

PETROLOGY OF THE BASALTIC

ACHONDRITE METEORITES

Thesis by

Michael B. Duke

In Partial Fulfillment of the Requirements

For the Degree of

Doctor of Philosophy

California Institute of Technology

Pasadena, California

1963

ABSTRACT

Mineralogical and textural evidence indicates that the basaltic achondrites originated in one or more magmatic episodes in a variety of cooling environments that resulted in textures ranging from gabbroic to diabasic. Chemical compositional and mineralogical variations are consistent with a common origin for the basaltic achondrites by magmatic differentiation. The characteristics of the mineralogical, major element and trace element variations are similar to those of the Skaergaard intrusion, but the basaltic achondrite magmas started from different compositions and crystallized under much lower partial pressures of oxygen (in the stability field of metallic iron) than did the magmas of the Skaergaard intrusion. The differentiation trends shown by the basaltic achondrites indicate that the starting material had calcic plagioclase and was depleted in alkalis with respect to chondritic meteorites, in which the plagioclase is sodic.

Brecciation is a conspicuous feature of most basaltic achondrites, which can be most satisfactorily subgrouped on the basis of breccia type as brecciated eucrites (monomict breccias), eucrites (unbrecciated), and howardites (polymict breccias). Petrographic evidence suggests that some textural metamorphism and brecciation were produced by shock effects that accompanied impact events on the surface of the parent body. The abundances of basaltic achondrite falls are consistent with a surface-sampling mechanism such as meteorite impact ejection. A preponderance of near-surface samples and the distinct differences between the basaltic achondrites and chondrites suggest that the moon is the probable parent body of the basaltic achondrites.

ACKNOWLEDGEMENTS

The problem was suggested by L. T. Silver, who acted as the writer's thesis advisor and offered stimulating criticism and advice during all stages of the research.

The cooperation of the following people, who generously supplied specimens and thin sections for this work, is gratefully acknowledged.

Dr. M. H. Hey, Senior principal scientific officer,
Department of Mineralogy, British Museum(Natural History)

Dr. C. B. Moore, Assistant Professor of Geology and Chemistry,
Arizona State University

Dr. W. v. Engelhardt, Director, Mineralogisch-Petrographisches
Institut Der Universitat Tubingen

Professor B. Mason, Curator of Mineralogy, American Museum
Of Natural History

Dr. E. P. Henderson, Associate Curator, Division of Mineralogy
and Petrology, U. S. National Museum

Dr. B. C. Roy, Geological Survey of India

Dr J. F. Lovering, Department of Geophysics, Australian
National University

Professor P. W. Gast, University of Minnesota

Dr. E. Anders, Enrico Fermi Institute for Nuclear Studies,
University of Chicago

Dr. K. Keil, University of California, La Jolla

A. Chodos and A. D. Maynes, staff analysts of the Division of Geological Sciences, California Institute of Technology, were extremely helpful in discussing analytical techniques. Dr. Maynes made new chemical analyses of meteorites and mineral separates. E. Bingham made the spectrographic analyses. R. v. Huene made excellent thin sections and polished thin sections and provided special assistance on a number of problems.

The writer wishes to thank Professor Harrison Brown for his interest and cooperation and for allowing the use of an unpublished analysis of Pasamonte by A. D. Maynes. E. M. Shoemaker provided stimulating ideas and discussion in regard to impact and shock events as recorded in the meteorites.

Financial support for general materials, chemical analyses and photographic equipment and materials was provided from the research program of L. T. Silver under A. E. C. contract AT(04-3)-427. Travel funds were provided from N. A. S. A. contract *NsG 56-60*. A grant from the Geological Society of America covered the cost of four new chemical analyses. The writer had a National Science Foundation Graduate Fellowship for the years 1960-1962.

TABLE OF CONTENTS

ABSTRACT

ACKNOWLEDGEMENTS

I.	INTRODUCTION	1
	Definition of basaltic achondrites	1
	Previous investigations	1
	Scope of this work	2
	Samples and Thin Sections	4
II.	TEXTURES AND STRUCTURES	7
	Introduction	7
	Meteorite descriptions	10
	Nuevo Laredo	10
	Sioux County	17
	Juvinas	21
	Stannern	25
	Pasamonte	29
	Bholghati	31
	Jonzac	32
	Moore County	32
	Serra de Mage	33
	Shergotty	37
	Petersburg	38
	Bialystok	44
	Pavlovka	44
	Frankfort	46
	Yurtuk	47
	Binda	47

Kapoeta	49
Estherville	51
Crab Orchard	52
Discussion	54
Introduction	54
Subclassification	54
Magmatic episode; rate of crystallization	58
Crystal settling	60
Late magmatic episodes	62
Brecciation and possible shock effects	63
Post-accumulation effects and possible repeated brecciation	67
Liquids of basaltic composition represented by bulk meteorites	68
III. CHEMICAL COMPOSITION OF THE BASALTIC ACHONDRITES AND SOME OF THEIR CONSTITUENT MINERALS	70
Bulk chemical analyses	70
General compositional features	85
Analyses of the Sioux County meteorite	88
Variation diagrams	88
Normative mineral variations	92
Composition of the Shergotty meteorite	97
Composition of minerals	101
Mineral compositions in the Shergotty meteorite	115
IV. MINERALOGY	120
Introduction	120

Pyroxenes	120
Color	120
Optical properties; composition	121
Plagioclase	137
Introduction	137
Composition of feldspar separates	138
Optical properties of plagioclase	138
Optic angle of plagioclase	148
Structural state; X-ray diffraction	151
Composition of plagioclase in other meteorites	155
Maskelynite	155
Summary of plagioclase data	158
Free Silica	164
Olivine	167
Metallic iron and the distribution of nickel between metal and silicates	170
Other minor mineral phases	176
V. PETROLOGIC TRENDS	180
VI. TRACE ELEMENT DISTRIBUTION	198
VII. NUCLEAR DATA	209
Pb ²⁰⁷ / _{Pb} ²⁰⁶ absolute ages	209
Uranium-helium ages	211
Potassium-argon ages	212
The isotopic composition of strontium; Rb-Sr model ages	212
Cosmic ray exposure ages	215

Primordial isotopic abundances	216
VIII. A HYPOTHESIS FOR THE ORIGIN AND HISTORY OF THE	
BASALTIC ACHONDRITES	218
Classification of basaltic achondrites	218
Correlations of meteorites in various subgroups	221
Characteristics of the available population of	
basaltic achondrites	224
Deduction of the probable parent body of the	
basaltic achondrites	228
REFERENCES	234
APPENDIX	239

INTRODUCTION

Definition of basaltic achondrites

The basaltic achondrites are a chemically and texturally diverse group of meteorites which have general similarities of mineralogy and textures in common with terrestrial basaltic rocks. They are composed primarily of calcic plagioclase and pyroxene and have magmatic textures ranging from gabbroic to basaltic.

Previous classifications have divided the basaltic achondrites into "eucrites" and "howardites", which Mason⁽¹⁾ has combined in a group called pyroxene-plagioclase achondrites. The basaltic achondrites as defined here differ from the basaltic-type achondrite group of Urey and Craig⁽²⁾ and the calcium-rich group of Prior⁽³⁾ in that the calcium-rich pyroxene achondrites Angra dos Reis, Nakhla and Lafayette are not included. The silicate phase of mesosiderites, which was recognized by Prior⁽⁴⁾ to be similar to the basaltic achondrites, is included in the basaltic achondrite classification in this work.

Previous investigations

Many of the major features of the basaltic achondrites have been described by previous investigators. Summaries of the earliest work on these meteorites are contained in Wahl⁽⁵⁾ and Michel⁽⁶⁾. It had been recognized at that time that the magmatic textures of the basaltic achondrites were similar to terrestrial diabases and Wahl's work on the pyroxenes established the presence of low calcium clinopyroxene (pigeonite) in the basaltic achondrites. Michel studied the plagioclase of meteorites and contributed useful information on the petrography of the basaltic achondrites. Chemical analyses had shown some of the basaltic

achondrites to be saturated with respect to silica and Berwerth⁽⁷⁾ described the occurrence of tridymite and quartz as minerals of these meteorites. It had been noted that the majority of known basaltic achondrites were brecciated and the early workers concluded that they resembled terrestrial volcanic tuff-breccias.

No petrological study of the basaltic achondrites as a group has been carried out since 1912, but some good descriptive papers on individual meteorites have been published. Among these are LaCroix⁽⁸⁾ on the Bereba meteorite; Foshag⁽⁹⁾ on the Pasamonte meteorite; and Henderson and Davis⁽¹⁰⁾ and Hess and Henderson⁽¹¹⁾ on the Moore County meteorite. Hess and Henderson argued for a process of magmatic crystal accumulation on the basis of preferred orientation of plagioclase and pyroxene grains. A paper by Game⁽¹²⁾ reported a detailed investigation of the plagioclase of the Juvinas meteorite. Zavaritskii and Kvasha⁽¹³⁾ gave some information on meteorites that have fallen in the USSR. A compilation of chemical analyses of basaltic achondrites was given by Urey and Craig⁽²⁾.

More recently, a number of the basaltic achondrites have been analyzed by newly developed techniques for minor and trace elements and for a variety of isotopic systems. Absolute age calculations have been made from some of the isotope relationships, while other elemental and isotopic data has been considered in theories of the origin and evolution of the meteorites and the solar system. The lack of closely correlated detailed petrographic and chemical data has made the interpretation of many aspects of the minor element and isotopic data difficult.

Scope of this work

The intent of this work is to provide the detailed textural, mineralogical and chemical data necessary for the formation of an adequate model for the origin and history of the basaltic achondrites. New bulk chemical

analyses, analyses of co-existing minerals, optical and structural data for minerals, trace element analyses and petrographic observations are combined with older data, mainly chemical, to outline reasonable magmatic histories of the achondrites. Isotopic data has been compiled from the literature and discussed in the context of the present work. Petrographic evidence on the nature of post-magmatic events is presented. The paper is divided into eight sections:

(I) Introduction

(II) Textures and Structures - A meteorite by meteorite description of the microscopic and macroscopic physical features of these achondrites, with a discussion of the principal events in the histories of the meteorites as inferred from textural observations.

(III) Chemical Composition of the Basaltic Achondrites and some of their Constituent Minerals - Older and new bulk chemical analyses and analyses of mineral separates. Systematics of compositional variations among the achondrites.

(IV) Mineralogy - A description of minerals, including composition and crystal-structure data, observations on sub-solidus transformations in pyroxene and observations on polymorphic variations of plagioclase and silica.

(V) Petrologic Trends - A discussion of compositional and mineralogical variations in these basaltic achondrites based on observational and experimental data on differentiation of terrestrial basaltic magmas.

(VI) Trace Elements - New determinations of trace elements in meteorites and mineral separates. Trace element variations are compared to the variations shown by rocks of the Skaergaard intrusion. The relation of achondrites to chondrites is examined.

(VII) Nuclear Data - A compilation of absolute age calculations, cosmic ray exposure ages and primordial isotopic abundances, with discussion based on the chemical and textural observations made in this work.

(VIII) Summary and Conclusions - From a summary of the principal features of the basaltic achondrites, aspects of their origin and history are considered. Limits are placed on the nature and identity of the parent body of these meteorites.

Samples and Thin Sections

Table 1 gives a list of the meteorite samples available for this work. Meteorite samples available only for non-destructive analysis are indicated. Table 2 gives an indexed list of all thin sections available for study and gives the repository for each thin section. This collection of thin sections of basaltic achondrites is probably the most comprehensive collection ever studied by a single investigator.

TABLE 1
SPECIMENS STUDIED IN THIS WORK

<u>Meteorite</u>	Specimens available for <u>Macroscopic study</u>	<u>Source</u>
Bialystok	Fragment, 0.8g	E.P. Henderson, U.S.Nat.Mus.
Binda	Fragment, 5g	J.F. Lovering, Aust. Nat.Univ.
Crab Orchard	Fragment, 40g	B. Mason, Am.Mus. Nat.Hist.
Estherville	Fragment, 1g	C.B. Moore, Ariz. State Univ.
Juvinas	Stone, 50g	B. Mason
	Stone and fragments, 30g	W.v. Engelhardt, Tübingen Univ.
Moore County	Powder, 4g	E.P. Henderson
	Cut slab	C.B. Moore
Nuevo Laredo	Original stone, 250g	
Pasamonte	Two stones, 40g	C.B. Moore
Pavlovka	Fragment	E.P. Henderson
Petersburg	Cut slab	C.B. Moore
Serra de Mage	Complete stone, 30g	B. Mason
Shergotty	Cut stone	E.P. Henderson
	Fragments, 30g	Roy, Geol. Survey of India
Sioux County	Fragment	P. Gast, Univ. of Minn.
	Fragment	E. Anders, Univ. of Chicago
	Stone	C. B. Moore
Stannern	Fragment and powder	W. v. Engelhardt
	Fragment	C. B. Moore
	Fragment	B. Mason
Yurtuk	Stone, 70g	E.P. Henderson

TABLE 2

THIN SECTIONS STUDIED IN THIS WORK

<u>Meteorite</u>	<u>Label</u>	<u>Source</u>
Bholghati	BM-1915,140	M. Hey, Br. Mus. Nat. Hist.
Bialystok	BM-96257	M. Hey
	CTT-Bial-1,2	
Binda	CTT-Bin-1	
Crab Orchard	CTT-CbO-1,2	
Estherville	CTT-E-1	
Frankfort	BM-43055	M. Hey
Jonzac	BM-19974	M. Hey
Juvinas	CTT-Juv-1,2,3,4	
	BM-45845	M. Hey
Kapoeta	UCLJ-1,d	K. Keil, Univ. Calif. La Jolla
Moore County	CTT-MC-1	
Nuevo Laredo	CTT-NL-1,2	
Pasamonte	CTT-Pas-1	
Pavlovka	BM-55255	M. Hey
Petersburg	BM-32053(3)	M. Hey
	CTT-Pet-1	
Serra de Mage	CTT-SdM-1	
Shergotty	U.S.N.M.-321	E.P. Henderson, U.S. Nat. Mus.
	BM-41020(2)	M. Hey
	CTT-Sh-1	
Sioux County	CTT-SC-1,2,3	
Stannern	CTT-St-1,2,3	
	BM-46970(4)	M. Hey

II

TEXTURES AND STRUCTURES

Introduction

Textures observed in the basaltic achondrites can be ascribed to two different genetic types, those related primarily to the crystallization histories and those related to the mechanical fragmentation histories of these meteorites. The development of the chemical compositional features of the meteorites can be seen in magmatic and metamorphic textures and some limits on the physical and chemical conditions of the crystallization history can be obtained from study of these textures. Brecciation is a conspicuous textural feature of most of these meteorites and analysis of the fragmental textures can lead to some understanding of the post-crystallization history of the basaltic achondrites. Some meteorites show evidence of post-accumulation chemical effects and clasts in some brecciated meteorites may have undergone magmatic crystallization, metamorphism, fragmentation, and recrystallization processes before their final fragmentation and accumulation. Following the final accumulation of the fragments, the brecciated materials were compacted enough to survive as meteorites.

This section gives descriptions of the textures observed in a number of basaltic achondrites along with an interpretation of the manner in which they developed. The origin of some of the textures can not be a matter of much controversy. In some cases, however, there may be more than one possible interpretation of the genesis of a texture and in a few cases only speculative interpretations can be made. The textural descriptions are given on a meteorite by meteorite basis, but most of the interpretation is reserved for a summary at the end of this section.

Textural descriptions are not independent of compositional and mineralogical properties of the meteorites. Where reference is made, in this section, to mineral composition or to bulk meteorite composition, the reader can refer to later chapters for supporting detail. Table 3 gives a summary description of the minerals of the basaltic achondrites which enter into the textural descriptions.

Table 3

Minerals of the Basaltic Achondrites

Pyroxenes

Pigeonite; monoclinic pyroxene in CaSiO_3 - MgSiO_3 - FeSiO_3 system with low CaSiO_3 content. Generally described by $\text{Fe}/\text{Fe}+\text{Mg}$ content.

Hypersthene; orthorhombic pyroxene in MgSiO_3 - FeSiO_3 system with less than 4% CaSiO_3 .

Ferroaugite; monoclinic pyroxene in CaSiO_3 - MgSiO_3 - FeSiO_3 system with high CaSiO_3 content, high $\text{Fe}/\text{Fe}+\text{Mg}$.

Feldspar

Plagioclase; feldspar with composition primarily described by the proportion of albite $\text{NaAlSi}_3\text{O}_8$ and anorthite $\text{CaAl}_2\text{Si}_2\text{O}_8$.

In these meteorites the plagioclase generally has greater than 80% anorthite molecule.

Maskelynite; amorphous plagioclase

Free Silica

Tridymite

Quartz

Cristobalite

Other Minerals

Metallic iron, troilite (FeS), ilmenite, chromite, whitlockite (phosphate), magnetite.

METEORITE DESCRIPTIONS

Nuevo Laredo

The first complete petrographic and textural description of Nuevo Laredo is presented as part of this study.

Except for a corner which had been broken off and lost, the original 500 gram stone had a complete fusion crust. The crust is greenish black and filled with spherical cavities up to .03 mm in diameter; the cavities apparently represent bubbles of volatiles which were formed during the fusion in atmospheric flight (Plate 1a). Rills of glossy black glass which flowed over the fusion crust have fewer spherical cavities. The fusion crust consists of three portions (Plate 3a). An outer zone, about 0.05 mm thick, is composed of dense brown glass in which the spherical cavities are conspicuous. An intermediate zone, generally about 0.05 mm thick, is primarily colorless glass into which a few plagioclase laths extend from the interior. The intermediate zone grades into an interior zone of darkened crystalline material which appears to mark the limit of the chemical effects of the fusion process.

In the hand specimen (Plate 1b), dark lithic fragments make up about fifty percent of the surface. The largest dark fragment has a maximum dimension of about five centimeters. At some point in the spectrum of fragment sizes, an arbitrary distinction must be made between fragments and matrix, because there is an apparent continuum of fragment sizes from the coarsest lithic fragments to the finest fragmental material in the matrix. Also, crystal fragments vary in dimensions and an arbitrary cutoff must be made between groundmass and crystal fragments. In Nuevo Laredo, it is convenient to call fragments larger than 1 mm lithic or crystal fragments, and smaller fragments are included in the category of matrix. Fragments greater than 1 mm make up approximately forty percent

of the surface area of the meteorite, and fragments greater than 10 mm make up ten to fifteen percent of the meteorite (visual estimate).

When a sample of the meteorite was crushed for mineral separation purposes, it was noted that some fragments were very resistant to crushing. A retained 38 mesh fraction of resistant fragments was separated for special study. The fragments were of two types, dark gray lithic fragments and light gray fragments composed primarily of matrix material (Plate 3b). Most of the fragments are equant or sub-spherical. Some shaping may have been produced by abrasion during crushing of the meteorite. However, on the broken surface of the meteorite and on many of the resistant dark lithic fragments there are some very smooth surfaces. The smoothness of these surfaces, which occur primarily on black pyroxene grains, causes some fragments partially exposed on the surface of the meteorite to appear as smooth hemispheres which are suggestive of the appearance of chondrules in chondritic meteorites. They are different from chondrules in that the smooth surfaces rarely extend over more than a hemisphere. The composition and internal textures of these resistant rounded lithic fragments are similar to those of larger more angular lithic fragments in the meteorite. It would appear that the rounding which is observed on some fragments is due to mechanical effects.

At low magnification in thin section, it is difficult to distinguish lithic fragments from what is more properly called matrix material. In (Plate 2a) the field contains primarily matrix material, but some lithic fragments occur in which the crystal size is only slightly greater than that of the matrix. The matrix consists of fine-grained fragmental material which in some portions has an average grain size of less than

ten microns. In these areas the matrix is brown and nearly isotropic. Between crossed nicols, very small spots of birefringence apparently represent very fine-grained crystal fragments. Even in portions of the matrix in which the average fragment size is ten microns to thirty microns, the overall effect between crossed nicols is a mass of very low birefringence, although if attention is focussed on individual grains, they can be identified as pyroxene or feldspar on the basis of their birefringence.

Because of the fine grain size of many of the lithic fragments and the identical mineralogy of fragments and matrix, the boundaries may be indistinct and seemingly gradational as in Plates 2a and 2b. Crystals apparently do not cross fragment-matrix boundaries. Rather, the indistinct nature of the boundaries appears to be due to overlapping of the fine-grained matrix onto lithic fragments with irregular shapes.

Fragments of nearly opaque brown "glass" are scattered sparsely throughout the meteorite. Although the material is optically isotropic, an X-ray diffraction pattern of an uncrushed globule of "glass" showed plagioclase and clinopyroxene diffraction peaks, which indicates that the "glass" is cryptocrystalline. In one place, "glass" fragments form a discontinuous vein-like feature (Plate 4a). Many of the fragments are separated from one another by fine-grained groundmass, which indicates that the glass has not been formed in place. Distribution of the "glass" fragments in the veinlike arrangement is probably due to mechanical effects related to brecciation.

In one of the "glass" fragments, two clinopyroxene (pigeonite) grains about 0.8 mm in length are present (Plate 4b). The grains have skeletal terminations, but sharply defined prism boundaries, and are interpreted as phenocrysts in the basaltic magma cooled rapidly to form the "glass".

This is the only feature observed in this study of basaltic achondrites which, can be described as porphyritic texture with any certainty. The basaltic achondrites, in general, show non-porphyritic textures, perhaps due to the lack of preservation of large fragments in which such textures could be observed, but more probably due to the nature of the sequence of crystallization in the basaltic magmas. Both plagioclase and pyroxene apparently began to crystallize at the same time during the cooling history of the magmas.

Special thin sections were prepared of a number of the more resistant fragments. The following discussion of the textures of fragments in Nuevo Laredo is derived primarily from study of the thin sections of these separated fragments. Most of the textures observed resemble textures of terrestrial diabasic rocks which occur as shallow intrusive rocks. Compositional zoning within individual lithic fragments is further direct evidence that these materials originally crystallized from liquid phases.

Aside from the "glass" described above, the textures observed are holocrystalline and represent average grain sizes from 0.01 to about 1 mm. The overall average grain size is about 0.3 mm. The finest-grained fragments have intergranular textures, with anhedral pigeonite and ferroaugite grains filling interstices between thin plagioclase plates. Plate 5a shows fragment with an intermediate grain size composed primarily of plagioclase laths and clinopyroxene grains in intergranular to sub-ophitic texture. Cristobalite occurs between plagioclase and pyroxene grains in a relationship which suggests that it is a primary magmatic mineral. Plate 5b shows a fragment with sub-ophitic texture in which the pyroxene is as coarse as 1 mm.

In coarser fragments plagioclase occurs both as laths and as irregular interstitial grains. The plagioclase laths of Nuevo Laredo have composition of An_{85} , but the interstitial plagioclase is more sodic and some grains as sodic as An_{65} have been observed. The interstitial plagioclase is commonly found in association with accumulations of troilite, suggesting that both minerals were concentrated in the late stages of crystallization (Plate 6a).

Pigeonite and ferroaugite are generally greenish brown with many slight color variations in single grains and between grains. In some grains, a small amount of inversion of pigeonite to colorless hypersthene causes color variations. Ferroaugite is lighter in color than pigeonite and may be responsible for some of the variability of color. Variations of $Fe/Fe+Mg$ have not been detected in the pigeonite, but if present could produce additional variability of color. Both pigeonite and ferroaugite contain abundant inclusions and the density of inclusions may affect the color.

Although there is a small amount of partial inversion of pigeonite to hypersthene, there is little evidence of exsolution phenomena. The two features are expected to be coupled because the calcium content of pigeonite is generally greater than the hypersthene structure can hold and calcium-rich pyroxene must be exsolved before inversion can occur. Under high magnification fine planes parallel to (001) in both pigeonite and ferroaugite can be seen. These may be crypto-exsolution lamellae, but could possibly represent twinning of the clinopyroxene. Ferroaugite occurs in distinct grains which can be physically separated from pigeonite. In thin section the two pyroxenes can be distinguished by determination of the optic angle.

Both pigeonite and ferroaugite contain oriented and unoriented inclusions. In the plagioclase, blebs and rod-like inclusions are concentrated in the (010) and (110) planes. Bleb inclusions also occur along curved fractures in the plagioclase. The inclusions are transparent, with an index of refraction greater than that of the plagioclase. They are probably colorless, but have a bluish tint as a result of the index contrast with the plagioclase. Oriented inclusions are common in the plagioclase of the finer-grained basaltic achondrites. Michel⁽⁶⁾ gave a detailed description of oriented inclusions in Stannern and other meteorites. The suggestion by Michel and other earlier investigators that the inclusions have pyroxenic composition has not been proved or disproved. Plate 6d shows a plagioclase grain with oriented inclusions.

In the clinopyroxenes, rod-like inclusions less than 20 microns long are concentrated in (110) planes and are elongated parallel to *c*. Many of these inclusions are opaque and have the reflectivity of ilmenite (Plate 6c). Inclusions also are concentrated along (001) planes; they are generally too small to be identified and may be opaque or non-opaque.

Quartz is present associated with troilite and ilmenite in the interstices of some lithic fragments (Plate 7a). The pyroxene in these areas tends to be corroded and clouded with opaque inclusions. Cristobalite is colorless and inclusion-free (Plate 5a). It does not commonly occur in areas with large concentrations of opaque minerals. No evidence of inversion of cristobalite to quartz was noted.

Ilmenite, troilite and chromite are the opaque minerals which have been identified in the magmatic textures. Ilmenite is most abundant and chromite is scarce. Ilmenite and troilite occur in grains or aggregates

of grains up to 0.5 mm, but most opaque grains are less than 0.1 mm in diameter. The total opaque mineral content is 3% or less. Troilite and some ilmenite are concentrated in the interstices with sodic plagioclase. In some fragments, the clinopyroxenes which occur with interstitial plagioclase, ilmenite and troilite (with or without quartz) have a corroded aspect suggestive of reaction (Plate 7a). It is possible that some corrosion of pyroxene and formation of troilite occurred in a late magmatic buildup of sulfur vapor pressure.

Metallic iron makes up less than 0.1% of the meteorite occurs in small amounts in fragments consisting primarily of orthopyroxene and plagioclase. The pyroxene of these fragments has non-uniform interference colors (Plate 7b). Because the orthopyroxene appears variable and because the normal pyroxene of the meteorite is predominantly pigeonite of uniform optical properties, the metallic iron is believed to have been produced by reduction of iron-rich pigeonite to produce hypersthene, free silica, metallic iron and perhaps some calcic pyroxene. Detailed study of the composition of the reaction products would be necessary to establish the validity of this hypothesis. The reaction of pigeonite to form hypersthene, free silica and metal is shown more conclusively in a fragment from the Sioux County meteorite.

The textures of fragments in Nuevo Laredo are predominantly fine-grained textures which are similar to those of terrestrial diabases. The fine-grained textures, the presence of cristobalite (which probably formed metastably), the lack of inversion of pigeonite (unstable at low temperature) and the presence of porphyritic "glass" suggest very rapid rates of cooling. The textural aspects of some troilite, which occurs in interstices with corroded pyroxene suggest that some late

stage magmatic reaction occurred. The overall uniformity of pyroxene composition suggests that brecciation and accumulation have occurred with little mixing of diverse chemical systems, although textural variations are substantial. The metamorphic effect which has caused the reduction of silicate to metal cannot be accurately placed in the time sequence with respect to the brecciation, and could represent a post-accumulation feature. The meteorite is friable, but it was compact enough to withstand passage through the earth's atmosphere and must have undergone some post-accumulation compaction.

Sioux County

The petrography of the Sioux County meteorite has not been described previously. Externally, the meteorite has a dark black fusion crust similar to that of the Nuevo Laredo. A broken surface shows many lithic fragments set in a fine-grained friable groundmass (Plate 8a and 8b). The groundmass is lighter than that of the Nuevo Laredo reflecting an abundance of very white plagioclase. The lithic fragments are medium- to coarse-grained equigranular aggregates of black pyroxene and white plagioclase. The coarse-grained fragment shown in Plate 8b has as coarse as any texture observed in the basaltic achondrites.

The average grain size of lithic fragments is much coarser than those in Nuevo Laredo. Consequently, there are more crystal fragments larger than 1 mm in Sioux County than in Nuevo Laredo. The average grain size of the matrix of Sioux County seems to be somewhat greater than that of Nuevo Laredo. Plate 9a shows a photomicrograph at low magnification of a portion of the meteorite which contains a medium-grained lithic fragment surrounded by finer-grained fragmental material. Some portions of the groundmass have overall low birefringence between crossed nicols, but the abundance of very fine-grained groundmass is low

in Sioux County. The boundaries between lithic fragments and matrix are sharply marked in many places, but where the pyroxene of the lithic fragments has been strongly granulated, it is more difficult to make the distinction. Plates 10a and 10b show at higher magnification a portion of the boundary between the lithic fragment and matrix shown in Plate 9a.

The medium-grained lithic fragment shown in Plate 9a is typical of Sioux County and is shown in greater detail in Plate 10a. The plagioclase grains are tabular rather than lathlike. They show much more mechanical distortion than the minerals of Nuevo Laredo. The pigeonite has fine lamellae parallel to (001) which may be exsolution lamellae. The pigeonite, commonly, is twinned on (100).

Some pigeonite twins have partially inverted to hypersthene in an irregular fashion. Plate 9b shows a partially inverted pigeonite grain in which areas within the central portions have inverted, leaving an irregular rim of pigeonite. The contacts between pigeonite and hypersthene are irregular and, but for the evidence that the grain was originally twinned on a clinopyroxene twin law, might be interpreted as a zonal relation in which hypersthene was first to crystallize. The geometrical irregularity of the inversion may be controlled by variations of composition in the pigeonite; if the pigeonite rims were more calcic than the cores, inversion might proceed from the center outward. No test of this possibility has been made.

Two fragments, a medium-grained fragment shown in Plate 8a and the coarse-grained fragment shown in Plate 8b were sampled for chemical and mineralogical analyses. The medium-grained fragment has about equal proportions of pigeonite and hypersthene the coarse-grained fragment

contains some pigeonite, but is primarily hypersthene and plagioclase. The pigeonite is brown and the hypersthene colorless. They both contain numerous inclusions. The color of the pyroxene in coarse grains may be controlled primarily by the inclusions, because both pigeonite-rich and hypersthene-rich fragments have black pyroxene grains.

The difference of grain size between the two lithic fragments suggests that the coarser has cooled and crystallized more slowly. The greater abundance of hypersthene in the coarser fragment is consistent with the formation of hypersthene by inversion from pigeonite following magmatic crystallization. More inversion occurs in the fragment which has the coarser texture and which has probably cooled more slowly.

Tridymite is the most abundant polymorph of silica in the meteorite and occurs interstitially in the gabbroic textures in grains up to 0.1 mm. Ilmenite and troilite are the most abundant opaque minerals in the primary textures; they generally occur interstitially to the plagioclase and pyroxene in grains that are generally smaller than 0.5 mm.

Corrosion of pyroxene with production of troilite and free silica is shown by some fragments; the free silica in these textures is quartz. The proportion of quartz to primary tridymite is small. The corroded pyroxene is lighter in color and has lower birefringence than the unaltered pyroxene. Plate 11a shows a fragment with corroded pyroxene.

In some fragments, pigeonite has been replaced by a finer-grained aggregate of colorless to yellow pigeonite. The recrystallized portions have fewer inclusions and grade into inclusion-filled normal pigeonite. There is no special concentration of opaque minerals in the recrystallized portions, but the fine-grained material is difficult to study by optical means. Recrystallization of pigeonite in this manner is shown

in Plate 11b. More distinctive examples of this type of recrystallization are described for the Juvinas meteorite.

Plate 12a shows a pigeonite-rich fragment in which a portion of the brown pigeonite has reacted to form colorless hypersthene and troilite. The troilite is concentrated at the boundaries of the hypersthene grain, which has a different crystallographic orientation than the host pigeonite. Plates 12b and 12c show the occurrence of metallic iron with orthopyroxene in what is interpreted as a post-magmatic reaction texture.

Mechanical deformation effects are pronounced and, in some cases, extreme. Thoroughly fractured pigeonite grains and plagioclase grains with distorted and offset twinning and cleavage lamellae are shown in Plates 10a and 13a.

Some portions of this meteorite show what may be post-aggregation recrystallization, especially of matrix material. Plate 13b shows an area which has an overall fragmental aspect with irregular plagioclase and pyroxene grains surrounded by very fine-grained matrix material. At some edges there are sharp contacts between fine-grained and coarser material, but at one edge the grain size grades from fine-grained to coarser material. In plane light, it is difficult to see boundaries between adjacent plagioclase grains within this area. The larger plagioclase grains have slightly undulatory extinction, but the smaller grains do not show undulatory extinction, which is in contrast with plagioclase fragments immediately outside the area which show strong undulatory extinction. These features strongly suggest that recrystallization of fragmental material has taken place after aggregation of the breccia.

Another possible example of matrix recrystallization is shown in Plates 14a and 14b. In crossed nicols, the area has a fragmental

appearance, not unlike the matrix material in Plates 10a and 10b. In plane light the boundaries between adjacent plagioclase grains are obscure and the plagioclase apparently forms a continuous network. This feature suggests that some post-accumulation sintering has occurred.

The magmatic textures of Sioux County are much coarser than those of Nuevo Laredo and suggest gabbroic rather than basaltic affinities. The slower rate of crystallization suggested by the texture is consistent with a larger amount of inversion of pigeonite to hypersthene in Sioux County. Corrosion of pyroxene with the formation of quartz and troilite has occurred to a lesser extent than in Nuevo Laredo, but is present as a possible late magmatic reaction. Some pyroxene grains show evidence of reduction to metallic iron after the original magmatic crystallization, but at an unknown time with respect to the late stage magmatic events or with the brecciation and accumulation history.

Brecciation has produced a much larger amount of mechanical deformation in Sioux County than in Nuevo Laredo. The coarse-grained lithic fragments are quite friable due to thorough fracturing of the pyroxene and plagioclase. This is in contrast to the toughness of the finer-grained dark fragments of Nuevo Laredo. There is less very fine-grained matrix material in Sioux County than in Nuevo Laredo. There is some evidence of post-accumulation recrystallization of the finer-grained matrix material.

Juvinas

The petrology of Juvinas has been discussed previously by Rose⁽¹⁴⁾, Wahl⁽⁵⁾, Michel⁽⁶⁾ and LaCroix⁽⁸⁾.

In external appearance, Juvinas is very much like Nuevo Laredo. The fragmental groundmass is light gray and lithic fragments are dark

gray to black. Lithic fragments reach as much as 3 cm in maximum dimension (Plate 15a). The fusion crust is black and contains spherical cavities as does that of Nuevo Laredo.

The matrix material of Juvinas is similar to that of Nuevo Laredo, but on the average is coarser.

The difference in average grain size of the matrix may directly reflect the coarser grain sizes in the magmatic textures of Juvinas in comparison with Nuevo Laredo. Some portions of the matrix in Juvinas have the sintered appearance described for Sioux County.

The fragments observed in thin section have medium-grained sub-ophitic and ophitic textures (Plates 15b and 16a). The sub-ophitic textures are composed of plagioclase laths with a length/width ratio of about four, intergrown with anhedral pigeonite and ferroaugite. The plagioclase laths generally have compositions of about An_{90} , and, uncommonly, show compositional zoning. Interstitial plagioclase may be as sodic as An_{65} . Many of the plagioclase grains have cloudy inclusion-filled cores and clear rims.

The ophitic textures show randomly oriented plagioclase laths up to 1 mm in length crowded into equant pigeonite or ferroaugite grains up to 4 mm in diameter. It seems clear that much of the plagioclase in these fragments crystallized before pyroxenes began to crystallize. It is possible, but has not been shown, that the plagioclase laths in the ophitic textures have variable compositions.

Pigeonite shows little sign of exsolution, but as in Nuevo Laredo there are planar features parallel (001) which may be exsolution lamellae. In some fragments, pigeonite has partially inverted to hypersthene. The amount of hypersthene is small, but more is present than in Nuevo Laredo.

The pigeonite of the sub-ophitic and ophitic fragments commonly shows twinning on (100) which may give striking fringe effects in crossed nicols (Plate 15b).

Inclusions, possibly of pyroxene, cloud the central portions of many plagioclase grains. The rims of many plagioclase grains, however, are inclusion-free. Tridymite occurs in the fragments with magmatic textures as colorless plates which have hexagonal patterns of oriented colorless inclusions of higher index.

Many of the fragments in Juvinas show partial recrystallization of clinopyroxene to fine-grained aggregates. Plates 17a and 18b show various aspects of this type of recrystallization. The recrystallization crosses features such as grain boundaries and twinning planes and grades into unrecrystallized pyroxene; structures of the unrecrystallized pyroxene can be followed into the recrystallized areas (especially cleavages in Plate 17a) and in 18b original planes marked by rows of minute opaque inclusions can be seen in a completely recrystallized fragment. The recrystallized fine-grained pigeonite is lighter in color than the unaffected pigeonite (Plate 17b), which may indicate that some chemical transformations have accompanied the recrystallization. Where plagioclase is present at the edges of recrystallized pyroxene areas, it is apparently unaffected, except for the possibility that the inclusion-free rims may be related to the recrystallization of pyroxene (Plate 18a).

In the interstices of some sub-ophitic fragments, corroded pyroxene is filled with opaque grains of troilite, ilmenite and metallic iron. Quartz is commonly associated in these interstices (Plates 19a and 19b).

Plate 20 shows a fractured pyroxene grain in which troilite has crystallized along the fractures. In the vicinity of the fractures, the

pyroxene is colorless or yellow as opposed to the brown unaffected pyroxene, and small areas of clinopyroxene with different optical orientation have developed. In one case, clinopyroxene was observed in very fine grains along a fracture in an hypersthene grain (inverted from pigeonite) which suggest that fracturing and replacement by sulfide occurred after inversion and, therefore, after much, if not all, of the magmatic crystallization.

The recrystallization and reaction textures described above have been observed, to some degree, in most of the basaltic achondrites, but are most pronounced in Juvinas. A unique feature of Juvinas, the presence of miarolitic(?) cavities within fragments with ophitic texture was reported by Rose⁽¹⁴⁾ and succeeding investigators Wahl⁽⁵⁾; LaCroix⁽⁸⁾. The cavities contain euhedral crystals of monoclinic pyroxene, plagioclase and troilite. The crystals are large enough that Rose was able to measure interfacial angles of the clinopyroxene. The occurrence of conspicuous silicate recrystallization may be related to the development of troilite along fractures and the formation of the cavities. Both features suggest that a sulfide-rich volatile phase was built up in the late stages of crystallization of the meteorite.

The magmatic textures of Juvinas are medium-grained sub-ophitic and ophitic textures such as are common in terrestrial diabases. There has been some inversion of pigeonite to hypersthene, but not as much as in Sioux County; tridymite is the stable form of free silica. The textural and mineralogical features suggest moderate cooling rates intermediate between those of Nuevo Laredo and Sioux County. Late stage magmatic alterations by sulfide-rich vapors may have caused most of the recrystallization effects. Brecciation did not mix fragments of diverse chemical

composition, but individual lithic fragments show compositional variations in individual grains, especially in the plagioclase. There may have been some sintering of matrix material after accumulation of the breccia.

Stannern

Previous petrographic descriptions have been given by Wahl⁽⁵⁾ and Michel⁽⁶⁾. A modern detailed study of this meteorite has been carried out by von Engelhardt⁽¹⁵⁾.

Stannern is similar to Nuevo Laredo and Juvinas in external appearance; it has a dull gray fine-grained groundmass and the lithic fragments are also dull gray. The lithic fragments have intergranular textures composed primarily of laths of plagioclase from 0.5 to 1.0 mm in length intergrown with dark minerals which are rarely larger than 0.5 mm. The laths commonly appear to be oriented in sub-parallel arrangements or in radiating structures. Plates 21a and 21b show external views of Stannern. In Plate 21b conspicuous dark veins are shown; these are not present in all fragments of the meteorites.

The fusion crust is similar to that of Nuevo Laredo. The three zones of brown glass, colorless glass and internal darkening are present. Plagioclase laths extend into the brown glass in the Stannern section, which indicates that plagioclase was the last mineral to be fused in the rapid formation of the fusion crust.

Most of the lithic fragments studied in thin section are fine-grained plagioclase and pyroxene in intergranular or sub-ophitic intergrowths. Plates 22a to 23b show typical lithic fragments. Limited areas show parallel orientation of plagioclase laths, as suggested from macroscopic observation. Some lithic fragments show radiating aggregates of plagioclase.

class laths with interstitial pyroxene. No phenocrysts could be distinguished. The textures with parallel or radiating laths have been observed only in Stannern and serve to distinguish it texturally from other basaltic achondrites.

Pigeonite is the most abundant pyroxene, but hypersthene is abundant in some fragments. Exsolution lamellae of augitic pyroxene exsolved from pigeonite create a relict herringbone pattern in some twinned grains which have subsequently inverted to hypersthene (Plate 22a). Other pyroxene grains have irregular intergrowths of hypersthene and pigeonite, with pigeonite generally confined to the rims. This is believed to be caused by inversion of pigeonite grains from the core outward. Along some fractures, pigeonite apparently embays hypersthene, but in other cases, the reverse relation is present.

Quartz is the only polymorph of silica found in Stannern. Plate 23a shows a typical occurrence, in which quartz rimmed by troilite is found between plagioclase laths in a fragment with sub-ophitic texture. Quartz in this textural position probably has crystallized directly from the magma.

Reaction of pyroxene to form troilite and quartz is observed in some fragments. Plate 23b shows a strongly corroded pigeonite grain which is optically continuous over a sizable area where it has been partly replaced by troilite and quartz. The remaining pyroxene is colorless whereas the unaltered pyroxene is brown. The proportions of magmatic quartz and secondary quartz can not be established for Stannern, but if this meteorite is similar to Sioux County and Juvinas, which contain magmatic tridymite and secondary quartz, the amount of secondary quartz is probably small. Ilmenite grains up to 0.1 mm also occur in the interstices with

troilite.

A few lithic fragments show pyroxene recrystallization similar to that found in Juvinas, where localized areas have suffered recrystallization to finer-grained pigeonite. These textures are not common, however, in Stannern.

Stannern is marked by a substantial amount of mechanical deformation; most plagioclase shows undulatory extinction or deformation of twin lamellae. Both plagioclase and pyroxene are commonly badly fractured, (Plate 24a). Some fracturing took place before reaction of the pyroxene to form sulfide, because some troilite is concentrated along fractures.

Most of the conspicuous dark veins shown on Plate 21b are composed of brown amorphous material which in some places is isotropic, but in other spots shows evidence of a cryptocrystalline structure (Plates 24b to 25b). The veins are interwoven in some portions of the meteorite and vary in thickness from a few microns to 0.2mm. Within some of the veins there are fractures oriented perpendicularly to the walls of the veins. In the brown amorphous or cryptocrystalline veins there is no apparent concentration of opaque material. The localization of the veins is not uniform, but in general they tend to occur between coarse and fine portions of the meteorite. Along most veins there is evidence of offset which includes both matrix and lithic fragments. The veins are certainly of a post-accumulation origin and apparently represent a partial re-brecciation of the material. It will be important to learn if the veins represent material actually melted and quenched or represent very limited zones of extreme mechanical reduction to cryptocrystalline grain sizes. Along one vein, which seems to be related to the brown veins, there is a concentration of opaque material which is probably troilite. This vein

suggests that some introduction of sulfide has occurred after the initial brecciation-aggregation history. Fragments of amorphous material similar to that which makes up the brown veins occur in other portions of the meteorite, which suggests that more than one post-accumulation mechanical event occurred.

The groundmass of Stannern is similar to that of Nuevo Laredo. The finer-grained portions of the matrix have grain sizes that are sub-microscopic. These areas tend to be dark brown and nearly opaque as well as isotropic. Some portions of the groundmass show sintering, but the meteorite is generally quite friable. Some portions of the groundmass have undergone post-accumulation fracturing concurrent with the formation of the brown veins. Plates 26a and 26b show a portion of a lithic fragment which has been offset in a post-aggregation event along with the adjacent matrix.

The magmatic textures of Stannern are primarily fine-grained textures with basaltic or diabasic affinities; they are finer-grained than those of Juvinas, but coarser than those of Nuevo Laredo. The radiating and sub-parallel arrangements of laths are conspicuous features which have only been observed in Stannern. The magmatic textures are consistent with an origin in a shallow intrusive environment.

Late stage reaction of pyroxene with sulfur has produced sulfide and quartz. Ilmenite also may be concentrated in these interstitial positions. Subsequent to a brecciation and accumulation event, distinct mechanical deformation occurred as shown by offset lithic fragments and matrix, and this deformational event was accompanied by the formation of brown amorphous veins and perhaps movement of some sulfide. A small amount of sintering of the fine-grained matrix has occurred after initial aggregation.

Pasamonte

Pasamonte was originally described by Foshag⁽⁹⁾. External views are shown in Plates 27a and 27b. The groundmass is light gray, but lithic and crystal fragments have pyroxene which is yellow, brown or black and plagioclase that is white; very fine-grained or glassy fragments are gray or black. The fusion crust differs from those of the other meteorites in that a polygonal fracturing of the crust is well developed; polygonal fracturing is developed only locally on the fusion crusts of the other meteorites.

Plates 28a to 29b show textures of different lithic fragments which show sheaf-like textures of pyroxene and plagioclase laths and very fine-grained intergranular, sub-ophitic and ophitic textures, in which the grain sizes vary from 0.01 to 3 mm. Despite the wide variety, all are comparable to textures found in terrestrial basaltic or diabasic rocks. All observed fragments are non-porphyrific.

Although there may be some compositional variation among the assemblage of lithic fragments, the most important compositional variations appear to be reflected in the compositional zoning of pyroxene in the medium-grained fragments. Plate 29a shows a portion of one fragment in which pigeonite varies from colorless in the cores ($Fe/Fe+Mg=0.5$) to yellow brown in the rims ($Fe/Fe+Mg=0.65$). Brown ferroaugite is concentrated in interstitial positions. Both ferroaugite and yellow brown pigeonite tend to be clouded with troilite inclusions. As the pyroxene shows a normal compositional zonation that is consistent with concentration of iron-rich pyroxene at the late stages of crystallization, it must be concluded that troilite was concentrated also in later stages of crystallization. There is a clear difference between the concentration

of opaque minerals in the interstices of Juvinas and Pasamonte. In Pasamonte there is no obvious corrosion of pyroxenes during the sulfide crystallization episode. The total variation of pyroxene composition found in this fragment is substantially the same as the variation of pyroxene composition found in the entire meteorite. As in other meteorites which have basaltic textures, interstitial plagioclase is generally more sodic than that of the laths.

The pigeonite is, for the most part, homogeneous with respect to exsolution or inversion. A few fine unidentified lamellae parallel (001) are present in some grains. The pyroxene of Pasamonte has better crystal form than in other basaltic achondrites. Except for the concentration of inclusions in the yellow brown pigeonite of the rocks, the pigeonite of the medium-grained fragments is generally more free of inclusions than the pigeonite of Juvinas, Sioux County, Stannern or Nuevo Laredo. These aspects of Pasamonte allow it to be distinguished from most other basaltic achondrites, but the reasons for the differences are not at all clear, as its bulk composition is very similar to other basaltic achondrites.

Tridymite is the only form of silica which has been observed. No conspicuous metamorphic textures were observed. There is little sign of mechanical deformation in the lithic and crystal fragments which form the breccia.

The groundmass material of Pasamonte does not have as high a percentage of sub-microscopic fragments as does Nuevo Laredo or Stannern. This may be due to the somewhat coarser average grain size of Pasamonte. The number and variety of lithic fragments greater than 1 mm suggests a comparison with the Pavlovka and Frankfort meteorites which will be

described below. The variety of compositions of crystal fragments reflects the compositional zoning within the lithic fragments, but has been previously attributed by Foshag⁽⁹⁾ to mixing of fragments in a polymict breccia.

The history of this meteorite seems to have consisted first of a magmatic episode from which crystallization of a variety of fine to medium-grained textures resulted. There was little fracturing with late stage formation of sulfides as in Juvinas or Stannern, although troilite may have been concentrated in the interstices of the diabasic textures during the late magmatic stages. The average grain size of the textures is somewhat less than that of Juvinas and greater than that of Stannern.

After the magmatic episode, a mechanical event brecciated the meteorite and only mixed in the breccia fragments which are seemingly related to one another. The groundmass material shows no strong evidence for post-accumulation sintering following the brecciation event.

Bholghati

No previous description of Bholghati has been found in the literature, although it has been recognized as a basaltic achondrite. A single thin section was examined.

Bholghati shows a texture comparable to that of Sioux County (Plate 30a). The section contains only a few lithic fragments, up to 5 mm in diameter, composed of tabular plagioclase and pyroxene. The pyroxene is predominantly hypersthene with conspicuous exsolution lamellae indicative of inversion from pigeonite. Some uninverted or only partially inverted pigeonite is present. The maximum grain size in the fragments is about 0.7 mm. One fragment (0.3 mm diameter) of dense brown cryptocrystalline material is present. It is similar to the brown vein material in Stannern

but might be comparable to the basaltic "glass" in Nuevo Laredo. In general the groundmass material has mineralogy similar to that of the lithic fragments.

Although finer-grained, the lithic fragments of Bholghati resemble those of Sioux County and suggest a gabbroic rather than a basaltic affinity. This similarity is suggested also by the presence of well defined exsolution lamellae and a great deal of inversion of pigeonite. Unfortunately, compositional data for Bholghati is poor; no 2V measurements could be made because the thin section obtained from the British Museum was too large to be studied with the universal stage. Beside the magmatic textures, brecciation is the only other conspicuous textural feature.

Jonzac

This meteorite has been described previously by Wahl⁽⁵⁾, Michel⁽⁶⁾, and LaCroix⁽⁸⁾. A single, unsatisfactory thin section was available for examination. There are no well preserved lithic fragments as a result of fracturing during preparation of the thin section. The texture appears to be similar to that of Juvinas, consisting primarily of pigeonite and plagioclase laths up to 2.5 mm long. Metamorphism of brown pigeonite to fine-grained yellow or colorless pigeonite is abundant.

Moore County

Moore County has been described in detail by Henderson and Davis⁽¹⁰⁾ and Hess and Henderson⁽¹¹⁾. It is one of three unbrecciated meteorites studied in this work.

Plate 30b shows an unpolished cut surface. The texture is medium-grained equigranular. Some portions of the meteorite have visibly greater concentrations of plagioclase than others. A few small veins of

colorless glassy (?) material cut across one corner.

Plate 31a shows a photomicrograph of a typical area in thin section. Plagioclase and pyroxene are both tabular rather than lathlike. The plagioclase shows little compositional variation. The pyroxene is predominantly pigeonite, with exsolution lamellae of diopsidic pyroxene parallel (001). Portions of the pigeonite, bounded by (001) lamellae and (110) cleavages have inverted to hypersthene. The hypersthene has subsequently exsolved calcic pyroxene parallel to (100). A single augite grain was observed in thin section Plate 31b. Tridymite, containing needle-like inclusions which may be apatite (Hess and Henderson⁽¹¹⁾), is present interstitially. Troilite and ilmenite are concentrated along pyroxene and plagioclase grain boundaries. Metallic iron is the principal phase in the portions of the meteorite separable with a hand magnet.

The texture of Moore County is gabbroic rather than basaltic and Hess and Henderson were able to show that there is a planar orientation of plagioclase and pyroxene grains. This was interpreted by them to indicate that crystal settling played a part in the magmatic history of the meteorite.

Fragments with textures similar to Moore County are not common in the brecciated meteorites. However, crystal fragments in many of the brecciated meteorites such as Petersburg and Pavlovka could well represent fragments of a Moore County type. It is not surprising that few Moore County fragments are found, because Moore County is quite friable. Hess and Henderson could only make a suitable thin section after impregnating the meteorite with a binding material.

Serra de Mage

The petrography of this meteorite has not been described previously

in any detail. The external features of the meteorite are similar to those of Moore County. The meteorite has an equigranular texture of medium-to coarse-grained white plagioclase and brown pyroxene. On the scale of the thin section there is inhomogeneity of distribution of plagioclase and pyroxene; Plate 32a shows what may be a layer of plagioclase grains. The meteorite has the coarsest texture observed in any of the basaltic achondrites. The one fragment studied is unbrecciated, but whether the entire meteorite was brecciated or unbrecciated is uncertain.

The coarseness of grain size allows the study of the fusion crust developed over individual plagioclase and pyroxene grains. Externally, the fusion crust is greenish black; in thin section it is pale green over both pyroxene and plagioclase; there are few spherical cavities in the fusion crust. Over both pyroxene and plagioclase, the fused material grades abruptly into unaltered material; whereas there is no observable effect on the crystalline plagioclase, there is a dark zone within the pyroxene, similar to the darkening observed in the brecciated meteorites (Plates 33a and 33b).

The pyroxene of Serra de Mage is primarily hypersthene (Plate 34a). The hypersthene contains abundant lamellae of monoclinic pyroxene of moderate birefringence. The coarser lamellae make a large angle with the orthopyroxene (100) planes and probably have resulted from the exsolution of augite from original pigeonite. Thin lamellae parallel to the orthopyroxene (100) planes also are present and are interpreted as exsolution features formed from the hypersthene after the original pigeonite inverted.

The plagioclase composition of Serra de Mage is very uniform and there is no sign of more sodic interstitial plagioclase. Tridymite grains

are rare. A few isolated grains of metallic iron apparently are due to magmatic crystallization, as are some coarse troilite grains (Plates 31b and 34c).

Troilite also occurs along fractures in pyroxene, where it is associated with a small amount of clinopyroxene, and, in one place, a mineral of low birefringence which may be quartz (Plate 32b). The meteorite is pervasively fractured. Some of the fractures contain brown amorphous material and reddish staining which may be products of terrestrial alteration.

A modal analysis of the meteorite gave the following mineral proportions:

	<u>Wt. %</u>
Hypersthene	38%
Augite (as exsolution lamellae)	2%
Plagioclase	56%
Troilite	2%
Others	2%

The small number of grains present in a thin section of a coarse-grained material limits the accuracy of the modal analysis, but it is clear that the plagioclase content of Serra de Mage is much greater than that of other basaltic achondrites with the possible exception of the plagioclase-rich portions of Moore County.

The orientations of fifteen plagioclase grains were determined on the universal stage. Figure 1 is a stereographic projection of the positions of the pole of (100) with respect to the pole of the thin section. There is a tendency for the poles of (100) to group near the pole of the thin section. The petrofabric evidence suggests a preferred orientation

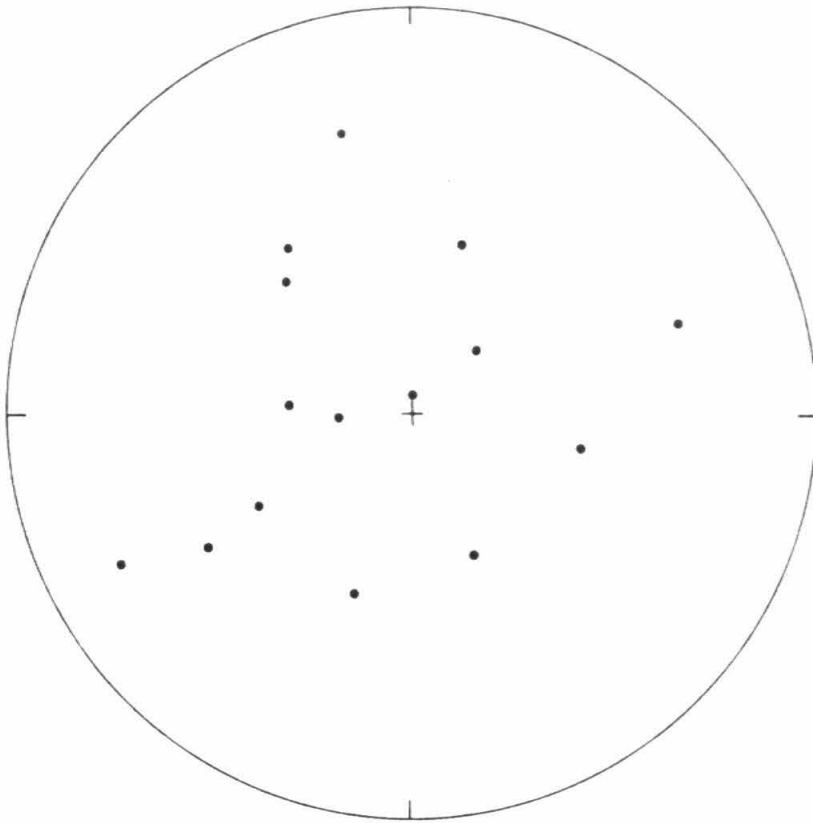


Figure 1. Poles of 100 plotted with respect to the pole of the thin section for 15 plagioclase grains of Serra de Mage.

in support of the modal evidence that plagioclase has been enriched in this meteorite by crystal settling.

Shergotty

Shergotty has been described previously by Tschermak⁽¹⁶⁾ and Michel⁽⁶⁾. The meteorite has a deep black fusion crust which is opaque in thin section and can not be subdivided into distinct zones. On a broken surface the meteorite is dull greenish gray (Plate 35a). White maskelynite laths and green pyroxene prisms show a very well defined planar fabric. The oriented fabric, which can be observed in every sample available for this study, has not been reported in previous investigations.

Plates 35b, 36a and 36b show photomicrographs of the meteorite. Pyroxene laths are up to 10 mm long, but rarely more than 1 mm wide. Isotropic maskelynite grains, with the form of plagioclase laths, are up to 3 mm long. Interstitial to the maskelynite and pyroxene are small amounts of brown or colorless, nearly amorphous material. This material is not amorphous, but appears strongly strained when examined in immersion oils. Whitlockite, a phosphate, occurs as stubby hexagonal prisms. Magnetite is the principal opaque mineral along with small quantities of troilite. Plates 36a and 36b show the distribution of minor phases in a portion of one thin section.

The pyroxene consists of pigeonite and augite, both with variable optic angles. Both occur in the same pyroxene lath, commonly with augite forming a rim around pigeonite; there may be more augite than pigeonite. Plate 37 shows a pyroxene lath displaying a zonal arrangement of pigeonite and augite. The pyroxene also shows zonal color variations from colorless at the core to light yellow on the rims, similar to the variations described for the pyroxene of Pasamonte but not as extreme. Con-

centrations of opaque grains occur in the yellow rims.

A modal analysis of Shergotty gives the following proportions:

	<u>Wt. %</u>
Pyroxene	76%
Plagioclase (maskelynite)	21%
Whitlockite	1%
Amorphous material	1%
Opagues	1%

Shergotty is distinct from other basaltic achondrites in a number of features: (1) magnetite and whitlockite are present, (2) the plagioclase is An₅₀ rather than An₉₀, (3) primary augite is nearly as abundant as pigeonite, and (4) the pyroxene content of Shergotty is greater.

Besides the metamorphic effect which has transformed plagioclase into the amorphous maskelynite, other presumably related effects are present. Some pyroxene grains show regions which are strongly strained and do not go to extinction between crossed nicols in any position of rotation of the microscope stage. Some of the phosphate shows patchy or undulatory extinction. The amorphous material in the interstices may owe its origin to the same metamorphism

The primary texture of Shergotty is apparently a magmatic texture; the origin of the planar orientation is not certain, but it does not appear to be a deformational structure and may be a result of crystal settling in the magma. The metamorphism, primarily of plagioclase to maskelynite, is believed ascribable to transformation in strong shock (see later discussion).

Petersburg

No previous complete petrographic description of this meteorite has been published. Smith⁽¹⁷⁾ and Wahl⁽¹⁸⁾ have given partial descriptions.

Petersburg is brecciated, with gray and black lithic fragments and colorless, yellow brown or black crystal fragments set in a fine-grained gray matrix (Plate 38a). Small fragments of metallic iron are abundant and a number of rims of metal around silicate grains appear unique to this meteorite (Plate 38b). The abundance of metal causes exposed surfaces to have a slight rusty appearance. The aggregate is dense and not friable, in contrast to all other brecciated meteorites studied here.

Lithic fragments show two principal types of textures. Plate 39a shows a portion of one thin section (CIT - Pet. 1) in which the lithic fragments have, for the most part, fine-grained sub-ophitic textures such as those of Nuevo Laredo, Stannern and Juvinas. The grain sizes in these lithic fragments vary from 0.1 mm to about 1 mm. The pyroxene of these fragments is primarily brown pigeonite, which in some cases has partially inverted to hypersthene. These fragments probably could not be distinguished from fragments of similar grain size in Stannern.

Plate 39b shows a portion of a thin section (BM- 32053) which contains fragments which have fine-grained equigranular textures, which will be referred to as granoblastic textures. These fragments are composed of colorless to yellow pigeonite, which in some cases has conspicuous (001) exsolution lamellae; clear, inclusion-free plagioclase, which is rarely twinned and has no apparent development of cleavage and small interstitial grains of tridymite. Plates 40a and 40b show different granoblastic fragments. The fragment shown in Plate 43a has one of the most equant textures observed in granoblastic fragments. The fragment shown in Plate 40b has not developed a texture as equant, but there are few vestiges of any original magmatic texture. These granoblastic textures are considered to represent recrystallization textures, but the mechanism of the

recrystallization is not known. The textures are suggestive of high rank thermal metamorphism as observed in terrestrial granulites. It is conceivable that these textures represent contact phenomena between freshly solidified magmas and new intrusions, or they could represent the result of a more pervasive type of metamorphism. The granoblastic textures are an important textural feature of Petersburg and other basaltic achondrites, but there are no clearly transitional textures between the magmatic and granoblastic textures, which makes difficult an interpretation of their relationship.

A feature which has been observed in several granoblastic fragments are sets of fractures which are more pronounced in the plagioclase. Plates 41a and 41b show two different lithic fragments with conspicuous fracture patterns. The fractures occur in sub parallel sets that are more or less continuous over the fragments and are unrelated to the orientation of the mineral grains. These fracture patterns are qualitatively similar to sets of fractures reported by Chao⁽¹⁹⁾ in materials from the Ries Basin which have apparently undergone strong shock, during the meteorite impact.

Plates 42a and 42b show a noteworthy fragment which has had a complicated history. In plane light, the fragment shows some aspects which resemble diabasic textures, especially two lathlike plagioclase forms at the left side of the picture. Fractures in the plagioclase laths tend to be perpendicular to the length, but are related to a sub-parallel fracture pattern that covers a large part of the fragment. Boundaries between laths and other irregular plagioclase areas are not clearly defined. The pyroxene, which is primarily pigeonite, is granular, but seems to be confined to clusters. In crossed nicols, the plagioclase has a non-uniform low

birefringence caused by its fine-grained feathery aspect. This textural feature is interpreted as a metamorphic effect that has more strongly affected plagioclase than pyroxene, because the present pyroxene grain size is similar to the grain size of the lathlike forms and dissimilar to the present size of the plagioclase crystallites. The presence of original lath forms suggests that the metamorphism has occurred without large amounts of mechanical deformation. Although the starting materials were somewhat different and the final state of the plagioclase is different, this fragment has some similarities in its metamorphism with the metamorphism observed in Shergotty. In both cases the plagioclase has gone to a finer-grained aggregate whereas the pyroxenes have not been greatly affected. In both cases there is no indication of strong mechanical deformation accompanying the metamorphism. It seems probable that in both cases the metamorphism has been essentially isochemical and, indeed, confined to the plagioclase. These textures are interpreted due to shock loading of the original material. The occurrence of a fragment which has undergone shock metamorphism in a breccia which contains fragments that have not undergone as extreme metamorphism indicates that the shock event preceded the final accumulation of the breccia. Since the fragment does not have a true magmatic texture, it is also probable that before the shock metamorphism, it previously had undergone a magmatic and a recrystallization event. This is one of the most complex histories observed in a single fragment in a basaltic achondrite.

Other clasts present in the breccia include dense cryptocrystalline fragments which may possibly represent either basaltic "glass" or material similar to that of the brown veins of Stannern. Many fragments are composed primarily of aphanitic material which contain a few small grains

of plagioclase or pyroxene (Plate 43a). One fragment is composed of equant medium-grained crystals of pigeonite with only a few plagioclase tablets (Plate 43b). The pyroxenes are approximately 1 mm in diameter and have prominent exsolution lamellae. This texture may represent an accumulate of pigeonite during a magmatic episode. No compositional data was obtainable on the fragment.

There are plentiful crystal fragments in the breccia, which include angular fragments of strongly strained hypersthene ($Fe/Fe+Mg = 0.2 - 0.5$), broken and strained fragments of pigeonite ($Fe/Fe+Mg = 0.6$, approximately), plagioclase, and some small fragments with felty extinction similar to that in Plate 42b. The hypersthene, which occurs in grains up to 5 mm in diameter, rarely shows exsolution lamellae ascribable to original pigeonite. Some lamellae parallel (100) are present, but in one fragment the lamellae are concentrated in the most strongly strained portions of the grain (Plate 44a). Griggs, et al (1960) have reported the exsolution of clinopyroxene from orthopyroxene under conditions of strong non-hydrostatic stress. It is possible that strong deformation related to the brecciation of the meteorite has produced the exsolution effects. Another hypersthene fragment shows fractures at about 45° to (100) which may have been produced during the mechanical disruption of original rock material (Plate 44b).

The metal rims around some silicate grains, predominantly hypersthene, are unique to Petersburg. In thin section, oxidation of the metal has made it difficult to observe the relations of metal to the surrounding groundmass. The included grains have fragmental appearance, as shown in Plate 45a. It is probable that the rims developed around the orthopyroxene grains before the fragments were finally accumulated in the breccia.

An argument for this view is the fact that the metal fragments are easily separable from surrounding groundmass, but the included pyroxene is very difficult to free entirely from the metal by mechanical means (picking with a needle). The irregular distribution of metal in rims and in fragments and the tendency to rim only orthopyroxene grains are suggestive of a pre-accumulation origin for the rims. However, some metal apparently rims fragmental aggregates of plagioclase and pyroxene. It is possible that the metal was introduced between two fragmentation events.

The history of Petersburg is more complex than any of the meteorites yet described. The original mineralogy and many of the textures have formed during one or more magmatic episodes under a variety of chemical and physical conditions which allowed a great variety of mineral compositions and grain sizes to form. Many of the original textures have been recrystallized to granoblastic textures, but it is not possible to determine at what time this recrystallization occurred relative to the initial fragmentation of the material. There are few textures which suggest more than one fragmentation event for the meteorite, but it is not impossible that a number of fragmentation events have produced the brecciated material. There is abundant evidence that the mechanical effects accompanying fragmentation were extreme. The metamorphic effect shown in Plates 42a and 42b are interpreted as due to shock and probably accompanied a brecciation event, but it was not necessarily a brecciation event related to the final accumulation of the meteorite as we know it. Some recrystallization has occurred after the final accumulation of the breccia and Petersburg is the most coherent of the basaltic achondrites which has been studied in this work.

Bialystok

Externally, the meteorite has an appearance similar to Pasamonte. The groundmass is light gray and clasts consist of black aphanitic lithic(?) fragments, intergrowths of yellow pyroxene with plagioclase, or fragments with both yellow and black pyroxene with plagioclase. In the small sample studied, the largest fragment was about 5 mm in diameter. Many of the lithic fragments are partly rounded, but of irregular shape.

The two types of textures found in Petersburg are present in the lithic fragments. Fine-grained intergranular or sub-ophitic textures are abundant (Plate 46a) as well as granoblastic textures (Plate 46b). One clast, consisting of orthopyroxene and plagioclase fragments embedded in a rusty amorphous groundmass, resembles the outer portions of the metal rims in Petersburg (Plate 47a). Another fragment consists of black opaque material intergrown with a strained plagioclase grain (Plate 47b). Many individual crystal fragments are composed of relatively coarse plagioclase, colorless to yellow pigeonite, or hypersthene. There appears to be less hypersthene than in Petersburg. The textural evidence for the pre-aggregation history of Bialystok is similar to that of Petersburg.

The groundmass of Bialystok has undergone some sintering after the final accumulation of the breccia. For instance, the region surrounding the granoblastic fragment shown in Plate 40a has many aspects shown by the portion of Sioux County shown in Plate 13b. Plagioclase in this area does not show pronounced undulatory extinction and contiguous plagioclase grains do not show obvious boundaries in plane light.

Pavlovka

Pavlovka has been described previously by Zavaritskii and Kvasha⁽¹³⁾.

A small piece is shown in Plate 48a . The groundmass is light gray and carries a variety of black, yellow and white lithic and crystal fragments; it is quite friable.

The thin section contains only a few small lithic fragments which have sub-ophitic plagioclase-pigeonite intergrowths. Most of the fragments are pyroxene or plagioclase crystal fragments; the pyroxene varies from colorless to deep brown, which is indicative of a large variability of pyroxene composition. A few fragments of olivine are present.

Plate 48b shows a fragment which has a texture similar to the portions of recrystallized breccia described in Sioux County (Plate 13b), that is, the texture has a fragmental appearance, but has been recrystallized. A complicated history of brecciation, recrystallization and re-brecciation is suggested by this fragment.

Another fragment consists of fragmental clinopyroxene and plagioclase in a black amorphous matrix (Plate 49a). One clinopyroxene grain in the fragment is a lath about 1.5 mm long and 0.2 mm wide, which resembles the pyroxene of Shergotty rather than the pyroxenes of the more common basaltic achondrites. The nature of the black amorphous material is not known, but the material is not composed of metallic iron, troilite, or a coarsely crystalline oxide phase. Metallic iron does occur in another fragment, where it encloses pyroxene and plagioclase fragments.

Many of the pyroxene fragments are strongly strained and plagioclase fragments commonly show undulatory extinction and deformed twin lamellae. One orthopyroxene fragment (Plates 49a and 49b) which is uniform in plane light shows, in crossed nicols, arrangements of blebs of lower birefringence (but approximately the same index of refraction) along planes which make angles of about 45° with the prismatic cleavage. This may be

a texture analogous to the recrystallization of some of the plagioclase of Petersburg to feathery aggregates, as the recrystallization is, apparently, isochemical and has produced a finer texture from a coarser one. A similar texture has been observed in the Tatouhine meteorite, a hypersthene achondrite. Plate 50 shows a photomicrograph of Tatouhine in crossed nicols. Although there has been substantial recrystallization, an X-ray diffraction pattern of Tatouhine shows that only hypersthene is present. The qualitative comparison of metamorphic effects in a fragment from a basaltic achondrite and a hypersthene achondrite does not show, necessarily, a close relation between the two meteorite types, but suggests that the materials have undergone similar post-crystallization events. The mineralogy of Tatouhine, however, is an allowable derivative of the basaltic achondrites and the two types of meteorites may have related magmatic origins.

The brecciation of Pavlovka has removed most evidence of the magmatic history. The large size of some hypersthene fragments (Plate 51a) suggests gabbroic rather than basaltic affinities, but some fine-grained magmatic textures are present. The presence of a fragment of recrystallized breccia suggests a repeated brecciation history for this meteorite. In one portion of the thin section an area of brown amorphous groundmass grades into normal groundmass (Plate 49a); this is probably a post-accumulation effect.

Frankfort

The thin section contains only a few lithic fragments composed of a fine-grained intergranular aggregate of plagioclase laths and pyroxene. Most of the fragments are hypersthene with strongly undulatory extinction; they are as large as 5 mm in diameter. Smaller pyroxene grains show a

wide variation of color indicative of a wide variation of composition. The proportion of hypersthene to pigeonite is much greater than in Petersburg and there is a lower content of plagioclase than in most of the other basaltic achondrites.

Although one must infer that the minerals were formed originally in a magmatic episode, the brecciation event effectively has removed most textural evidence of the magmatic history. The large size of some hypersthene fragments and the abundance of hypersthene suggests that more gabbroic-type material than basaltic-type material has been mixed in the breccia.

Yurtuk

Only a external examination was made of the Yurtuk fragment shown in Plate 51b. The meteorite is similar, in external appearance, to Pasamonte, Petersburg, Bialystok and Pavlovka. Rounded to sub-rounded lithic fragments from less than 0.5 mm to about 1 mm, consisting of brown and yellow pyroxene intergrown with plagioclase, are common. Grains less than 0.5 mm are, in general, monomineralic fragments of plagioclase or pyroxene. A black vein, similar in external appearance, to the veins of Stannern (cf. Plate 21b), traverses the fragment. The color variation of pyroxenes in the lithic and crystal fragments suggests that there is a wide variation of pyroxene composition.

Binda

Plate 52a shows an external view of a small portion of the meteorite. There is abundant gray groundmass which includes coarse-grained equigranular lithic fragments and angular crystal fragments. An accumulation of dense dark gray material occurs on one edge of the fragment and is visible on the cut surface.

The meteorite is composed of medium to coarse tabular grains of plagioclase and hypersthene, both of which show evidence of extreme mechanical deformation. The dark gray cryptocrystalline areas, which appear to be dark fragments on the cut surface shown in Plate 52a, are shown in a photomicrograph in Plate 53a. Their relation to other grains is not unambiguous. They completely surround some crystal fragments and apparently extend apophyses into crystalline material at the upper edge of Plate 53a. There are gradations of grain size and color from black in the densest areas to brown or gray at some boundaries with the groundmass. These features suggest that the dark areas have formed after the accumulation of the breccia. Other portions of the dark material, such as the one at the lower right hand corner of the picture seem to be fragments. A possible explanation for the seemingly ambiguous textural relations is that the black material has been redistributed in mechanical events following its original formation or accumulation in the breccia. It is difficult to say from the observed relations whether the material was originally present as fragments or whether it formed in place as material similar to the veins of Stannern.

In crossed nicols, the dark areas show numerous points of birefringent material and actually appear to be less dense than in plane light (Plate 53b). The picture under crossed nicols amplifies the effects of the very strong mechanical disruption which the meteorite has undergone. Both pyroxene and plagioclase show pronounced undulatory extinction. At the lower left corner of Plate 53a a contact between plagioclase and pyroxene is marked by a zone of granulation which is shown in Plate 54a. The zone of granulation is darker than the normal pyroxene or plagioclase and contains some material that is isotropic in crossed nicols. More

evidence of extreme mechanical deformation is shown in Plate 54b, which shows deformed exsolution (100) lamellae in orthopyroxene.

The original magmatic textures of Binda apparently had gabbroic affinities. The lithic fragment shown on Plate 52a had an average grain size of at least 3 mm. On the cut surface, the pyroxene has a fairly uniform color, both within the lithic fragment and in the matrix, which suggests that there is no large variation of pyroxene composition. From inspection of the cut surface, it is estimated that plagioclase makes up between ten and twenty percent of the meteorite by volume. These observations must be tempered by the fact that the size of the sample is only a few times that of the largest lithic fragment. It is possible that this texture could have developed by very strong fragmentation of a geometrically limited portion of original material and the breccia is more similar to a terrestrial tectonic breccia than an accumulation breccia.

Kapoeta

Photomicrographs of Kapoeta are shown in Plates 55a to 58b. The meteorite consists of, for the most part, broken fragments of pyroxene which show a wide variety of colors, and include both orthopyroxene and clinopyroxene. Some of the clinopyroxene grains show (001) exsolution lamellae.

Plate 55a shows a small lithic fragment that consists of a plagioclase lath intergrown with brown pigeonite in a texture similar to that of Juvinas or Stannern. This was the only diabasic lithic fragment observed. Plate 55b shows a "granoblastic" fragment which resembles the Petersburg fragment shown in Plate 40b. Plate 56a shows a fragment which resembles the recrystallized groundmass textures described for Sioux County (Plate 13b) and Pavlovka (Plate 48b). Plate 56b shows a fragment similar

to one described in Petersburg (Plate 43a). It consists of a micro-crystalline groundmass that encloses a few angular grains of pyroxene and plagioclase. This textural type are of uncertain origin.

An aspect of Kapoeta that has proved of interest recently with respect to the meteorite's content of "primordial" rare gases is a distinction between the color of various portions of the matrix. The distinction is primarily one of grain size, as shown by Plates 57a to 58b which compare fields in reflected and transmitted light. The dark portions correspond to very fine-grained matrix, the lighter portions correspond to more coarsely crystalline material. A pervasive sub-parallel fracture pattern is most apparent in the darker more finely crushed portions and suggests that the darker portions represent a mylonite-like material. It is clear that the light-dark structure has been developed after the initial brecciation and accumulation event which mixed fragments of the various rock types observed in the thin sections.

"Primordial" rare gases are trapped in the darker portions. It is possible that a shock event has produced the "light-dark" structure and has trapped the rare gases. Such a shock metamorphic process has been proposed by Fredricksson and Keil⁽²⁰⁾.

The magmatic history of Kapoeta has been obscured by the recrystallization and mechanical events which are more clearly observed. The mineralogy is apparently similar to that of Pavlovka or Petersburg, and probably had similar magmatic origins. Many of the lithic fragments have textures which suggest recrystallization of original magmatic textures or of groundmass. The post-accumulation mechanical history has been extreme and may well be due to metamorphism under strong shock conditions.

Estherville

Estherville is a mesosiderite, but Prior⁽⁴⁾ noted that the silicate phase of mesosiderites had a composition similar to the basaltic achondrites. Merrill⁽²¹⁾ described Estherville and concluded that it was a metamorphosed fragmental aggregate. In this work a small sample of the silicate material was studied.

The texture observed in thin section is not homogeneous. It is inequigranular and large grains appear to be angular and perhaps fragmental (Plate 59a). The texture is in some respects similar to the recrystallized breccia textures of Sioux County and Pavlovka (cf. Plate 13b; Plate 48b). The minerals identified in this section include olivine, hypersthene, plagioclase, tridymite, whitlockite, metallic iron and troilite.

An aggregate of olivine grains shown in Plate 59b has a number of larger uniform grains with irregular areas of finer-grained material which have an aspect similar to the recrystallization textures of Juvinas (cf. Plate 17a). The entire olivine aggregate has a rim marked, on the inside, by a discontinuous zone of metallic iron grains and, on the outside, by a narrow zone of hypersthene. The rim is probably a reaction product of the olivine, which is clearly out of equilibrium with the tridymite that occurs abundantly in the section.

The orthopyroxene is variable in composition from about $Fe/Fe+Mg = 0.15$ to 0.30 . Many of the larger grains have concentrations of opaque and nonopaque inclusions near, but not at, the grain boundaries (Plate 60a). Outside the zone of inclusions there is, commonly, an inclusion-free area in optical continuity with the rest of the grain. It is not known whether the composition of the rim orthopyroxene is the same as that of the core.

The orthopyroxene of finer grains is filled with inclusions and is generally more iron-rich.

Plagioclase occurs, in part, as large plates which have irregular outlines and in which the plagioclase commonly shows pericline and carlsbad twinning. In some portions, plagioclase also occurs as narrow laths showing, predominantly, albite twinning.

Tridymite occurs as clear irregular grains up to 0.5 mm in diameter with no special textural features. The phosphate has low birefringence and small negative 2V; it may be concentrated in areas richest in metal.

The metal phase of the mesosiderites, according to Prior⁽¹⁾, shows intrusive relations to the silicate portions. The metal and troilite within this fragment of silicate material is discontinuous and clearly has not been injected into the silicates. The evidence observed here is consistent with the view of Merrill who concluded that a fragmental aggregate had been metamorphosed. The reaction relations observed here represent an attempt by the silicates to equilibrate during the metamorphism.

Without further study it is not really possible to say much about the history of the Estherville mesosiderite. The texture resembles a recrystallized fragmental texture of the type which might result from static metamorphism of a meteorite such as Petersburg or Pavlovka. The compositional range of the silicates is somewhat limited and the most important point to be brought out here is that the mineralogy is consistent with the hypothesis that the basaltic achondrites and the mesosiderites have had similar magmatic histories and may be, in fact, directly related.

Crab Orchard

Crab Orchard is a mesosiderite reported by Mason⁽¹⁾ to contain pigeonite. A preliminary study of the meteorite shows it to have many fea-

tures in common with Estherville. The pyroxenes have a variety of compositions and include both pigeonite and orthopyroxene, which generally have distinct reaction rims. A small amount of olivine is also present along with plagioclase. The metallic iron is irregularly distributed and is not entirely continuous, which suggests that it was originally fragmental and, along with the silicates, has undergone thermal metamorphism. The histories of the mesosiderites are clearly quite complex, since magmatic, fragmentation and recrystallization processes are required. It will be of extreme importance to learn whether the metal now present in the mesosiderites is directly related to the basaltic material or has been mixed in the breccia from a separate source.

Discussion

Introduction

A sequence of events can be traced through the textural features of the basaltic achondrites. The initial event in every case was a magmatic episode, but magmatic crystallization took place in a variety of cooling environments. Metamorphism possibly related to the magmatic episode is a conspicuous feature in a few meteorites, but is a minor feature in most. Most of the achondrites are brecciated, and a few recrystallization features may be related to the brecciation event. Post-accumulation recrystallization has occurred in some meteorites and most have undergone enough compaction to allow them to exist as small coherent bodies. A few meteorites show post-accumulation veining. This portion of the paper discusses some of the implications of the textural observations.

Subclassification

In the Rose-Tschermak-Brezina system (Brezina⁽²²⁾), the basaltic achondrites were subdivided into eucrites (=augite-anorthite achondrites), howardites (hypersthene-olivine-augite-anorthite achondrites), and shergottites (augite-maskelynite achondrites). It was shown by Wahl⁽⁵⁾ that the principal clinopyroxene of the meteorites is pigeonite, rather than augite. Mason⁽¹⁾, who has included the shergottites with the eucrites, has proposed that the subdivisions eucrites (=pigeonite-anorthite achondrites) and howardites (=hypersthene-anorthite achondrites) be retained. The classification is basically sound, but is complicated due to (1) the complete inversion or nearly complete inversion of pigeonite to hypersthene in some meteorites, and (2) the occurrence of pigeonite in most of the howardites.

Brown⁽²³⁾ and Mason⁽¹⁾ have pointed out that the chemical compositions of the basaltic achondrites fall into two principal groups which closely correspond to the eucrite-howardite mineralogical classification; the howardites have low Fe/Fe+Mg and low CaO compared to the eucrites.

The description of Petersburg given above suggests that the chemical classification has a fault. Petersburg is a brecciated meteorite which has a wide range of pyroxene compositions from magnesian hypersthene to iron-rich pigeonite. The variation is continuous; it is not a case of mixing pigeonite of a single composition with hypersthene of a single composition. The meteorite has a very inhomogeneous distribution of crystal and lithic fragments and it is apparent that a sample could be taken in which there might be a high proportion of magnesian hypersthene, which would put the meteorite in the howardite class, although the bulk chemical composition puts it in the eucrite class of Mason. Most of the howardites in Mason's classification also contain a wide range of pyroxene compositions, but have more of the magnesian hypersthene and less iron-rich pigeonite in contrast to Petersburg, which apparently has a higher concentration of the iron-rich pyroxenes. The difference between Petersburg and the howardites of Mason's classification is the degree of mixing which has been accomplished following the brecciation and during accumulation of the fragmental debris of which the meteorites are comprised. If the chemical subdivisions can be crossed because of superimposed mechanical mixing effects, it is more significant if a purely textural classification, which describes the degree of mixing more precisely, is used.

Wahl⁽¹⁸⁾ divided the basaltic achondrites into monomict (limited compositional variability) and polymict (wide compositional variability)

brecciated meteorites. If the monomict brecciated meteorites are called eucrites and the polymict brecciated meteorites are called howardites, the textural classification is very similar in its groupings to the mineralogical and chemical classifications, but has the advantage of not having to place a chemically inhomogeneous meteorite in a chemical or mineralogical classification.

The description of the Pasamonte meteorite given above points out a difficulty in classifying a meteorite according to Wahl's classification. Whereas the overall composition of the lithic fragments is fairly uniform, there is a good deal of compositional zoning of the pyroxene, which leads to a variation of composition in the crystal fragments of the breccia. To circumvent this difficulty, the following classification of the eucrite-howardite group is suggested:

Eucrites: Monomict breccias, in which the lithic fragments are generally similar in bulk composition and the mineral composition in the entire meteorite shows no greater variation than the internal variation shown within lithic fragments.

Howardites: Polymict breccias, in which the lithic fragments show variations of bulk composition, in which the crystal fragments differ in composition from the minerals found in the lithic fragments, or in meteorites that contain no lithic fragments, there is a wide variation in the composition of crystal fragments.

All unbrecciated basaltic achondrites of this type are called eucrites. Hence, eucrite fragments occur in most, if not all, howardites. The following table gives the classifications for the meteorites studied in this work.

Classifications for Basaltic Achondrites

Studied in This Work

<u>Unbrecciated Eucrites</u>	<u>Brecciated Eucrites</u>	<u>Howardites</u>
------------------------------	----------------------------	-------------------

Moore County	Nuevo Laredo	Petersburg
Serra de Mage	Juvinas	Bialystok
Shergotty	Stannern	Pavlovka
	Sioux County	Kapoeta
	Bholghati	Frankfort
	Binda	Yurtuk
	Jonzac	

Mesosiderites

Crab Orchard

Estherville

Magmatic episode; rate of crystallization

On the basis of grain size and shape the basaltic achondrites show similarities to terrestrial basalts, diabases and gabbros. The basaltic portions have intergranular or sub-ophitic textures in which the grain size generally varies from about 0.01 mm to 1 mm and the plagioclase grains are elongated thin laths. Nuevo Laredo, Stannern and Pasamonte, as well as some lithic fragments of the howardites have textures similar to those found in terrestrial extrusive basalts and hypobysal diabase intrusions. Sub-ophitic and ophitic fragments from Juvinas have grain size from 1 mm to 4 mm and broader plagioclase laths, which are more suggestive of textures found in comparatively shallow diabase intrusions. The textures of Sioux County, Moore County, Serra de Mage, Bholghati and Binda are primarily equant textures from 0.7 mm to 6 mm in grain size and are more akin to terrestrial gabbroic rocks that have formed in deep seated environments.

Exsolution and inversion features of the pigeonite can be used as indicators of the rates of cooling during or following magmatic crystallization. According to Hess⁽²⁴⁾, the behavior of pigeonite under various types of cooling histories is as follows:

- (1) With rapid cooling, homogeneous pigeonite may persist as a metastable phase at lower temperatures.
- (2) With an intermediate cooling rate, pigeonite exsolves lamellae of augite along (001) planes.
- (3) With slow cooling, after exsolution of augite, pigeonite inverts to hypersthene, which may, in turn, exsolve augitic pyroxene parallel to (100).

Nuevo Laredo, Sioux County, Juvinas and Stannern have pigeonite with

Fe/Fe+Mg between 0.58 and 0.67. These meteorites show thin lamellae which probably represent exsolution of augite previous to partial inversion to hypersthene. For these meteorites there is a general tendency for the amount of inversion to be directly related to grain size. Nuevo Laredo has only a small amount of hypersthene, whereas the coarsest fragment in Sioux County consists almost entirely of hypersthene.

Moore County and Serra de Mage show broader clinopyroxene lamellae and a larger volume of exsolved clinopyroxene. Moore County pigeonite has partially inverted to hypersthene and Serra de Mage has completely inverted to hypersthene. This is consistent with the grain size relations, as Serra de Mage is more coarse-grained than Moore County. Completely inverted pigeonite is known from terrestrial intrusions such as the Skaergaard intrusion (Brown⁽²⁵⁾) and the Stillwater intrusion (Hess⁽²⁴⁾).

The rate of inversion of a simple iron-magnesium clinopyroxene is probably a function of the dissimilarity between orthopyroxene and clinopyroxene structures (Brown⁽²⁵⁾). Bowen and Schairer⁽²⁶⁾ found that the transformation was more sluggish in the intermediate compositions, for which the most structural dissimilarity occurs, than for the iron-rich or magnesium-rich clinopyroxenes.

However, for the Pasamonte pigeonite, inversion controlled simply by the iron-content of the pyroxene can not be called upon, for neither the magnesium-rich cores or the iron-rich rims have partially inverted to hypersthene although the grain size of some of the pigeonite is coarser than that of Stannern or Nuevo Laredo. It is possible that the calcium content, which must be reduced by exsolution before inversion can occur, plays a part in the inversion of pigeonite to hypersthene.

With these cautions in mind, it can be suggested that the inversion

properties shown by the pigeonite of the basaltic achondrites are consistent with the textural evidence in indicating that the different meteorites formed under a variety of cooling conditions. In general, for pyroxenes of similar composition, there is a tendency for the most extensive inversion to occur in the more coarse-grained pigeonite.

Crystal settling

Planar orientation of plagioclase and pyroxene in Moore County and Serra de Mage and the great enrichment of plagioclase in Serra de Mage indicate that crystal settling has occurred during the magmatic history of the basaltic achondrites. The preferred orientation shown by Shergotty may be related to crystal settling.

The occurrence of crystal settling is one of the few features of the achondrites which can be used to limit the size of the parent body of the meteorites. The accumulation of crystals is a function of the rate at which crystals settle and of the rate of crystallization of the magma. In a simple, non-convecting magma, the rate of settling is a function of physical and thermal constants for the magma and crystals and the size of the gravitational field. Limits on the rate of crystallization can not be set accurately, but the grain size of Moore County and Serra de Mage are similar to grain sizes found in terrestrial layered gabbroic intrusions, for which cooling rates can be estimated.

The problem is not completely specified for the meteorites, because the distance through which crystals settle as well as their rate of settling is important. One can make the assumption that the crystals which accumulate on the floor of a magma chamber have settled from a certain thickness of overlying magma, say ten meters, but this assumption can not be tested. However, it may be a limiting assumption.

Accumulation of olivine from 900 feet of overlying magma has occurred in the olivine layer of the Palisade sill (Walker⁽²⁷⁾) and it is possible that a fairly large thickness of magma must be depleted of its crystals in order to form an accumulate.

The rate of crystallization of thick sills has been investigated from the point of view of heat flow calculations by Jaeger⁽²⁸⁾. For diabase sills greater than about 200 meters thick, much of the sill is found to crystallize at rates of from one centimeter to three centimeters per year. If crystals have accumulated from a ten meter layer of magma, some of the crystals must have settled at rates of from 3 to 10 meters per year. If plagioclase crystals 1 mm in radius (assuming the grains to be spherical), with specific gravity of 2.7, settle in a magma of specific gravity 2.65 with a viscosity of 10^{11} poises, are to attain terminal settling velocities of 3 meters per year, a simple Stokes' Law calculation indicates that the size of the gravitational field must be on the order of the earth's gravity. If the viscosity of the magma is a factor of 100 lower, as is quite possible for an iron-rich basaltic magma, the size of the gravitational field would be 100 times smaller than that of the earth. It is clear that this calculation is not subject to exact determination for a number of reasons. The calculations seem to show that the process of crystal settling should not be expected in a parent body smaller than 1/100 earth radius, and would be more probable, the larger the size of the parent body. Unfortunately, within the limits of the calculation, most bodies which might be suggested as the parent of the basaltic achondrites would fit. The most important conclusion suggested by the observation that crystals have accumulated in some basaltic achondrites is that a mechanism is available for the magmatic differentiation deduced from the chemical and mineralogical evidence

presented in succeeding chapters.

Late Magmatic Episodes

The details of the magmatic episode (or episodes) of the basaltic achondrites are discussed in the chapters on Chemical Composition, Mineralogy and Petrologic Trends. The chemical changes in late magmatic or deuteric episodes and in post-magmatic metamorphism are not of sufficient magnitude to be reflected in bulk chemical composition and are best summarized from the petrographic evidence.

In the interstices of many of the magmatic textures there are concentrations of opaque minerals, in which ilmenite and troilite predominate. In some interstices, corroded pyroxene is associated with troilite, ilmenite and quartz. A reaction relation with pyroxene combining with sulfur to form troilite and free silica (magnesium and calcium probably recombine as orthorhombic or monoclinic pyroxenes) is the simplest one that can be envisioned. It may be that the ilmenite is also released from solid solution in the pyroxene during the reaction.

Especially in Juvinas fracturing of pyroxene grains has been followed by crystallization of troilite along the fractures. In the vicinity of the fractures, the pyroxene is somewhat bleached and some reaction may have occurred. In Juvinas, a buildup of sulfide vapors in the late stages may have been responsible for the formation of miarolitic cavities. Sulfide reaction may have been responsible for some of the conspicuous recrystallization textures in Juvinas, where colorless or yellow fine-grained pigeonite has replaced coarser brown pigeonite.

More limited in extent are reactions which apparently involve the reduction of iron-rich pyroxenes to metal. Unfortunately, the time sequence of formation of metallic iron in these textures can not be definite-

ly established. The metal may have formed in a metamorphism following the brecciation event. In one lithic fragment of Juvinas, a small grain of metallic iron occurs along with sulfide and ilmenite in an area rich in corroded pyroxene and quartz (Plates 19a and 19b).

Brecciation and Possible Shock Effects

Most of the basaltic achondrites have been brecciated. There are, unfortunately, a few clear cut lines of evidence which can be used to determine the process by which the brecciation occurred, but two principal possibilities exist. The basaltic achondrite breccias may represent volcanic breccias (or volcanic-sedimentary tuff-breccias) or they may represent tectonic breccias, among which impact breccias may be included.

Many of the early investigators concluded that the basaltic achondrites are tuff-breccias, principally on the basis of the obvious association of volcanic textures in the rock fragments of the breccias. It is not possible to completely discount the possibility that some of the basaltic achondrites, especially the howardites, have their origin in explosive volcanic events. There are some features of the achondrites, however, that may be difficult to reconcile with a volcanic brecciation process.

For explosive volcanism to occur it is probable that a gas phase with a large vapor pressure must build up. There is no petrographic evidence for the presence of a substantial vapor phase during the magmatic history of the meteorites. The only volatile element that appears in the mineralogy is sulfur in troilite. If explosive volcanism is to be called upon, a volatile component such as N, CO, or CO₂ or perhaps noble gases must be assumed. Large contents of noble gases occur in the dark

portions of the Kapoeta meteorite (Zahringer⁽²⁹⁾), but whether concentration of noble gases could reach levels high enough to produce explosive volcanism is not known.

There is an aspect of the monomict brecciated eucrites which seems to be difficult to reconcile with a tuffaceous origin. Although there is some variability of textures of lithic fragments within the monomict breccias, the variation of textures between meteorites is much greater. It is possible to distinguish with little difficulty Sioux County, Juvinas, Stannern and Nuevo Laredo on the basis of the textures of the lithic fragments. All of these meteorites are apparently monomict, with little mixing of different mineral compositions and all have very similar bulk compositions. It appears that the principal distinguishing factors are the textures which indicate a variety of cooling conditions during the magmatic episode (or episodes). The fact that these meteorites are monomict, similar, but distinct, suggests that they represent localized fragmentation of the original rocks. This seems inconsistent with a tuffaceous accumulation history, although the possibility that the meteorites represent materials brecciated in place along volcanic pipes can not be eliminated. The polymict breccias might well be tuffaceous in origin.

Impact brecciation may produce textures similar to those found in volcanic breccias. A cratering event may give products which have some features in common with terrestrial tectonic or fault breccias (material brecciated in place) or with tuffaceous breccias (material ejected from the crater). Plate 61 shows an example of breccia from the Brent Crater, Ontario, Canada, which is probably of meteorite impact origin (Millman, et al⁽³⁰⁾). The sample comes from a core through the crater floor, but

the breccia may represent material which fell back into the crater. This particular breccia type occurs only in a limited portion of the core, so it can not be said that it is a typical meteorite impact breccia. The general features of this breccia can be compared with the brecciated basaltic achondrites, and especially the thin section of Bholghati (Plate 30a). Although the mineralogy is different (the Brent breccia has been formed from a granitic gneiss), both breccias have been formed from crystalline rather than sedimentary material. There is a similar range of fragment sizes and shapes in both breccias and there seem to be similar types of strained crystal fragments in each breccia. This comparison shows that it is permissible for some of the brecciation of the basaltic achondrites to be of impact origin.

It is probably the case that fragment size and form distribution will not provide uniquely determinative criteria for impact breccias or volcanic breccias. There are a number of textures in the basaltic achondrites which seem to be consistent with metamorphism by strong shock and can be suggested to be of an impact origin.

The most probable example of a shock metamorphosed basaltic achondrite is Shergotty, an unbrecciated meteorite (See Plates 35a to 36b). In Shergotty, plagioclase has been transformed to an amorphous state while pyroxene has been only slightly affected and the original magmatic texture has been maintained. Although all of the structural aspects of Shergotty were not maintained, Milton and DeCarli⁽³¹⁾ have shown that shock loading (peak pressure of about 250 kilobars) can produce a similar texture in a terrestrial gabbro. Examples of a similar nature have been reported by Chao⁽³²⁾ from the Ries Basin, where feldspar and quartz have

been made amorphous, leaving biotite and other dark minerals essentially unaltered. There seems to be little doubt that the transformation observed in Shergotty was produced by shock metamorphism.

Although maskelynite, the amorphous plagioclase of Shergotty, has been reported in older descriptions of basaltic achondrites, no truly amorphous plagioclase has been observed in the other meteorites studied in this work. A number of the howardites contain plagioclase fragments which apparently are single crystal fragments when viewed in plane light, but show feathery extinction properties which give them an overall low birefringence in crossed nicols. The most striking example of feathery plagioclase is shown by a lithic fragment in Petersburg (Plates 42a and 42b) where the feathery plagioclase is intergrown with pyroxene and the plagioclase has some semblance of original crystal form. Similar textures have not been reported from terrestrial volcanic rocks and this is interpreted to be a Shergotty-like metamorphic texture. Because it is a fragment within a breccia that contains apparently unmetamorphosed fragments, it is clear that the metamorphism preceded final accumulation of the breccia. If the interpretation is correct, it would imply that some of the fragments in the Petersburg breccia underwent a shock event previous to accumulation of the breccia.

Neither the demonstration that some fragments in the brecciated basaltic achondrites probably have had a shock history nor the demonstrated similarity between the brecciated basaltic achondrites and meteorite impact breccias is proof that all of the brecciation is due to impact events. It is possible that some combination of impact events and volcanic events have produced the breccias. However, the simplest hypothesis that apparently can explain all of the mechanical features

observed in the basaltic achondrites is that the brecciation has been predominantly impact brecciation.

Post-Accumulation Effects and Possible Repeated Brecciation

In Sioux County, there are some portions of the matrix which apparently have undergone recrystallization (Plate 13b). Fragments of a similar type have been described in many of the howardites (Pavlovka, Plate 48a; Kapoeta, Plate 56a) where they occur with fragments that have original magmatic textures or various recrystallization textures. The appearance in the polymict breccias of recrystallized matrix material implies two generations of brecciation, separated by a recrystallization episode. More complicated combinations of brecciation and recrystallization might exist, but would be extremely difficult to recognize petrographically.

The mesosiderites show post-accumulation recrystallization, in which some mineralogical changes occurred. An environment for thermal metamorphism of fragmental material must have been accessible in order to form the mesosiderites as we now know them.

Stannern and Yurtuk have dark veins that have formed after accumulation of the breccias. These veins may be very finely granulated material along localized zones in the meteorites. There has been some displacement along many of the veins in Stannern, which suggest that the veins are related to some type of post-accumulation mechanical disruption episode. Fredricksson et al⁽³³⁾ have been able to produce dark veins in chondritic meteorites in shock loading experiments. A shock process may be involved in the formation of the veins of Stannern and Yurtuk.

In Kapoeta, strong mechanical disruption following accumulation of the breccia has produced light and dark portions. The dark portions are

the most highly pulverized. Fredricksson and Keil⁽²⁰⁾ believe that a shock process has produced the dark portions. If that is true, the shock process undergone by Kapoeta has been quite different than that undergone by Shergotty and the reason for the differences is not apparent at the present time.

Whether the veins of Stannern and Yurtuk and the dark portions of Kapoeta have been produced by shock processes is a matter for some further investigation. In any case, there is good evidence that mechanical processes were active after the final accumulation of the brecciated meteorites. It is possible that a process capable of removing a meteorite from its parent body and placing it in an orbit which intersects the earth's orbit should produce discernible effects in the meteorite. Some of the post-accumulation effects noted in the meteorites may be related to the final ejection event, but post-accumulation effects are minor in the basaltic achondrites. Considering some of the extreme mechanical effects observed in the brecciated basaltic achondrites and the shock effects shown by Shergotty, it seems probable that the final ejection took a lesser amount of mechanical energy than did the initial brecciation.

Liquids of basaltic composition represented by bulk meteorites

With the summary of magmatic and post-magmatic features of the basaltic achondrites, it is possible to comment about how closely the meteorites might represent the basaltic liquids from which they formed. This discussion is important to succeeding discussions of the compositional variations of the basaltic achondrites.

For the eucrites, which by definition do not have mixed chemical compositions, there is reason to believe that the meteorites that have

predominantly fine-grained non-porphyrific basaltic textures may truly represent the composition of the liquids from which they crystallized, minus any volatile phase that escaped. For the meteorites with gabbroic texture, which it is not always possible to predict whether they represent liquid compositions, it can be supposed that in the cases of Moore County and Serra de Mage, which show evidence of crystal accumulation, they do not. In other cases, as in the coarsest fragments in Sioux County, they may adequately represent silicate melts.

For the howardites, in which brecciation has mixed fragments with diverse chemical and textural histories, it is clear that the meteorites do not represent liquid compositions. Depending on the degree of mixing of diverse systems, however, it is possible that the howardites can approach compositions of liquids in the basaltic system.

III

CHEMICAL COMPOSITION OF THE BASALTIC ACHONDRITES
AND SOME OF THEIR CONSTITUENT MINERALS

Bulk Chemical Analyses

Chemical analyses of basaltic achondrites are given in Table 4. The sources of the data are (1) the literature compilation made by Urey and Craig⁽²⁾, (2) new total meteorite analytical data obtained during the course of this work, and (3) partial chemical analyses, particularly for alkalis, from Edwards⁽³³⁾ and from this work. For use in making some comparisons, CIPW norms have been calculated from the chemical analyses (Table 5). The method by which the norms are calculated is given by Washington⁽³⁴⁾ and yields a calculated mineralogical assemblage that closely resembles the mineralogy observed in the meteorites. In a few cases, norms have been recalculated using a combination of old and new analytical data. These norms are clearly of lesser reliability than those calculated from good analytical data.

In order to select the better older analyses for comparative purposes and to understand the expected accuracy of older analytical data, the following comparisons are made:

(1) Alkali values from both old and new analyses are compared with Na and K determinations of Edwards⁽³³⁾, Gast⁽³⁵⁾ and Geiss and Hess⁽³⁶⁾ in Table 6. The old analyses are found to be variable in reliability and tend to overestimate the alkali contents (especially K). The new analyses agree well with the independent determinations of alkalis.

(2) Table 7 gives data for new flame photometer analyses of seven plagioclase separates. The method used was that described by Brannock and Shapiro⁽³⁷⁾. Comparison with the normative

TABLE 4

CHEMICAL ANALYSES OF BASALTIC ACHONDRITES

1. Sioux County, composite
2. Sioux County, lithic fragment
3. Sioux County
4. Pasamonte
5. Pasamonte
6. Stannern
7. Stannern
8. Juvinas
9. Juvinas
10. Nuevo Laredo
11. Tchervony Koot
12. Peramiho
13. Bereba
14. Cachari
15. Jonzac
16. Macibini
17. Binda
18. Padvarminkai
19. Moore County
20. Serra de Mage
21. Shergotty
22. Shergotty
23. Luotolax
24. Yurtuk
25. Le Teilleul
26. Frankfort
27. Petersburg
28. Zmenj
29. Pavlovka
30. Mëssing

TABLE 4
CHEMICAL ANALYSES OF BASALTIC ACHONDRITES

	Brecciated Eucrites							
	<u>1*</u>	<u>2*</u>	<u>3</u>	<u>4*</u>	<u>5**</u>	<u>6*</u>	<u>7**</u>	<u>8*</u>
SiO ₂	49.29	49.60	49.96	48.59	48.20	49.33	47.94	49.32
TiO ₂	0.60	0.52	0.75	0.65	0.07	0.96	0.41	0.68
Al ₂ O ₃	12.84	12.75	12.04	12.70	13.91	12.34	11.19	12.64
FeO	18.25	18.22	18.44	19.58	17.04	17.92	20.05	18.49
MgO	7.08	7.35	7.02	6.77	6.47	6.36	7.14	6.83
CaO	10.39	10.13	10.00	10.25	10.24	10.58	10.36	10.32
Na ₂ O	0.42	0.42		0.45	0.31	0.60	0.75	0.42
K ₂ O	0.04	0.04	0.03	0.05	0.06	0.08	0.13	0.05
Cr ₂ O ₃	0.31	0.36		0.33	0.30	0.28	0.35	0.30
MnO	0.53	0.53	0.59	0.56	0.42	0.50	----	0.53
P ₂ O ₅	0.09	0.09	0.27	0.10	----	0.13	0.14	0.07
Fe(met.)	0.05	----		0.00	2.64	0.02	----	0.04
FeS	<u>0.45</u>	<u>0.03</u>	----	<u>0.06</u>	<u>0.19</u>	<u>0.72</u>	<u>0.86</u>	<u>0.53</u>
	100.46	100.11		100.37	99.85	100.09	99.32	100.29
H ₂ O	0.01			0.01		0.02		0.03
H ₂ O	0.13			0.27		0.24	0.30	0.02

* New analysis, by A. D. Maynes, California Institute of Technology

** Taken from Urey and Craig⁽²⁾ All iron recalculated as FeO.

Taken from Gast⁽³⁵⁾

TABLE 4
CHEMICAL ANALYSES OF BASALTIC ACHONDRITES

	Brecciated Eucrites							
	<u>9**</u>	<u>10*</u>	<u>11**</u>	<u>12**</u>	<u>13**</u>	<u>14**</u>	<u>15**</u>	<u>16**</u>
SiO ₂	49.02	49.46	48.80	49.32	48.48	48.47	48.32	49.10
TiO ₂	0.58	0.95	0.71	0.42	0.60	0.07	0.52	0.74
Al ₂ O ₃	13.39	11.78	13.44	11.24	12.25	13.94	12.74	11.71
FeO	17.56	20.10	18.47	19.99	18.76	19.98	17.76	15.99
MgO	6.80	5.46	6.98	7.15	6.50	6.84	7.42	8.43
CaO	10.72	10.40	11.48	10.84	11.12	8.62	10.48	10.31
Na ₂ O	0.40	0.57	0.52	0.40	0.15	0.92	0.91	0.62
K ₂ O	0.17	0.05	0.12	0.25	0.22	0.13	0.22	0.66
Cr ₂ O ₃	0.31	0.29	0.21	----	0.88	0.06	0.33	0.51
MnO	0.21	0.56	0.63	----	0.25	0.78	0.28	0.42
P ₂ O ₅	0.17	0.11	----	----	0.12	0.06	0.16	0.09
Fe(met.)	----	0.00	----	----	----	----	----	----
FeS	<u>0.27</u>	<u>0.21</u>	<u>0.25</u>	<u>0.80</u>	<u>0.57</u>	<u>0.05</u>	----	----
	99.60	99.98	101.61	100.41	99.90	99.92	99.13	98.58
H ₂ O	0.30	----			0.18			
H ₂ O	0.14	0.14			0.15	0.20		

* New analysis, by W. Blake, California Institute of Technology.

** Taken from Urey and Craig.⁽²⁾ All iron recalculated as FeO.

TABLE 4

CHEMICAL ANALYSES OF BASALTIC ACHONDRITES

	Brecciated Eucrites		Unbrecciated Eucrites			
	<u>17**</u>	<u>18**</u>	<u>19**</u>	<u>20**</u>	<u>21**</u>	<u>22*</u>
SiO ₂	50.50	47.21	48.16	43.42	50.21	50.10
TiO ₂	-----	-----	0.32	-----	-----	0.92
Al ₂ O ₃	8.84	10.49	15.57	27.20	5.90	6.68
FeO	15.29	16.17	15.02	6.56	21.85	18.66 ^b
MgO	16.15	9.00	8.41	3.18	10.00	9.40
CaO	6.15	12.18	11.08	14.53	10.41	10.03
Na ₂ O	0.28	1.20	0.45	1.59 (0.25) ^a	1.28	1.28
K ₂ O	0.13	0.86	0.09	0.20 (0.00) ^a	0.57	0.16
Cr ₂ O ₃	0.75	-----	0.44	0.32	-----	0.18
MnO	0.51	-----	0.31	0.58	-----	0.50
P ₂ O ₅	0.03	-----	-----	-----	-----	0.71
Fe(met.)	-----	1.56	-----	-----	-----	-----
FeS	-----	S 0.51 C 0.43	0.82	0.11	-----	-----
	<u>98.63</u>	<u>99.61</u>	<u>100.67</u>	<u>97.70</u>	<u>100.22</u>	<u>100.11</u>
H ₂ O				0.01		
H ₂ O				1.71		

* New analysis, by A. D. Maynes, California Institute of Technology Preliminary data.

** Urey and Craig (2) All iron recalculated as FeO.

a Plus 1.49% Fe₂O₃.

b Deduced from modal analysis.

TABLE 4
CHEMICAL ANALYSES OF BASALTIC ACHONDRITES

	Howardites*							
	<u>23</u>	<u>24</u>	<u>25</u>	<u>26</u>	<u>27</u>	<u>28</u>	<u>29</u>	<u>30</u>
SiO ₂	48.05	49.45	48.14	51.53	49.21	48.18	50.91	53.11
TiO ₂			0.19				0.03	
Al ₂ O ₃	13.41	9.66	11.35	8.05	11.05	8.06	6.30	8.20
FeO	18.56	15.61	16.71	13.19	20.41	14.66	17.42	18.99
MgO	8.67	17.40	13.93	17.59	8.13	16.81	14.69	8.48
CaO	10.40	6.39	7.88	7.04	9.01	5.48	6.24	5.79
Na ₂ O			0.22	0.45	0.82	1.75	2.04	1.93
	0.29	0.31		(0.15) ^a			(0.13) ^a	
K ₂ O			0.24	0.22		0.38	0.43	1.19
				(0.02) ^a			(0.02) ^a	
Cr ₂ O ₃	0.60	0.04	0.53	0.42	0.42	0.38		0.98
MnO	0.25	0.72	0.22			2.17	0.30	
P ₂ O ₅		0.01	0.17			0.08		
Fe(met.)						0.32		
FeS	<u> </u>	<u> </u>	<u>0.27</u>	<u>0.63</u>	<u>0.16</u>	<u>1.32</u>	<u> </u>	<u>1.01</u>
	100.68	99.59	99.85	98.91	98.79	99.59	98.46	99.68
H ₂ O			0.06					
H ₂ O			0.16				0.44	

* All analyses taken from Urey and Craig.⁽²⁾

a Alkali values determined by Edwards.⁽³³⁾

TABLE 5
NORMS FOR BASALTIC ACHONDRITES

	Brecciated		Eucrites					
	1	2	4	5	6	8	10	11
Or	0.2	0.2	0.3	0.3	0.4	0.3	0.3	0.7
Ab	3.6	3.6	3.8	2.6	5.1	3.6	4.8	4.4
An	32.8	32.8	32.5	36.4	30.8	32.5	29.4	34.0
Wo	7.7	7.1	7.4	6.0	8.8	7.8	9.1	9.6
En	17.6	18.3	16.9	16.1	15.8	17.0	13.6	17.3
Fs	33.3	33.3	34.8	33.2	32.0	33.2	35.1	33.5
Fo								0.1
Fa								0.2
Q	2.6	3.1	2.0	3.3	3.7	3.3	4.2	
Ap	0.2		0.2		0.3	0.2	0.3	
Ilm	0.5		1.2	0.1	1.8	1.3	1.8	1.4
Cr	1.1		0.5	0.5	0.4	0.5	0.4	0.3
Fe/Fe+Mg	0.59	0.58	0.61	0.60	0.61	0.60	0.65	0.60
An/Ab+An	0.89	0.89	0.89	0.93	0.84	0.89	0.85	0.87

TABLE 5

	NORMS FOR BASALTIC ACHONDRITES Brecciated Eucrites							Eucrite
	12	13	14	15	16	17	18	19
Or	1.5	1.3	0.8	1.3	3.9	0.9	5.1	0.6
Ab	3.4	1.3	7.8	7.7	5.2	2.4	10.2	3.8
An	28.1	32.1	33.5	30.0	27.2	22.5	20.7	40.2
Wo	10.8	9.4	3.7	8.7	9.8	3.3	16.6	6.2
En	17.7	16.2	15.5	17.2	21.0	39.9	9.9	20.4
Fs	36.0	33.2	34.6	29.7	28.8	28.2	13.2	26.6
Fo			1.1	0.9		0.2	8.8	0.4
Fa			2.7	1.8		0.1	12.8	0.6
Q	1.3	3.3			0.5			
Ap		0.3	0.1	0.3	0.2	0.1		
Ilm	0.8	1.1	0.1	1.0	1.4			0.6
Cr		1.3	0.1	0.5	0.6	1.1		0.7
Fe/Fe+Mg	0.61	0.61	0.63	0.57	0.51	0.35	0.50	0.50
An/Ab+An	0.85	0.93	0.80	0.77	0.75	0.93	0.58	0.90

TABLE 5
NORMS FOR BASALTIC ACHONDRITES

	Eucrites			Howardites				
	20*	22	23	24	25	26**	27	28
Or		0.9	1.6	1.7	1.4			2.2
Ab	2.6	10.8			1.8	1.0	6.9	14.8
An	72.8	12.1	35.7	25.4	29.3	21.1	26.5	13.1
Wo		14.0	6.6	2.6	3.6	5.7	7.6	5.7
En	7.8	23.4	21.1	35.4	28.4	43.8	20.1	18.2
Fs	12.0	32.3	33.2	24.5	24.9	24.0	37.2	13.3
Fo			0.4	5.6	4.4		0.1	16.6
Fa			0.6	4.3	4.2		0.2	13.3
Q		0.9				1.2		
Ap		1.6			0.4			0.2
Ilm		1.8			0.4			
Mt		2.2						
Cr		0.3	0.9	0.1	0.8	0.4		0.6
Fe/Fe+Mg	0.53	0.51	0.54	0.40	0.40	0.29	0.58	0.36
An/Ab+An	0.97	0.49	0.96	0.94	0.90	0.95	0.79	0.43

* Calculated from alkali data estimated from analyzed mineral separates

** Calculated with alkali data from Edwards(33)

TABLE 5

NORMS FOR BASALTIC ACHONDRITES

	Howardites	
	<u>29*</u>	<u>30</u>
Or		7.0
Ab	1.0	16.3
An	16.4	10.2
Wo	4.9	7.7
En	36.5	21.1
Fs	32.5	34.0
Fo		
Fa		
Q	3.9	0.8
Ap		
Ilm		
Cr		
Fe/Fe+Mg	0.36	0.55
An/Ab+An	0.94	0.30

* Calculated with alkali data from Edwards(33)

TABLE 6

ALKALI CONTENTS OF SOME BASALTIC ACHONDRITES

	Old Analyses		New Analyses*		Edwards (33)		Gast (35)	Geiss and Hess(36)
	Na	K	Na	K	Na	K	K	K
Juvinas	0.31	0.14.	0.31	0.04	0.33	0.04		
Stannern	0.57	0.11	0.44	0.07	0.43	0.07		
Nuevo Laredo			0.42	0.04	0.41	0.05	0.04	
Sioux County			0.31	0.03			0.03	
Pasamonte	0.24	0.05	0.33	0.04	0.38	0.06	0.04	
Moore County	0.33	0.07					0.02	
Frankfort	0.34	0.18			0.15	0.02		
Pavlovka	1.52	0.34			0.13	0.02		
Petersburg	0.61				0.45	0.05		
Shergotty	0.96	0.48	0.96	0.15				0.15
Padvarninkai	0.90	0.71						0.10

* Taken from new total meteorite analyses. Alkalies were determined by flame photometer using the method described by Brannock and Shapiro.⁽³⁷⁾

TABLE 7

ALKALI CONTENTS OF PLAGIOCLASE SEPARATES

DETERMINED BY FLAME PHOTOMETRIC ANALYSIS

	<u>1</u>	<u>2</u>	<u>3</u>	<u>4</u>	<u>5</u>	<u>6</u>	<u>7</u>
Sample Weight	.1014g	.1004g	.1150g	.0981g	.0879g	.1120g	.0504g
Raw Data							
Na ₂ O	1.56 .06*	1.06 .04	0.74 .04	1.05 .03	0.98 .01	1.45 .02	0.56 .01
	1.55 .02	1.03 .02	0.71 .01				
K ₂ O	0.18 .02	0.08 .02	0.03 .01	0.08 .01	0.07 .01	0.13 .01	0.05 .01
	0.16 .02	0.06 .02	0.03 .01				
Reduced Data							
Na ₂ O	1.68 ^a	1.03	0.64	1.07	1.11	1.33 ^b	1.11
K ₂ O	0.18 ^a	0.07	0.02	0.08	0.08	0.13 ^b	0.10
Wt. % Ab	14.0	8.4	5.3	8.8	9.1	11.2	9.1
Wt. % Or	1.5	0.6	0.1	0.7 ²	0.7 ²	1.1	0.8 ²
Norm. Plag. Ab from Or total met. analysis	14.5			9.8	9.8	10.3	
	1.5			0.8	0.6	0.8	

* Error stated is reproducibility of flame photometer measurement
a Corrected for 10% pyroxene impurity, determined microscopically
b Corrected for 10% tridymite impurity, determined microscopically

- | | | | |
|---|----------------------------------|---|-------------------------|
| 1 | Nuevo Laredo, P200, 1.0aNM, STBE | 5 | Sioux County |
| 2 | Moore County | 6 | Pasamonte, Pa200, 0.8aM |
| 3 | Serra de Mage | | STBE 2.65 |
| 4 | Juvinas, 1.8aNM, 2.74 2.77 | 7 | Petersburg |

plagioclase of the new analyses shows agreement within 1% Ab and 0.3% Or. Besides showing that the analytical techniques give comparable results, this comparison indicates the usefulness of the norm in giving average plagioclase compositions for these meteorites. The comparison indicates that the Al_2O_3 content of the pyroxene of these meteorites is low, for small amounts of Al_2O_3 in the pyroxene, which is more abundant than plagioclase, would tend to make the normative plagioclase composition more calcic than the modal* composition.

(3) Normative plagioclase compositions are compared with plagioclase compositions deduced from optical determinations in Table 8. For old analyses and old optical data, there is considerable lack of agreement due to (a) inaccuracies in the chemical analyses and (b) the small number of optical determinations which were made on meteorites in which there is significant compositional variation of the plagioclase (see Part IV, Mineralogy). Where comparison is possible, the older optical data shows good agreement with new chemical and optical data, which suggests that the older optical data are more accurate than the older chemical analyses.

(4) Fe/Fe+Mg ratios for old and new analyses of the same meteorite are compared in Table 9. There is good agreement for Stannern, Juvinas and Pasamonte and fair agreement for Shergotty. Comparison also is made between normative and modal Fe/Fe+Mg for Petersburg and Serra de Mage for which agreement is not good. In the case of Petersburg, a very inhomogeneous meteorite, the discrepancy probably reflects sampling problems which bias samples towards more magnesian

*The terms mode and modal pertain to the mineralogy of the meteorites rather than to calculated normative minerals.

TABLE 8

COMPARISON OF NORMATIVE AND MODAL PLAGIOCLASE COMPOSITIONS

	Modal Composition, (deduced from optical properties)		Normative Composition	
	%An		%An	
	Older work (Range)	This work (Average)	Old Analyses	New Analyses
Stannern	86-88 ^{1a}	80	79	84
Juvinas	90-91 ^{1a}	90	89,	90
Jonzac	84-86 ^a	--	77	--
Peramiho	88 ^a	--	85	--
Petersburg	86-88 ^a	86	79	--
Pavlovka	90-97 ^a	--	25	94*
Frankfort	94-95 ^a	--	79	95*
Iuotolax	90-93 ^a	--	96	--
Zmenj	83 ^{1/2} ^a	--	43	--
Mëssing	75 ^a	--	30	--
Le Teilleul	78 ^a	--	90	--
Béréba	87 ^b	--	93	--
Macibini	86 ^c	--	75	--
Moore County	90 ^d	90	90	--
Pasamonte	88 ^e	86	93	89
Nuevo Laredo	--	85	--	85
Sioux County	--	90	--	90
Binda	--	90	93	--
Serra de Mage	--	95	82	95**
Shergotty	--	--	39	49

a Michel⁽⁶⁾ deduced from extinction angles on albite-carlsbad twins.

b Lacroix, deduced from index of refraction.

c Haughton and Partridge, deduced from index of refraction.

d Hess and Henderson, deduced from index of refraction.

e Foshag(), Deduced from index of refraction.

* Calculated, using alkali values of Edwards(33)

** Composition of analyzed plagioclase separate, this work.

TABLE 9

COMPARISON OF Fe/Fe Mg RATIOS IN OLD AND NEW ANALYSES

	Fe/Fe+Mg Old Analyses	Fe/Fe+Mg New Analyses
Juvinas	0.58	0.60
Stannern	0.60	0.61
Pasamonte	0.60	0.61
Shergotty	0.55	0.51
	Fe/Fe+Mg Modal	Fe/Fe+Mg Normative
Petersburg	0.58	0.32
Serra de Mage	0.53	0.44

pyroxenes. For Serra de Mage the error may lie in the analytical data.

In general, it appears that the older chemical analyses had poor determinations of the alkalis which are present only in small quantities. For the major oxides, SiO_2 , Al_2O_3 , CaO , FeO and MgO , the old analyses appear to be at least adequate.

General compositional features

The compositions of the basaltic achondrites are those of simple basaltic systems in which the components are chiefly plagioclase and pyroxene. The correlation between normative and modal mineral compositions is good, which indicates that the minerals of the mode are simple and not too complicated by solid solution phenomena such as the solubility of sodium and aluminum in some pyroxenes.

Table 10 compares the compositions and norms of Binda, a magnesium-rich achondrite, Juvinas, an iron-rich achondrite and a tholeiitic olivine basalt from Kilauea (Tilley⁽³⁸⁾, p. 50, analysis 2). The norms of the basaltic achondrites show approximate saturation with respect to silica and therefore suggest the comparison with terrestrial saturated (tholeiitic) basalts.

The Juvinas meteorite has some general similarities to the terrestrial basalt. The notable difference is the low alkali content of the meteorite, which leads to some striking differences in the norms of the two analyses. The amount of normative plagioclase in the terrestrial basalt is somewhat greater and it is much more albitic than is the normative plagioclase in the meteorite. There is a larger proportion of normative diopside (calcium-magnesium-iron pyroxene) in the pyroxene component of the terrestrial basalt.

TABLE 10

COMPARISON OF TWO BASALTIC ACHONDRITES TO A TERRESTRIAL
THOLEIITIC (SILICA SATURATED) BASALT

	Analyses				Norms		
	Binda ^a (Mg-rich)	Juvinas ^b (Fe-rich)	Basalt ^c		Binda	Juvinas	Basalt
SiO ₂	50.50	49.32	49.43	Q	—	3.3	0.7
Al ₂ O ₃	10.49	13.39	12.92	Or	0.8	0.3	3.1
Fe ₂ O ₃	n.d.	—	3.14	Ab	2.4	3.6	18.3
FeO	16.17	12.64	8.34	An	22.5	32.5	23.8
MgO	16.15	6.83	9.24	Di	6.3	16.0	23.3
MnO	0.51	0.53	0.18	Hy	65.1	42.0	20.3
CaO	6.15	10.32	11.02	Ol	0.3	—	—
Na ₂ O	0.28	0.42	2.22	Ilm	—	1.3	5.4
K ₂ O	0.13	0.05	0.52	Mt	—	—	4.5
H ₂ O	n.d.	0.02	0.17	Ap	0.1	0.2	0.7
H ₂ O	n.d.	0.03	0.01	Tr	—	0.5	—
TiO ₂	n.d.	0.68	2.85				
P ₂ O ₅	0.03	0.07	0.26				
Cr ₂ O ₃	0.75	0.30	n.d.				
FeS	—	0.53	—				

a Urey and Craig(2)

b This work

c Tilley(30)

Binda shows greater dissimilarity to the terrestrial basalt. The amounts of aluminum, calcium and alkalis are much lower in Binda and the magnesium content is much higher in Binda than in the terrestrial basalt. In the norm, Binda shows much less feldspar component and the feldspar is much more calcic than in the terrestrial basalt. The abundance of pyroxene is much greater in Binda and there is very little normative diopside component.

A notable difference between the Juvinas analysis and the terrestrial basalt analysis is the oxidation state of iron. Appreciable amounts of Fe_2O_3 have not been reported in any of the new analyses of basaltic achondrites. This is in contrast to the terrestrial basalt which contains about three percent of Fe_2O_3 which is calculated as magnetite in the norm and occurs, in part, as magnetite in the mode. In contrast, small amounts of metallic iron are present in the norms and modes of the newly analysed meteorites. These differences are an important indication that the basaltic achondrites crystallized under conditions of very low partial pressure of oxygen. In the laboratory study of the MgO-FeO-SiO_2 system (Bowen and Schairer⁽²⁶⁾) it was reported that ferric iron was present in liquids that were in equilibrium with pyroxenes and the metallic iron of the sample container. Muan⁽³⁹⁾ showed that in the system $\text{FeO-Fe}_2\text{O}_3\text{-SiO}_2$ the liquid in equilibrium with fayalite, silica and metallic iron contained about one percent Fe_2O_3 . The partial pressure of oxygen for that equilibrium is less than 10^{-12} atmospheres. The low content of Fe_2O_3 in the basaltic achondrites apparently is consistent with crystallization under conditions of equilibrium between ferrous iron-bearing silicates and metallic iron. This conclusion agrees with the observed mineralogy in the basaltic achondrites.

Analyses of the Sioux County meteorite

The two new analyses of the Sioux County meteorite are important because they are indicative of the compositional variations found in the brecciated eucrites. The samples which were selected for analysis were a single medium-grained lithic fragment which was freed from most surrounding matrix material and a bulk sample which contained a high proportion of fine-grained matrix material. Comparison of the two analyses (1 and 2) shows no clear difference between the two portions of Sioux County, but indicates the type of compositional variation expected between lithic fragments and matrix or between different lithic fragments in a brecciated eucrite.

Variation diagrams

Figure 2 gives variation diagrams for the various oxides (weight percent) in the basaltic achondrites plotted against Fe/Fe+Mg (mode percent). The ratio Fe/Fe+Mg is used because it reflects the relative degree of magmatic differentiation in a set of basaltic rocks. Because, in general, the pyroxene and olivine crystallizing from a basaltic magma have a smaller Fe/Fe+Mg than the magma, fractional crystallization tends to drive Fe/Fe+Mg in the melt towards higher values. Partial melting would reverse the trend, in that the liquid would have a progressively lower Fe/Fe+Mg.

The data plotted in the variation diagrams includes all but the most obviously incorrect analyses. The old analyses of Padvarninkai, Pavlovka, Zmenj and Serra de Mage have been rejected because they contain fifteen to twenty percent of normative olivine. Olivine is not abundant in the modes of these meteorites and by analogy with newly analyzed meteorites, the norms and modes should agree closely. New data for Pavlovka and Serra de Mage indicates that alkalis have been

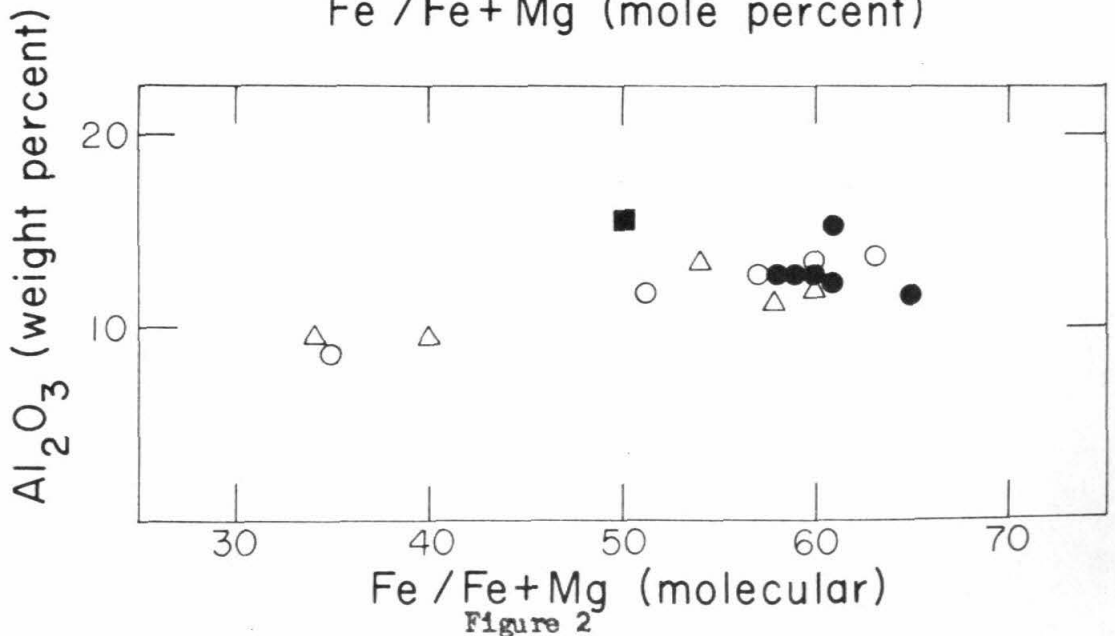
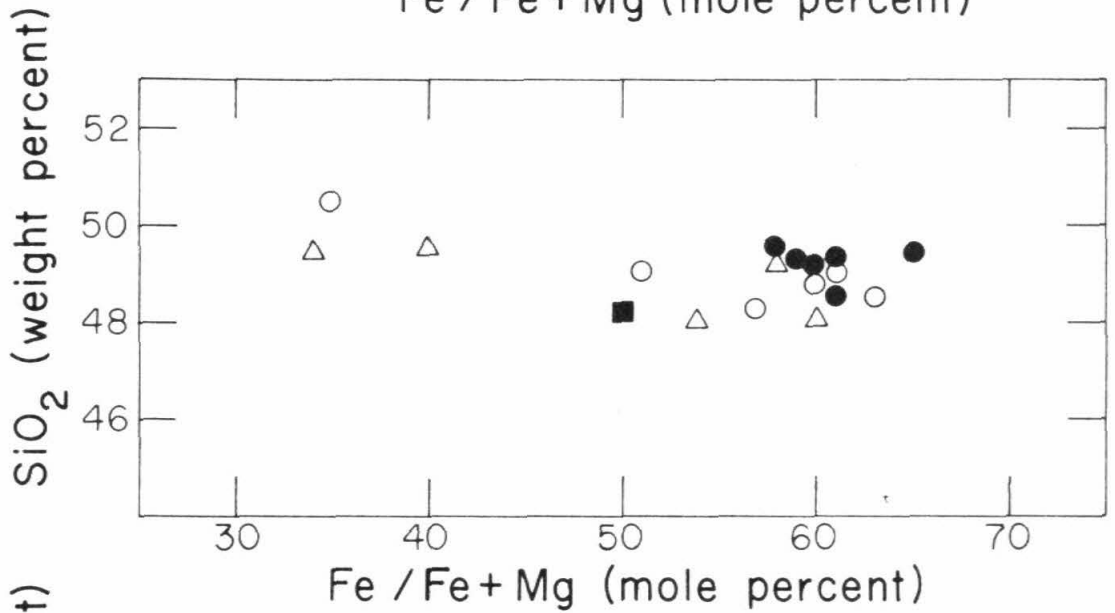
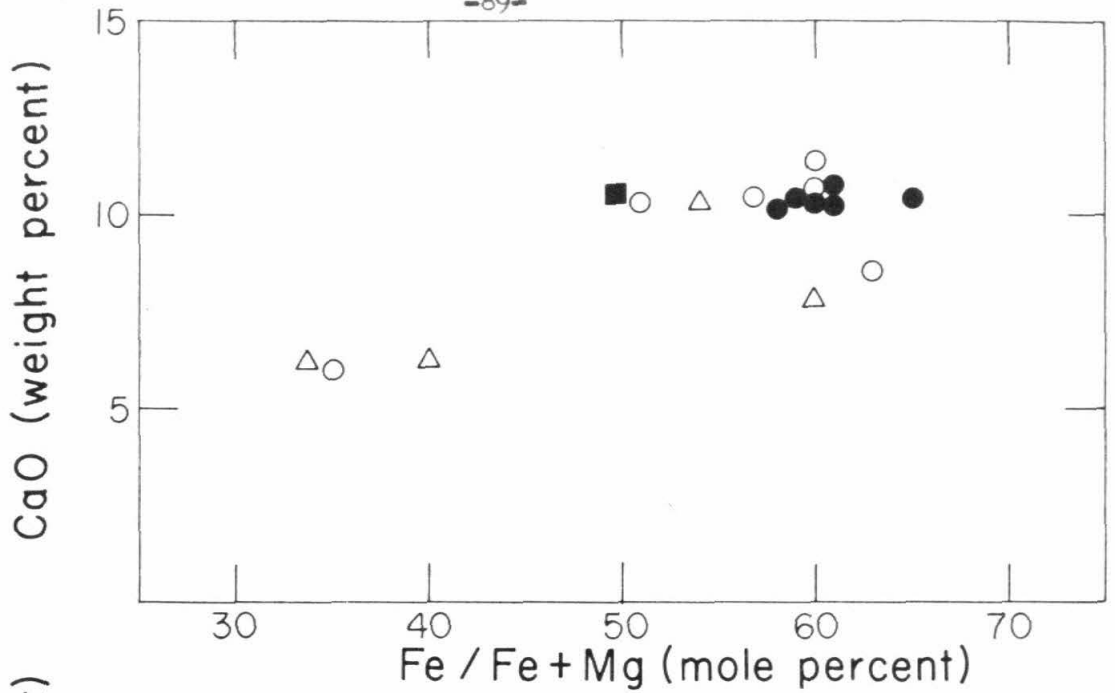


Figure 2

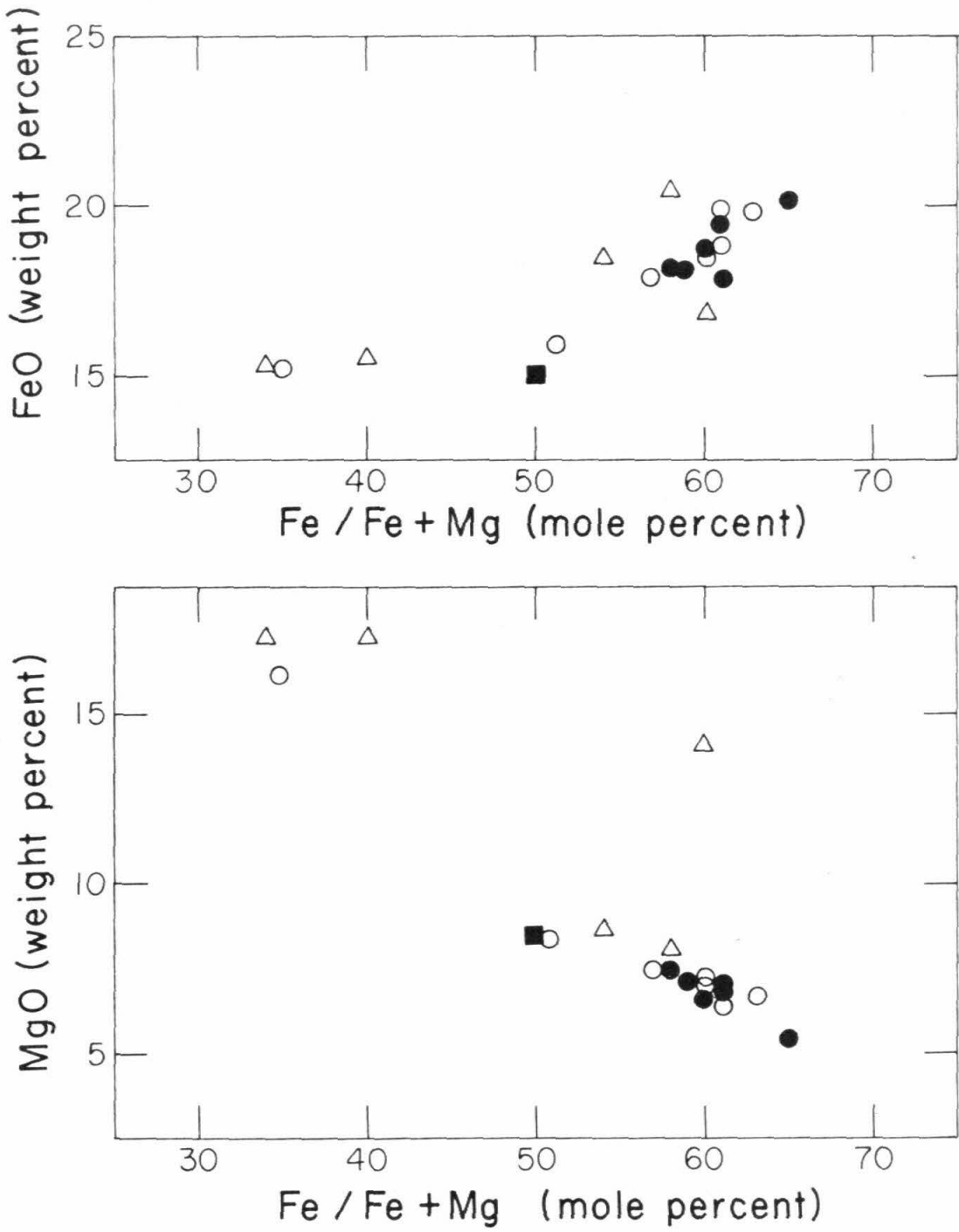


Figure 2

overestimated in the older analyses, which leads to an increase in normative olivine. The combination of high alkali values and normative olivine in Padvarninkai and Zmenj suggests that the old alkali determinations were erroneous. The old analysis of Mässing has been discarded because it shows about three percent $\text{Na}_2\text{O}+\text{K}_2\text{O}$ which is probably an incorrect determination. The composition of Shergotty is not included on the variation diagrams and is discussed separately.

On the variation diagrams, the following distinctions have been made: new analyses are indicated by solid circles, old selected analyses are indicated by open circles (eucrites) and open triangles (howardites). The Moore County meteorite, an unbrecciated eucrite, for which the older analysis by Henderson and Davis⁽¹⁰⁾ is apparently an excellent analysis, has been marked by a solid square.

On the basis of $\text{Fe}/\text{Fe}+\text{Mg}$ ratios, the existing analyses can be divided into two groups, one with $\text{Fe}/\text{Fe}+\text{Mg}$ greater than 0.5 and one with $\text{Fe}/\text{Fe}+\text{Mg}$ less than 0.4. The gap is not considered to be real in terms of the magmatic histories of these meteorites, but the groupings help simplify discussion. The two groups are, essentially, the groups distinguished in the chemical classification of basaltic achondrites proposed by Brown⁽²³⁾ and Mason⁽¹⁾. In terms of the classification used in this work, the iron-rich group contains three howardites (Petersburg, Luotolaks, Mässing) and the magnesium-rich group contains one eucrite (Binda).

The calcium content is higher for the iron-rich group than for the magnesium-rich group. There is no discernible variation of CaO within the iron-rich group. The SiO_2 content is rather uniform for the whole assemblage of basaltic achondrites. The magnesium-rich group may have

slightly higher values than the iron-rich group and there may be a slight increase of SiO_2 with increasing $\text{Fe}/\text{Fe}+\text{Mg}$ in the iron-rich group. For the iron-rich group, the older analyses seem to be systematically lower than the newer analyses.

There is a significant variation of FeO , which increases from the magnesium-rich to the iron-rich basaltic achondrites. The trend of absolute enrichment in iron is a principal justification for comparing the compositional trends in the basaltic achondrites with those of the Skaergaard intrusion, which is well known as a differentiated gabbroic intrusion which shows strong enrichment in iron in the later stages of differentiation. The magnesium content declines from the magnesium-rich group to the iron-rich group.

An important function of a variation diagram can be to show that groups of rocks share common relationships. The significant feature of these variation diagrams is that some regularities can be distinguished. Without further elaboration it might be argued, on the basis of these diagrams, that most of the basaltic achondrites have close chemical affinities.

Normative mineral variations

Further details of the compositional variability of the basaltic achondrites can be obtained by comparison of normative mineral abundances.

Although some of the norms have been calculated from a combination of old major element analyses and new alkali analyses and are substantially better than norms calculated from the original analyses, the only old analyses for which variations of normative mineral composition have been plotted in variation diagrams are the selected analyses used in plotting Figure 2. For some normative components, only the good recent

analyses are used.

Figure 3 gives the variation of the amount of normative anorthite as a function of $Fe/Fe+Mg$. There is a distinct trend from the magnesium-rich basaltic achondrites which have lower anorthite content to the iron-rich achondrites which have higher anorthite content. Many iron-rich basaltic achondrites have similar compositions, and much of the scatter of the older analyses may be due to analytical error. If only the good analyses are used, it is possible to suggest that there is a slight decrease of normative anorthite with increase of iron above $Fe/Fe+Mg = 0.6$. The Moore County meteorite has an anorthite content distinct from the main group of iron-rich basaltic achondrites. It shows a higher plagioclase content which may be a result of accumulation of plagioclase during the magmatic episode.

Figure 4 gives the variation of normative plagioclase composition as a function of $Fe/Fe+Mg$. The composition of normative plagioclase is sensitive to errors in alkali determinations and to errors in alumina determinations. Therefore, the old analyses probably have considerable scatter due to analytical error. Nevertheless, it seems probable that there is a general increase in the alkali content of the plagioclase with increasing $Fe/Fe+Mg$.

Figure 5 shows the variation of the normative wollastonite component ($CaSiO_3$) in the good analyses. There is a general increase in wollastonite component as $Fe/Fe+Mg$ increases. The combined decrease in normative anorthite content and the increase of normative wollastonite causes the calcium content to remain essentially constant in the iron-rich basaltic achondrites.

A survey of the norms indicates that in general the basaltic achon-

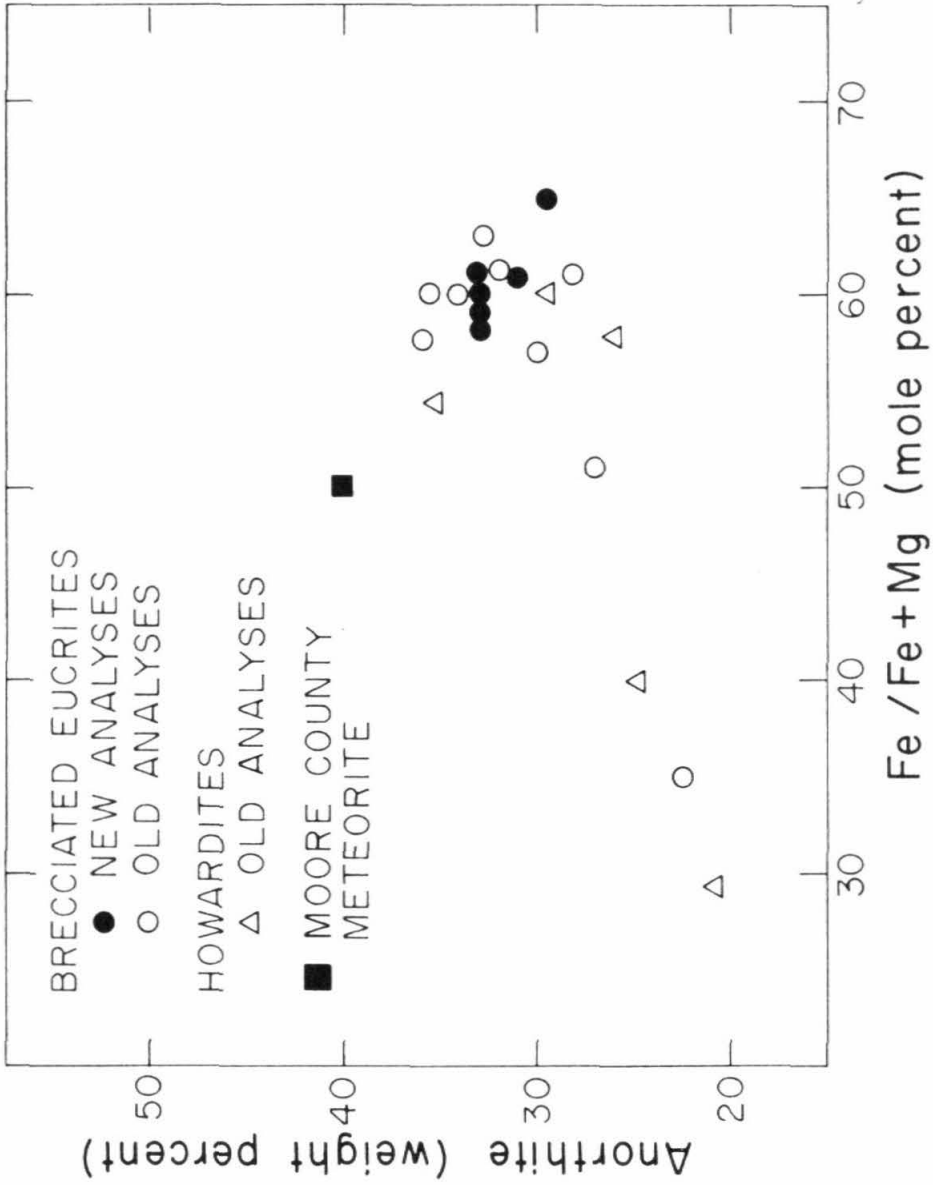


Figure 3

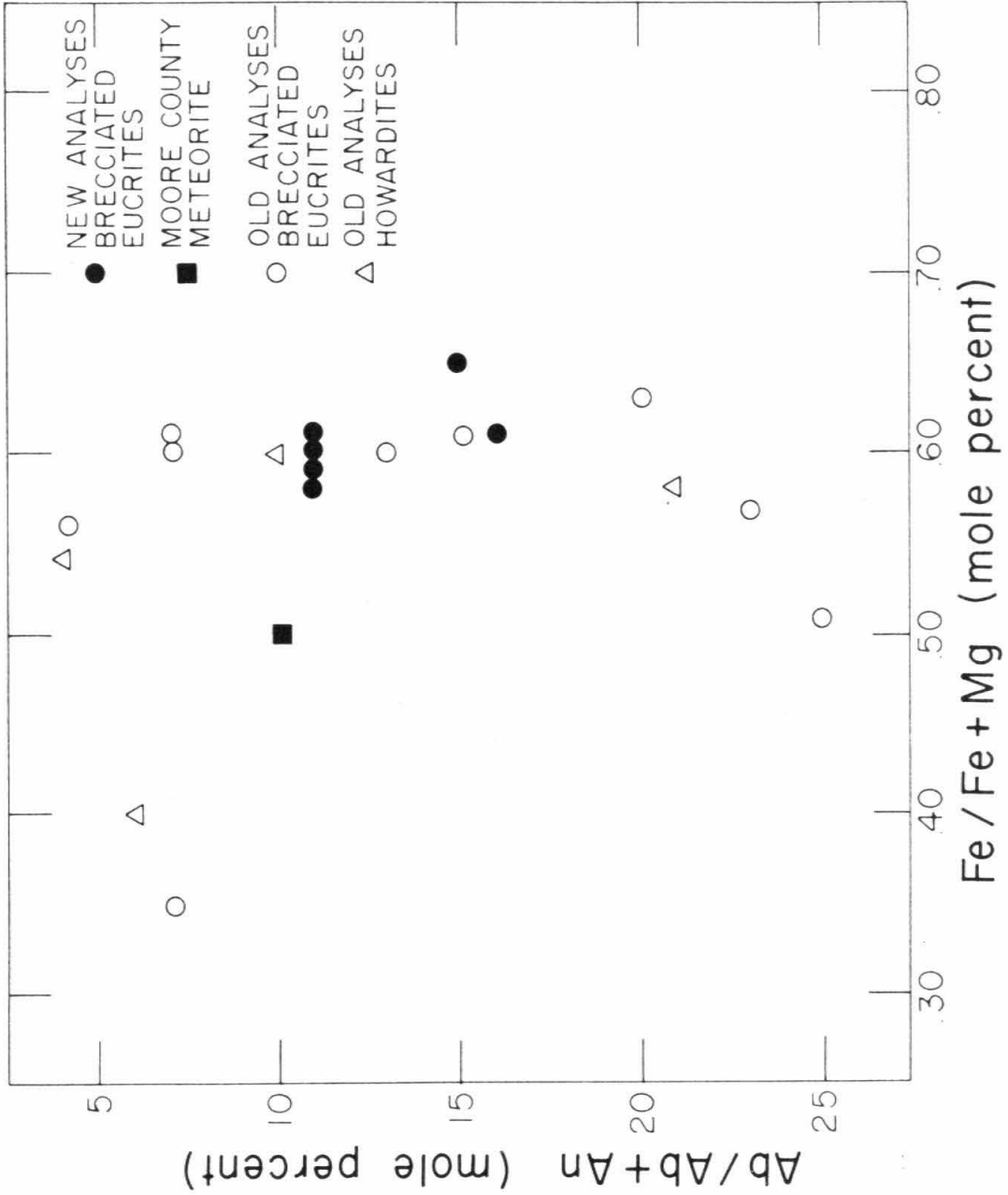


Figure 4

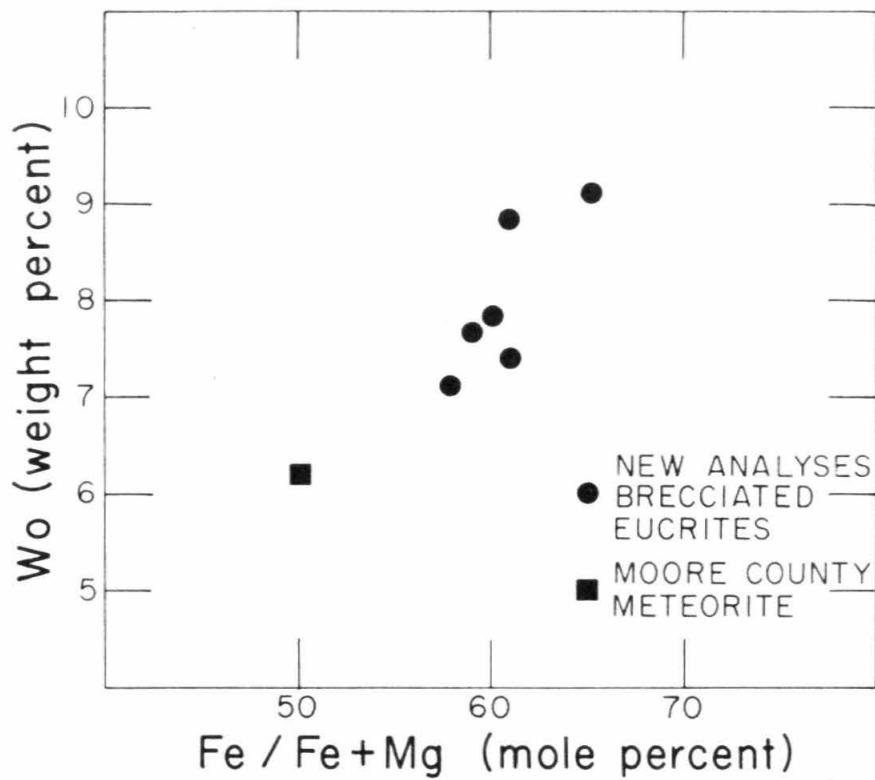


Figure 5

drites are either slightly oversaturated or slightly undersaturated with respect to silica. This corresponds to the presence of small amounts of free silica or small amounts of olivine in the modes. Some meteorites which have modal free silica may be slightly undersaturated with respect to silica in the norm because of solution of Al_2O_3 in the pyroxene. Al_2O_3 in the pyroxene is calculated as feldspar molecule, which takes up silica, rather than as pyroxene molecule, which can be calculated as $Al \cdot AlO_3$ in analogy to the metasilicate formula and causes an apparent deficiency in SiO_2 . For the iron-rich basaltic achondrites, there is a tendency for the amount of normative free silica to increase with increasing $Fe/Fe+Mg$, (Figure 6). Moore County has modal free silica, but has normative olivine, due to the presence of Al_2O_3 in the pyroxene. The amount of modal free silica may have been affected by crystal settling in the case of Moore County.

Composition of the Shergotty meteorite

New analytical data for the Shergotty meteorite indicate that Shergotty has an exceptional composition. This conclusion had been suspected by the older analytical data, but has now been substantiated. Table 11 compares the analyses and norms of Shergotty and Juvinas.

The most striking difference between the two meteorites is the composition of the plagioclase, which is about An_{50} in Shergotty and An_{90} in Juvinas. The total amount of plagioclase is much less in Shergotty than in Juvinas and is reflected by the much smaller content of Al_2O_3 in Shergotty. The $Fe/Fe+Mg$ in Shergotty is slightly smaller than that of Juvinas, but the normative wollastonite component in the pyroxene is substantially larger. Two compositional features also not present in the other meteorites studied here are the occurrence in Shergotty of 0.71% P_2O_5 which reflects the modal occurrence of whitlockite and the

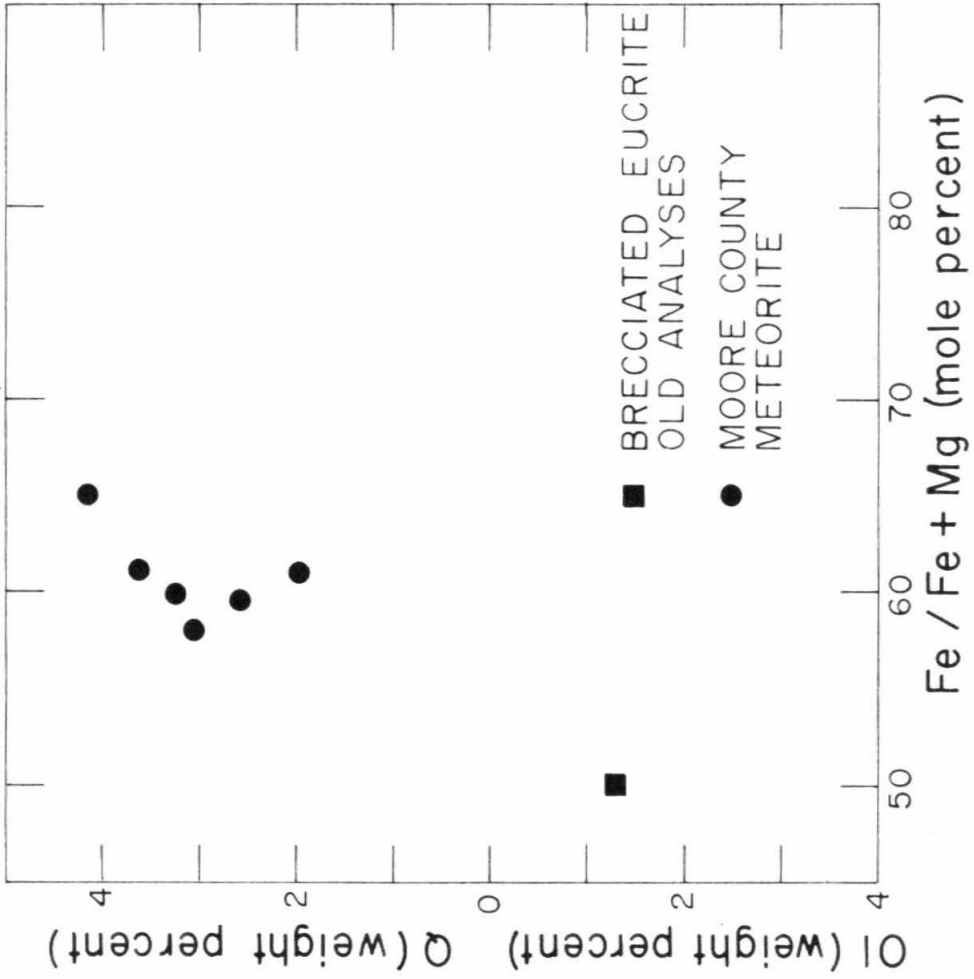


Figure 6

TABLE 11

COMPARISON OF CHEMICAL COMPOSITIONS OF SHERGOTTY AND JUVINAS

	Analyses			Norms	
	Shergotty	Juvinas		Shergotty	Juvinas
SiO ₂	50.10	49.32	Or	0.9	0.3
TiO ₂	0.92	0.68	Ab	10.8	3.6
Al ₂ O ₃	6.68	12.64	An	12.1	32.5
Fe ₂ O ₃	1.49	----	Wo	14.0	7.8
FeO	18.66	18.49	En	23.4	17.0
MnO	0.50	0.53	Fs	32.3	33.2
CaO	10.03	10.32	Q	0.9	3.3
MgO	9.40	6.83	Ap	1.6	0.2
Na ₂ O	1.28	0.42	Ilm	1.8	1.3
K ₂ O	0.16	0.05	Cr	0.3	0.5
P ₂ O ₅	0.71	0.07	Mt	2.2	---
Cr ₂ O ₃	0.18	0.30	Fe/Fe+Mg	.51	.60
Fe(met.)	----	0.04	An/Ab+Or+An	.49	.89
FeS	----	<u>0.53</u>	Wo/Wo+En+Fs	.20	.13
	100.11	100.29			

presence of ferric iron, which occurs modally as magnetite.

Whereas the other basaltic achondrites studied in this work seem to follow fairly simple compositional trends, Shergotty fits none of the trends. With existing data it is not possible to determine the manner in which Shergotty attained its compositional features, but some possible explanations can be suggested for the differences between Shergotty and the other basaltic achondrites. It is possible that the paths of crystallization in basalt systems are strongly influenced by oxygen partial pressure (Osborne⁽⁴¹⁾). Shergotty is different from other basaltic achondrites in that it contains magnetite rather than metallic iron which indicates that oxidation conditions were different in Shergotty than in the other achondrites. Further investigation of the paths of crystallization of basaltic magmas under various partial pressure of oxygen could shed some light on the possibility that Shergotty and the other basaltic achondrites differentiated from the same parent material under different P_{O_2} regimes.

It is also possible that Shergotty differentiated from a different parent material. In that case, it would be necessary to postulate a previous differentiation event to produce the variation between the parent material of Shergotty and the parent material of the other basaltic achondrites. A similar initial differentiation may be necessary to explain the relation of basaltic achondrites to chondrites.

A third possibility is that Shergotty and the other basaltic achondrites differentiated from a similar parent material under different P-T conditions. The higher the pressure, the more favored is the solid solution of aluminum in pyroxenes (Boyd and England⁽⁴²⁾). If aluminum preferentially goes into pyroxene, there must be a concurrent increase

of the alkali component of the feldspar an increase in the amount of calcium available for the formation of pyroxene. As both of these features are found in the comparison of Shergotty and other basaltic achondrites, differentiation of Shergotty under higher total pressures may be partly responsible for the observed differences.

Composition of minerals

One of the most fundamental sets of data which can be obtained for a rock or meteorite is the composition of the minerals which make up the rock. For this purpose a number of mineral separations have been made by heavy liquid, magnetic and chemical techniques. A number of problems have been encountered which have not been solved in a completely satisfactory way and, in fact, may be impossible to deal with in the context of the small sample size available for making mineral separations on meteorites.

For those meteorites with fine-grained magmatic textures, the problem of liberation of the mineral grains is acute. The problem is even more acute with regard to making mineral separations of meteorites where there is a great deal of finely crushed matrix material. The Frantz magnetic separator can not handle materials ground to finer than about 300 mesh due to the interference of electrostatic effects and the clumping of grains. This limits separation of very fine material to heavy liquid or chemical techniques. If much of the material must be ground to 300 mesh in order to free mineral grains, adequate mineral separation becomes difficult. In Nuevo Laredo, where many of the lithic fragments have very fine-grained textures, there is always a biasing in the mineral separates towards the coarser-grained portions.

For mineral grains completely free of binary intergrowths, the Frantz

separator can efficiently fractionate plagioclase and free silica from pyroxenes, but can not efficiently separate various pyroxenes such as the pigeonite and ferroaugite that occur in the iron-rich basaltic achondrites or the pyroxenes of variable composition in the howardites. For Nuevo Laredo and Juvinas, where pigeonite is the most abundant pyroxene, pigeonite separates have been made, but ferroaugite compositions must be determined by other means as indicated below. For those meteorites where pyroxene compositions are variable, there is no obvious way in which to get either a completely reliable composite pyroxene separate or a separate of one of the principal pyroxene phases. This difficulty is heightened by the problem that in the meteorites with variable pyroxene compositions there tend to be variable quantities of inclusion material which may affect the magnetic properties of the grains.

Heavy liquid separations have been made using methylene iodide, tetrabromoethane and acetone. These liquids allow the separation of free silica from plagioclase and the separation of very fine-grained matrix fragments of intermediate density from plagioclase and pyroxene. Separations of small samples are expedited with the use of a centrifuge. The problem of separation of the pyroxenes has not been attempted by heavy liquid techniques because their separation would require the use of a liquid of higher specific gravity such as Clerici solution. Although it is possible that separation of pyroxenes could be made in a correctly adjusted Clerici solution the irregular distribution of inclusions in the pyroxenes and the compositional variations of the pyroxenes would make the separation inefficient. The limiting factor for making mineral separations in many cases is the size of the sample that is available. In meteorite studies, the availability of large samples

is limited and only fairly efficient mineral separation techniques can be used.

The calcic plagioclase present in the basaltic achondrites decomposes in HCl. For cases where it is desirable to eliminate plagioclase completely from pyroxene concentrates, magnetic and heavy liquid separation can be followed with acid treatment to remove any remaining plagioclase. The reverse situation, chemical removal of plagioclase component from a magnetic and/or heavy liquid concentrate of plagioclase, possibly could be used to obtain chemical compositional data on plagioclase. Analyses of the acid soluble and acid insoluble portions of meteorites were reported in the older meteorite literature (see Wahl⁽⁵⁾ and Michel⁽⁶⁾). In those cases, previous concentration of minerals had not been made.

Table 12 gives analyses of mineral separates made in this study and some analyses made in previous studies. Partial analyses for alkalis in feldspar separates have been given in Table 7. Because of the inefficiencies of mineral separation, many of these analyses have unknown amounts of contaminants. Some limits can be put on the amounts of contamination by calculating norms for the mineral analyses. This is especially useful in trying to establish the amount of aluminum in the pyroxenes. By using a calculation which assumes that all alkalis in the pyroxene analysis are due to plagioclase contamination a lower limit on the aluminum content in the pyroxene can be calculated. The upper limit to the aluminum content in the pyroxene is set by the value reported in the chemical analysis.

The data for Nuevo Laredo pyroxene separates has been used in conjunction with X-ray fluorescence and diffraction analysis to establish the composition of the co-existing augite and pigeonite in Nuevo Laredo

TABLE 12
MINERAL SEPARATE ANALYSES

	<u>M1</u>	<u>M2</u>	<u>M3</u>
SiO ₂	41.62	47.82	50.56
TiO ₂	0.56	0.87	0.29
Al ₂ O ₃	2.45	1.82	27.86
Fe ₂ O ₃	0.77	0.01	—
FeO	30.19	34.15	2.29
MnO	0.85	0.92	0.07
CaO	7.40	4.35	14.91
MgO	8.64	8.90	0.86
Na ₂ O	0.11	0.08	1.49
K ₂ O	0.03	0.03	0.12
P ₂ O ₅	0.08	—	—
	<u>99.70</u>	<u>98.95</u>	<u>99.45</u>

NORMS

Or	0.2	Or ₂	0.2	Or ₃	0.7	Or ₁
Ab	0.9	Ab ₁₃	0.7	Ab ₁₃	12.6	Ab ₁₅
An	6.1	An ₈₅	4.5	An ₈₄	69.0	An ₈₄
Wo	12.6	Wo ₁₄	7.1	Wo ₈	2.1	Wo ₂₁
En	21.5	En ₂₄	21.9	En ₂₄	2.1	En ₂₂
Fs	56.1	Fs ₆₂	61.9	Fs ₆₈	5.7	Fs ₅₇
Ol	—		1.0		—	
Q	0.3		—		6.7	
Ap	0.2		—		—	
Mt	0.8		—		—	
Ilm	1.1		1.7		0.5	

TABLE 12

MINERAL SEPARATE ANALYSES

	<u>M4</u>	<u>M5</u>	<u>M6</u>
SiO ₂	49.30	49.80	49.37
TiO ₂	0.16	---	0.62
Al ₂ O ₃	30.32	5.60	1.55
Fe ₂ O ₃	---	---	1.83
FeO	1.18	28.16	26.44
MnO	0.02	tr	0.37
CaO	15.73	7.03	4.60
MgO	0.42	10.96	15.54
Na ₂ O	1.66	0.26	---
K ₂ O	0.20	0.10	---
P ₂ O ₅	---	---	---
	<u>98.99</u>	<u>101.91</u>	<u>100.32</u>

NORMS

Or	1.2	Or ₁	0.6	Or ₄		
Ab	14.1	Ab ₁₆	2.2	Ab ₁₄		
An	74.7	Ang ₈₄	13.5	Ang ₈₂		
Wo	1.4	Wo ₃₂	8.9	Wo ₁₀	9.5	Wo ₁₀
En	1.0	En ₂₄	27.2	En ₃₉	38.7	En ₄₇
Fs	1.9	Fs ₄₄	46.4	Fs ₅₁	46.8	Fs ₄₃
Q	4.4					
Mt					2.7	
Ilm	0.3				1.1	
Cor					1.6	

TABLE 12

MINERAL SEPARATE ANALYSES

	<u>M7</u>	<u>M8</u>
SiO ₂	46.70	46.59
TiO ₂	0.06	—
Al ₂ O ₃	33.20	33.42
Fe ₂ O ₃	1.59	—
FeO	—	0.80
CaO	17.40	16.40
MgO	0.27	—
Na ₂ O	1.16	2.04
K ₂ O	0.08	0.20
	<u>100.48</u>	<u>99.68</u>

NORMS

Or	0.5		1.1	Or ₁
Ab	9.8	Ab ₁₁	17.3	Ab ₁₈
An	85.2	Ang ₉	81.5	Ang ₁
Wo	0.7			
En	0.7			
Q	2.1			
Mt	2.3			
Ilm	0.1			

TABLE 12
MINERAL SEPARATE ANALYSES

	<u>M9</u>	<u>M10</u>	<u>M11</u>
SiO ₂	48.49	56.4	49.72
TiO ₂	1.22	0.2	0.56
Al ₂ O ₃	2.03	26.7	2.16
Fe ₂ O ₃	—	1.3	0.58
FeO	32.34	—	23.67
MnO	0.80	—	0.55
CaO	4.14	10.0	10.04
MgO	11.43	—	12.54
Na ₂ O	0.09	5.31	0.21
K ₂ O	0.06	0.41	0.08
	<u>100.60</u>	<u>100.3</u>	<u>100.31</u>

NORMS

Or	0.3	Or ₆	2.2	Or _{2.3}	0.5	Or ₇
Ab	0.7	Ab ₁₂	45.1	Ab ₄₉	1.7	Ab ₂₇
An	5.0	An ₈₂	47.9	An ₄₉	4.5	An ₆₆
Wo	6.5	Wo ₈	0.5		18.9	Wo ₂₂
En	26.5	En ₃₆			27.5	En ₃₈
Fs	54.5	Fs ₅₆			38.3	Fs ₄₀
Ol	4.6				6.5	
Q			2.5			
Mt			1.2		0.8	
Ilm	2.3		0.5		1.1	

TABLE 12

References

- M1 Nuevo Laredo, pyroxene (New analysis, A.D. Maynes, CIT)
- M2 Nuevo Laredo, pyroxene (New analysis, A.D. Maynes, CIT)
- M3 Nuevo Laredo, plagioclase (New analysis, A.D. Maynes, CIT)
- M4 Nuevo Laredo, plagioclase (New analysis, A.D. Maynes, CIT)
- M5 Pasamonte, pyroxene (Foshag⁽⁹⁾)
- M6 Moore County, pyroxene (Henderson and Davis⁽¹⁰⁾)
- M7 Moore County, plagioclase (Henderson and Davis⁽¹⁰⁾)
- M8 Juvinas, plagioclase (Game⁽¹²⁾)
- M9 Juvinas, pyroxene (New analysis, tentative, A.D. Maynes, CIT)
- M10 Shergotty, maskelynite (New analysis, tentative, A.D. Maynes, CIT)
- M11 Shergotty, pyroxene (New analysis, tentative, A.D. Maynes, CIT)

and Juvinas. Separates with various augite-pigeonite proportions were treated with HCl in order to remove plagioclase. The separates were analyzed by X-ray fluorescence for Ca/Fe ratios and the relative intensities of the (220) diffraction peaks for augite and pigeonite were established by X-ray diffraction. Table 13 gives the intensity ratios; Figure 7 plots $I_{Ca}/I_{Ca} + I_{Fe}$ from X-ray fluorescence against $I_{Aug}/I_{Aug} + I_{Pig}$ from X-ray diffraction. The points lie on a straight line, which, when extrapolated to diffraction peak ratios of zero and one, gives the Ca-Fe relations for pure augite and pure pigeonite. The extrapolation to zero augite indicates that the pyroxene of one of the mineral separates (Analysis M2) is essentially pure pigeonite. By using a lever rule, the abundance of augite in the total meteorite sample, marked by the open box, is fixed at 25% of the total pyroxene or about 15% of the total meteorite.

Figure 8 shows the composition of normative pyroxene from the analyzed mineral separates and total meteorite analyses of Nuevo Laredo and Juvinas. For Nuevo Laredo, the $MgSiO_3$ content of each pyroxene is about 25%. By application of the lever rule to the points equivalent to mineral analysis M2 and the bulk chemical analysis, the composition of augite in Nuevo Laredo (in proportion 1:3 to pigeonite) is $Ca_{33}Mg_{23}Fe_{44}$, which is very close to the normative pyroxene of Analysis M4. The ratio of augite to pigeonite is similar in Juvinas and Nuevo Laredo. Applying the lever rule to the data from Juvinas, an augite composition of $Ca_{31}Mg_{31}Fe_{38}$ is indicated. The iron-rich nature of these calcium-rich pyroxenes indicates that a more precise term for them is ferroaugite.

Analyses M-2 and M-9 give the best determinations of pigeonite compositions that have been made for these meteorites. The analysis of

-110-
TABLE 13

X-RAY FLUORESCENCE AND X-RAY DIFFRACTION DATA FOR
PIGEONITE-FERROAUGITE MIXTURES

	Fluorescence I_{Ca}/I_{Fe+Ca}	Diffraction $I_{Aug}/I_{Aug+Pig}$ (220 Peak)
Juvinas		
#41	.125	.06
#42	.214	.25
Nuevo Laredo		
#29(Total meteorite)	---	.24
#46	.288	.35
#43	.283	.38
#48	.323	.48
#44	.176	.14
#24(M2, pigeonite)	.105	---

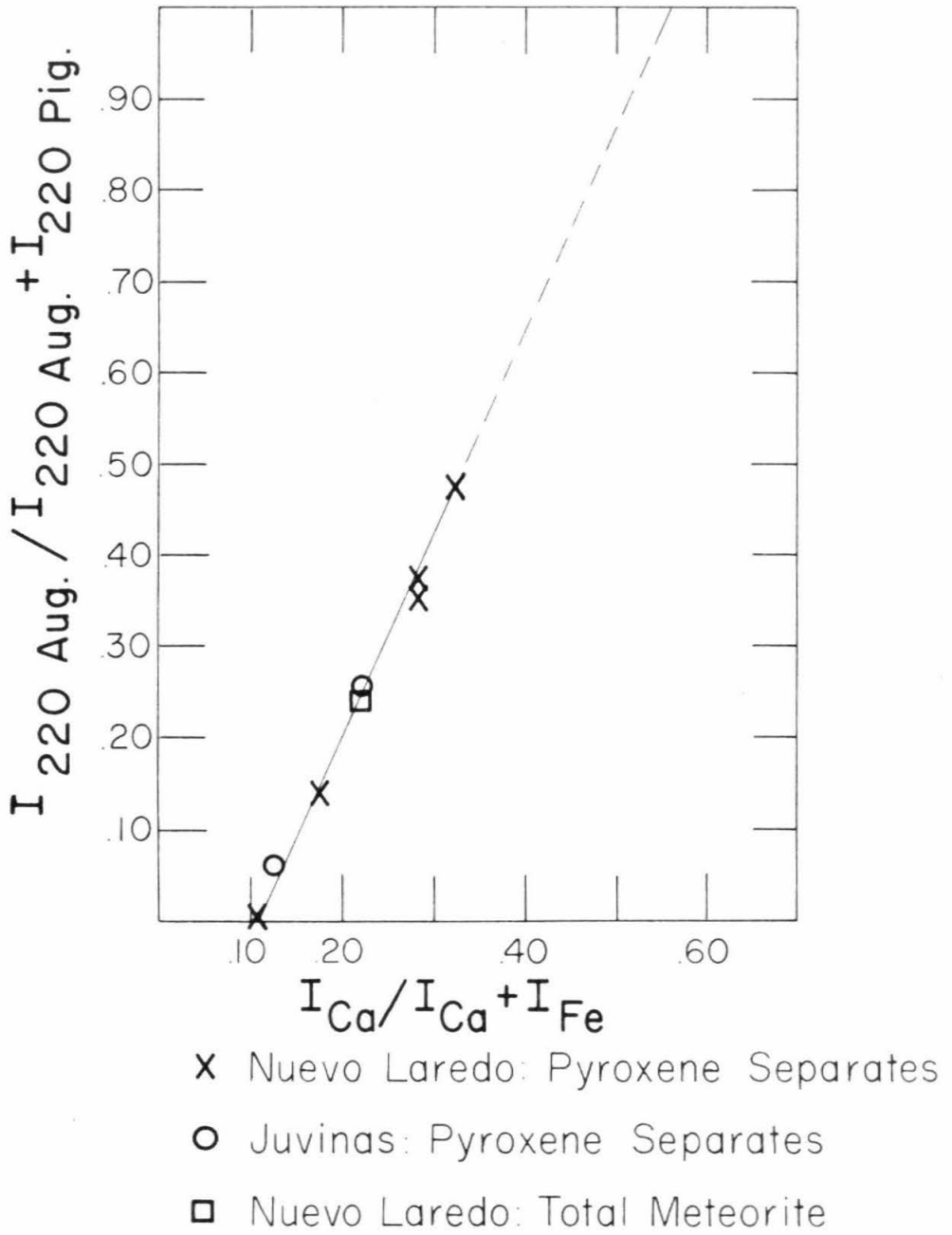


Figure 7

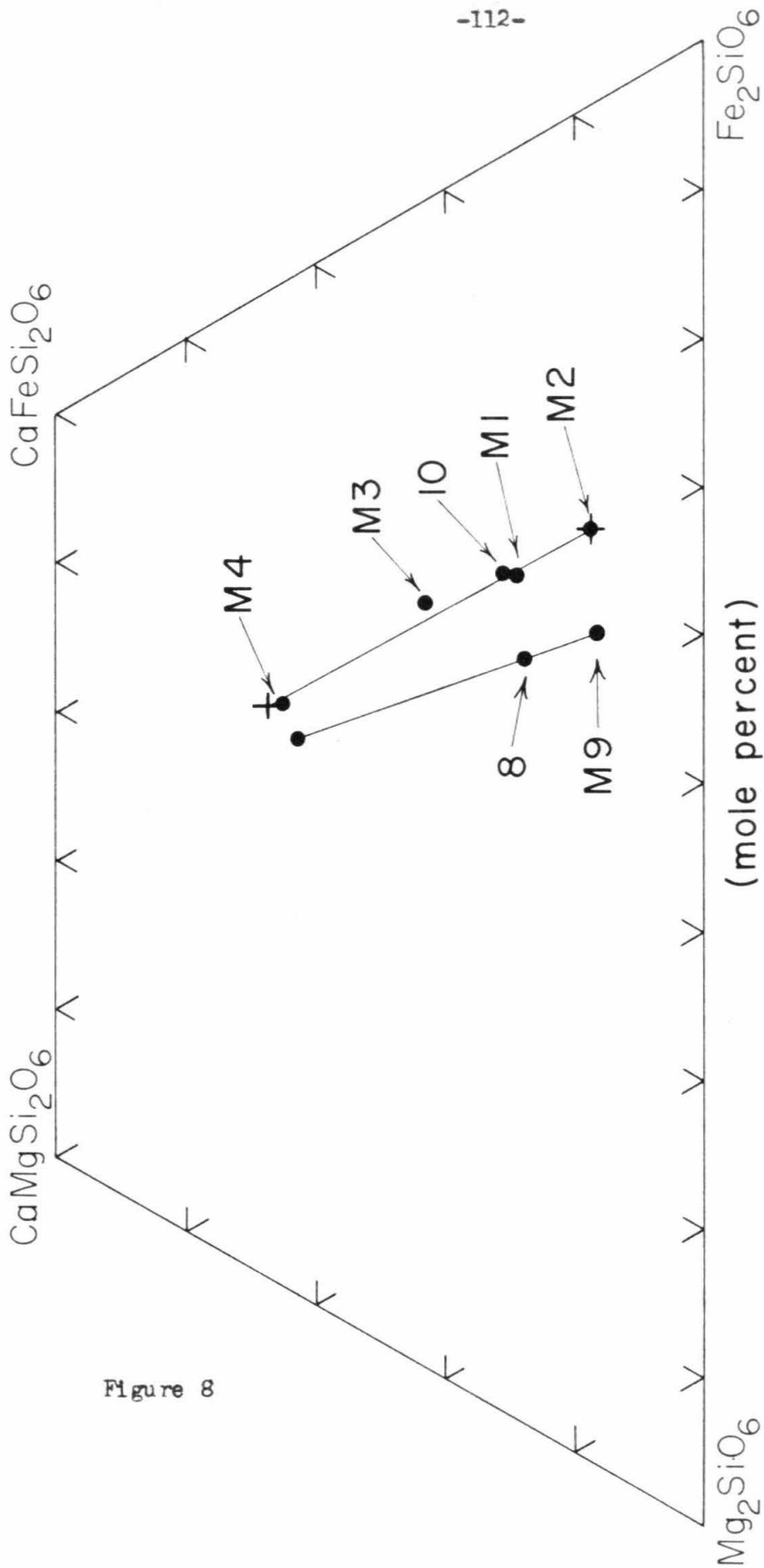


Figure 8

Nuevo Laredo pigeonite is consistent with an iron-rich pigeonite that contains about eight mole percent wollastonite component. The composition of this pigeonite is as iron-rich as any known from terrestrial occurrences. In the Skaergaard intrusion, more iron-rich systems contain the assemblage fayalite-augite-quartz rather than the assemblage pigeonite-augite (Wager and Deer⁽⁴⁰⁾). More highly differentiated basaltic achondrites could be presumed to have fayalite and quartz rather than pigeonite. The Juvinas pigeonite has a lower ratio of Fe/Fe+Mg but is otherwise similar to the Nuevo Laredo pigeonite.

The plagioclase separates partially analyzed for alkalis indicate a plagioclase composition of about An₈₅ for Nuevo Laredo (Table 7). The total analysis of the plagioclase separate gives a normative plagioclase composition of about An₈₅. The plagioclase separate was contaminated, however, by pyroxene and free silica. The pyroxene component of the purest plagioclase separate may be contained in the higher-index inclusions common to the plagioclase of the iron-rich basaltic achondrites.

Consideration of the four analyses from Nuevo Laredo, which have a wide range of pyroxene-plagioclase ratios, but for which the normative plagioclase compositions are uniform, indicates that the Al₂O₃ content of the pyroxene is small. Large amounts of alumina in the pyroxene would lead to more calcic normative plagioclase in the pyroxene-rich separates. Assuming that the plagioclase has a uniform composition of Ab₁₅, and all alkalis in the pyroxene analysis are due to feldspar contamination, the maximum allowable Al₂O₃ in the pyroxene is about 0.4%. The larger Or-Ab ratio of the pyroxene concentrates probably is due to rounding errors in the determination of the very small K₂O content. These values of Al₂O₃ in the pyroxene are somewhat lower than the Al₂O₃ reported by Hess and Henderson(1949) for the pyroxene of Moore County (Analysis 6), but are

consistent with values reported for pyroxenes of Kapoeta (Fredriksson and Keil⁽²⁰⁾). If there is any sodium and potassium in the pyroxene, the Al_2O_3 values are greater than those calculated from the norm.

According to the norm the analysis of "pigeonite" from Pasamonte made by Foshag⁽⁹⁾ included about 15% plagioclase (Analysis M5). It is likely that this is not a representative sample either of the total pyroxene composition of Pasamonte (compare it with the normative pyroxene of the bulk analysis) or of the average pigeonite composition. The wide variation of Fe/Fe+Mg shown by pyroxenes in Pasamonte and the presence of both pigeonite and ferroaugite make it difficult to obtain a representative pyroxene sample.

The analyses of plagioclase and pyroxene from Moore County are less suspect of contamination because the coarser grain size of that meteorite should facilitate mineral liberation. However, the pyroxene analysis may not be representative of the total pyroxene due to the presence of augite in exsolution lamellae (Hess and Henderson⁽¹¹⁾) and as individual grains (this work). There may be some variation of plagioclase composition which gives rise to a more calcic normative plagioclase than that of the analyzed plagioclase, but the observed discrepancy would be expected if the pyroxene does contain as much as 1.5% Al_2O_3 . On the other hand, the determination of alkalis made on a sample of plagioclase from Moore County in this work gives somewhat lower values than the data of Henderson and Davis⁽¹⁰⁾ and is in better agreement with the optical data.

The analysis of plagioclase from Juvinas is difficult to understand completely because it was shown by Game⁽¹²⁾ that the optical properties measured for that plagioclase indicated a more calcic composition than is indicated by the chemical analysis. The composition of the plagioclase

determined by Game is considerably more alkalic than that determined in this work (Table 3). The separational technique used by Game apparently concentrated more alkali-rich plagioclase, which probably corresponds to a concentration of interstitial plagioclase. As the interstitial plagioclase tends to be untwinned, optical determinations may have been biased towards less abundant more calcic grains.

Mineral compositions in the Shergotty meteorite

The average grain size in Shergotty is coarser than in many of the other basaltic achondrites and it was expected that good separations would be possible. Consideration of the analyses of a maskelynite separate and a pyroxene separate, taken in conjunction with the total meteorite analysis, yields evidence bearing on the efficiency of the mineral separation as well as the true compositions of the minerals.

Table 14 compares the norms calculated from the analysis of the mineral separates (M-9; M-10) and the bulk chemical analysis. The normative plagioclase from the bulk analysis is in good agreement with the composition of the analyzed maskelynite and the normative pyroxene of the bulk analysis is in agreement with the analyzed pyroxene composition. However, some significant discrepancies exist. The normative plagioclase composition of the pyroxene analysis gives a more calcic composition and has a larger orthoclase/albite ratio than the analyzed maskelynite. The normative feldspar of the bulk analysis has more orthoclase than the analyzed maskelynite and the normative pyroxene of the total analysis contains less wollastonite component than the analyzed pyroxene. The pyroxene analysis shows significant undersaturation with respect to silica. These discrepancies suggest that the pyroxene has small amounts of aluminum and alkalis in solid solution.

TABLE 14

NORMS FOR SHERGOTTY TOTAL METEORITE AND MINERAL SEPARATE ANALYSES

	Maskelynite		Pyroxene		Total Meteorite	
Or	2.2	Or _{2.3}	0.5		0.9	Or _{3.6}
Ab	45.1	Ab ₄₉	1.7		10.8	Ab ₄₇
An	47.9	An ₄₉	4.5		12.1	An ₄₉
Wo	0.5		18.9	Wo ₂₂	14.0	Wo ₂₀
En	---		27.6	En ₃₈	23.4	En ₃₉
Fs	---		38.2	Fs ₄₀	32.2	Fs ₄₁
Fo	---		2.5		---	
Fa	---		4.0		---	
Q	2.5		---		0.9	
Ap	---		---		1.6	
Ilm	0.5		1.1		1.8	
Cr	---		---		0.3	
Mt	1.2		0.8		2.2	

The normative feldspar composition of the total meteorite analysis differs from the composition of the maskelynite. For the total meteorite analysis, the amount of potassium that must be in solution in the pyroxene to remove the discrepancy is equivalent to 0.08 weight percent of K_2O in the pyroxene, which is identical to the value determined for the pyroxene separate. This suggests that all of the sodium, potassium and aluminum in the pyroxene analysis is in solid solution in the pyroxene. It implies that the pyroxene separate had essentially no maskelynite as a contaminant.

The mineral analyses can be used to reconstitute the total meteorite analysis. Table 15 gives the reconstituted analysis and compares it with the total meteorite analysis. The proportions of maskelynite and pyroxene have been specified by the sodium contents of the three analyses and the only other restriction placed on the calculation is that the sum of all minerals is 100%. The amount of calcium due to the phosphate is fixed by the amount of P_2O_5 . TiO_2 , Fe_2O_3 , MnO and Cr_2O_3 can be matched in an arbitrary manner, so the comparison between the reconstituted analysis and the total meteorite analysis is not significant for those oxides. The significant feature of the comparison is the close agreement for the major oxides Al_2O_3 , FeO , CaO , and MgO . SiO_2 is in good agreement if there is about three percent of modal SiO_2 . These values are in reasonable agreement with the modal analysis given for Shergotty in Chapter II.

These comparisons serve as an internal check on the chemical analyses, but also they substantiate the conclusion that the Shergotty pyroxene has about two percent Al_2O_3 and small amounts of sodium and potassium. The amount of aluminum in the Shergotty pyroxene appears to be greater than

TABLE 15

RECONSTITUTED TOTAL METEORITE ANALYSIS FOR SHERGOTTY

	Pyroxene (73.5%)	Maskelynite (20.5%)	Quartz (2.0%)	Apatite (1.5%)	Others* (2.5%)	Calc. Total	Observed Total
SiO ₂	36.54	11.56	2.00	----	----	50.10	50.10
TiO ₂	0.41	0.04	----	----	0.45	0.90	0.92
Al ₂ O ₃	1.58	5.48	----	----	----	7.06	6.68
Fe ₂ O ₃	0.42	0.26	----	----	0.80	1.48	1.49
FeO	17.40	----	----	----	0.97	18.37	18.66
MnO	0.40	----	----	----	0.10	0.50	0.50
CaO	7.38	2.05	----	0.80	----	10.23	10.03
MgO	9.21	----	----	----	----	9.21	9.40
Na ₂ O	0.15	1.08	----	----	----	1.23	1.28
K ₂ O	0.06	0.08	----	----	----	0.14	0.16
P ₂ O ₅	----	----	----	0.70	----	0.70	0.71
Cr ₂ O ₃	----	----	----	----	0.18	0.18	0.18

* Includes ilmenite, magnetite and chromite.

in the other basaltic achondrite pyroxenes and indicates another compositional difference between Shergotty and the other meteorites.

IV

MINERALOGY

Introduction

The minerals described in this section include pyroxenes, plagioclase, free silica, olivine, metallic iron and other minor phases. The section gives the detailed variations of the principal minerals as determined by optical and X-ray methods. Emphasis is placed on those properties which have been shown to be useful in the determination of mineral compositions or the structural state of minerals. The section also includes some X-ray fluorescence and emission spectrographic data on the nickel content of metallic iron of the basaltic achondrites and on the distribution of nickel between metal and silicates in these and other meteorites.

Pyroxenes

Color

The principal pyroxenes of the basaltic achondrites are pigeonite, ferroaugite and hypersthene. Some of the hypersthene crystallized directly from the magma. In coarse grains it varies from colorless for compositions of $Fe/Fe+Mg = 0.2$ to yellow for compositions of $Fe/Fe+Mg = 0.4$, but it is colorless in thin section. Hypersthene which has formed from pigeonite by inversion may appear dark brown or black in large grains because of abundant inclusions. Pigeonite varies from yellow to deep brown or black in coarse grains in the composition range 0.5 to 0.67. In thin section, the color varies from colorless to yellow brown. In many of the meteorites where pigeonite contains abundant inclusions the color, in thin section, is brown or green and, in large grains, is greenish black. Ferroaugite is light brown in thin section and may be gray,

brown or black in coarse grains depending upon the concentration of inclusions.

Optical properties; composition

Indices of refraction of pyroxenes have been determined by immersion methods using a variable monochromator to match oil and mineral indices. For orthopyroxenes, n_z was measured on grains showing parallel extinction; for clinopyroxenes, n_y was measured on (100) or (001) parting flakes where the orientation of the indicatrix can be determined by use of the off-center optic axis figure (Slawson and Peck⁽⁴³⁾; Hess⁽²⁴⁾).

By the use of more than one oil of known dispersion, both the index of refraction of the minerals in N_{D} light and the absolute dispersion of the minerals can be determined. Table 16 gives the data for pyroxenes that show relatively little compositional variation. For a given oil, both the range and the average wave lengths where the appropriate index matched that of the immersion oil are given. In Figures 9 to 11 the data are plotted on Hartmann nets (Winchell and Winchell⁽⁴⁴⁾, p. 281) on which absolute dispersions are linear functions of wave length. In order to use these diagrams for the determination of indices of refraction, a line representing the dispersion of the oil ($n_F - n_C$) is drawn between the base at $C=654\mu$ and the vertical line at $F=486\mu$. Through the point representing the index of the oil in N_{D} light, a line is drawn parallel to the oil dispersion curve. This line gives the index of refraction of the immersion oil as a function of wave length. To determine the index of refraction of a mineral grain, the index is matched with that of the oil at some wave length. The intersection of the vertical line representing the match wave length and the oil index also is the intersection of the wave length line with the line giving

TABLE 16

WAVE LENGTHS AT WHICH MINERAL INDEX AND IMMERSION OIL INDEX
ARE MATCHED
FOR PYROXENES OF SOME BASALTIC ACHONDRITES

	n_{oil} *	(a) Pigeonite, n_y		<u>Average</u>
		<u>No. Meas.</u>	<u>Range</u>	
Nuevo Laredo	1.708	9	470-530	510
	1.718	6	540-580	567
	1.730	3	680-682	681
Juvinas	1.708	3	500-520	510
	1.718	4	578-598	587
Stannern	1.708	5	465-500	479
	1.730	5	555-590	575
Moore County	1.700	3	520	520
	1.708	3	555-565	559
	1.718	1	670	670
Sioux County (analyzed frag.)	1.718	4	612-640	610
Bialystok	1.718	7	525-602	541
(b) Ferroaugite, n_y				
Nuevo Laredo	1.708	4	518-578	538
	1.718	4	590-630	605
	1.730	1	610	610
Juvinas	1.718	2	570-605	587

* Shillaber immersion oils. Corrected for temperature to 25°C

TABLE 16,
(Continued)

(c) Hypersthene, n_z

	<u>n_{oil}</u>	<u>No. Meas.</u>	<u>Range</u>	<u>Average</u>
Juvinas	1.718	2	490-500	495
	1.730	1	595	595
Stannern	1.730	10	472-528	498
	1.740	8	545-630	587
Moore County	1.708	1	470	470
	1.718	5	500-544	528
	1.730	5	600-668	620
Binda, fragment	1.690	5	498-505	500
	1.700	6	550-562	556
Sioux County Analyzed fragment	1.718	3	460-470	467
Sioux County Coarsest fragment	1.730	5	520-560	543
	1.718	4	460-475	466
Serra de Mage	1.708	6	480-488	483
Tatouhine	1.678	1	490	490
Hypersthene	1.680	2	502-503	503
Achondrite	1.682	4	506-508	508
	1.690	3	554-562	559
	1.696	1	625	625
	1.700	1	675	675
Shalka	1.678	3	487-493	490
	1.680	4	492-499	496
	1.682	4	505-512	508
	1.690	3	548-556	552
	1.696	3	599-605	600

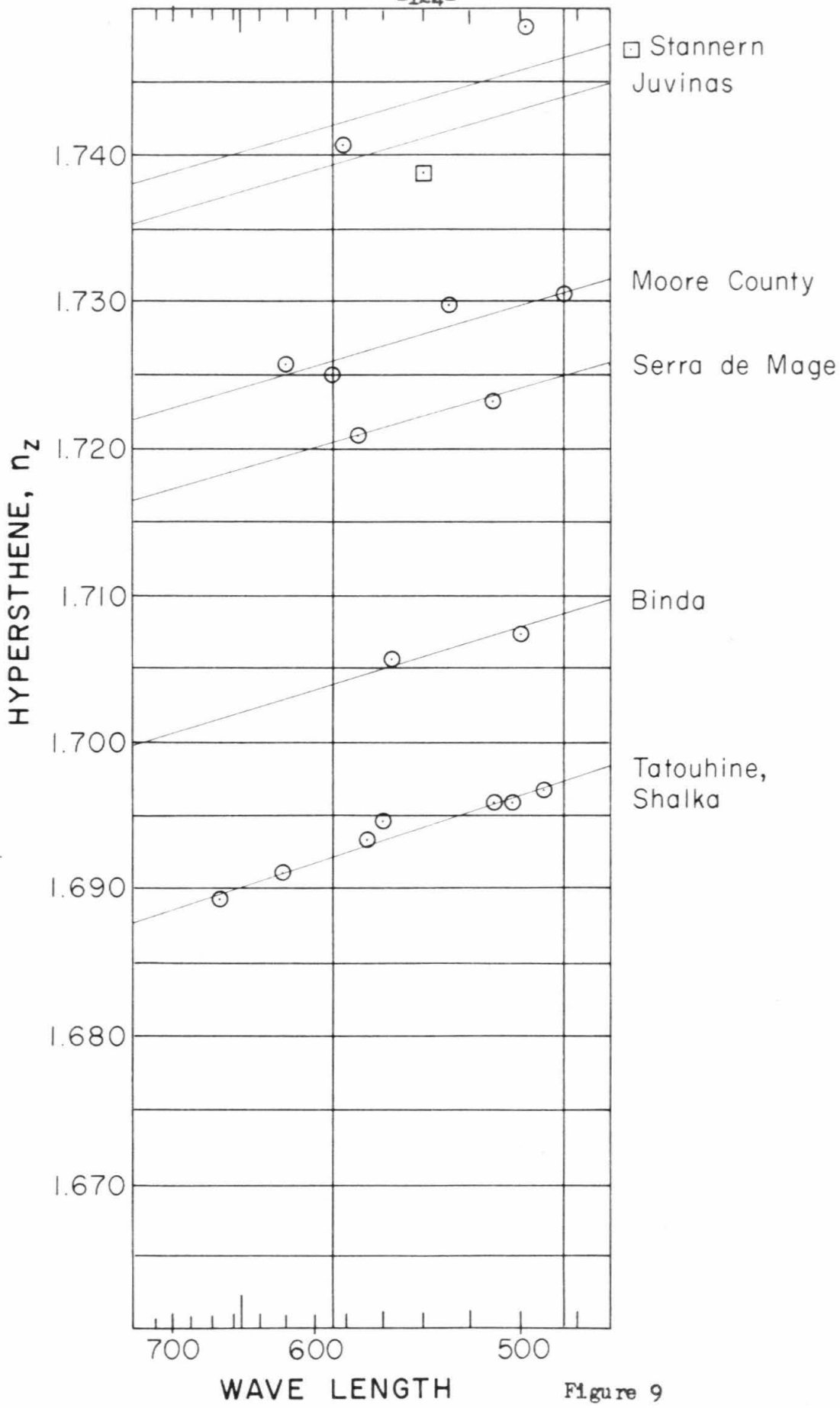


Figure 9

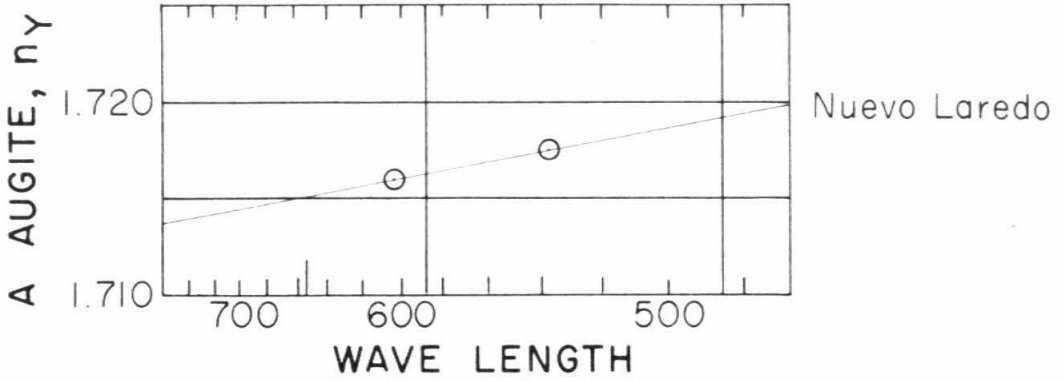


Figure 10

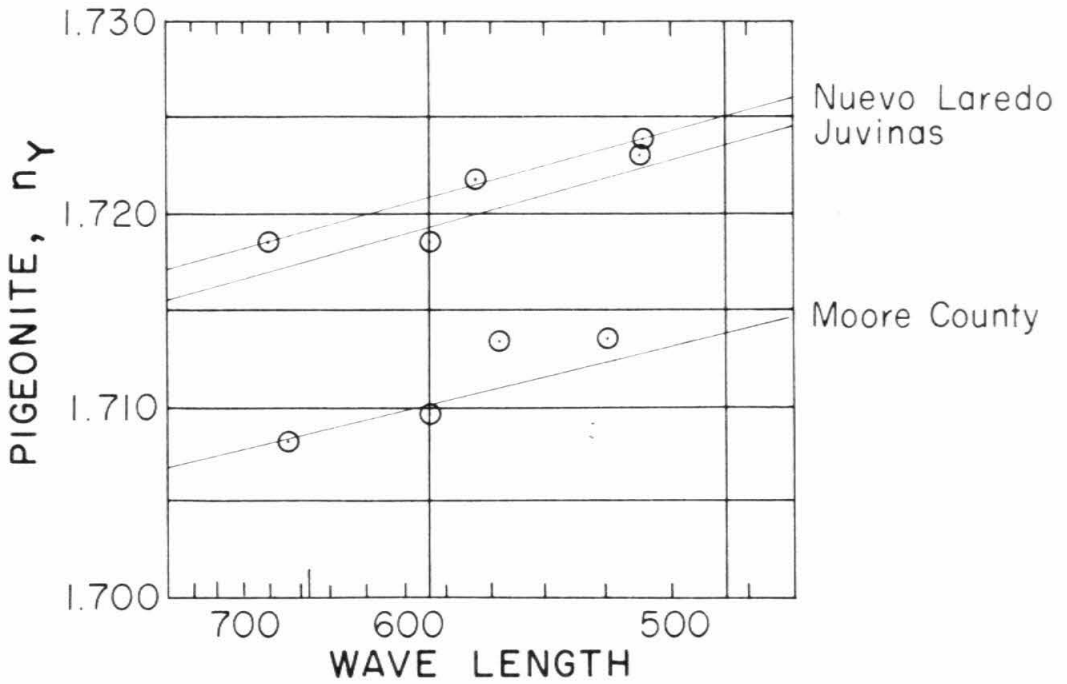


Figure 11

the index of the mineral as a function of wave length. The mineral dispersion curve is then used to obtain the index of refraction for Na_D light.

There is some scatter of the data especially for iron-rich pyroxenes for a number of reasons:

(1) In many of the samples studied there is limited but real variation of the pyroxene composition.

(2) The presence of inclusions which cloud grains and of fine exsolution lamellae interferes with determination of the exact wave length at which mineral and oil indices are matched. In extreme cases central illumination instead of Becke line tests must be used.

(3) The clinopyroxenes may not lie exactly on parting surfaces which may lead to a small discrepancy in the determination of n_y . In some samples where both clinopyroxene and orthopyroxene are present, it is possible to confuse an off-center nearly uniaxial clinopyroxene interference figure with an off-center orthopyroxene interference figure with large $2V$.

The mineral dispersion curves have been determined only for the orthopyroxene of the Shalka and Tatouhine calcium-poor achondrites. These meteorites have rather uniform pyroxene composition and have pyroxene which is magnesium-rich and has refractive indices below 1.700. For these compositions, immersion oils were available at intervals of .002; for index of refraction above 1.700, immersion oils were only available for intervals of .01. The dispersion curves for the two well determined pyroxenes have been assumed to be valid over the range of composition of the orthopyroxenes and have been assumed equal to the dispersion for the clinopyroxenes. Dispersion is not a sensitive function of composition and the assumption seems valid, but should be tested for samples of homogeneous iron-rich pyroxenes.

Figures 9 to 11 show that the data for the various pyroxenes can be fit to the dispersion curves with a scatter of not more than $\pm .002$ in most cases. For the pyroxenes of Shalka and Tatouhine, the index of refraction in Na_D light is probably correct to within $\pm .0005$. Temperature information was obtained from a thermometer mounted on the microscope stage. Corrections have been made for temperature and were generally less than .001. The immersion oils were calibrated with an Abbe refractometer.

Table 17 gives the indices of refraction in Na_D light for those pyroxenes which can be standardized by comparison with the Fe/Fe+Mg ratio of the bulk chemical analysis. Also given are data from this and other studies of optic angles and extinction angles. For clinopyroxenes the indices of refraction are insensitive to variations in calcium content, whereas the optic angle is a function of calcium content (See Hess⁽⁴⁵⁾). It has been reported by others (Foshag⁽⁹⁾; v. Engelhardt⁽¹⁵⁾) that there is a continuous variation of optic angles in calcium-poor clinopyroxenes from the typical 0° of pigeonite to about 30° in the Pasamonte and Stannern meteorites. Investigation of the pyroxenes of Nuevo Laredo and Juvinas showed, however, that there is not a continuum of pyroxene compositions, but that pigeonite with optic angle from 0° - 10° coexists with augite with optic angle from 35° - 40° . The indices for pyroxenes of Nuevo Laredo and Moore County have been standardized relative to composition by means of the analyzed mineral separates given in Part III.

In Figure 12 are plotted the indices of refraction of the pyroxenes studied as a function of composition. These data only include those meteorites where reliable chemical analyses (see Part III) exist and where there is small variability of pyroxene composition. The iron-

TABLE 17

COMPOSITIONS USED FOR STANDARDIZATION OF PYROXENE OPTICAL PROPERTIES

Hypersthene	n_z	Fe/Fe+Mg
Stannern	1.743	0.61 ^a
Juvinas	1.739	0.61 ^b
Moore County	1.725	0.50 ^a
Binda	1.704	0.35 ^a
Tatouhine	1.692	0.24 ^a
Shalka	1.692	0.22 ^a
Pigeonite	n_y	Fe/Fe+Mg
Nuevo Laredo	1.721	0.67 ^b
Juvinas	1.718	0.61 ^b
Sioux County	1.715	0.58 ^a
Moore County	1.710	0.50 ^b
Ferroaugite		
Nuevo Laredo	1.716	0.56 ^b

a Normative ratio

b From analyzed pyroxene

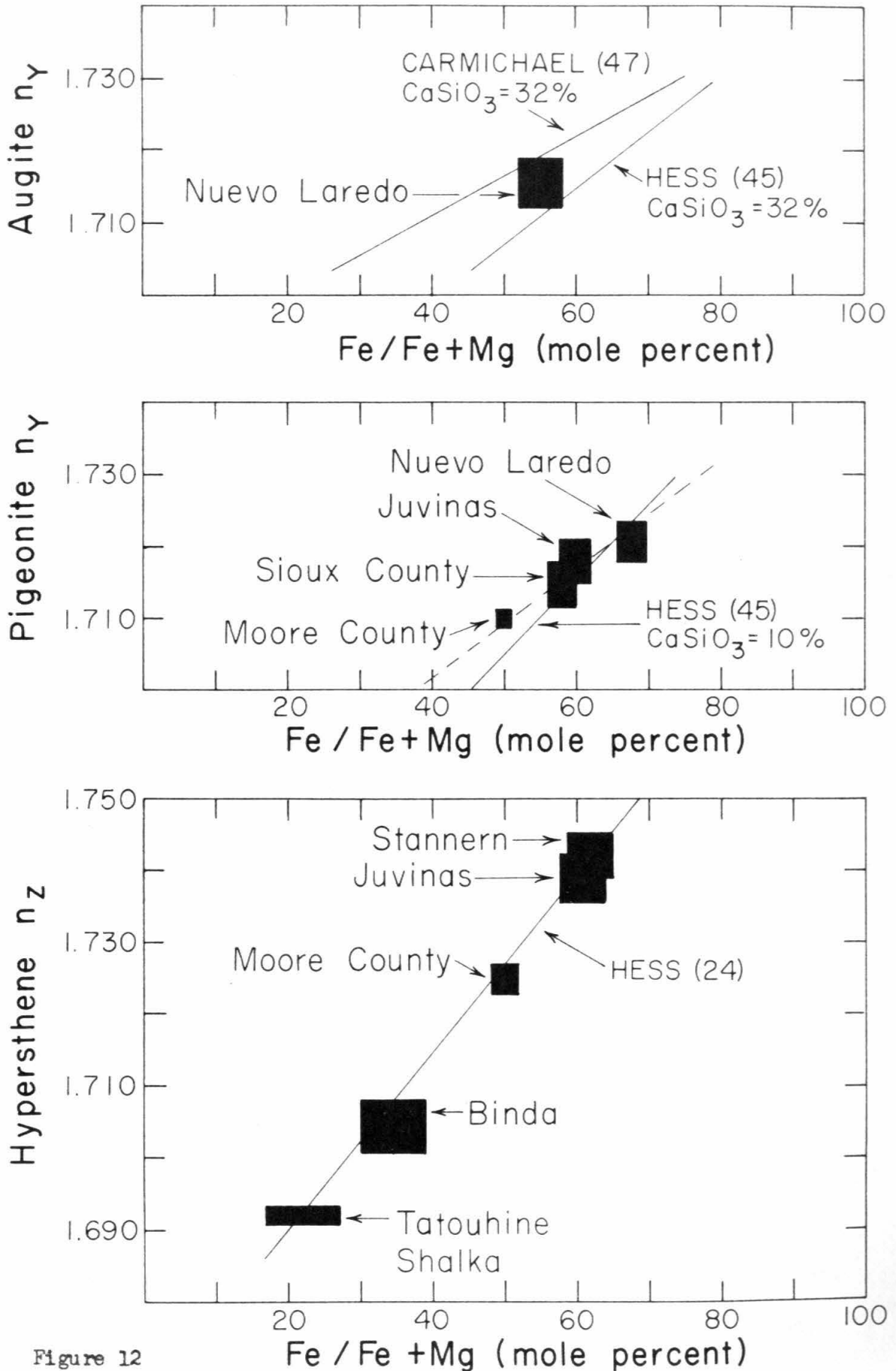


Figure 12

magnesium ratios for the two hypersthene achondrites have been obtained from a norm calculated from the analyses given by Urey and Craig⁽²⁾. The data of Figure 12 are compared to determinative curves previously published by Hess⁽⁴⁵⁾, Carmichael⁽⁴⁷⁾ and Hess⁽²⁴⁾. For the pigeonite, the determinative curve has been plotted for a constant 10% of CaSiO_3 molecule, for augite, a constant 32% CaSiO_3 . For the orthopyroxenes the fit of the points from the meteorites is good and one can reasonably expect to be able to determine orthopyroxene compositions from the indices to within one mole percent FeSiO_3 of the true composition.

The curves presented by Hess⁽⁴⁵⁾ for clinopyroxenes were based on few empirical data in the iron-rich compositions. It is not surprising, then, that the values obtained for the clinopyroxenes of the basaltic achondrites differ somewhat from his curves. In the case of pigeonites the deviation is not too great for the range considered, but the dashed line of Figure 12 has been used to determine compositions of other pigeonites in this study. For ferroaugite, Carmichael⁽⁴⁷⁾ presented curves that more closely fitted data for ferroaugites from acid glasses. The single value for ferroaugite from Nuevo Laredo falls between the curves of Carmichael and Hess; optical determinations of augite compositions are subject to uncertainty of about 5% of any of the major components.

There is only a little data on the Al_2O_3 content of pyroxenes from the basaltic achondrites. From the four analyzed mineral separates from Nuevo Laredo an estimate of the alumina content can be made by noting that the normative plagioclase compositions differ slightly in the plagioclase-rich and pyroxene-rich concentrates. Although it may represent a biased sampling of the plagioclase, which shows some compositional variation, the difference between the two plagioclase compositions can be

explained if there is from 0.3-0.4% Al_2O_3 in the pyroxene. This figure is somewhat smaller than the 1.5% Al_2O_3 reported by Hess and Henderson⁽¹¹⁾ for a pyroxene separate from Moore County, but is consistent with the electron microprobe analyses of pyroxenes from Kapoeta (Fredriksson and Keil,⁽²⁰⁾) which gave values of about 0.5% for Al_2O_3 . It is evident that the clinopyroxenes of the basaltic achondrites have quite low alumina contents.

Table 18 gives index measurements for meteorites in which the pyroxene shows substantial compositional variation.

Table 19 gives the composition of pyroxenes from meteorites for which chemical data are inadequate and from meteorites where there is a large variation of composition. These compositions have been taken directly from the standard curves given in Figure 12.

The variability of pyroxene composition from Pasamonte and Petersburg arises from different causes. In Pasamonte the variation is primarily due to compositional zoning during crystallization (See Plate 23b). One set of data from Pasamonte (fragment) is from a single lithic fragment separated from the breccia. This shows a wide range of variation in pyroxene composition that is not greatly increased by adding observations made on the total meteorite sample, even when an attempt was made to find the extreme pyroxene compositions present.

The compositional variation in Petersburg arises from the brecciation and mixing of diverse lithologies shown by this meteorite. Most of the grains for which indices have been measured are individual fragments of orthopyroxene which do not show any obvious composition zoning in thin section. These grains have been mixed with clinopyroxenes which are generally more iron-rich than the orthopyroxene. The clinopyroxene

TABLE 18

INDEX OF REFRACTION DATA FOR PYROXENES OF SOME METEORITES

WITH VARIABLE PYROXENE COMPOSITIONS

(Wave length, λ , at which mineral and immersion oil refractive indices are matched)

	No. of measured grains					
	<u>1</u>	<u>2</u>	<u>3</u>	<u>4</u>	<u>5</u>	
n_{oil}^*	1.708	1.700	1.708	1.708	1.708	1.690
440	-	2	-	-	-	-
440-460	-	1	-	-	-	-
460-480	-	1	-	2	2	-
480-500	-	-	-	4	1	-
500-520	-	1	-	2	-	2
520-540	2	1	-	2	-	1
540-560	-	2	-	1	-	1
560-580	-	2	1	-	-	-
580-600	-	1	-	-	-	11
600-620	-	2	1	-	-	8
620-640	-	-	-	-	-	1
640-660	-	-	-	-	-	2
660	-	2	1	-	-	-

- 1 Petersburg, hypersthene, n_z
- 2 Petersburg, pigeonite, n_y
- 3 Pasamonte, pigeonite, n_y
- 4 Pasamonte, ferroaugite, n_y
- 5 Estherville, hypersthene, n_z

* Shillaber immersion oils, $N_F - N_C$ 0.29. Data corrected to 25°C.

TABLE 19

COMPOSITION OF PYROXENES DEDUCED FROM OPTICAL DATA

(Parenthesis give average values)

	Hypersthene (Fe/Fe+Mg)	Pigeonite (Fe/Fe+Mg for 10% CaSiO ₃)	Ferroaugite (Fe/Fe+Mg for 32% CaSiO ₃)
Nuevo Laredo	—	0.67	0.56
Juvinas	0.58	0.61	0.58
Stannern	0.60	0.62	—
Sioux County	0.58	0.59	—
Sioux County, coarsest fragment	0.57	0.59	—
Bialystok	—	0.60-0.70(0.65)	—
Pasamonte, fragment	—	0.48-0.70(0.64)	0.73
Petersburg	0.24-0.45(0.32)	0.58	—
Binda, fragment	0.32	—	—
Estherville	0.16-0.28(0.20)	—	—
Serra de Mage	0.44	—	—
Moore County	0.50	0.50	—
Tatouhine(hypersthene	0.23	—	—
Shalka achondrites)	0.23	—	—

of Petersburg is pigeonite and is generally filled with inclusions that do not allow easy measurement of refractive index. Although it is not possible to determine the proportion of iron-rich pigeonite to magnesium-rich orthopyroxene by optical means, the chemical analysis by Smith⁽¹⁷⁾ shows a much higher iron content than would be indicated by the average orthopyroxene optical data. This suggests that, in the sample analyzed by Smith, pigeonite was relatively more abundant than hypersthene.

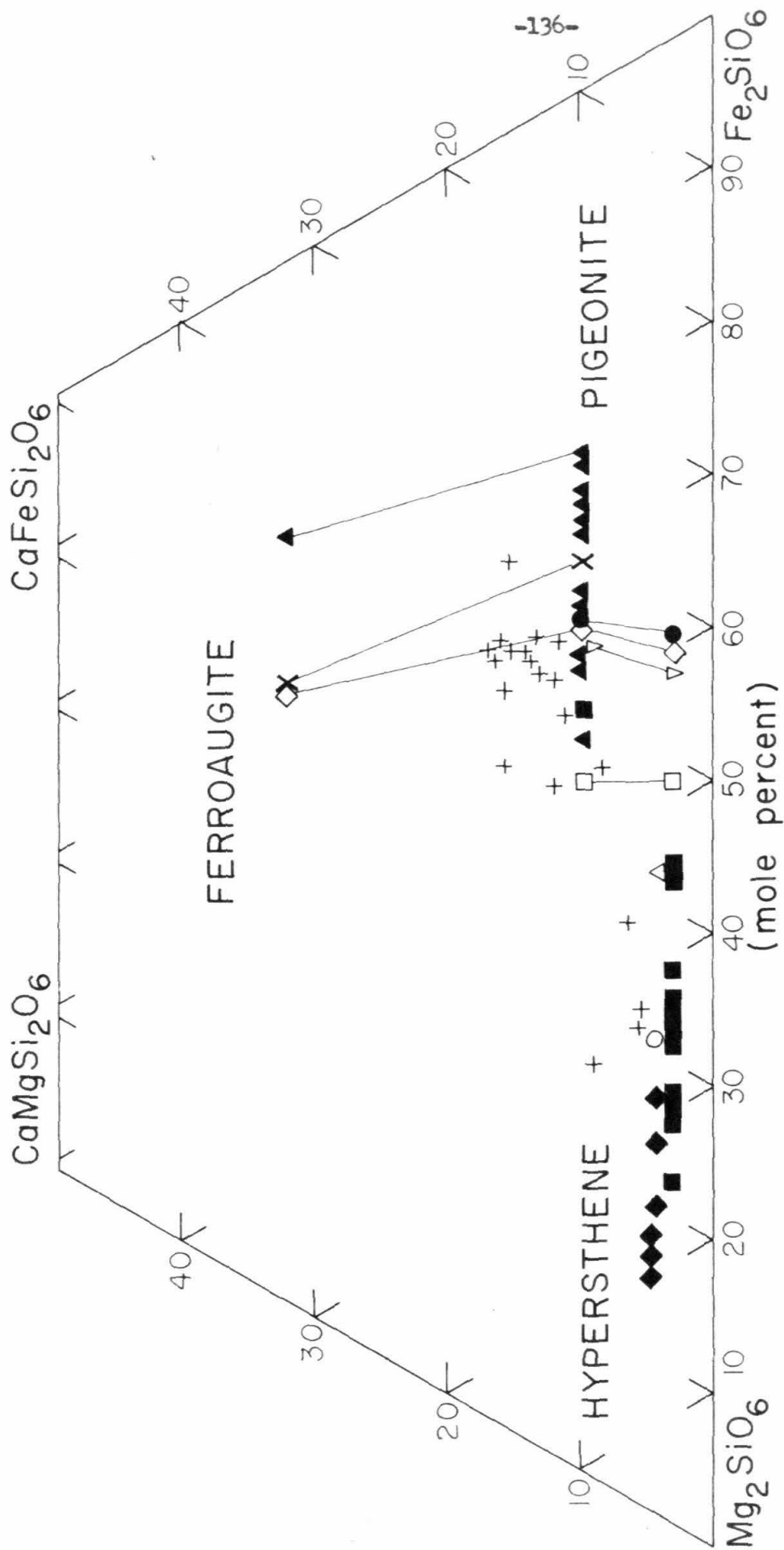
Without direct observations made on lithic fragments it is difficult to determine whether hypersthene has crystallized directly from the magma or has formed by inversion from pigeonite. In the Stillwater complex, Hess⁽²⁴⁾ has shown that there is a distinct Fe/Fe+Mg at which pigeonite replaces hypersthene as the primary magmatic pyroxene. It might be expected that a similar relation holds for the basaltic achondrites. However, only limits can be placed on the composition at which the transition takes place. The most magnesian pigeonite observed is the pigeonite of Serra de Mage, which has entirely inverted to hypersthene. The most iron-rich hypersthene which is definitely of direct magmatic crystallization is that of Binda. The composition at which primary hypersthene is replaced by primary pigeonite in the basaltic achondrites appears to be between Fe/Fe+Mg = 0.35 and 0.45. If the composition of pyroxene could be determined easily and accurately in thin section, it is probable that a study of Petersburg or another howardite could give more precise information as to the composition at which hypersthene is replaced by pigeonite as the primary magmatic pyroxene.

The discovery of independent grains of augite in Nuevo Laredo and Juvinas led to a search for augite in other basaltic achondrites. A single grain of augite was found in a thin section of Moore County.

Augite has also been observed in Sioux County, Pasamonte, and Stannern, although there is still some question as to the continuity of the calcium variation in Stannern and Pasamonte clinopyroxenes. In Shergotty, both augite and pigeonite are present in zonal relationships in the same grain (Plate 28c). The pigeonite has $2V$ which varies from 0° to 15° and the augite varies from 30° to 40° . There are definite discontinuities of the optic angle across the boundaries shown in Plate 28c.

Figure 13 represents graphically the measured and inferred compositions of pyroxenes in the basaltic achondrites studied here. As, in general, the calcium contents of the low-calcium pyroxenes have not been determined, the CaSiO_3 content of the orthopyroxenes has been assumed to be 3%. For the pigeonites, it has been assumed that there is a regular decrease in calcium content from 10% CaSiO_3 to 8% CaSiO_3 over the range $\text{Fe}/\text{Fe}+\text{Mg} = 0.5$ to 0.67 . Some of the pigeonite in Pasamonte and Stannern may have more CaSiO_3 than is indicated on the diagram. Where the petrographic data is available, the distinction between hypersthene formed by inversion and hypersthene which has crystallized directly from the magma has been made.

A more complex discussion of the pyroxene variations is given in the section on Petrologic Trends. The general features are: (1) for the magnesium-rich meteorites, hypersthene is the stable pyroxene phase; (2) for intermediate compositions, pigeonite is the primary magmatic phase, but much of the pigeonite has inverted to hypersthene; (3) pigeonite is abundant in the iron-rich meteorites; (4) ferroaugite occurs only in meteorites with $\text{Fe}/\text{Fe}+\text{Mg}$ greater than 0.5 and is only abundant in meteorites with $\text{Fe}/\text{Fe}+\text{Mg}$ greater than 0.6 . Perhaps the most important feature of this diagram is that the pyroxene compositional variation



Pyroxenes of Some Basaltic Achondrites

- ▲ Pasamonte ● Stannern ○ Binda
- × Nuevo Laredo □ Moore County ◇ Estherville
- ◇ Juvinas △ Serra de Mage + Normative
- ▽ Sioux County ■ Petersburg

Figure 13

appears to be continuous. Although the meteorites can be divided into groups on the basis of chemical composition, the pyroxenes show a continuous variation. The pyroxene of the Estherville mesosiderite fits into the trend. The continuous variation gives strong indication that the basaltic achondrites, including eucrites, howardites, and mesosiderites, have a common type of magmatic origin. It is of interest to note that the determinations of pyroxene compositions made by Fredriksson and Keil⁽²⁰⁾ on the Kapoeta howardite indicate that the pyroxene of that meteorite spans the entire range reported here for the basaltic achondrites.

Plagioclase

Introduction

Calcic plagioclase is an abundant constituent of the basaltic achondrites. The general features of plagioclase as it occurs in sub-ophitic textures have been well described by Michel⁽⁶⁾. Michel also measured extinction angles for albite-carlsbad twins and established the compositions of scattered grains in a number of basaltic achondrites and mesosiderites. He has also supplied data on the optical properties of the maskelynite from Shergotty. Other information on plagioclase properties and compositions can be obtained from the descriptive papers for the various meteorites (Berwerth,⁽⁴⁸⁾ LaCroix⁽⁸⁾; Haughton and Partridge⁽⁴⁶⁾; Foshag⁽⁹⁾; Hess and Henderson⁽¹¹⁾). In general, these papers provide good descriptions of the habit of the plagioclase, but contain little compositional data. Only three determinations of index of refraction were found in a search of existing literature. The work of Game⁽¹²⁾ stands out as a good study of the compositional variation of plagioclase from a single meteorite (Juvinas).

Composition of feldspar separates

Four analyses of feldspar concentrates have been reported in this work. In order to establish more clearly the variations of alkalis in the plagioclase of basaltic achondrites and to provide chemically analyzed standards for optical and X-ray diffraction studies, plagioclase separates were analyzed by flame photometer using the method outlined by Brannock and Shapiro⁽³⁷⁾. These analyses are given in Table 7. The Nuevo Laredo and Pasamonte feldspar separates have small amounts of pyroxene impurity which have been estimated in grain mounts of the samples. The reproducibility of the analyses is within 5% for Na_2O and between 10% and 20% for K_2O , which is adequate for the purposes of mineralogic comparison where both of these elements are low.

The sodium contents determined here are equivalent to albite contents of the feldspar of from 5% to 15%; orthoclase contents vary between 0.2 and 1.5%. There is a regular variation of orthoclase content with albite content as shown in Figure 14.

The regular variation of potassium and sodium contents is of importance for two reasons:

(1) It shows that the feldspars of the basaltic achondrites can be considered a coherent group.

(2) The variation is consistent with a model of fractional crystallization of basaltic magma.

Optical properties of plagioclase

Indices of refraction have been measured for plagioclase by the method of Tsuboi⁽⁴⁹⁾ using the variable monochromator to match oil and grain indices. The Hartmann net published in Winchell and Winchell⁽⁴⁴⁾ (p. 281) was used to obtain indices in Na_D light. The Tsuboi method

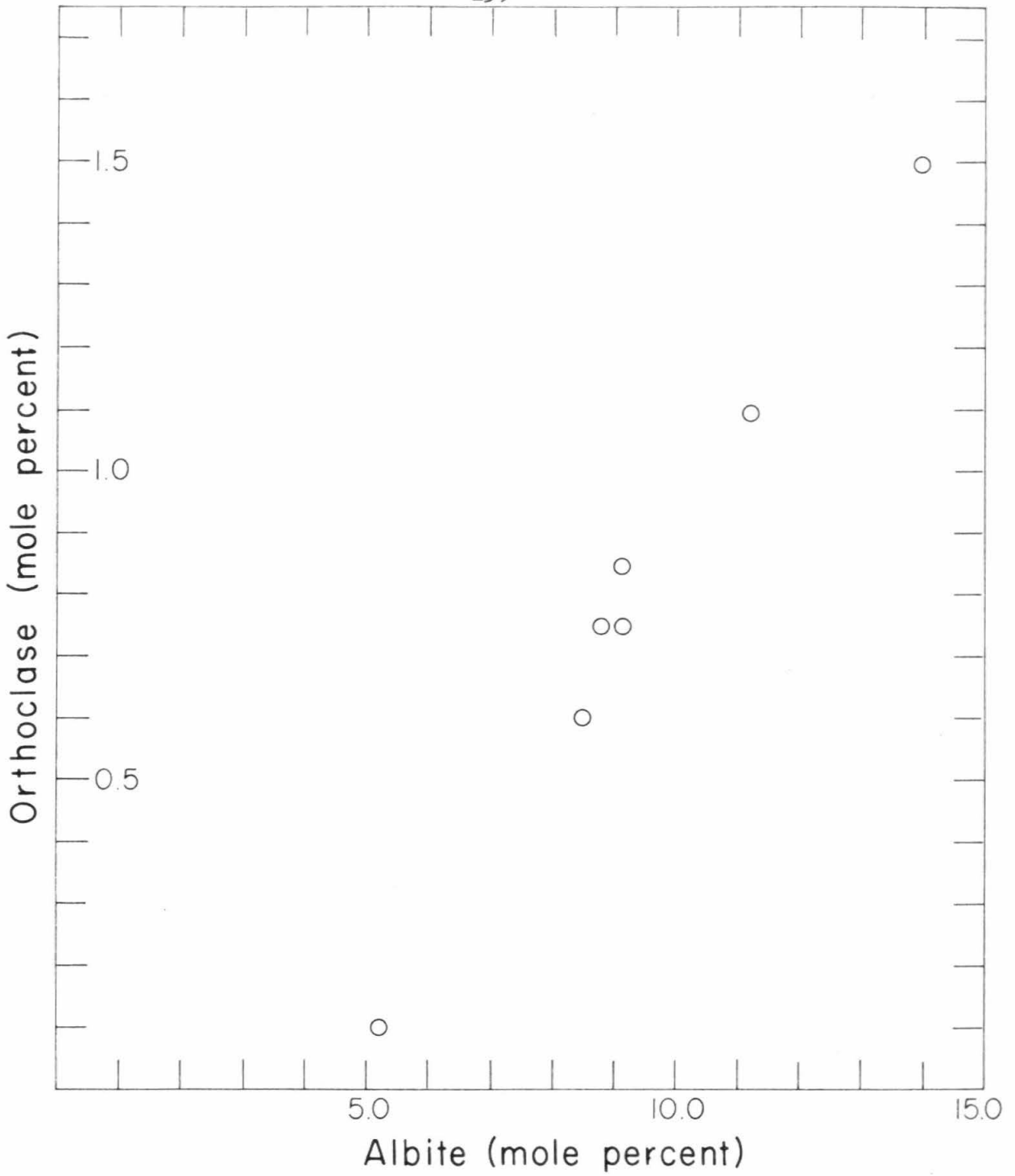


Figure 14

consists of measuring the apparent refractive indices on (001) or (010) cleavage flakes. The two orientations are not always distinguishable, but the apparent index n_x^a only differs by .001 for the two orientations in the compositional range studied. There are, presumably, differences between "volcanic" and "plutonic" structural types, but the indices of refraction of the two types do not differ greatly for calcic plagioclase (Smith⁽⁵⁰⁾).

The principal difficulties encountered in these determinations were:

(1) Inclusion-filled grains make precise determination of the matching wave length difficult. This can lead to an error of perhaps $\pm .002$ in the index of refraction, and to a biasing of the data if there is a preferential concentration of inclusions as a function of composition.

(2) The cleavages of the feldspar in the basaltic achondrites are poorly developed. Some error may therefore be introduced by grains which do not lie directly on the cleavage plates. The error introduced by misorientation is probably not more than $\pm .001$, for special effort was made to find grains with uniform interference colors indicating parallel upper and lower surfaces.

For an inclusion-free grain the index of refraction of the grain can be matched to that of the oil with an accuracy of about $5m\mu$ in wave length, which, at a maximum, corresponds to about .0005 in the index of refraction. Temperature corrections were less than .001 and introduce even smaller uncertainties.

Some of the uncertainties of the individual measurements are compensated by the usefulness of the method in the measurement of a large number of grains in a single sample. At its best, the method could be used to measure about 50 grains in an hour. For the basaltic achondrites,

where there are substantial variations of composition in some meteorites, the method was indispensable. Table 20 gives the results of index measurements on feldspar samples from basaltic achondrites and mesosiderites. Figure 15 presents histograms giving the frequency distribution of index of refraction for each sample.

From consideration of the limitations of the method mentioned above it would appear probable that the variations noted in individual samples are real. The Serra de Mage plagioclase sample shows the spread expected when all possible interferences are at a minimum. The spread of the Moore County determinations is possibly due to the poor development of cleavages, but may be due in part, to a small compositional variation between accumulated crystals and interstitial overgrowths. In the other samples the ranges are much greater than can be explained by the probable errors, and are indicative of the compositional zoning inferred from petrographic study. The variations observed here are comparable to those found by Game⁽¹²⁾ in Juvinas. The bimodal distribution of plagioclase indices for the Sioux County fragments may be due to mixing between the selected fragments and the surrounding material which could not be entirely eliminated during sampling.

Table 21 gives the index of refraction data composition for those samples which have been analyzed. The data is presented graphically in Figure 16. For comparison, the curve presented by Tsuboi⁽⁴⁹⁾ is also shown. There is a significant discrepancy between his curve and the best fit to the new data. Tsuboi used one feldspar with composition An_{80} and one feldspar of composition An_{100} to establish his curve. The data for the basaltic achondrites presented here is more comprehensive. The curve fitted to the new data has been used to determine the average

TABLE 20

INDEX OF REFRACTION DATA FOR PLAGIOCLASE

(Wave length, λ , at which the apparent index of refraction, n_x^i , matches the index of refraction of the immersion oil)

	Number of Measured Grains							
	<u>1</u>	<u>2</u>	<u>3</u>	<u>4</u>	<u>5</u>	<u>6</u>	<u>7</u>	<u>8</u>
n_{oil}^*	1.568	1.576	1.568	1.568	1.568	1.568	1.568	1.570
480	-	-	11	1	1	6	6	-
480-500	4	-	12	3	3	5	5	-
500-520	2	-	10	2	12	6	8	7
520-540	6	-	9	1	6	5	5	3
540-560	4	-	2	-	12	5	-	8
560-580	3	2	1	1	9	2	1	1
580-600	1	11	3	1	4	-	-	3
600-620	3	13	1	1	4	-	-	2
620-640	1	12	-	-	-	-	-	-
640-660	1	1	1	-	-	-	-	-
660	-	1	-	-	-	-	-	-
Ave. n_x^i [*]	1.570	1.580	1.574	1.574	1.571	1.573	1.573	1.573

- | | |
|-----------------|---------------|
| 1 Petersburg | 6 Bialystok |
| 2 Serra de Mage | 7 Juvinas |
| 3 Sioux County | 8 Estherville |
| 4 Binda | |
| 5 Pasamonte | |

* Shillaber immersion oils, $n_F - n_C$.019. The data have been corrected for temperature to a standard 25°C. Immersion oils were calibrated with an Abbé refractometer.

* Index obtained by using Hartmann net, Winchell and Winchell (,) p.281

TABLE 20

(Continued)
Number of measured grains

	9			10		11	12	13	14
	1.572	1.570	1.574	1.566	1.570	1.572	1.568	1.572	1.570
n _{oil}									
480	-	-	-	5	-	1	1	1	-
480-500	-	-	-	3	-	8	3	2	-
500-520	-	2	-	5	-	10	5	8	2
520-540	-	8	-	6	-	11	4	7	2
540-560	1	2	9	6	-	12	18	7	4
560-580	1	1	1	6	1	5	12	9	11
580-600	-	1	-	7	-	2	13	2	4
600-620	2	-	-	3	2	-	4	3	2
620-640	1	-	-	5	1	1	2	4	3
640-660	-	-	-	-	-	-	-	2	-
660	-	-	-	-	2	-	-	5	-
Ave. n _x [!]		1.576			1.567	1.576	1.570	1.574	1.570

- 9. Moore County
- 10. Stannern
- 11. Sioux County, analyzed fragment
- 12. Nuevo Laredo, 1.0a M
- 13. Sioux County, coarsest fragment
- 14. Nuevo Laredo, 1.8a NM

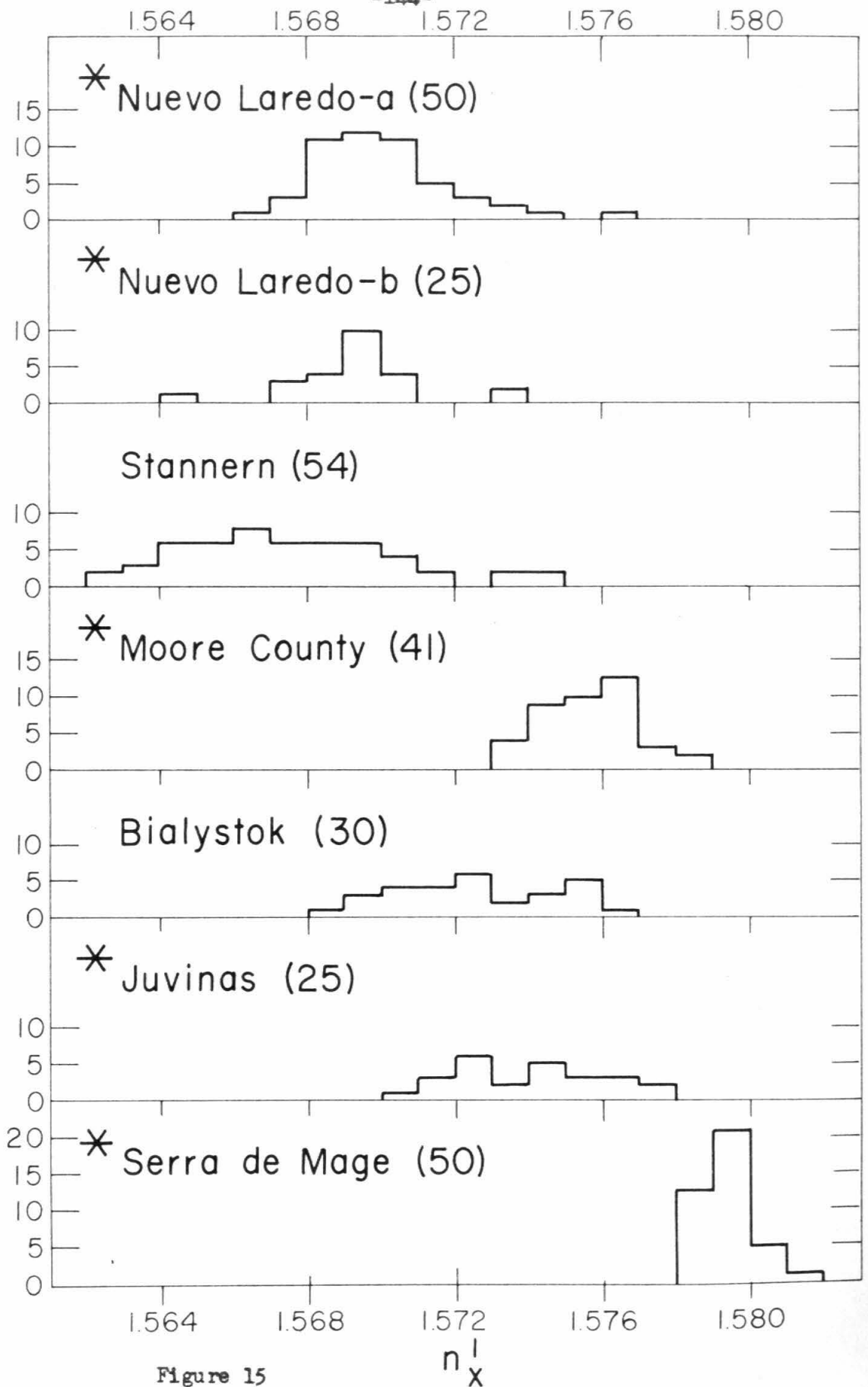


Figure 15

n_x

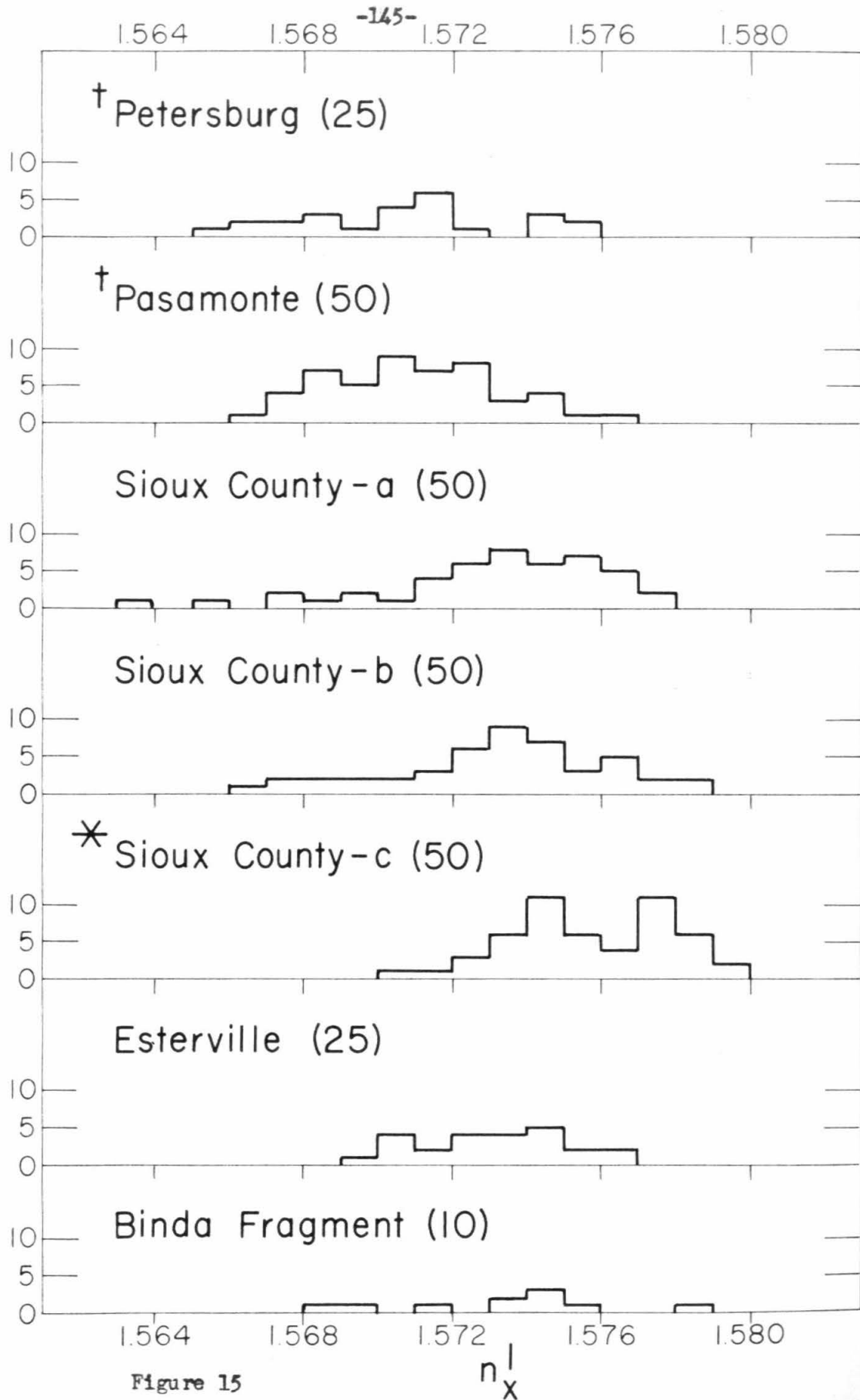


Figure 15

n_x

TABLE 21

COMPOSITION OF PLAGIOCLASE DEDUCED FROM INDEX OF REFRACTION DATA

(a) Analyzed Separates

	n_x' *	%An	Sample
Nuevo Laredo-a	1.570	85	1.0a M
Nuevo Laredo-b	1.569	84	1.5a M
Pasamonte	1.571	88	Fragment, lithic
Juvinas	1.574	90	Anal. Plag.
Moore County	1.5755	90.5	Total met.*
Sioux County-c	1.576	91	Anal. Frag.
Serra de Mage	1.579	95	Total met.

(b) Deduced compositions

	n_x'	%An	
Sioux County-a	1.573	88	Total met.
Sioux County-b	1.574	90	Coarsest frag.
Stannern	1.567	80	Total met.
Bialystok	1.572	87	Total met.
Petersburg	1.571	86	2.76
Estherville	1.573	88	Total met.
Binda	1.574	90	Lithic frag.

* Samples labeled total met. refer to samples separated by floating on liquid of density about 2.9, which should include most of the plagioclase in the sampled meteorite.

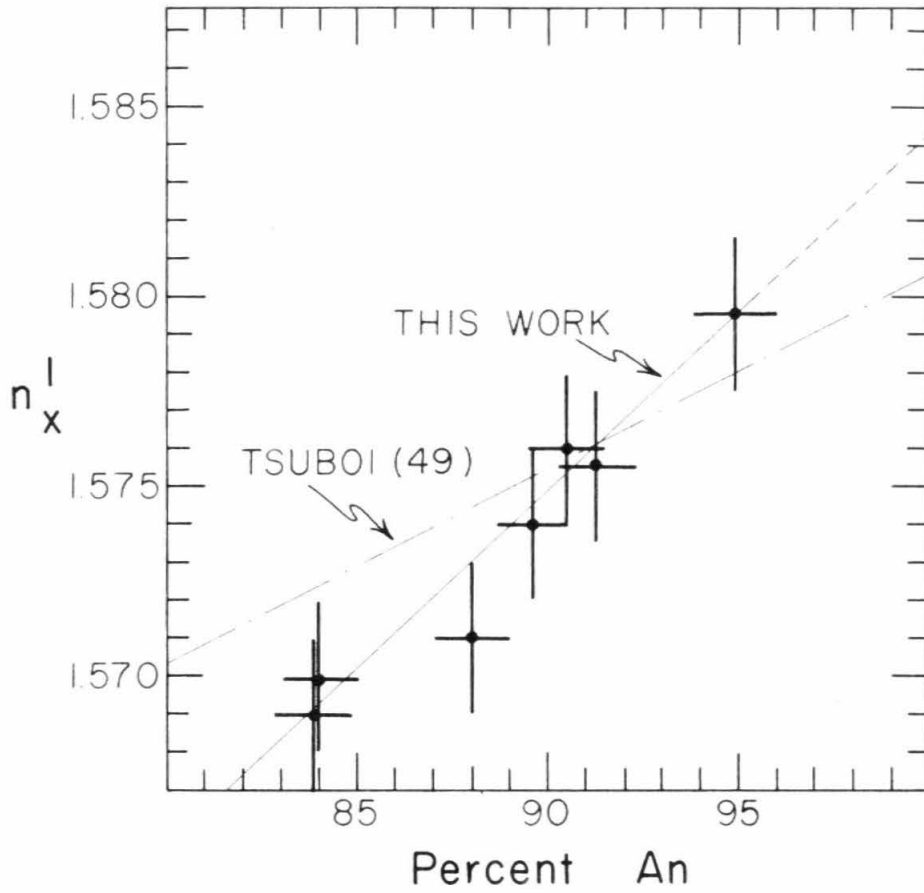


Figure 16. Crosses give limits of error.

feldspar compositions given in Table 21.

Optic Angle of Plagioclase

Optic angles of feldspar grains were measured by standard universal stage techniques. Only grains where the emergence of two optic axes could be measured were used. Measurements were made on thin sections of Nuevo Laredo, Pasamonte, Moore County, Petersburg, Serra de Mage, Sioux County. Game⁽¹²⁾ has given optic angles for feldspar in Juvinas, and von Engelhardt⁽¹⁵⁾ has presented data for feldspar in Stannern. The variations shown by the 2V determinations are given in Table 22.

The optic angle determinations show little variation in Serra de Mage, Moore County and Sioux County, but quite large variability in Nuevo Laredo, Pasamonte, Stannern and Juvinas. Figure 17 plots 2V against composition for the calcium-rich plagioclase feldspars. For comparative purposes, the curves for "volcanic" and "plutonic" plagioclase given by Smith⁽⁵⁰⁾ are also shown. It is probable that both compositional and structural differences are involved in the variations of 2V. The range of compositions which would be indicated by the variation of 2V seems consistent with the compositional variations indicated by index of refraction determinations, but the average values for the optic angles fall near the curve for natural "plutonic" plagioclase. As other studies indicate that at least some of the plagioclase of Juvinas has "volcanic" affinities, it is suggested that the 2V determinations are biased towards measurements on more coarsely crystalline plagioclase with "plutonic" affinities. 2V determinations on plagioclase from the finer-grained basaltic achondrites do not give uniquely interpretable data. Serra de Mage and Moore County meteorites, which have gabbroic rather than basaltic textures, have uniform optic angles which fall on the curve for natural

TABLE 22

2V DETERMINATIONS FOR PLAGIOCLASE OF SOME BASALTIC ACHONDRITES

	<u>No. of Measurements</u>	<u>Range</u>	<u>Average</u>
Nuevo Laredo	8	77-83(-)	81
Pasamonte	10	74-84(-)	77
Moore County	3	75-76(-)	76
Serra de Mage	3	78-79(-)	79
Juvinas*	57	75-82(-)	78
Stannern	6 9	67(-)-88(+)	-
Petersburg	5	67(-)-87(+)	86**(-)

* Game (12)

** v. Engelhardt (15)

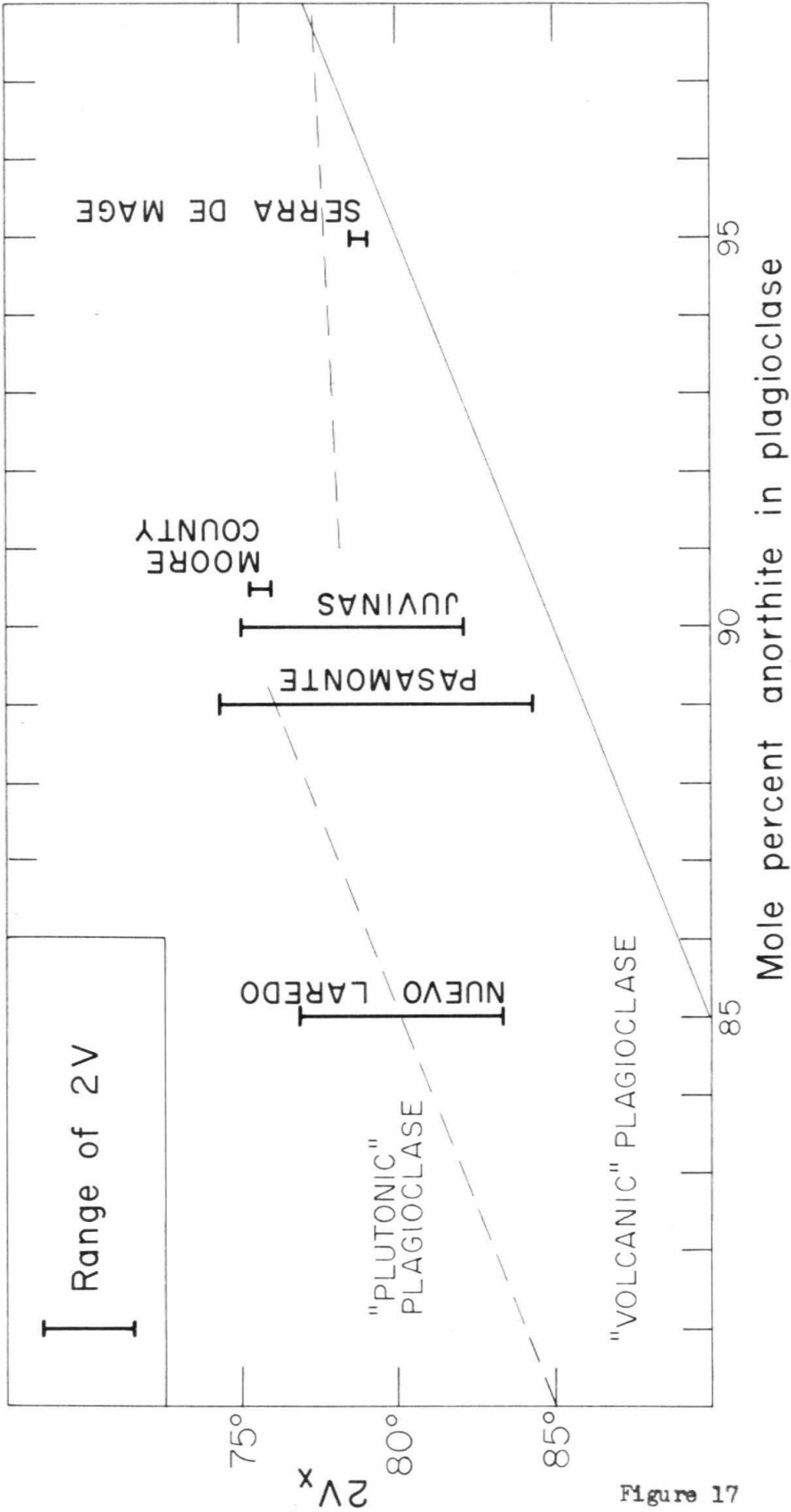


Figure 17

plagioclase.

Structural State; X-ray diffraction

X-ray diffraction analysis using a Phillips diffractometer was used to obtain structural data for plagioclase by the method of Smith and Yoder⁽⁵¹⁾. Plagioclase powders were slurred with acetone on a glass slide to make a thin even coating. Copper K_{α} radiation with a nickel filter was used. The slit and collector were 1° . The chart ran at $\frac{1}{2}$ inch per minute or $\frac{1}{2}$ degree per minute. Each run was made at least three times, always scanning towards higher angles. The reproducibility of the parameter $2\theta_{(131)} - 2\theta_{(\bar{1}\bar{3}\bar{1})} (= \Delta 2\theta)$ is about $\pm .02$ degrees. By measuring $\Delta 2\theta$ for natural and heated plagioclase, Smith and Yoder were able to obtain curves relating $\Delta 2\theta$ and composition for "plutonic" and "volcanic" structural types.

Table 23 and Figure 18 give the variation of $\Delta 2\theta$ for plagioclase samples from the basaltic achondrites. These new points have been plotted with several points given by Smith and Yoder⁽⁵¹⁾ including artificially prepared feldspars and feldspars from ~~terrestrial~~ layered intrusions. Although the accuracy of the X-ray determinations is considered to be $\pm .02^{\circ}$ in both the present work and the previous experiments, the fit of the points to regular curves suggests that the data is actually precise to about $\pm .01^{\circ}$.

The new data allow details of the variation in the range An_{80} to An_{100} to be outlined. Previous work (Smith and Yoder⁽⁵¹⁾) has suggested that there are no differences between "volcanic" and "plutonic" plagioclase detectible by X-ray diffraction in this region. In detail there is a small difference among the samples studied in this work. The three

TABLE 23

 $2\theta_{131} - 2\theta_{1\bar{3}1} (= \Delta 2\theta)$ FOR PLAGIOCLASE FROM SOME BASALTIC ACHONDRITES

	%An	$\Delta 2\theta$
Serra de Mage, analyzed	95 .001	2.28 .002
Moore County, analyzed	91	2.26
Sioux County	90	2.25
Sioux County, coarsest frag.	90	2.24
Juvinas	88	2.15
Stannern	80	2.14
Nuevo Laredo	82	2.14
Juvinas, analyzed	90.5	2.22
Pasamonte, analyzed	88	2.20
Pasamonte, fragment	87	2.13
Estherville	89	2.17
Nuevo Laredo, analyzed	85	2.17
Sioux County, analyzed frag.	90	2.24

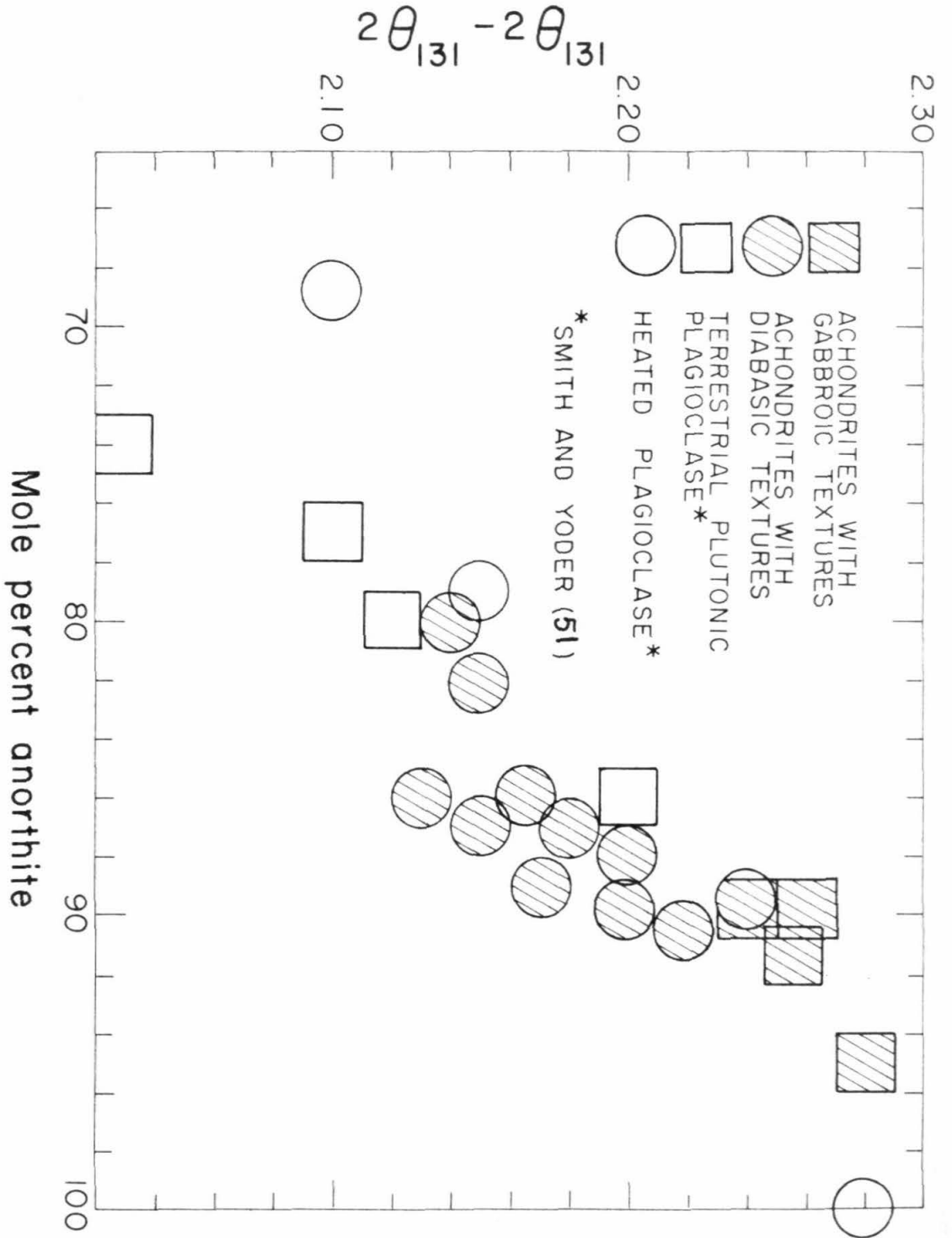


Figure 18

feldspar samples which fall on the upper curve are Sioux County, Moore County and Serra de Mage. These three meteorites are characterized by having gabbroic textures and clinopyroxenes that have largely inverted to orthopyroxenes. The first observation signifies slow crystallization, the second indicates slow cooling to allow sub-solidus transformations to occur. Both indicate that these three meteorites have origins more akin to "plutonic" than to "volcanic"; that is they come from very slowly cooled systems where plagioclase could invert to "low temperature" forms.

Plagioclase feldspars from Nuevo Laredo, Pasamonte and Juvinas occur in "volcanic" textures and the clinopyroxenes are not at all or only partially inverted to orthopyroxene. Both features indicate rapid cooling and the properties of these feldspars should approach those of the artificial feldspars. The plagioclase of Juvinas, which shows a variety of reactions to heat treatment (Game⁽¹²⁾) may contain "intermediate" structural types.

The plagioclase samples from meteorites that have "volcanic" or basaltic textures show a regularity of variation in $\Delta 2\theta$ that is different from the "plutonic" feldspar curve. The points have lower $\Delta 2\theta$ for identical compositions and lie along the extension of the curve for "volcanic" plagioclase more sodic than An_{80} given by Smith and Yoder⁽⁵¹⁾. The artificial plagioclase with composition $An_{89.4}$ prepared by Smith and Yoder, however, lies on the "plutonic" rather than the "volcanic" curve. The reason for this discrepancy is unknown. It does seem probable, however, that "volcanic" (or "intermediate") and "plutonic" plagioclase can be distinguished even for the very calcic feldspars present in the basaltic achondrites.

Composition of Plagioclase in other meteorites

There is only a minimal amount of data that can be gathered from the literature concerning the composition of plagioclase in basaltic achondrites not studied here. Until the work of Game⁽¹²⁾ the extent of the compositional variations of plagioclase in basaltic achondrites was not appreciated and previous investigators had only measured a limited number of grains in their studies. Michel⁽⁶⁾ gave compositions of plagioclase from twelve basaltic achondrites and six mesosiderites deduced from extinction angle measurements on albite-carlsbad twins, (Table 24). In general, the range of compositions determined by Michel are close to the normative feldspar concentration for those meteorites that have been analyzed. (See Chemical Composition).

Indices of refraction have been reported previously for plagioclase from Bereba (LaCroix⁽⁸⁾), Moore County (Hess and Henderson⁽¹¹⁾), Pasamonte (Foshag⁽⁹⁾), Macibini (Haughton and Partridge⁽¹⁴⁶⁾). These data have been employed to infer compositions which are given in Table 24.

Maskelynite

The plagioclase of two meteorites, Shergotty and Padvarninkai, has been replaced completely by an amorphous material to which Tschermak⁽¹⁶⁾ gave the name maskelynite. Amorphous plagioclase is also a common constituent of chondritic meteorites.

The maskelynite of the Shergotty meteorite has been studied in this work. The findings tend to confirm the earlier investigations of Tschermak⁽¹⁶⁾ and Michel⁽⁶⁾. The chemical analysis of a separated maskelynite sample (Analysis M-10, p. 107) indicates that the maskelynite has an average composition of $Or_2Ab_{49}An_{49}$. Density determinations were made on the analyzed sample by adjusting the density of a tetrabromoethane-

TABLE 24

PLAGIOCLASE COMPOSITIONS DEDUCED FROM OPTICAL DATA GIVEN IN OLDER STUDIES

(a) Michel,⁽⁶⁾ based on extinction angles of albite-carlsbad twins

Euclrites, Howardites	%An
Stannern	86-88 $\frac{1}{2}$
Juvinas	90-91 $\frac{1}{2}$
Jonzac	84-86
Peramiho	88
Petersburg	86-88
Pavlovka	90-97
Frankfort	94-95
Luotolax	90-93
Zmenj	83 $\frac{1}{2}$
Massing	75
Le Teilleul	78

Mesosiderites

Vaca Muerta	96
Dona Inez	87
Llano Del Inca	87-87 $\frac{1}{2}$
Crab Orchard	92 $\frac{1}{2}$
Morristown	97
Estherville	96 $\frac{1}{2}$
Mincy	87 $\frac{1}{2}$
Hainholz	92

(b) Lacroix(), based on index of refraction.

Bereba	87
--------	----

(c) Haughton and Partridge(), based on index of refraction

Macibini	86
----------	----

acetone mixture to match the density of the crystals. The density of the maskelynite varied between 2.42 and 2.58, with an average of 2.576 in the analyzed sample. The index of refraction varies between 1.540 and 1.548, with an average of 1.546 in the analyzed sample. The upper limit is well defined, but the lower limit of index values may be less than 1.540.

The index and density data for the maskelynite are of interest because they are not comparable to the properties of plagioclase glass prepared by quenching from a melt. For plagioclase glass of composition An_{50} , Schairer, et al⁽⁵²⁾ find an index of refraction of 1.529, whereas the maskelynite has an index of refraction of 1.546. The mean index of refraction of crystalline An_{50} is 1.558. The maskelynite, therefore, has an index of refraction which is intermediate between that of crystalline plagioclase and plagioclase glass prepared by quenching of a melt.

The variations of density and index of refraction may be a function either of compositional variations or structural state of the maskelynite. No evidence has been obtained concerning possible compositional variations of the maskelynite. Some maskelynite grains in thin section show index of refraction contrasts that follow what apparently were original twin planes in the crystals. This observation suggests that some of the index and density variation is due to the structural state of the plagioclase glass.

It seems probable that the transformation of plagioclase to maskelynite took place during passage of a strong shock. The density of the maskelynite, which is between that of crystalline plagioclase and the synthetic plagioclase glass, is consistent with the petrographic

observations that little volume change has occurred during the metamorphism. In contrast, breccia fragments from the Ries Basin described by Chao⁽³²⁾ have amorphous plagioclase in which the density and index is that of synthetic plagioclase glass and the experiments of Milton and De Carli⁽³¹⁾ produced amorphous plagioclase which has an index of refraction equivalent to the synthetic plagioclase glass of the same composition. It may be that the metamorphism undergone by Shergotty occurred in somewhat different conditions than the experimental conditions or those which produced the Ries Basin occurrences. No correlated index of refraction and chemical analyses have been made for maskelynite in chondrites.

Summary of plagioclase data

Data has been given which describes the compositional, optical and structural variations of plagioclase encountered in the basaltic achondrites. A number of the important features are summarized here.

Plagioclase in these meteorites is generally quite calcic and the average plagioclase composition varies between An₈₀ and An₉₅. The exception to this statement is Shergotty, in which the plagioclase is An₅₀. Within individual meteorites, especially those with finer-grained basaltic or diabasic textures, the plagioclase shows compositional variability that is more extreme, in many cases, than the total variability shown by the average plagioclase composition in the entire group of meteorites (again excluding Shergotty). In Juvinas, for example, the index of refraction data indicate that plagioclase compositions vary from An₉₅ to An₆₅. Because of the extreme variation within individual meteorites, it is difficult to discern the effect of mixing of different systems in the polymict breccias, although the data of Michel⁽⁶⁾

extends the range of plagioclase composition towards more calcic varieties in howardites and mesosiderites, where it is reported that some plagioclase is as calcic as An_{98} .

Optical and X-ray diffraction data supports the petrographic textural evidence that the plagioclase originally crystallized under a wide variety of cooling regimes. Optic angle determinations are subject to biasing towards coarser grains which generally tend to have low temperature or plutonic affinities. X-ray diffraction data give average values for the structural state and suggest that those meteorites which have fine-grained basaltic or diabasic textures have plagioclase with high temperature or volcanic affinities. The X-ray diffraction data indicate that the meteorites which have coarser textures with gabbroic affinities have plagioclase with low temperature or plutonic structural state. The coarse grain size of many of the plagioclase fragments of the howardites suggests that they have plutonic affinities.

Shock metamorphism has produced a transformation of plagioclase in Shergotty to a glassy state that has a higher density than plagioclase glass prepared by quenching of a melt. The structural properties of the maskelynite are not known.

The relation of plagioclase and pyroxene compositions gives valuable information concerning magmatic differentiation of basaltic rocks. It also may give information concerning the conditions of crystallization of the minerals for those cases where anomalous values are observed. Two types of information can be obtained: (1) comparison of average plagioclase and average pyroxene compositions for the total meteorites or (2) comparison of plagioclase and pyroxene compositions in individual lithic

fragments. For the eucrites, the two methods give essentially the same results, for all lithic fragments have similar compositions.

For the howardites, individual lithic fragments may vary widely in composition. It may be easier, however, to obtain average mineral compositions by using the norms calculated from the chemical analyses. Such average values are biased because the total sample includes some crystals which have been formed in early stages of the crystallization of the magma and are more calcic (in the case of the plagioclase) or more magnesian (in the case of the pyroxene) and some crystals which are relatively enriched in alkalis or iron, but the mix of crystals does not necessarily represent the average composition of the starting system. On the other hand, the lithic fragments that one can sample from the howardites are generally the finer-grained textures which may more closely resemble liquid compositions. The coarser pyroxene and plagioclase of the howardites are rarely seen in intergrowth relations.

For the mesosiderites, many of which have undergone some homogenization in a metamorphic event, only average plagioclase and pyroxene compositions can be determined. In the case of Estherville, the average mineral compositions have been deduced from optical determinations. For Vaca Muerta, the optical data of Michel⁽⁶⁾, who made a number of determinations on samples that were represented to him as different meteorites, but were all samples of the same meteorite, has been combined with the iron-magnesium ratio of the acid insoluble portion given by Prior⁽⁴⁾.

Table 25 and Figure 19 give the variation of plagioclase and pyroxene compositions for some of the basaltic achondrites and meso-

TABLE 25

COMPOSITION OF CO-EXISTING PLAGIOCLASE AND PYROXENE IN SOME
BASALTIC ACHONDRITES*

(a) This work	%An	Fe/Fe+Mg
Pasamonte, fragment	86	0.64
Sioux County, total	88	0.59
Sioux County, cst. frag.	90	0.57
Sioux County, an. frag.	91	0.59
Nuevo Laredo-a	85	0.65
Nuevo Laredo-b	84	0.65
Stannern	80	0.61
Moore County	90	0.50
Bialystok	87	0.65
Juvinas	90	0.59
Petersburg	86	0.58
Serra de Mage	95	0.44
Estherville	89	0.20
Binda, fragment	90	0.32

(b) Older work, meteorites not examined in this study

Jonzac	85	0.57
Peramiho	88**	0.61
Pavlovka	93**	0.36
Frankfort	94**	0.29
Inotolax	91**	0.54
Zmenj	83	0.36
Massing	75	0.55
Le Teilleul	78	0.40
Bereba	87**	0.61
Macibini	86	0.51

* Deduced from optical data.

** Normative and modal plagioclase compositions agree within 5% An.

Ab / Ab+An (mole percent)

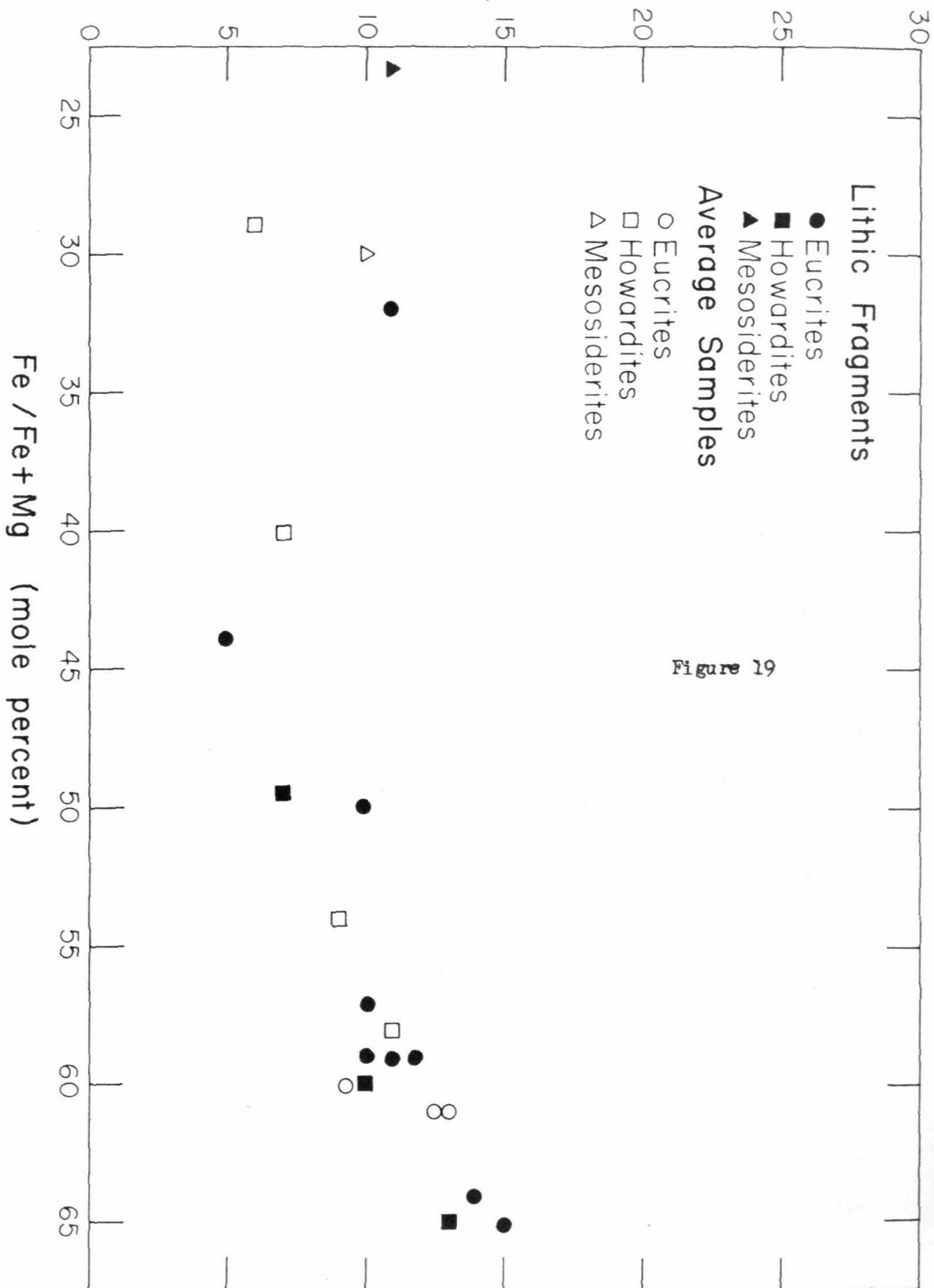


Figure 19

siderites. The general features of the variations seem to be: (1) the more sodic plagioclase is generally associated with the more iron-rich pyroxene; (2) the plagioclase associated with the more magnesian pyroxenes in lithic fragments, in the Binda eucrite and in the mesosiderites consistently ^{has} an average composition of about An_{89} , which seems to be a limiting composition for the magnesium-rich systems; (3) the howardites apparently have a component of more calcic plagioclase and give average compositions as calcic as An_{95} ; (4) the plagioclase of Serra de Mage, in which crystal accumulation probably has occurred, is more calcic than the plagioclase of Moore County, although the pyroxene compositions are similar. This latter relation suggests that the very calcic plagioclase of Serra de Mage and the howardites represents the earliest plagioclase formed during the magmatic episode and was separated by crystal settling from the magma. It will be argued in a later portion of this work that the first basaltic achondrite magmas were probably not saturated with plagioclase. If that hypothesis is true, it will be expected that very calcic plagioclase should coexist only with pyroxene more iron-rich than that which was separating from the magma at the point that plagioclase first began to separate. More detailed study of the coexisting very calcic plagioclase and magnesian pyroxene in lithic fragments might verify the hypothesis.

The composition of the coexisting plagioclase and pyroxene of Shergotty do not fit the generalizations stated above. The much higher alkali content of the Shergotty plagioclase makes it aberrant with respect to all basaltic achondrites studied in this work. It is of importance to establish whether Shergotty-like plagioclase exists

in fragments in the howardites. The work of Michel⁽⁶⁾ suggests that the howardites Massing, LeTeilleul and Zmenj may have a component of plagioclase that is more sodic than the plagioclase that occurs generally in the basaltic achondrites.

Free Silica

Quartz and tridymite were first reported as constituents of basaltic achondrites by Berwerth⁽⁷⁾ and subsequent investigations have verified and extended his observations. In this study, tridymite has been newly observed in Serra de Mage, Sioux County, Estherville and Petersburg. Cristobalite and quartz occur in Nuevo Laredo. Quartz has been discovered in small amounts in Juvinas and Sioux County. Table 26 summarizes the occurrence of free silica in the basaltic achondrites. An apparent compositional control over the free silica polymorphs is made apparent by comparing the polymorphs as a function of Fe/Fe+Mg (molecular) taken from the bulk chemical analyses.

The free silica most commonly occurs in interstices between plagioclase and pyroxene grains where it has apparently been among the last minerals to crystallize. Plate 5a, cristobalite in Nuevo Laredo; Plate 28b, tridymite in Pasamonte; Plate 23a, quartz in Stanern). The grain size of the free silica is generally smaller than the average grain size of the coexisting pyroxene and plagioclase. In the interstitial positions the free silica commonly occurs in intergrowths with troilite and ilmenite and with interstitial (labradoritic) plagioclase. In many of the finer-grained textures, the free silica is inclusion-filled and difficult to distinguish from interstitial plagioclase.

TABLE 26

FREE SILICA POLYMORPHS IN SOME BASALTIC ACHONDRITES

	Tridymite	Quartz*	Cristobalite	Fe/Fe+Mg
Estherville	x			0.20
Serra de Mage	x	o?		0.44
Moore County	x			0.50
Sioux County	x	o		0.58
Petersburg	x			0.58
Juvinas	x	o		0.60
Pasamonte	x			0.61
Stannern		x		0.61
Jonzac		x?		0.58
Peramiho		x?		0.61
Bereba		x?		0.61
Nuevo Laredo		o		0.65

* Quartz that has crystallized directly from the magma is designated by (x). Quartz that occurs in association with troilite and corroded pyroxene is designated (o).

In contrast to its interstitial occurrence in magmatic textures, some free silica has been formed as a reaction product. Plate 19a shows a corroded pyroxene grain from Juvinas in which troilite has locally replaced the silicate and quartz has been formed. In Sioux County, pyroxene has been reduced to metallic iron with the liberation of free silica (Plate 11b). These phenomena have been observed in most of the earlier studies of the brecciated basaltic achondrites (see, e.g. von Engelhardt⁽¹⁵⁾). Many of the earlier investigators (Wahl⁽⁵⁾) were especially impressed by these evidences of reaction and presumed that most of the quartz was formed by reaction*.

There are three reasons for believing that most of the free silica is present as a primary magmatic mineral.

(1) The meteorites are slightly oversaturated with respect to silica, and free silica should be a stable magmatic phase.

(2) There is not enough troilite or metal to explain 3% to 5% free silica in the norm as a product of reaction. In Juvinas, Sioux County and Nuevo Laredo where primary tridymite or cristobalite and secondary quartz occur, the primary free silica is more abundant than is the quartz.

(3) There is an apparent compositional control over the polymorph of free silica present. The presence of quartz rather than tridymite in the iron-rich meteorites is consistent with lower melting temperatures for the silicates of those meteorites.

*In most of the earlier studies, the opaque minerals were identified as magnetite and the quartz forming reaction was presumed to be $3\text{FeSiO}_3 + \frac{1}{2}\text{O}_2 = \text{Fe}_3\text{O}_4 + 3\text{SiO}_2$. Two reactions are more probable:
(1) $\text{FeSiO}_3 \xrightarrow{-2} \text{Fe} + \text{SiO}_2 + \frac{1}{2}\text{O}_2$ or (2) $\text{FeSiO}_3 + \frac{1}{2}\text{S}_2 \xrightarrow{-} \text{FeS} + \text{SiO}_2 + \frac{1}{2}\text{O}_2$.

The major amount of free silica in the basaltic achondrites occupies textural positions where it is difficult to identify. In Nuevo Laredo, quartz was only observed rarely, whereas cristobalite is commonly seen in thin section. The quartz is confined to interstitial positions in some fragments where it is difficult to distinguish from plagioclase. There is no sign in any meteorite of incipient inversion of cristobalite or tridymite to quartz.

Free silica is not easily recognized in the fragmental groundmass of the brecciated meteorites although it must be present. There is apparently no depletion or enrichment of free silica in the groundmass, as the separate analyses of groundmass and an individual fragment in Sioux County both showed the same amounts of free silica. The normative silica content of the chemical analysis of Stannern agrees well with a modal analysis done by von Engelhardt⁽¹⁵⁾ on lithic fragments.

An interesting aspect of the distribution of free silica is that primary quartz and tridymite have not been reported together in an individual meteorite. In Juvinas and Sioux County, the quartz has a different textural position than the tridymite and is present in much smaller quantities than the tridymite. For those meteorites with $Fe/Fe+Mg$ of about 0.6, the amount of mixing of possible quartz- and tridymite-bearing materials is very small and the degree of chemical mixing must be slight. This is another indication that monomict breccias formed from limited samples of the original rocks.

Olivine

Olivine has been observed in this study as a single fragment in one thin section of the Pavlovka howardite and in nodular clusters in the Estherville and Crab Orchard mesosiderites. Zavaritskii and Kvasha⁽¹³⁾

give indices of refraction for olivine in Yurtuk and Zmenj. Prior⁽⁴⁾ has compiled chemical evidence for the composition of olivine in mesosiderites. Fredriksson and Keil⁽²⁰⁾ have determined the composition of five olivine grains from Kapoeta. The compositional data is given in Table 27. Olivine has also been reported in Frankfort, Pavlovka, Luotolax, Massing and Le Teilleul (Wahl⁽⁵⁾). It seems established that olivine is a rather rare constituent of the howardites and mesosiderites.

Olivine in the howardites occurs primarily as fragments not intergrown with other minerals. In the mesosiderites examined in this study, olivine is also fragmental, but has taken part in the recrystallization episode. The textural relations of the olivine, in the mesosiderites studied here suggest that it was in fragments mixed with other silicates and was not introduced by a pallasitic melt as suggested by Lovering⁽⁵³⁾.

One of the aspects of the basaltic achondrite assemblage that seems to be of some importance is the small amount of olivine in the more magnesian meteorites. This feature bears further investigation, which may be most advantageously pursued in the mesosiderites. Alternative possibilities are: (1) the parent material of the basaltic achondrites was saturated with respect to silica. This would entail a magmatic differentiation in order to explain the difference between the compositions of a saturated parent material and the compositions of chondrites, (2) olivine may have been strongly fractionated by a process of fractional crystallization or partial melting of an olivine-bearing parent material.

The most iron-rich basaltic achondrites have pyroxenes which

TABLE 27

OLIVINE IN SOME BASALTIC ACHONDRITES

	Olivine Composition	Fe/Fe+Mg Meteorite
Estherville	Fs ₂₀	0.20
Frankfort	x	0.29
Kapoeta	Fs ₈₋₃₀	0.30
Yurtuk	x	0.35
Zmenj	x	0.36
Pavlovka	x	0.40
Le Teilleul	x	0.40
Inotolax	Fs ₂₇	0.54
Massing	Fs ₂₇	0.55

approach compositions for which calcium-poor pyroxenes are unstable and are replaced by a mixture of iron-rich olivine and silica. Iron-rich olivine has not been observed, but more iron-rich meteorites than Nuevo Laredo might occur in which the phase assemblage fayalite-augite-plagioclase-silica could be expected.

Metallic iron and the distribution of nickel between metal and silicates

The textural relations of metallic iron in the basaltic achondrites have been illustrated in Chapter II. In Serra de Mage and Moore County small equant grains of metallic iron are probably of primary crystallization. In Sioux County, Stannern, Juvinas and Nuevo Laredo some of the metal is possibly of primary origin. In Nuevo Laredo and Sioux County some of the metal has apparently formed by post-crystallization reduction of pyroxene. In Petersburg, fragments of metal and orthopyroxene rimmed with metal are common, but the origin of the metal is not clear. In the mesosiderites, metallic iron-nickel has taken part in a metamorphic episode and it is difficult to understand the original relations between silicates and metal with our present knowledge of these meteorites.

The nickel content of the metal from five meteorites has been determined by X-ray fluorescence. Samples were separated with a hand magnet and mounted in the X-ray spectrometer between mylar sheets clamped to "Caplugs". The $Fe_{K\beta}$ and $Ni_{K\beta}$ emission peaks were measured with the LiF crystal. Standards used were three NBS steel spectrographic standards and one nickel-iron thin film previously analyzed by Chodos (personal communication). The data are given in Table 28 and the standard curve given in Figure 20. The compositions inferred for the meteoritic metal are given in Table 29. The samples were contam-

TABLE 28

X-RAY FLUORESCENCE DATA FOR THE NI CONTENT OF METALLIC IRON

	Counting Rate (x10 ³ cps)				
	<u>FeK_β</u>	<u>NiK_β</u>	<u>NiK_{α1}</u>	<u>I_{Ni}/I_{Fe}</u>	<u>Ni/Fe</u>
<u>Standards</u>					
NBS 408	20.41	.271	.059	.0104	0.0123
NBS 412a	14.73	.139	.052	.0059	0.0057
NBS 418	17.32	.093	.053	.0023	0.0011
17-17-20(thin film)	1.43	.775	.157	.431	0.2453
<u>Samples</u>					
Moore County	54.41	.106	.053	.0010	.001
Serra de Mage	11.58	.098	.051	.0010	.001
Petersburg	11.74	.341	.060	.0239	.025
Juvinas	8.44	.065	.051	.0016	.001
Estherville	10.02	.917	.081	.0824	.085

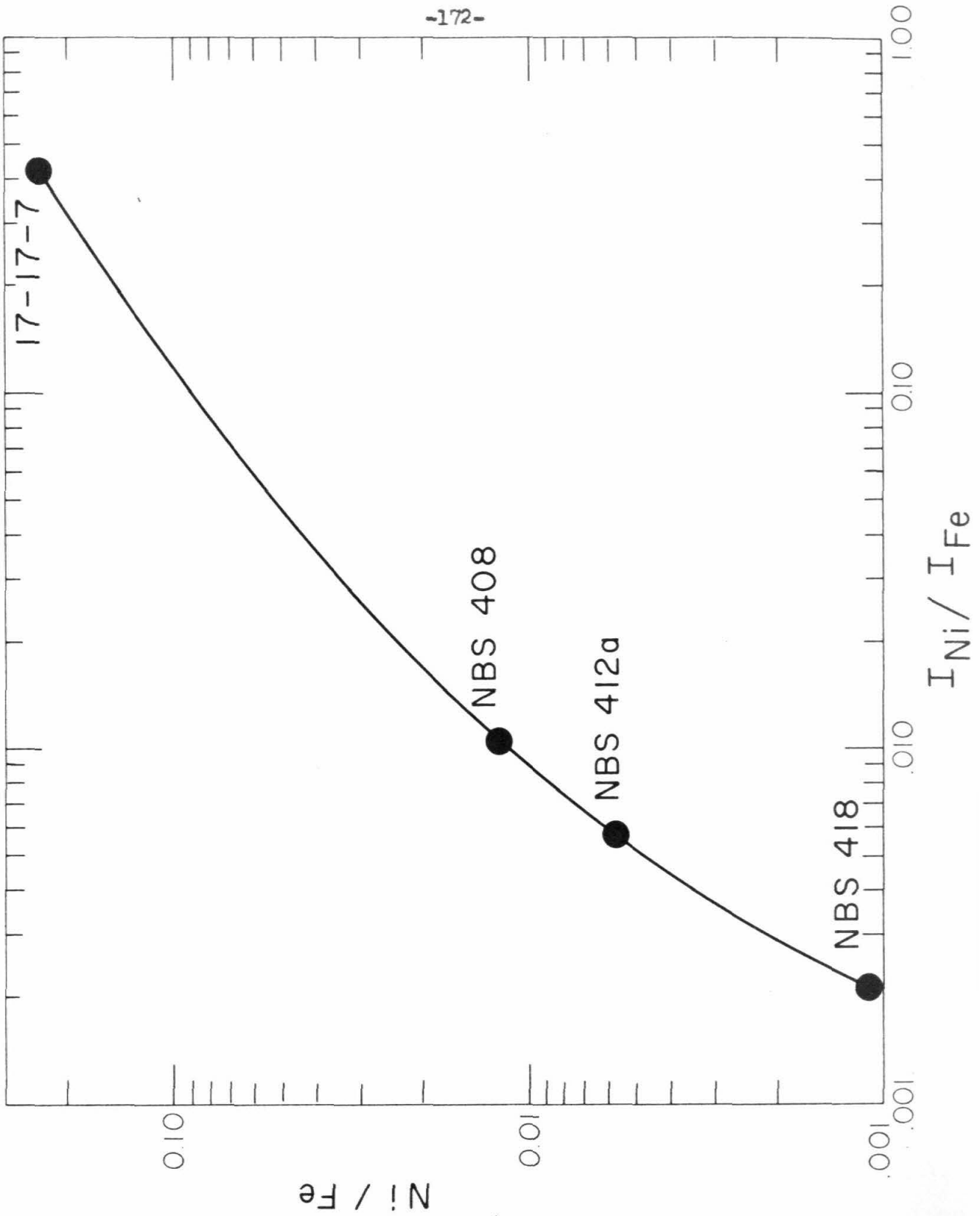


Figure 20

TABLE 29

NICKEL IN THE SILICATE AND METAL PHASES OF SOME METEORITES

(a) Nickel content of metallic iron in basaltic achondrites
X-ray Fluorescence

Estherville	8.5%
Petersburg	2.5%
Moore County	.1%
Serra de Mage	.1%
Juvinas	.1%
Nuevo Laredo	.1%

(b) Nickel content of minerals from various meteorites

Emission Spectrography

Clinopyroxenes (basaltic achondrites)	1-3 ppm
Plagioclase (basaltic achondrites)	1 ppm
Hypersthene (Richardton chondrite)	40 ppm
Olivine (Allegan chondrite)	30 ppm
Hypersthene (Tatouhine achondrite)	6 ppm
Enstatite (Norton Co. achondrite)	30 ppm
Troilite (Allegan chondrite)	1000 ppm

inated with indeterminate but small amounts of silicates. In the case of the three lowest values, the analyses may be in error by a factor of two due to silicate contamination, but such error is of no real significance, because the nickel contents of these samples were barely measurable over background. The important point is that for metal believed to be either of primary crystallization or post-crystallization reaction the nickel content is extremely low.

The nickel content of the metal from the Estherville mesosiderite is slightly lower than the range reported by Prior⁽⁴⁾ for the mesosiderites, but it is distinct from the metal of the eucrites and howardites.

The nickel content of the Petersburg metallic iron is intermediate between the metal of the mesosiderite and the primary metal of the basaltic achondrite. The Petersburg metal also is on the lower side of metal compositions normally found in other meteorites. With present data it is not possible to determine the relation of the nickel content of the metal in the meteorites to the silicate magmatic differentiation. There is a correlation which shows the nickel content of the metal to be greater for the more magnesian basaltic achondrites, but the small amount of data also is consistent with an external origin for the metal of Estherville and Petersburg.

Table 29 also gives emission spectrographic data for nickel contents of silicates from the basaltic achondrites as well as from other achondrites and chondrites. The problem faced in the analysis of chondritic silicates for nickel is that of removal of all of the metal which has very high nickel content.

The chondrite and calcium-poor achondrite pyroxenes were separated

magnetically and then treated with HCl in order to remove metal and sulfide contaminations. The olivine sample underwent only magnetic separation. The nickel contents reported here must be considered upper limits as small amounts of contamination may remain. No special procedures were used for the basaltic achondrite silicates as it was clear from the beginning that the nickel abundances in these silicates were at or below the 1mmp detectability limit of the emission spectrograph.

The general picture one gets of the nickel content of silicates from meteorites is that the nickel contents are extremely low. If one assumes that the metallic iron of chondrites has on the order of 10% nickel and that the silicates have 10% Fe, the fractionation factor $(Ni)_m(Fe)_m / (Fe)_m(Ni)_s$ is about 2×10^2 , a value which is comparable to $1.4 - 1.6 \times 10^2$ found by Zur Strassen ⁽⁷⁷⁾ for the distribution between silicate and metal at 1700-1800°C. There is, apparently, close to equilibrium fractionation of nickel between silicates and metal in the chondrites. More precise experimental and observational evidence might supply a thermometer for the silicate-metal equilibrium in chondrites.

The very large fractionation factor between metal and silicates is a possible reason for the depletion of nickel in the basaltic achondrites. As metallic iron is apparently a primary phase gravitational separation of early formed metallic iron could easily deplete a magma in any nickel it might still contain. The same would be true if the metal formed an immiscible liquid phase which could mechanically separate from the magma. The retention of relatively high nickel contents in terrestrial basaltic rocks is due to the presence of primary oxide phases which have much

lower fractionation factors with respect to silicates.

The presence of metallic iron as a primary phase in the basaltic achondrites could also result in the gravitational accumulation of metal-rich zones in an intrusion. It is possible that the metal of Petersburg and even of the mesosiderites is related to the gravitational separation of a liquid metal phase from a differentiated basaltic intrusion with an initially high nickel content.

Other minor mineral phases

In the modern descriptions of the basaltic achondrites, the opaque minerals are generally identified as troilite, ilmenite and chromite. These opaque minerals are of low abundance, so detailed information is difficult to obtain. Troilite is easily identifiable in reflected light by its pinkish color and anisotropy. Ilmenite is characterized by a dull metallic reflectivity and distinct anisotropy. Chromite is similar in reflectivity to ilmenite, but is isotropic. In general, it is impossible to distinguish chromite with certainty.

Through the courtesy of Dr. G. Arrhenius of the University of California at La Jolla and with the help of A. Chodos, a survey of opaque grains in a polished section of Nuevo Laredo was made with the electron microprobe analyzer. Ilmenite was found to be the most abundant opaque mineral, followed by troilite. Only a few scattered grains of chromite were found.

Many earlier investigators considered the opaque mineral assemblage to contain magnetite. In this study, magnetite has been observed only in the Shergotty meteorite.

The textural aspects of troilite and ilmenite have been described previously. Both opaque minerals, and especially troilite, are concen-

trated in the late-forming interstitial material in the fragments showing basaltic textures. Some troilite is found in veins that have probably formed in late magmatic stages or during metamorphic episodes.

One of the sulfide-rich veins of Stannern may be a post-brecciation vein.

There are small amounts of phosphate in the new chemical analyses of basaltic achondrites. In Shergotty there is a modal phosphate which Fuchs⁽⁵⁴⁾ identified as whitlockite, but in none of the iron-rich basaltic achondrites has a phosphate been positively identified. In Estherville, a phosphate with small negative 2V and indices of refraction $n_x = 1.620$, $n_z = 1.621$ is tentatively identified as whitlockite.

The mineralogy of the basaltic achondrites can be compared with that of the Skaergaard intrusion (Wager and Deer⁽⁴⁰⁾), a highly differentiated terrestrial basaltic intrusion. A convenient method of summarizing the mineralogical variations in both assemblages is given in Figure 21, which follows the pattern set by Wager and Deer. Figure 21 compares the compositions, but not the abundances, of the minerals that occur in both sequences. The most important difference between the two assemblages is the composition of the plagioclase, which in the basaltic achondrites is very calcic (An_{90}) and relatively invariant, but in the Skaergaard intrusion starts at more sodic compositions and becomes increasingly more sodic as the Fe/Fe+Mg increases. Another important difference is the absence of augitic clinopyroxene over most of the variational range in the basaltic achondrites, whereas augitic clinopyroxene is present over the entire observed range in the Skaergaard intrusion. Olivine is more abundant in the Skaergaard intrusion than in the basaltic achondrites, and reaches compositions as iron-rich as Fa_{44} in the lower portions, whereas the maximum iron content reported

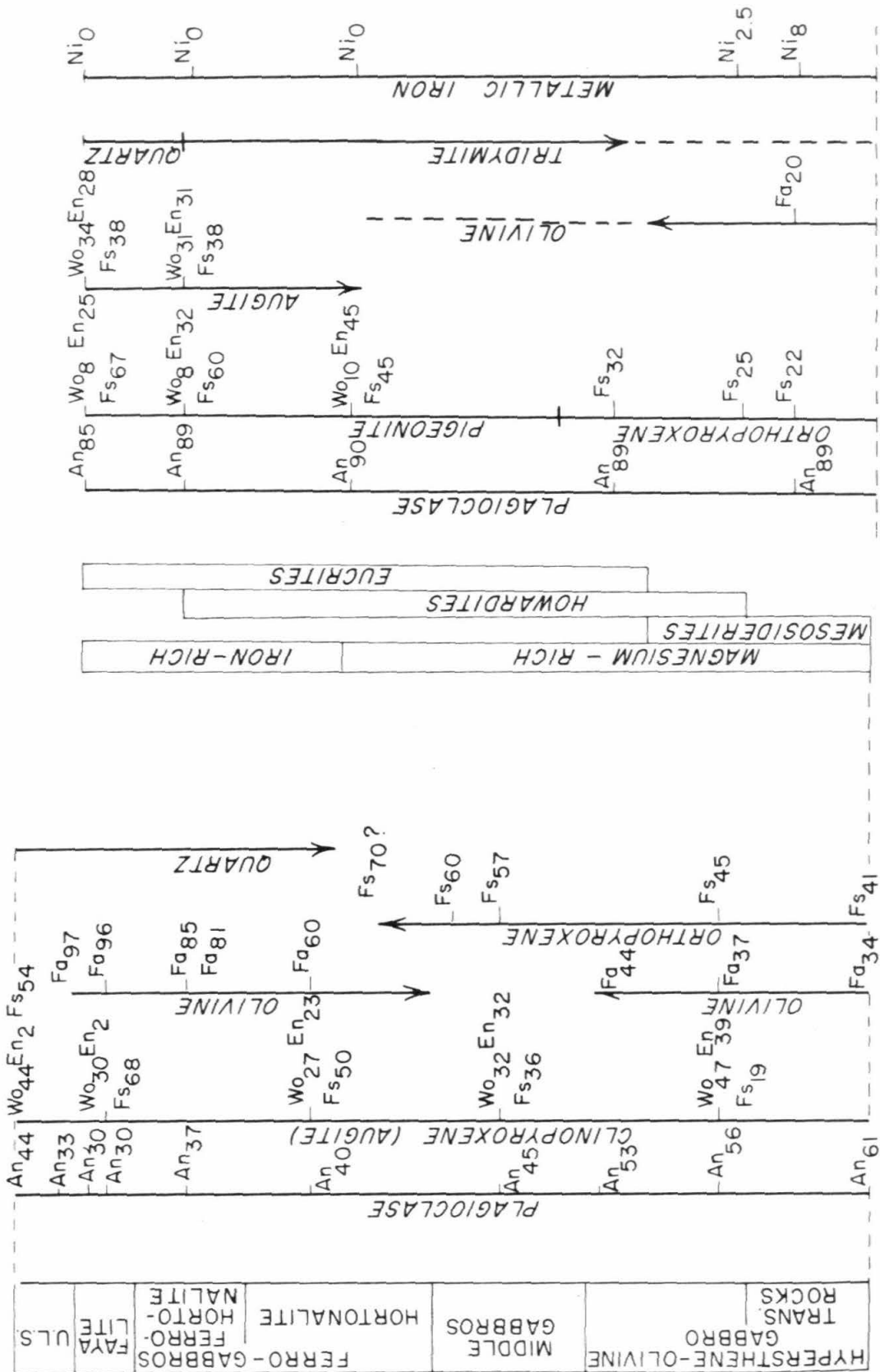


Figure 21

for an olivine in the basaltic achondrites is Fa_{30} . Orthopyroxene (inverted from pigeonite) in the Skaergaard intrusion disappears at compositions of about Fs_{70} , which is slightly more iron-rich than the pigeonite of Nuevo Laredo and some of the pigeonite of Pasamonte. Free silica is present throughout a greater range in the basaltic achondrites than in the Skaergaard intrusion. Although there are differences in detail, the mineralogy of the basaltic achondrites is similar to that of the Skaergaard intrusion and shows some of the same systematic variations of composition. The mineralogy of the basaltic achondrites, therefore, is consistent with a magmatic differentiation model for the basaltic achondrites.

PETROLOGIC TRENDS

It has been shown above that the mineralogical variations shown by the basaltic achondrites have some features in common with the mineralogical variations of terrestrial differentiated basaltic intrusions such as the Skaergaard intrusion. This discussion concerns the variations of the bulk chemical composition of the basaltic achondrites, which are examined in the light of experimental and observational evidence concerning the crystallization of basaltic magmas. The bulk compositional evidence suggests that the basaltic achondrites represent a set of compositional systems related by crystal-liquid fractionations in a single basaltic magma or in a set of similar basaltic magmas.

The normative components anorthite, enstatite and ferrosilite make up 75 percent or more of each of the basaltic achondrites and the variations of the proportions of these components are the first order compositional variations shown by the basaltic achondrites. This ternary system has not been studied experimentally, but it is possible to determine the boundary along which pyroxene, anorthite and liquid coexist by the use of ideal solution calculations (Figure 22). Table 30 summarizes the calculations employed to derive the cotectic and includes the pertinent thermodynamic data. Entropies of fusion for $MgSiO_3$ and $FeSiO_3$ were obtained by fitting an ideal solution model to the data of Bowen and Schairer⁽²⁶⁾ for the $MgSiO_3$ - $FeSiO_3$ system (Figure 23). The figure indicates that the solid solution of the pyroxenes can be described reasonably well by an ideal solution model. The binary and ternary systems are complicated by the incongruent melting of enstatite and the instability of ferrosilite, which allows the boundary curve in

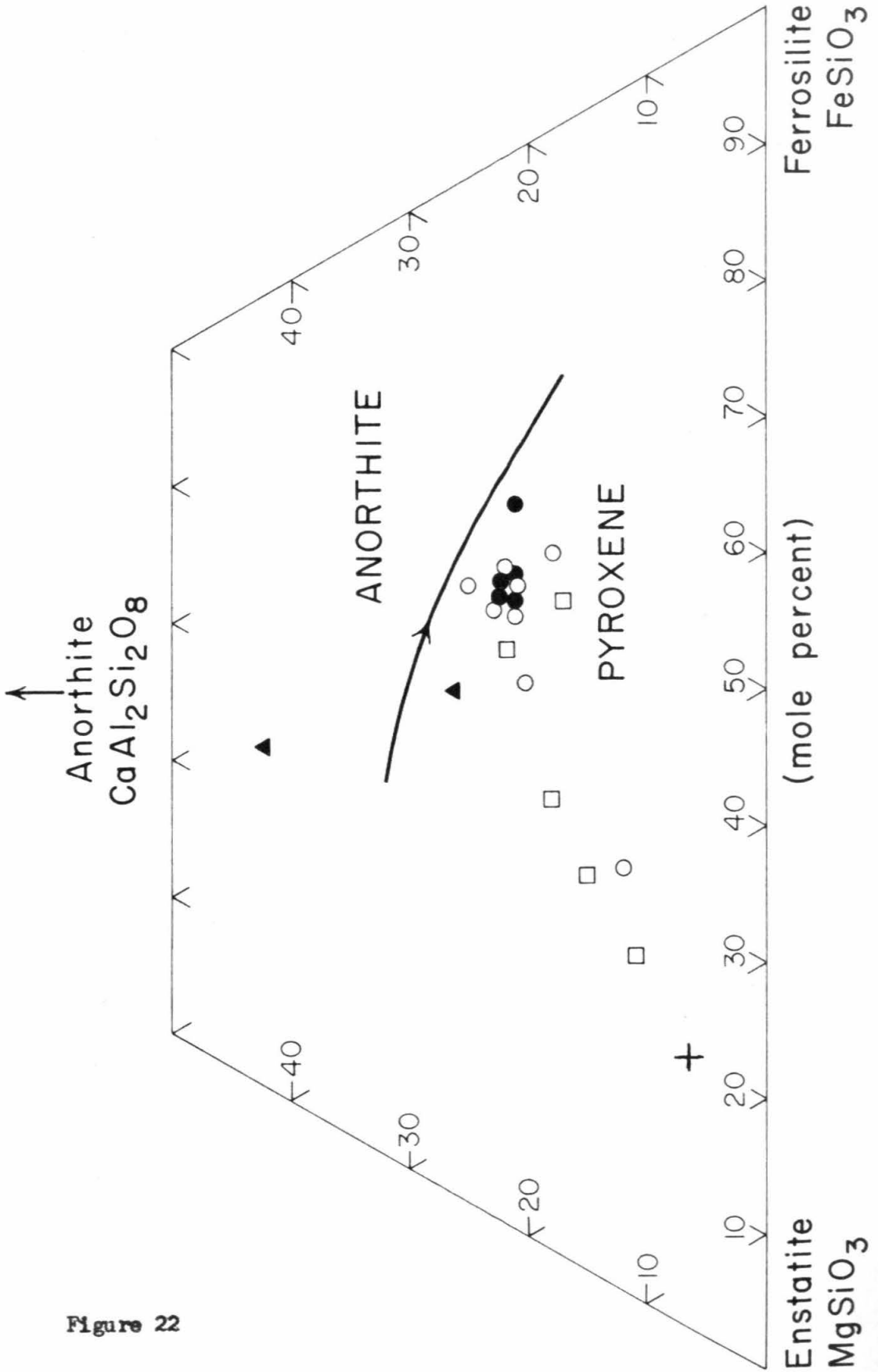


Figure 22

TABLE 30

CALCULATION OF COTECTIC IN THE $MgSiO_3$ - $FeSiO_3$ - SiO_2 SYSTEM

Components: 1 Anorthite
2 Enstatite
3 Ferrosilite

Equations:

$$x_1^l = e^{\frac{-\Delta S_{f_1}(T_1-T)}{RT}}$$

$$x_2^l/x_2^s = e^{\frac{-\Delta S_{f_2}(T_2-T)}{RT}}$$

$$x_3^l/x_3^s = e^{\frac{-\Delta S_{f_3}(T_3-T)}{RT}}$$

x_i^l (i = 1,2,3) Mole fraction of i in liquid
 x_i^s (i = 1,2) Mole fraction of i in solid
 ΔS_{f_i} Entropy of fusion of pure component i
 T_i Melting temperature of pure component i
 R Gas constant

The equations are subject to the restrictions:

$$x_2^s + x_3^s = 1; \quad x_1^l + x_2^l + x_3^l = 1$$

From these equations, isotherms can be calculated for the fields of pyroxene and anorthite stability. The intersections of the isotherms mark the boundary curve.

Thermodynamic data:

Anorthite	1823°K	8.1
Enstatite	1798	5.0
Ferrosilite	1413	6.0

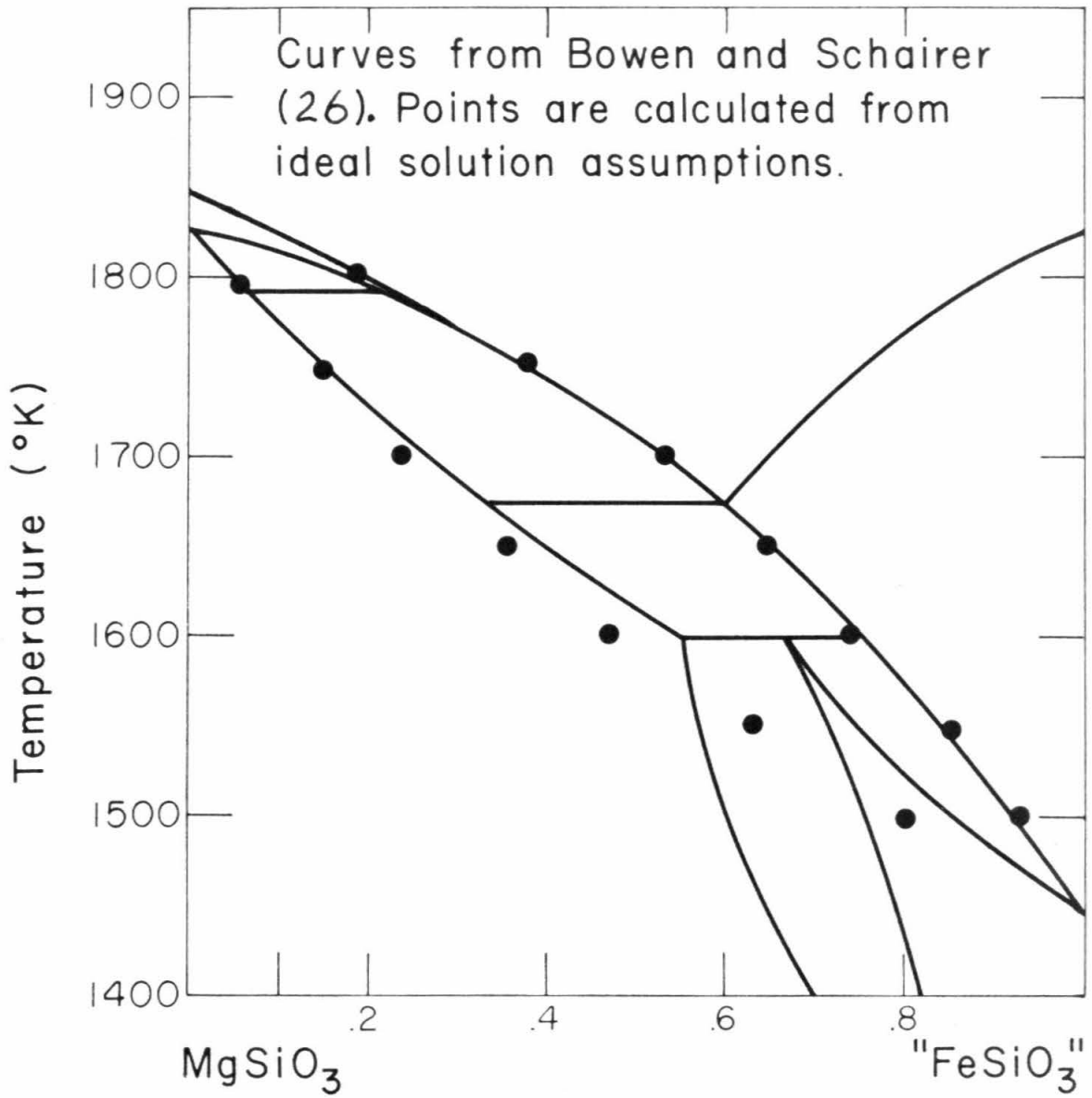


Figure 23

the ternary system to be calculated only for the regions of ternary behavior.

Table 31 gives the proportions of normative anorthite, enstatite and ferrosilite for the selected older and new analyses discussed in Chapter III and the modal proportions for some meteorites. These data are graphically presented in Figure 22. The composition of Shergotty is not considered in this discussion.

The most pronounced trend shown in Figure 22 is the general increase in the proportion of anorthite as the iron-magnesium ratio of the pyroxene increases. For the most iron-rich meteorites, there may be a decrease in the amount of anorthite as $Fe/Fe+Mg$ increases from 0.58 to 0.65. The limited range clumping of meteorite compositions does not allow a conclusive statement to be made, but these meteorites have compositions very close to the calculated cotectic and a decrease in the amount of anorthite is consistent with crystallization along the plagioclase-pyroxene-liquid boundary. These meteorites show textural evidence of co-crystallization of plagioclase and pyroxene and it has been argued in Chapter II that these meteorites are the most likely to represent the compositions of the liquids from which they crystallized.

Although it could be expected that the more magnesian basaltic achondrites do not represent the compositions of the liquids from which they crystallized and there is good evidence that Moore County and Serra de Mage do not represent liquids, there is a general trend of compositions from Estherville to Macibini and then to the most iron-rich achondrites which may be a trend of liquid compositional variation. Textural evidence is not available to indicate such trend, but it is possible to test the consistency of such a trend with what is known

TABLE 31

NORMATIVE PROPORTIONS OF An-En-Fs AND An-Fo-Fa-SiO₂

(a) Molecular proportions of An, En and Fs

Old Analyses	An	En	Fs
Bereba	22	30	48
Binda	12	57	31
Cachari	32	32	36
Chervony Koot	22	31	47
Frankfort	11	64	25
Jonzac	21	34	45
Le Teilleul	18	49	33
Luotolax	22	36	42
Macibini	20	40	40
Moore County	26	37	37
Peramiho	18	31	49
Petersburg	17	35	48
Yurtuk	15	56	29

New Analyses

Stannern	22	31	47
Juvinas	22	32	46
Sioux County	22	32	46
Pasamonte	21	31	48
Nuevo Laredo	21	26	53
Shergotty	8	45	47

Modal Analyses

Serra de Mage	42	33	25
Estherville	10	72	18

(b) Proportions by weight of An, Fo, Fa, SiO₂

	An	Fo	Fa	SiO ₂
Estherville	16	41	15	28
Hypersthene achondrites	0	60	13	27
P ₁	12	52	14	22
P ₂ Possible parent materials	8	68	12	12

about crystallization in the more complicated basaltic system.

Figure 24 gives an interpretation of the phase relations within the system $Mg_2SiO_4-Fe_2SiO_4-CaAl_2Si_2O_8-SiO_2$ based on interpolations from the experimentally known boundary systems. In this tetrahedron, the trend of compositional variation of the basaltic achondrites is indicated. Values for the compositional points are given in Table 31. The olivine-pyroxene-liquid surface (acghdf), the pyroxene-liquid stability field (efdcab), the pyroxene-anorthite-liquid boundary surface (efd) and the quaternary invariant point (d) are important to the discussion.

The silicate phase of Estherville has the smallest Fe/Fe+Mg ratio of the meteorites studied here, and this composition will be assumed to represent a liquid composition (called "Estherville liquid"). The question that is asked is whether the other compositions logically follow from this initial assumption. This can be answered by attempting to follow the course of crystallization of "Estherville liquid".

"Estherville liquid" is saturated with respect to SiO_2 , but the first phase to crystallize will be olivine. The olivine will be more magnesian than the liquid and the liquid will follow a curved path in a plane containing the initial composition of the liquid and the compositions of olivine that crystallizes from the magma. The liquid composition will reach the olivine-pyroxene-liquid boundary curve after approximately ten percent of the liquid has crystallized. Under conditions of equilibrium crystallization, the liquid will follow the pyroxene-olivine-liquid until the olivine-pyroxene-anorthite boundary is reached. Along this path some olivine reacts to form pyroxene, but the major effect is one of crystallization of

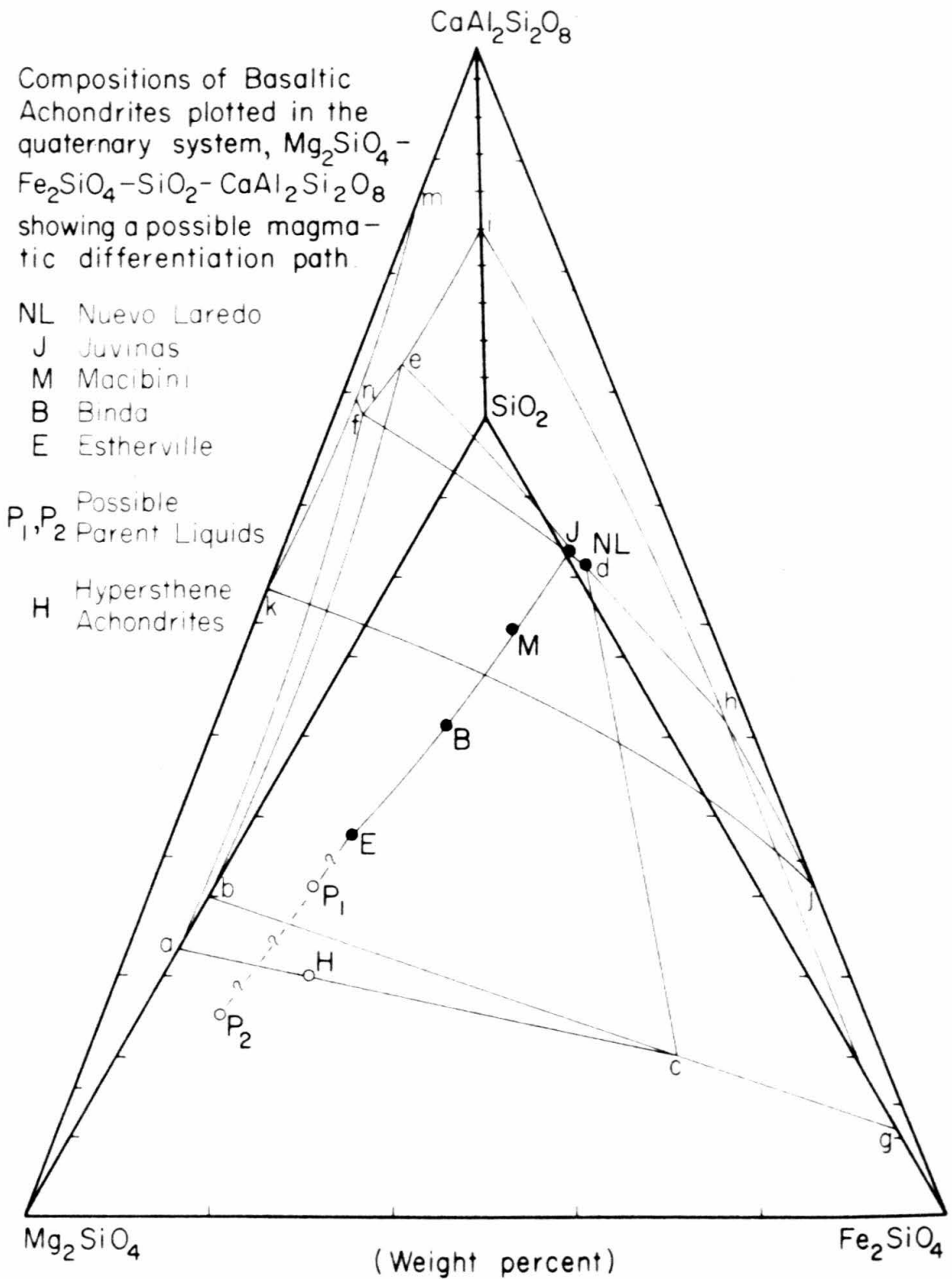


FIGURE 24

pyroxene. The liquid will reach the olivine-pyroxene-anorthite boundary when approximately 25 percent of the liquid remains and the liquid contains about 60 percent anorthite. Crystallization proceeds along the boundary curve with the remaining olivine reacting and pyroxene and plagioclase crystallizing until at some point short of the invariant point (d), the last liquid disappears just as the last olivine has reacted. The composition of the final liquid can be estimated to have $Fe/Fe+Mg = 0.4$ from tie lines given by Bowen and Schairer⁽²⁶⁾ for the binary system $MgSiO_3 - FeSiO_3$.

Because the $Fe/Fe+Mg$ ratio in the iron-rich meteorites is greater than 0.4, it is apparent that fractional crystallization is required. The principal effect of fractional crystallization on variations discussed above are the increase of the range of iron-magnesium ratios. In either equilibrium crystallization or fractional crystallization the amount of anorthite in the residual liquid reflects primarily the amount of pyroxene or olivine that has been extracted from the liquid. For a fractional crystallization path starting with "Estherville liquid" for complete removal of crystals, the liquid will move in a curved path to the olivine-pyroxene-liquid boundary and will intersect the boundary at a slightly more iron-rich composition than in the case of equilibrium crystallization. Because there is no olivine to react with the liquid, the liquid will follow a path in the field of pyroxene stability constrained to a plane that includes the composition of the liquid at the point at which the pyroxene stability field is reached and the line representing the compositions of the pyroxene that separate from the magma. Because the point at which the liquid first encounters the pyroxene stability field is

generally only slightly oversaturated with respect to silica, the constraining plane will be almost identical to the pyroxene-anorthite plane of Figure 22.

The trend of compositions for the magnesium-rich achondrites in Figure 22 can be examined with respect to known tielines for the binary system $MgSiO_3$ - $FeSiO_3$. Although they are subject to some modification within the "ternary" system, the tielines in the binary system should give a useful first approximation to tielines in the more complicated system. Figure 25 shows paths of crystallization of "Estherville liquid" for equilibrium crystallization and fractional crystallization with complete separation of crystals within the field of pyroxene stability. The fractional crystallization trend fits the compositional data for the basaltic achondrites. Although the paths of crystallization can not be considered to be precisely known, they suggest that the variational trend shown by the compositions of the basaltic achondrites do represent a trend of crystal-liquid fractionation. The fractional crystallization curve shown in Figure 25 is analogous to the trend of compositions shown by the meteorites in Figure 24.

Most of the crystallization path outlined in Figures 24 and 25 consists of crystallization in the pyroxene stability field. During this portion of the crystallization path, the amount of anorthite builds up to the point that the pyroxene-anorthite boundary surface is reached. If we now consider the addition of another component to the four component system, namely albite, it is possible to test the reality of the trend that has been outlined. If the magmas crystallized in a field where plagioclase was not separating from the liquid, it is expected that the plagioclase composition should not vary along

E ESTHERVILLE

B BINDA

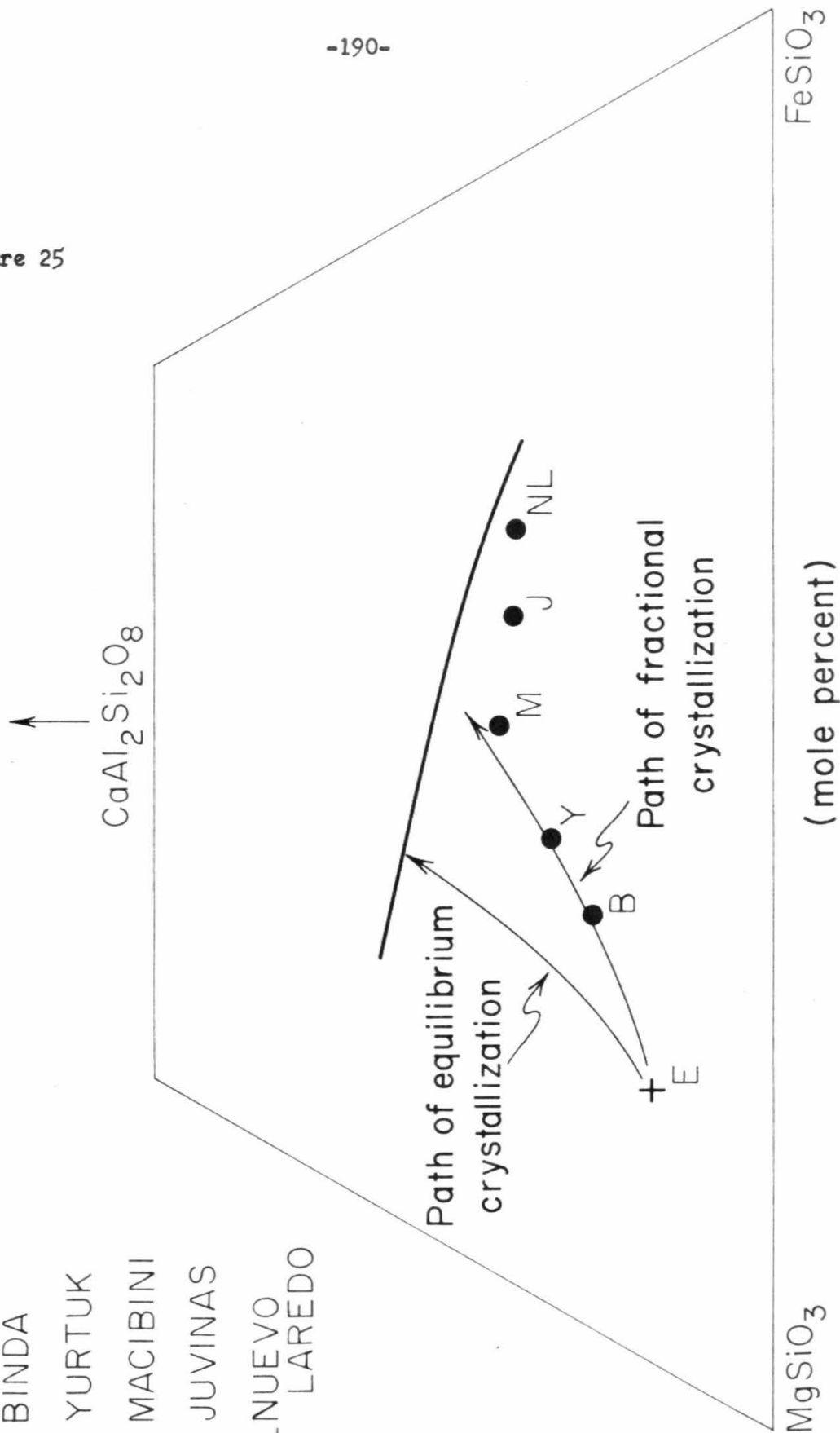
Y YURTUK

M MACIBINI

J JUVINAS

NL NUNUEVO
LAREDO

Figure 25



that portion of the path of crystallization. Consideration of Figure 19 shows that there is little variation of plagioclase composition, especially if lithic fragments alone are considered, for a rather wide range of pyroxene compositions. This relation is interpreted as a supporting argument that the paths of crystallization of the more magnesian basaltic achondrites have started from a plagioclase-depleted composition such as "Estherville liquid".

For the most iron-rich basaltic achondrites, the compositional variations shown in Figure 22 suggest that crystallization along a pyroxene-plagioclase boundary has occurred. For these systems, the composition of plagioclase becomes enriched in albite as the $Fe/Fe+Mg$ ratio increases, which is consistent with the expected variations along a pyroxene-plagioclase boundary.

The component of the basaltic achondrites that has not been considered to this point in the discussion of compositional variations is the wollastonite (calcium pyroxene) component. The effects of this component are difficult to assess in the same manner as in the previous discussion, but the variations of the normative pyroxene composition can be compared to the variations shown by the Skaergaard intrusion (Figure 26). Although the trend toward the calcic iron-rich pyroxene (hedenbergitic) compositions is shown by both assemblages, the Skaergaard compositions tend to show more strongly the enrichment in hedenbergite. This variation, and the distinct difference in the plagioclase compositions of the two suites, are the most pronounced compositional differences between the Skaergaard intrusion and the basaltic achondrites. Only some suggestions can be advanced as possible explanations of the differences.

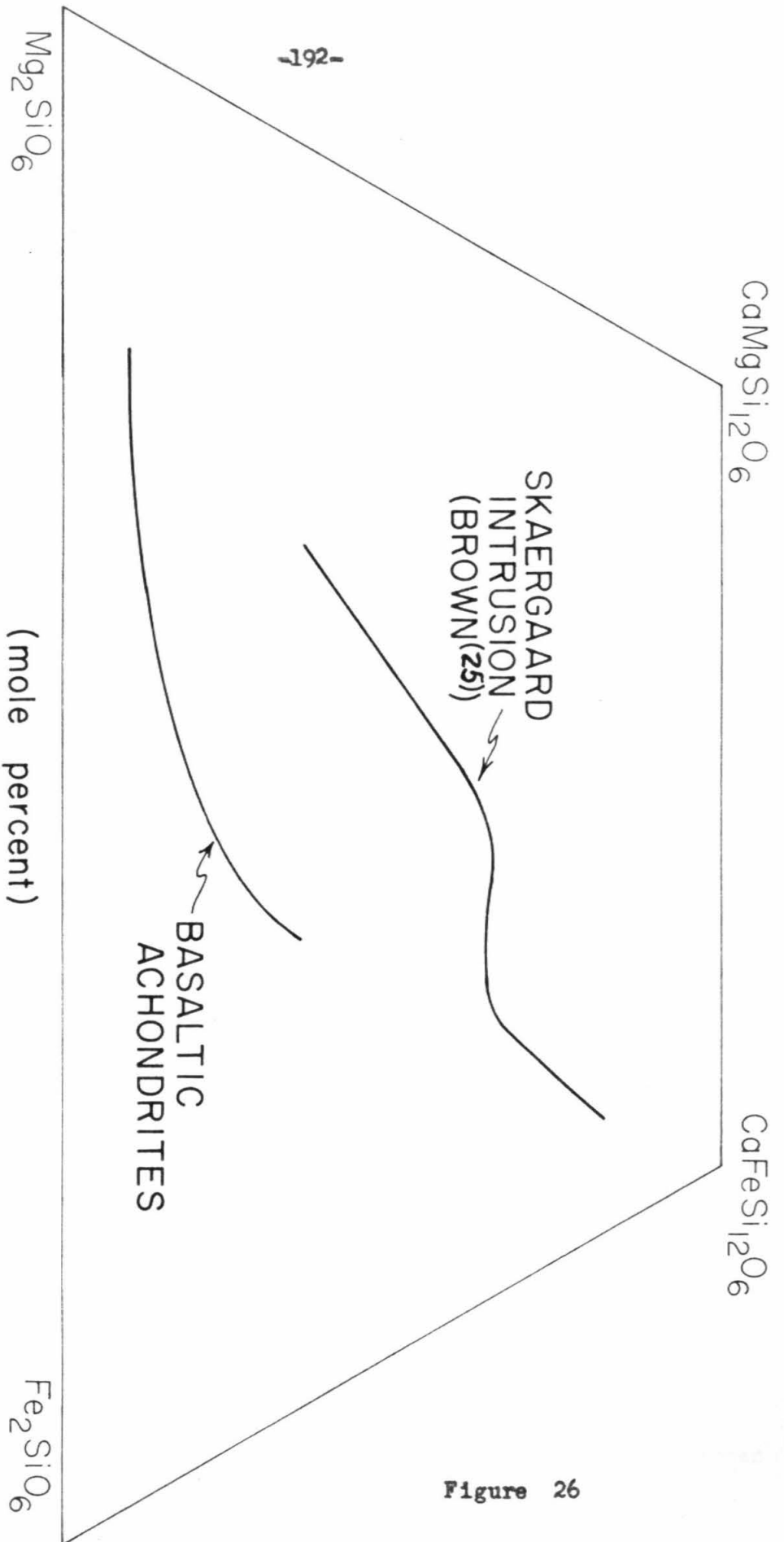


Figure 26

The starting composition of the magmas may have played a large part in the variations of the normative pyroxene composition. It can be argued that the reason for the important difference in the plagioclase compositions, in part, is due to the initial starting composition of the basaltic achondrite magma which did not allow the plagioclase component to change greatly its composition. In the case of the pyroxene composition, it may be that the starting compositions were different in that there was more olivine in the Skaergaard magma than in "Estherville liquid". With continued separation of olivine instead of pyroxene, the calcium pyroxene component may have been more strongly enriched in the Skaergaard trend.

A factor which may be of importance in determining the details of the variational trends in basaltic magmas is the role of the partial pressure of oxygen. Osborne⁽⁴¹⁾ has argued that crystallization under constant partial pressure of oxygen leads to enrichment of silica in a basaltic magma, whereas crystallization under a condition of "constant total composition" leads to the iron-enrichment trend observed in the Skaergaard intrusion and in the basaltic achondrites. The effects of oxygen partial pressure conditions intermediate between a fixed partial pressure and "constant total composition" is not known. From examination of the diagrams presented by Muan and Osborne⁽⁵⁵⁾ and Osborne⁽⁴¹⁾ however, it does not appear that the partial pressure of oxygen has a pronounced effect on crystallization in the magnesian portions of the system except at very high partial pressures of oxygen. For the basaltic achondrites, the presence of metallic iron and the low content of Fe_2O_3 indicates that the partial pressures of oxygen were low. Although the partial pressures of oxygen were somewhat higher

in the case of the Skaergaard intrusion, magnetite was not a major component until the later stages of crystallization. Although it is not possible to decide on the basis of present data, it seems more probable that the differences of the compositional trends shown by the basaltic achondrites and by the Skaergaard intrusions are due to initial compositional differences than to differing partial pressures of oxygen.

The demonstration that the compositions of the basaltic achondrites may be related by processes of magmatic differentiation provides an important means of setting limits on the composition of the parent material of the basaltic achondrites. In the previous discussions, it has been assumed that the "Estherville liquid" was the starting composition. That is not a unique assumption, but only one which can be reconciled with the data. The "Estherville liquid" composition is interpreted as being a limiting composition for the parent material, but it could represent the differentiation product from a more primitive material.

The limits that the "Estherville liquid" puts on the parent material are (1) the plagioclase content of the parent material was less than or equal to 15 percent and the plagioclase composition was approximately An_{90} , because the plagioclase composition of the parent material correspond to the plagioclase composition of the magnesian liquids, (2) the pyroxene composition was low in calcium probably a hypersthene composition, (3) the Fe/Fe+Mg ratio was less than or equal to 0.25. Possible more primitive parent magma compositions are given in Figure 24. The olivine-pyroxene proportions in the parent magma can not be determined from the present data, for there are a variety of initial compositions and processes by which a plagioclase-poor, olivine-pyroxene-bearing

magma could differentiate towards the "Estherville liquid" composition.

It is of fundamental importance, however, that the parent material of the basaltic achondrites is clearly distinct from the composition of the chondritic meteorites. The distinguishing feature between the chondrites and the parent material of the basaltic achondrites is the composition of the plagioclase. In chondrites, the composition of the plagioclase is quite sodic, in the basaltic achondrites the initial plagioclase composition necessarily was quite calcic.

The depletion of alkalis in the basaltic achondrites with respect to chondrites has been noted previously. Urey⁽⁵⁶⁾ and Gast⁽³⁵⁾ argued for a process of fractional volatilization of alkalis from chondritic material to explain the depletion. Urey⁽⁵⁷⁾ has suggested that the fractional volatilization took place during the magmatic history of the basaltic achondrites.

The demonstration that the plagioclase composition is calcic from the very beginning of the compositional variation trend of the basaltic achondrites and is satisfactorily explained on the basis of magmatic differentiation is a strong argument that the initial plagioclase composition was calcic. There is no evidence of depletion of alkalis over the differentiation path shown by the basaltic achondrites. The coupled sodium and potassium variations shown in Figure 14 also indicate that alkalis were behaving normally during the magmatic episode. These arguments indicate that the fractionation of alkalis between chondrites and the parent material of the basaltic achondrites is of a more fundamental nature than has been supposed previously. It is possible that the fractionation relates to a process that occurred during the accretion stages of the solar system. Volatilization may

have played a part in the fractionation of alkalis, but other possible chemical processes should be investigated.

Figure 24 can be used to suggest other types of meteorites which might be related to the basaltic achondrites as a product of magmatic differentiation. The magmatic differentiation trend presupposes a mechanism for removal of crystals from the liquids. In Moore County and Serra de Mage there is evidence of crystal accumulation and it may be supposed that crystal settling was a dominant mechanism by which the basaltic achondrites differentiated. If that is the case, one can specify what types of crystal accumulates might be expected.

If the initial parent material had a relatively large olivine content, it should have been possible to obtain dunites, as well as peridotites and pyroxenites. These accumulates could contain some calcic plagioclase, but its abundance would be low due to the low plagioclase content in the starting liquids. Meteorites which possibly fit these specifications are the hypersthene achondrites. These meteorites are composed primarily of hypersthene (Shalka and Tatouhine have hypersthene with $Fe/Fe+Mg=0.22$) with minor amounts of plagioclase (in Johnstown) and olivine (Mason⁽¹⁾, ⁽⁵⁸⁾). These meteorites could well be crystal accumulates from the earlier basaltic achondrite magmas. From later achondrite magmas, pyroxenites or anorthosites could form in similar manner to their occurrences in terrestrial layered intrusions.

The composition of the Nuevo Laredo meteorite lies very close to the quaternary invariant point (d) of Figure 24. For compositions more iron-rich than Nuevo Laredo, it might be expected that pigeonite would be replaced by an iron-rich olivine and silica. Instead of a mineral

assemblage consisting of plagioclase, pigeonite, ferroaugite and silica, the assemblage in the more iron-rich systems might be plagioclase, ferroaugite, olivine and silica. No meteorites with this type of composition have been found.

Another use of the differentiation trends is a specification of limits on the amounts of the various compositions which could be obtained by magmatic differentiation from an initial magma such as the "Estherville liquid". In the fractional crystallization trend shown in Figure 25, the amount of liquid remaining when the composition reaches the pyroxene-plagioclase-liquid boundary is between 25 percent and 30 percent of the initial liquid. This places minimum limits on the proportions of initial and starting compositions, because the proportions are maximized for the most extreme fractional crystallization and the compositional limits are greater than those indicated by the variation across the pyroxene stability field. It can be concluded that only a small fraction of the initial liquid can be represented in the very highly differentiated liquids such as that of the Nuevo Laredo meteorite.

TRACE ELEMENT DISTRIBUTION

Tables 32 to 34 give determinations of trace element abundances for the basaltic achondrites made, in this work, by emission spectrographic analysis and, in previous work, by a variety of other techniques. Where data can be compared, the spectrographic technique apparently yields values comparable to the other analytical data. In general, the spectrographic values are reproducible to about 20% of the amount present.

Included in the tables are trace element abundances in total basaltic achondrite samples, plagioclase and pyroxene separates from basaltic achondrites, and silicate fractions from chondrites and other non-basaltic achondrites. Also included for comparison are values for liquids of the Skaergaard intrusion (Wager and Mitchell⁽⁵⁹⁾).

Figure 27 gives the variation of trace elements in the total basaltic achondrite samples as a function of the Fe/Fe+Mg ratio. Most of the trace elements show general trends of enrichment or depletion with increasing Fe/Fe+Mg which can be compared with the direction of the trends in the Skaergaard suite. For many of the elements, the absolute abundances are quite different in the Skaergaard rocks and the basaltic achondrites, but the trends are similar. Enrichment of barium, strontium, rubidium, cesium, yttrium, lanthanum (and other rare earth elements), zirconium, and manganese occurs both in Skaergaard and in the basaltic achondrites with increasing Fe/Fe+Mg. Chromium and vanadium tend to decrease in both suites, but are more irregular in their variation in Skaergaard rocks than in the basaltic achondrites. Scandium tends to increase in the basaltic achondrites, but tends to decrease in

TABLE 32

EMISSION SPECTROGRAPHIC ANALYSES OF TOTAL METEORITE SAMPLES,

WITH COMPARISONS TO TRACE ELEMENT DATA OF OTHER WORK

AND TO TRACE ELEMENT CONTENTS OF ROCKS OF THE SKAERGAARD INTRUSION

	(ppm)									
	<u>1</u>	<u>2</u>	<u>3</u>	<u>4</u>	<u>5</u>	<u>6</u>	<u>7</u>	<u>8</u>	<u>9</u>	<u>10</u>
Ba	5	20	17	26	26	62	40 44 ^d	43	90	170
Co	120	3	-	-	3	3	1	53	35	22
Cr	4800	2600	4500	3200	2700	2700	2100 1200 ^b	170	75	1
Cu	48	2	7	3	4	3	2	130	220	360
Ga	-	-	-	-	-	-	1	17	20	21
Mn	2100	2900	2200	2400	2500	2500	3500	800	1220	1500
Ni	2000	3	2	4	3	3	8	170	50	1
Sc	16	30	18	30	32	33	40 45 ^b 43 ^c	12	15	9
Sr	29	75 69 ^a	81 80 ^a	70 83 ^a	81	92	100 84 ^a	350	500	470
Ti	800	2200	1100	1700	1900	3000	3000			
V	130	64	120	130	150	110	70	140	220	10
Y	10	20	10	18	24	37	30		13	45
Yb	3 0.5 ^c	3	2	4 1.7 ^c	3	5	5 2.3 ^c			
Zr	13	38	17	36	41	73	70	50	80	90
Fe/FetMg	.20	.59	.50	.61	.60	.61	.65	.33	.52	.58

TABLE 32

References

1. Estherville, this work
2. Sioux County, this work
3. Moore County, this work
4. Pasamonte, this work
5. Juvinas, this work
6. Stannern, this work
7. Nuevo Laredo, this work
8. Skaergaard intrusion, 1st liquid, Wager and Mitchell(59)
9. " " 2nd liquid, " "
10. " " 3rd liquid, " "

- a Gast(69)
- b Bate, et al(60)
- c Schmitt, et al(61)
- d Reed, et al (63)

TABLE 33

EMISSION SPECTROGRAPHIC DATA FOR PYROXENES FROM SOME BASALTIC ACHONDRITES

(ppm)

	Serra de Mage*	Juvinas**	Pasamonte**	Nuevo Laredo***
Ni	3	-	3	-
Mn	4000	4000	4000	5500-7100
Ti	900	2000	900	2300-5200
Cr	4000	3000	3000	4000-6700
V	100	80	100	100
Sc	30	50	50	60
Zr	20	40	20	60

* Fe/Fe+Mg 0.44

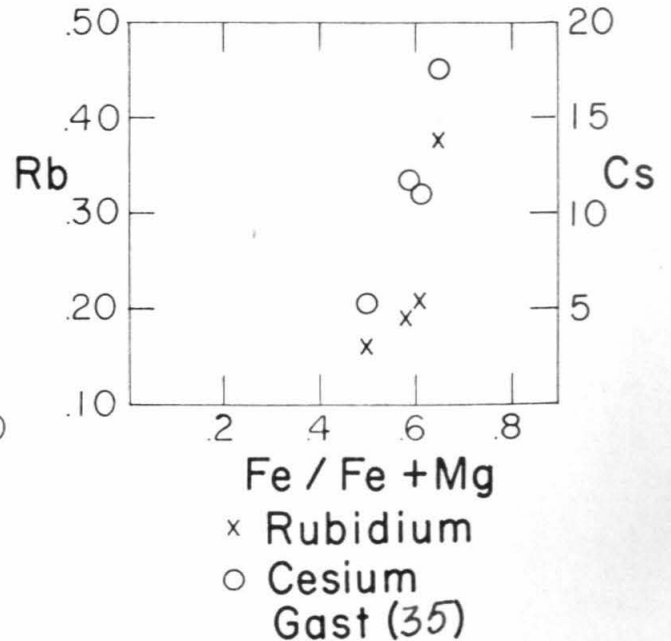
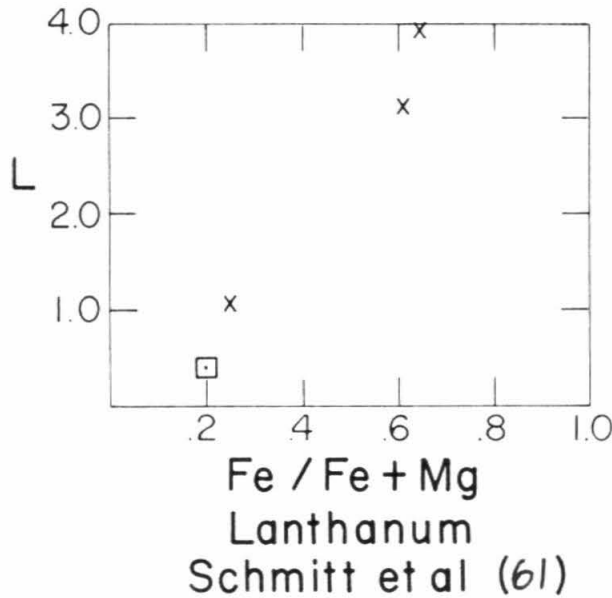
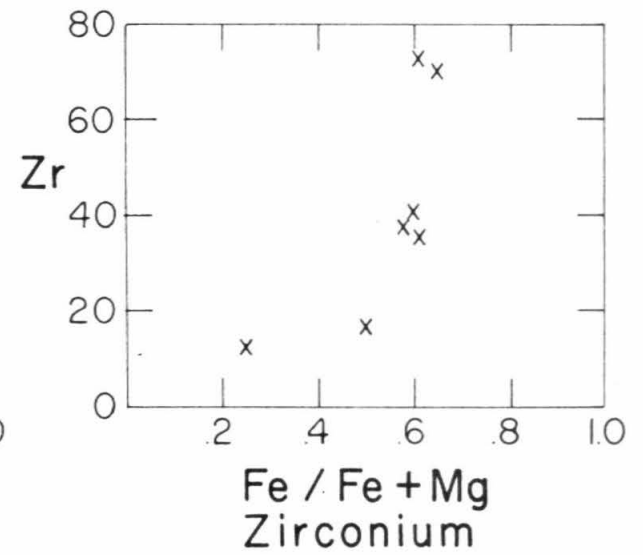
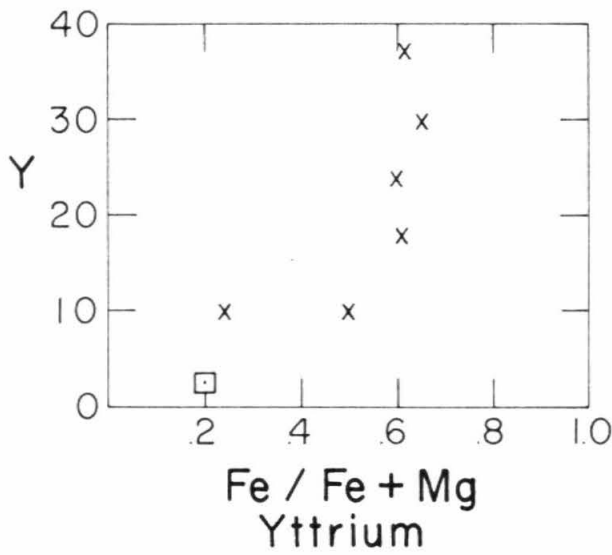
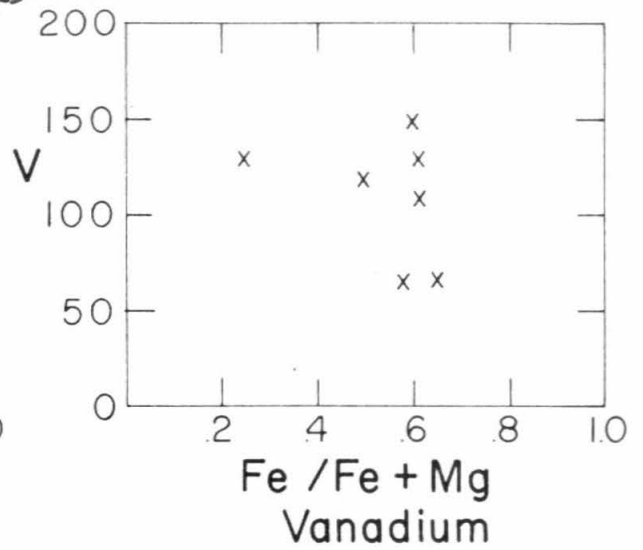
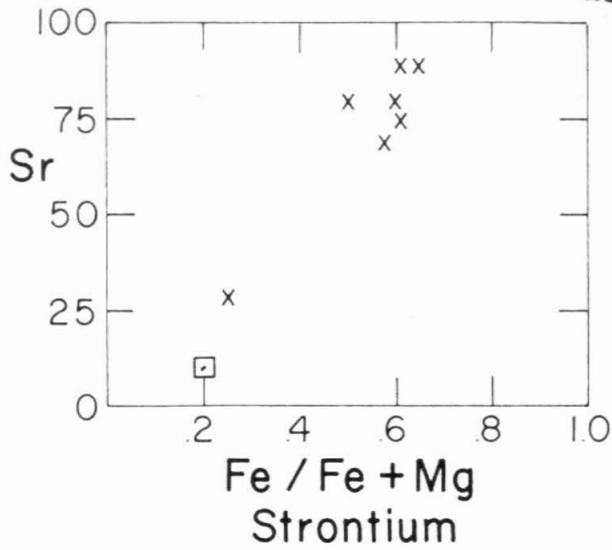
** Fe/Fe+Mg 0.61

*** Fe/Fe+Mg 0.65

TABLE 34

EMISSION SPECTROGRAPHIC DATA FOR PLAGIOCLASE OF THREE BASALTIC ACHONDRITES

	Serra de Mage (An ₉₅)	Moore County (An ₉₀)	Nuevo Laredo (An ₈₅)
Ni	-	-	-
Mn	30	100	600
Ti	-	80	1000
Cr	60	80	200
Sc	-	-	-
V	20	20	20
Zr	0	-	-
Ba	10	20	70
Sr	100	200	200
Y	-	-	20
Yb	-	-	2



Schmitt et al (61)

x Rubidium
o Cesium
Gast (35)

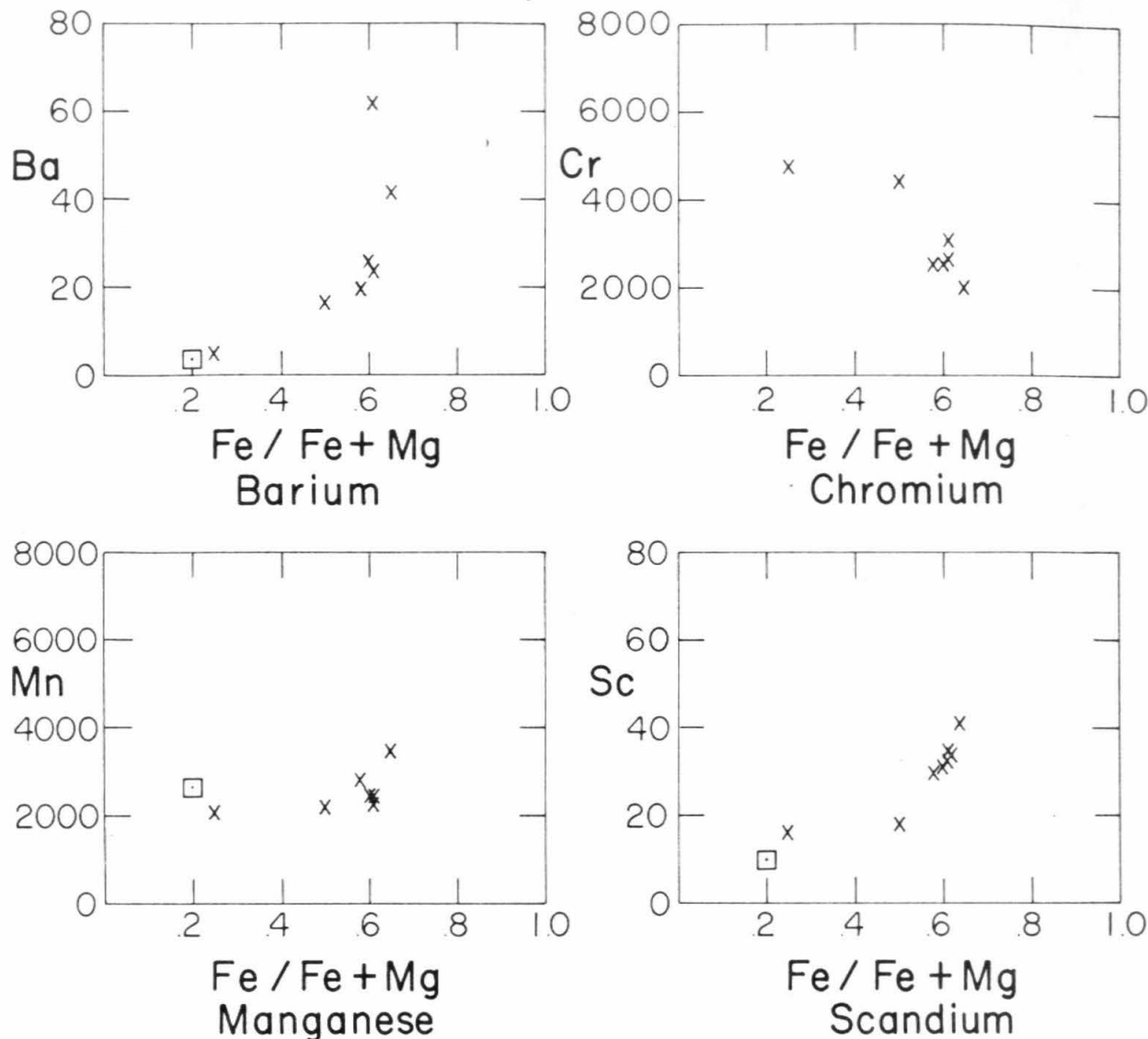


FIGURE 27

x Basaltic achondrites
□ Chondrites

Skaergaard.

The trace element analyses of the mineral separates from the basaltic achondrites show that the elements barium, strontium, and yttrium are concentrated in the plagioclase; the alkali metals rubidium and cesium are probably enriched in the plagioclase. Chromium, manganese, scandium and vanadium are concentrated in the pyroxenes. Zirconium in Nuevo Laredo does not show any marked tendency to occur in either phase, and may be concentrated in small amounts of a dispersed mineral which has not been identified. X-ray fluorescence analyses of the metallic iron shows that the nickel is concentrated with the metal (Part IV), and the cobalt is also presumed to be concentrated in the metal. Copper is a sulfophile element and is generally concentrated in the sulfide phase of the meteorites. In the Skaergaard intrusion, magnetite is the host mineral for much of the vanadium; chromium was concentrated in an early-forming chrome spinel. With these observations about the partition of trace elements between minerals, the similarities and differences between Skaergaard and the basaltic achondrites can be examined.

The elements which are concentrated in the plagioclase of both Skaergaard and the basaltic achondrites show similar variations. This statement holds primarily for the variations of barium, strontium, and the rare earths (and probably rubidium and cesium) which increase with increasing $Fe/Fe+Mg$. Chromium is concentrated in pyroxene in both suites and tends to enter the pyroxene in greater amounts than the concentrations in the magma and so becomes depleted in later stages of differentiation. Manganese is concentrated in the pyroxenes, but tends

to be concentrated in the residual liquids and increases slightly with differentiation. The vanadium of the basaltic achondrites is concentrated primarily in pyroxene and shows a general tendency towards depletion with increasing $Fe/Fe+Mg$. In the Skaergaard gabbros, vanadium is strongly concentrated in magnetite and drops sharply after magnetite appears. Scandium, which is concentrated in pyroxenes in both cases, shows little variation in Skaergaard, but shows a general increase in the basaltic achondrites. However, scandium does show a small increase in the early pyroxenes of Skaergaard with increasing $Fe/Fe+Mg$ (Wager and Mitchell,⁽⁵⁹⁾) and the difference between the two total liquid trends may be due to the stronger concentration of pyroxene component in the residual liquids of the basaltic achondrite system than in the Skaergaard rocks. The proportion of pyroxene in the basaltic achondrites rises to 70% of the total system in the last observed stages, but is only about 40% in similar Skaergaard rocks.

The depletion of nickel in the basaltic achondrites may be due to two processes. First, there is a very large fractionation factor which favors nickel in the metallic iron of the meteorites. The depletion of nickel in the basaltic achondrites may be due primarily to the separation of metallic iron from the silicate system during its magmatic history. Depletion of nickel during fractional crystallization may also have occurred. Comparison of the nickel contents of the silicate phases of chondrites and other achondrites suggests that, although the silicate phases of chondrites and achondrites are generally low in nickel, there is a somewhat greater nickel content than is present in

the iron-rich basaltic achondrites. It must be cautioned that the analyses for nickel in the silicate phase of the chondrites and achondrites must be considered upper limits due to possible contamination with very small amounts of metallic iron or sulfide. In Skaergaard rocks there is a well defined tendency for nickel to be concentrated in the most magnesian pyroxenes and, if the nickel contents of the silicate phases of the chondrites and pyroxene achondrites (which are more magnesian than the iron-rich basaltic achondrites) are greater than the nickel contents of the iron-rich basaltic achondrites, an analogous situation exists. The depletion of nickel in the basaltic achondrites may be due, in part, to the normal trends of fractional crystallization.

The general similarity and explainable differences between trace element variations in the basaltic achondrites and the Skaergaard intrusion is further evidence for a related type of igneous differentiation. The fact that most of the data from the achondrites fit into systematic trends further indicates that the achondrites have shared a common igneous history.

Comparison can be made of the trace element abundances of lithophile elements in the basaltic achondrites and the chondrites. It has been recognized previously that many of the trace elements in basaltic achondrites have quite different abundances than in the chondrites (Bate, et al⁽⁶⁰⁾; Gast, (35); Schmitt, et al⁽⁶¹⁾). The inclusion of the mesosiderite silicate phase and of magnesium-rich basaltic achondrites has allowed the variational trends of the achondrites to be

followed back into the presumably less differentiated compositions and allows a clear comparison between the basaltic achondrites and chondrites to be made.

The magnesium-rich basaltic achondrites show great similarity to the chondrites for many trace elements, including Ba, Mn, Sc, Sr, Y, La (and other rare earth elements). Schmitt, et al⁽⁶¹⁾ have shown that the spectrum of rare earth elements (the relative abundances of REE) is identical for chondrites and basaltic achondrites. As far as these elements are concerned, the basaltic achondrites could well represent samples of the silicate phase of chondrites.

As in the case of the major elements, the only trace elements which do not fit into the picture are the alkalis, rubidium and cesium, which are depleted in the achondrites. Rubidium and cesium do show, however, regular variations within the basaltic achondrites as a function of $Fe/Fe+Mg$. These variations are consistent with variations expected under conditions of fractional crystallization. It must be concluded that all the alkalis started from low concentrations and any fractionation of alkalis between chondrites and the parent material of the basaltic achondrites must have occurred before initiation of the magmatic sequence described here.

VII

NUCLEAR DATA

Various types of data involving determinations of isotopic abundances of elements have been obtained for basaltic achondrites. These data can be used to establish crystallization and cosmic-ray exposure ages and to establish the isotopic compositions of primordial matter.

One of the criticisms that can be made about most absolute age determinations yet made on meteorites is that they are, in general, model ages based on the assumption that two different types of meteorites have been separated from a single system at a precise time. Absolute age determinations on two or more minerals of the same meteorite would be of great value, but no definitive data on individual minerals from a single meteorite have been published.

Pb²⁰⁷/Pb²⁰⁶ absolute ages

Patterson⁽⁶²⁾ determined the lead isotopic composition in Nuevo Laredo. It was found that the lead of Nuevo Laredo had large amounts of radiogenic isotopes relative to the common lead. This is consistent with the expected fractionation of uranium, thorium and lead between silicate and sulfide phases and the great age of the system. Making the assumption that the common lead in Nuevo Laredo has the same isotopic abundances as the lead from the troilite of the Canon Diablo iron meteorite, Patterson calculated a Pb²⁰⁷/Pb²⁰⁶ age of 4.55 billion years for Nuevo Laredo. This age is presumed to correspond to the time that the uranium-lead system of Nuevo Laredo was separated from

the uranium-lead system of the iron meteorite.

The uranium-lead system of Nuevo Laredo appears to give very discordant ages for the separation of uranium and thorium from lead. Patterson⁽⁶²⁾ determined the amounts of uranium and thorium necessary to produce the observed quantities of lead in a 4.5 billion year decay interval. The following table presents the data on the absolute abundance of lead and the predicted amounts of uranium and thorium. For comparison, the observed amounts of uranium and thorium are given.

Pb abundance	0.7ppm	Patterson ⁽⁶²⁾
Predicted U	0.2	
Predicted Th	0.7	
Measured U	0.12	Reed, et al ⁽⁶³⁾
Measured Th	0.047	Bate, et al ⁽⁶⁰⁾

The amounts of lead measured by Patterson are almost twice that which would be produced by the measured amounts of uranium and thorium over a period of 4.5 billion years. Redeterminations of the Pb^{208} content of Nuevo Laredo by Reed, et al⁽⁶³⁾, when combined with the isotopic abundances of lead determined by Patterson, seem to confirm the absolute abundance of lead determined by Patterson. The data are consistent with a rather redistribution of uranium and lead in the meteorite system, but no petrologic evidence for a recent chemical episode has been observed. More study is necessary on the uranium-lead systems in the basaltic achondrites.

Uranium-helium ages

Data for uranium concentrations and He^4 concentrations are given below for some basaltic achondrites. From these data, assuming the Th/U ratio is known, a time can be calculated which may indicate the age of isolation of the uranium-helium system in the meteorite. Such ages are severely limited by the diffusion losses of helium from the system.

Meteorite	U	Th/U	He^4	Age
Nuevo Laredo ^{1,2,4}	.126ppm	3.8	1.3×10^{-5}	.45by
Pasamonte ³			6.1	3.6*
Shergotty ³			0.2	

1 Hamaguchi, et al⁽⁶⁴⁾

2 Reynolds and Lipson⁽⁶⁵⁾

3 Eberhardt and Hess⁽⁶⁶⁾

4 Bate, et al⁽⁶⁰⁾

* Based on unpublished uranium data of Wanke

For none of these meteorites have the uranium and helium determinations been made on the same sample and for Shergotty no uranium determination has been made. If one makes the first order assumption that the uranium contents are equal, it is clear that the three meteorites have suffered radically different losses of helium and any ages determined on the basis of helium and uranium data must be suspect.

POTASSIUM-ARGON AGES

Potassium-argon ages for basaltic achondrites are given in Table 35. These include data compiled by Anders⁽⁶⁷⁾ and Stauffer⁽⁶⁸⁾

The analytical data presented in this work indicate that the potassium of most of the basaltic achondrites is located in plagioclase and it is reasonable to expect that potassium is concentrated in the sodium-rich portions of those meteorites which show compositional variation in their plagioclase. The potassium content of different samples of the same meteorite may vary because of variations in the amounts of pyroxene and plagioclase or because of variations due to compositional zoning. It is unfortunate, therefore, that in many cases potassium and argon measurements have not been made on the same samples of the meteorites.

The calculated ages vary from 0.56 to 4.3 billion years. As the potassium-argon systems are known to be subject to diffusion losses of argon, the data can be considered to give minimum ages and are consistent with an original crystallization age of 4.5 billion years.

The isotopic composition of strontium; Rb-Sr model ages

Gast⁽⁶⁹⁾ has published determinations of rubidium and strontium isotopic contents and strontium isotopic compositions for Pasamonte, Sioux County, Moore County and Nuevo Laredo. His data are summarized in the following table:

TABLE 35
 POTASSIUM-ARGON AGES

Meteorite	K-Ar Age	Reference
Moore County	3.2	Geiss and Hess ⁽³⁶⁾
Pasamonte	3.8	Geiss and Hess
	4.3	Wanke and Konig (78)
Stannern	3.0	Vinogradov, et al(79)
Nuevo Laredo	3.1-3.6	Reynolds and Lipson(65)
Chervony Koot	2.7	Vinogradov, et al
Shergotty	0.56	Geiss and Hess
Padvarninkai	1.0	Gerling and Rik(80)
Pavlovka		
Yurtuk	2.6	Vinogradov, et al
Frankfort	5.1	Geiss and Hess

Meteorite	Plag. K/Ca	Sr(ppm)	Rb(ppm)	Rb/Sr	Sr ⁸⁷ /Sr ⁸⁶
Moore Co.	.0036	79.5	0.16	.0020	.7023
Sioux Co.	.0053	68.8	0.20	.0029	.7015
Pasamonte	.0076	82.9	0.23	.0028	.7008
Nuevo Laredo	.0109	81.1	0.36	.0043	.7027

From the trace element analyses done in this work, it is clear that most of the strontium and presumably the rubidium of the basaltic achondrites is located in the plagioclase. It is therefore of interest that Rb/Sr shows good correlation with K/Ca of plagioclase as determined in this work. The correlation indicates that Rb follows K and Sr follows Ca as would be expected. Rubidium does not increase as rapidly with respect to strontium as potassium does with respect to calcium, but as calcium in the plagioclase actually decreases, the comparison may not be valid.

The isotopic data are very similar and are in agreement within the limits of experimental error. One can conclude that the parent material of the basaltic achondrites had Sr⁸⁷/Sr⁸⁶ of about 0.702.

Gast presents a model for the age of differentiation of basaltic achondrites from chondrites on the basis of the time of separation of rubidium from strontium. His model ages of 4.3 and 4.7 billion years are in agreement with the Pb²⁰⁷/Pb²⁰⁶ and potassium-argon ages in indicating an age of about 4.5 billion years for the basaltic achondrites.

Cosmic ray exposure ages

The abundances of the isotope He^3 for six basaltic achondrites are given below:

Meteorite	He^3 (10^{-8} cc/g STP)	Reference
Pavlovka	9.5	Stauffer ⁽⁶⁸⁾
Shergotty	4.7	Eberhardt and Hess ⁽⁶⁶⁾
Petersburg	22.4	Stauffer
Pasamonte	7.9	Eberhardt and Hess
Stannern	33.8	Stauffer
Nuevo Laredo	4.0	Reynolds and Lipson ⁽⁶⁵⁾

The production rate of He^3 is not greatly dependent upon the composition of the meteorites and the shielding effects and diffusion losses for these meteorites have been found to be small by Stauffer⁽⁶⁸⁾. If the cosmic ray flux has been constant in space and in time the relative abundances of He^3 give relative times of exposure of the meteorites to cosmic rays. Absolute exposure ages have been determined for Shergotty and Pasamonte by the H^3 - He^3 method (Eberhardt and Hess⁽⁶⁶⁾). The relative and absolute exposure ages for the six basaltic achondrites are as follows:

Meteorite	Relative He^3 abundance	Exposure age
Shergotty	1.0	5 mill. yr.*
Pavlovka	2.0	10
Petersburg	4.8	24
Pasamonte	1.6	8*
Stannern	7.2	36
Nuevo Laredo	0.9	5

* Calculated from H^3 - He^3 data

If Stauffer's demonstration that shielding and diffusion effects are small is correct, these exposure ages should be correct within about 30% of the actual value. The lack of shielding effects suggests that sudden events were responsible for the original removal of the meteorites from shielded environments.

The important feature of the exposure ages is that they are measured in terms of millions of years as opposed to the crystallization ages of 4.5 billion years. The exposure ages are comparable to the expected lifetimes, with respect to collision, of bodies coming from the moon or asteroid belt (Öpik).

Primordial isotopic abundances

Gast⁽⁶⁹⁾ has established the primordial abundances of strontium isotopes in the basaltic achondrites as:

$$\text{Sr}^{87}/\text{Sr}^{86} = 0.702$$

$$\text{Sr}^{84}/\text{Sr}^{86} = 0.0561$$

Murthy and Schmitt⁽⁷¹⁾ have measured the isotopic composition of Sm, Eu and Gd in meteorites, including Pasamonte. They found that the isotopic compositions of the three elements are within 1% of their abundances in terrestrial materials.

Shima⁽⁷²⁾ measured the abundances of boron isotopes in Pasamonte and found the $\text{B}^{11}/\text{B}^{10}$ ratio to be about 5% lower than in some terrestrial basaltic rocks. Although there may be differences between the initial boron isotopic composition in meteorites and the earth, these may have been hidden by fractionation of boron in later chemical

processes.

As far as can be determined, there is no detectable difference in the primordial isotopic compositions of various elements, between the basaltic achondrites and rocks of the earth. Examinations of isotopic anomalies due to the initial presence of short lived radioactive elements has given negative results thus far (Reed, et al,⁽⁶³⁾ Bi²⁰⁹; Reynolds and Lipson,⁽⁶⁵⁾ Xe¹²⁹).

The howardite Kapoeta is of interest because of the large quantities of "primordial" noble gases which it contains (Zähringer⁽²⁹⁾). These gases, which are present in different isotopic abundances than expected from cosmic-irradiation of the meteorite, are trapped selectively in "glassy" black portions which Fredriksson and Keil⁽²⁰⁾ believe to have recrystallized during a shock event.

The mineralogy of Kapoeta indicates that it has undergone much of the same history as have the other basaltic achondrites, including magmatic differentiation, recrystallization and brecciation. The "primordial" rare gases have been trapped after an extended sequence of chemical and mechanical events. The nature of the trapping mechanism and the source of the "primordial" gases are not understood. When understood, they may yield valuable evidence pertaining to the history of the basaltic achondrites.

VIII

A HYPOTHESIS FOR THE ORIGIN AND HISTORY
OF THE BASALTIC ACHONDRITES

Chapters II to VI have presented textural and compositional evidence which indicates that the basaltic achondrites originated under magmatic conditions and share related compositional features that can be understood in terms of a history of magmatic differentiation. The meteorites originally crystallized in a variety of cooling environments which allowed textures analogous to those of terrestrial diabases (shallow intrusions) and gabbros (deep-seated intrusions) to be formed.

Evidence presented in Chapter II indicates that one, and perhaps more, fragmentation episodes followed the original magmatic crystallization. There is some evidence that the brecciation and some textural modifications were produced by impact-generated shock metamorphism.

This chapter combines some other lines of evidence with the compositional and textural evidence to attempt to deduce the identity of the parent body of the basaltic achondrites. The following arguments are used to suggest that the parent body of the basaltic achondrites is the moon. As far as is known, there are no lines of evidence that conflict with this hypothesis.

Classification of Basaltic Achondrites

Two methods have been used previously to sub-classify the basaltic achondrites. Brown⁽²³⁾ and Mason⁽¹⁾ suggested classifications based on bulk chemical composition. Figure 28 shows the diagram given by Mason⁽¹⁾ which plots CaO against the ratio Fe/Fe+Mg. The achondrites are divided into four principal groups on this basis: the enstatite achondrites, with low CaO and low Fe/Fe+Mg; the hypersthene achondrites

and ureilites with low CaO and intermediate Fe/Fe+Mg; and the two groups of calcium-rich basaltic achondrites. Two calcium-rich achondrites, Nakhla and Angra dos Reis are distinct because they consist almost entirely of calcium-rich pyroxenes. The chemical classifications specify that the magnesium-rich basaltic achondrites are howardites and the iron-rich achondrites are eucrites.

The sub-classification does not seem to be satisfactory in the case of the basaltic achondrites. In Chapter IV it has been shown that there is a continuum of mineral compositions from the most magnesian to the most iron-rich systems. It is probable that individual lithic fragments in the howardites, if their true proportions of pyroxene and plagioclase could be determined, would fill the apparent hiatus between the magnesium-rich and iron-rich basaltic achondrites. This possibility suggests that the apparent compositional grouping of the basaltic achondrites has been superimposed on an original chemical variation by the mechanical effects observed in the brecciation features of the meteorites. If this is the case, a sub-classification of the basaltic achondrites as proposed by Wahl⁽¹⁸⁾ and this work (Chapter II) which is based on description of the breccia type is to be preferred as a basis for assigning names to various groups of basaltic achondrites. It is an unfortunate aspect of the chemical classification that it does not recognize the contrast in compositions between most basaltic achondrites and a meteorite like Shergotty. It is concluded that the best sub-classification of the basaltic achondrites consists of a monomict breccia (brecciated eucrite) - unbrecciated (eucrite)-polymict breccia (howardite) grouping. The chemical classification is of some use, however, in indicating the relative degree of magmatic

differentiation of the meteorites.

A third type of subclassification of the basaltic achondrites, a classification according to original texture, has not been suggested in previous studies of the basaltic achondrites. As a means of giving names to meteorite groups, this sub-classification has the same disadvantage as the chemical classification in that the mechanical brecciation history of the meteorites has mixed systems with different original textural features. A classification on the basis of original texture is also hampered by the presence of recrystallization textures that have significantly altered original textures. Nevertheless, it is possible to distinguish between meteorites that have predominantly basaltic, or fine-grained igneous characteristics, and meteorites that have gabbroic, or coarse-grained igneous affinities. In general, the textural affinities are reflected by the mineralogical features such as the pyroxene inversion and exsolution features and the plagioclase structural state.

In Table 36 a list of basaltic achondrites and mesosiderites is given with their classification as magnesium-rich or iron-rich, breccia type, and original textural type. For some meteorites not studied in this work, older descriptions are available which allow the meteorites to be subclassified. Only meteorites which can be classified in more than one category are given.

Correlations of meteorites in various subgroups

From Table 36, cross-correlations can be made for meteorites that have been classified in more than one subgroup. Table 37 gives the numbers of meteorites which can be classified in various combinations of subgroups. There is a distinct correlation between magnesium-rich

TABLE 36

SUBCLASSIFICATION OF BASALTIC ACHONDRITES

	<u>Fe- Rich</u>	<u>Mg- Rich</u>	<u>Eu₀</u>	<u>Eu</u>	<u>Ho</u>	<u>Bas.</u>	<u>Gab.</u>
Béréba	x		x			x	
Bholghati	x		x				x
Bialystok	x				x	x	
Binda		x	x				x
Cachari	x		x			x	
Chervony Koot	x		x			x	
Frankfort		x			x		x
Jonzac	x		x			x	
Juvinas	x		x			x	
Kapoeta		x			x		x
Le Teilleul		x			x		x
Iuotolax	x				x		
Macibini	x		x			x	
Missing	x				x		
Moore County	x			x			x
Nuevo Laredo	x		x			x	
Padvarminkai	x		x			x	
Pasamonte	x		x			x	
Pavlovka		x			x		x
Peramiho	x		x			x	
Petersburg	x				x	x	
Serra de Mage	x?			x			x
Shergotty	x		x				x?
Sioux County	x		x				x
Stannern	x		x			x	
Yurtuk		x			x		x
Zmenj		x			x		x
Estherville		x			x		x
Crab Orchard		x			x		x

TABLE 37

CROSS-CORRELATIONS OF THE NUMBER OF METEORITES IN VARIOUS SUBGROUPS
FOR METEORITES THAT CAN BE CLASSIFIED IN MORE THAN ONE SUBGROUP

Subgroup	Brecciated Euclrites	Howardites	Basaltic	Gabbroic
Fe-rich	14	4	13	5
Mg-rich	1	8	0	9
Basaltic	11	2	x	x
Gabbroic	3	8	x	x

and gabbroic meteorites. This correlation is heightened by the fact that many of the magnesian pyroxene fragments in the iron-rich howardites appear to be fragments of material that originally had coarse-grained textures. It seems probable, therefore, that the magnesium-rich systems have formed under more deep-seated cooling environments than have the iron-rich systems, in which basaltic textures are more common.

Another correlation that may be significant is the correlation between the brecciated eucrite and iron-rich groups. This seems to suggest that the iron-rich meteorites have been less susceptible to mixing in the brecciation episode than have the magnesium-rich systems. The iron-rich systems, by the correlation discussed in the preceding paragraph and by the greater abundance of basaltic than gabbroic textures, appear to have formed in shallower environments.

It is suggested, therefore, that the lack of mixing of the brecciated eucrites is related to brecciation in shallower materials. The mixing shown by the howardites, conversely, may be related to sampling of deeper materials.

Characteristics of the available population of basaltic achondrites

Table 38 gives the proportions by number and weight of observed falls of basaltic achondrites of various subgroups. Many more and much greater masses of iron-rich, basaltic, and monomict achondrites have fallen than specimens of magnesium-rich, gabbroic and polymict basaltic achondrites.

It was argued above that the magnesium-rich basaltic achondrites in general formed in more deep-seated environments. The relative scarcities of magnesium-rich basaltic achondrites and basaltic achon-

TABLE 38

TEXTURAL AND COMPOSITIONAL GROUPS OF BASALTIC ACHONDRITE METEORITES

	Number of Falls	Total Weight
Iron-rich	25	225 kg
Magnesium-rich	10	10 kg
Brecciated eucrites	19	212 kg
Eucrites	3	9 kg
Howardites	13	14 kg
Basaltic	21	207 kg
Gabbroic	14	28 kg

drites with coarse-grained textures are consistent with a sampling process that did not effectively sample deeper material in the parent body. Most of the magnesium-rich basaltic achondrites are howardites which may have been exposed at the surface of the parent body after their accumulation. This adds to the evidence that suggests very strongly that the sampling mechanism has selectively removed near-surface materials from the parent body.

Although it can not be argued at this time with complete certainty, it is possible that the sampling process which has selected the basaltic achondrites preferentially is due to the same process which produced the observed brecciation and that this process is one of collision or meteorite impact. The presence of strongly shocked meteorites such as Shergotty, and the occurrence in some of the howardites of metamorphic textures similar to that of Shergotty, suggests that strong shock has played an important role in the histories of these meteorites. A process of removal of fragments from a parent body by meteorite impact would in general be confined to surficial regions and would tend to sample selectively regions closer to the surface.

If much of the brecciation of the basaltic achondrites can be ascribed to impact phenomena, it would appear that the monomict eucrites in general represent smaller impact events than the howardites, because the fragments in the howardites include coarse, magnesian fragments that are interpreted as representing much deeper original crystallization sites than those of the meteorites with basaltic textures

and iron-rich compositions.

The mixing shown by the monomict breccias may have occurred within a quite localized region, since the chemical differences between lithic fragments are small. The howardites, however, show mixing of chemical systems as well as systems with differing textural characteristics. The distinction between monomict and polymict breccias may be analogous to the distinction of "throwout" breccias and breccias formed in place during cratering events.

The size of impact events which may have ejected the basaltic achondrites from their parent body can be limited by the small amount of post-accumulation mechanical history that can be observed in the meteorites. Whereas Shergotty and some fragments in the howardites have undergone severe metamorphism that was probably shock metamorphism, the breccias have not undergone such extreme histories after their accumulation. It seems probable that if the brecciation and ejection of the basaltic achondrites both were produced by impact events, the events that ejected the meteorites were of smaller magnitude than the brecciation events. This line of reasoning gives another indication that a strong bias towards surface samples should be observed in the assemblage of basaltic achondrites.

A question that can not be answered at present is that of whether the mechanism of ejection of basaltic achondrites from the parent body is one which has given a random areal sample. It is possible that the basaltic achondrites represent a few discrete ejection events, in which case their compositions may reflect the compo-

sition of a limited area of the parent body. The difference in composition between Shergotty and the rest of the basaltic achondrites suggests that some areal variations occur, but it can not be determined whether Shergotty actually represents an unusual rock type on the parent body.

Deduction of the probable parent body of the basaltic achondrites

The above discussion attempts to explain the observed frequencies of falls of basaltic achondrites with respect to their expected abundances on the basis of surficial sampling of the parent body. It also proposes a sampling mechanism, meteorite impact, that seems consistent with the observed discrepancies in the abundances of the meteorite falls and with the petrographic evidence pertaining to the mechanical histories of the basaltic achondrites. The hypothesis presented should be considered tentative until the importance of volcanic activity as a brecciation and ejection mechanism can be studied more thoroughly, for if volcanic activity has been important in producing many of the textures, a number of plausible alternatives to the sampling mechanism might be proposed. At the present stage, however, it is of interest to suggest the implications of the meteorite impact sampling mechanism and to look to other lines of evidence for support or refutation of the proposed hypothesis.

If the impact-sampling mechanism is the true explanation for the features described above, it must be concluded that the most plausible parent body for the basaltic achondrites is the moon. The argument implies that the parent body of the basaltic achondrites

exists in the solar system at the present time, because we do not observe the effects of a complete disruption of the parent body. The basaltic achondrites make up about 6% of all meteorite falls and it must be concluded that they owe their ejections to events that are either fairly common or in which there is a large probability that some of the ejecta reaches the earth. The moon offers a surface that is accessible to repeated meteorite impacts and much of the material ejected from lunar impact events should eventually reach the earth if it does not fall back to the moon. Gault, et al⁽⁸¹⁾ have argued that a mass of fragments greater than the impacting mass should leave the moon at escape velocities. It would require a substantial focussing effect to generate the observed flux at the earth if the basaltic achondrites originated in ejection events on other terrestrial planets, on the moons of the major planets, or on a few larger asteroids. The clear difference between the chondrites and the parent material of the basaltic achondrites suggests the possibility of at least two distinct regions of origin, perhaps corresponding to an asteroidal origin for chondrites and a lunar origin for the basaltic achondrites.

A number of other lines of evidence seem to be consistent with a lunar origin for the basaltic achondrites:

- (1) There are some indications that the parent body of the basaltic achondrites is fairly large. The process of

crystal settling as indicated by orientation of crystals in Moore County and Serra de Mage is more favored in large bodies than in small ones. The evidence presented in Chapter V suggests that the compositional variations observed in the basaltic achondrites is consistent with pronounced fractional crystallization of the same order of magnitude observed in the Skaergaard intrusion. If crystal separation, which is essentially a gravitational process, has produced the fractional crystallization in both sequences, it is probable that the gravitational field in which the basaltic achondrites crystallized was not too different from that of the earth. The magmatic differentiation may be consistent with a lunar origin for the basaltic achondrites.

(2) It has been suggested in Chapter VII that the cosmic ray exposure ages are consistent with a lunar origin for the basaltic achondrites.

(3) The absolute ages (crystallization ages) of the basaltic achondrites are very old, which suggests that surface volcanic activity was confined to the early history of the parent body. This is consistent with the observed surficial features of the moon which do not suggest a large amount of recent volcanic activity.

(4) The distribution in time of meteorite falls has been studied by Millard and Brown,⁽⁷⁴⁾ who found the monthly

variation of basaltic achondrite falls to be random. There is an aspect of the pattern of fall of the basaltic achondrites, not studied by Millard and Brown, which may be of significance. Figure 29 gives the hour of fall statistics for basaltic achondrites and mesosiderites and compares them with similar statistics for all meteorites. The data was compiled with the help of the punched card system described by Brown and Goddard⁽⁷³⁾ The histogram for all meteorites(except the basaltic achondrites) has a distinct peak at 3:00 P.M. local time, whereas the basaltic achondrites apparently are concentrated around a peak at 9:00 A.M. as well as 3:00 P.M. Whereas there are about equal numbers of morning and afternoon falls for the basaltic achondrites, there are about twice as many afternoon falls as morning falls for the chondrites, which make up the majority of the other meteorite falls.

An afternoon fall indicates that the colliding meteorite has a higher velocity than that of the earth and catches up to the earth. A morning fall indicates that the meteorite is caught by the earth. For a given eccentricity, a meteorite orbit which crosses the earth's orbit will have a greater relative velocity, at the earth's orbit, the greater the semi-major axis of the orbit. For the chondrites, the afternoon peak may reflect average semi-major axes that are greater than those shown by the

basaltic achondrites. The difference of hourly distribution of basaltic achondrite and chondrite falls, therefore, gives another suggestion of a dual source for these groups of meteorites. The even distribution of morning and afternoon falls of basaltic achondrites may reflect orbits that are nearly circular, but have semi-major axes just smaller or just larger than one astronomical unit. These orbits would be consistent with a lunar origin for the basaltic achondrites.

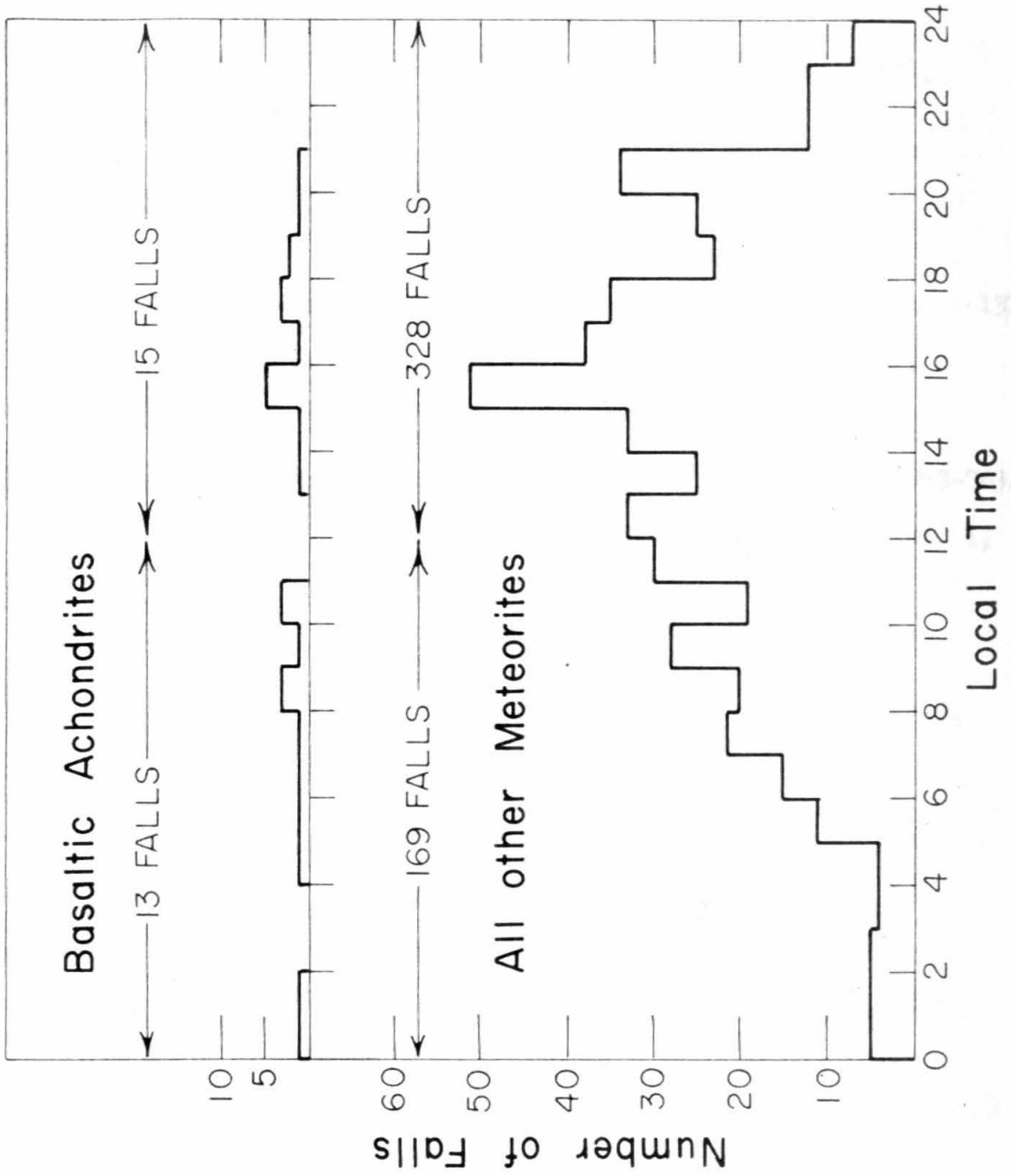


Figure 29

REFERENCES

1. Mason, B., Meteorites (1962), 274 pp.
2. Urey, H. C., and H. Craig, *Geochim. et Cosmochim. Acta* (1953),
Vol. 4, pp. 36-82.
3. Prior, G. T., *Mineralog. Mag.* (1920), Vol. 19, pp. 51-63.
4. Prior, G. T., *Mineralog. Mag.* (1918), Vol. 18, pp. 151-172.
5. Wahl, W., *Tschermaks Min. u. Petrog. Mitt.* (1907), Vol. 26, pp. 1-131.
6. Michel, H., *Tschermaks Min. u. Petrog. Mitt.* (1912), Vol. 31,
pp. 563-658.
7. Berwerth, F., *Sitzber. Akad. Wiss. Wien* (1912), Vol. 121, pp. 763-783.
8. LaCroix, A., *Arch. Museum Hist. Nat. Paris* (1926), ser. 6, Vol. 1,
pp. 15-58.
9. Foshag, W. F., *Am. Jour. Sci.* (1938), Vol. 35, pp. 374-382.
10. Henderson, E. P., and H. T. Davis, *Am. Mineral.* (1936), Vol. 21,
pp. 215-229.
11. Hess, H. H., and E. P. Henderson, *Am. Mineral.* (1949), Vol. 34,
pp. 494-507.
12. Game, P. M., *Mineralog. Mag.*, (1957), Vol. 31, pp. 656-671.
13. Zavaritskii, A. M., and L. G. Kvasha, Meteorites of the U.S.S.R.
(1952), pp. 221-235.
14. Rose, G., Cited in Wahl⁽⁵⁾.
15. Engelhardt, W. V., Preprint (1963).
16. Tschermak, G., *Sitzber. Akad. Wiss. Wien, Math.-Naturw. Kl.*,
Abt. I (1872), Vol. 65, pp. 122-146.
17. Smith, J. L., *Am. Jour. Sci.* (1861)², Vol. 31, p. 265.
18. Wahl, W., *Geochim. et Cosmochim. Acta* (1952), Vol. 2, pp. 91-117.

19. Chao, E. C. T., personal communication (1963).
20. Fredricksson, K., and K. Keil, *Geochim. et Cosmochim. Acta*,
in press (1963).
21. Merrill, G. P., *Proc. U. S. Nat. Mus.* (1921), Vol. 58, pp. 363-370.
22. Brezina, A., *Jahrb. k. k. Geol. Reichsanstalt.* (1904), Vol. 35,
pp. 151-276.
23. Brown, H., *Proc. Lunar and Planetary Colloquium* (1961), Vol. 2,
No. 4, pp. 30-36.
24. Hess, H. H., *Geol. Soc. Am. Memoir*, No. 80 (1960), 225 pp.
25. Brown, G. M., *Mineralog. Mag.* (1957), Vol. 31, pp. 511-543
26. Bowen, N. L., and J. F. Schairer, *Am. Jour. Sci.* (1935), Vol. 29,
pp. 151-217.
27. Walker, F., *Geol. Soc. Am., Bull.* (1940), Vol. 51, pp. 1059-1106.
28. Jaeger, J. C., *Am. Jour. Sci.* (1959), Vol. 257, pp. 44-54.
29. Zahringer, J., *Geochim. et Cosmochim. Acta* (1963), Vol. 26,
pp. 665-680.
30. Millman, P. M., B. A. Liberty, J. F. Clark, P. L. Wellmore and
Innes, M. J. S., *Dom. Observ. Pub.* (1960), Vol. 24, 43 pp.
31. Milton, D., and P. S. DeCarli, Preprint (1962).
32. Chao, E. C. T., personal communication (1963).
33. Edwards, G., *Geochim. et Cosmochim. Acta* (1955), Vol. 8, pp. 285-294.
34. Washington, H. S., *U. S. Geol. Survey, Prof. Paper No. 99* (1917),
pp. 1162-1180.
35. Gast, P. W., *Geochim. et Cosmochim. Acta* (1960), Vol. 19, pp. 1-4.
36. Geiss, J. and D. C. Hess, *Astrophys. Jour.*, (1958), Vol. 124,
pp. 224-236.

37. Brannock, L., and W. W. Shapiro, U. S. Geol. Survey, Bull., 1036-C
(1956), pp. 43-44.
38. Tilley, C. E., Jour. Petrology (1960), Vol. 1, pp. 47-55.
39. Muan, A., A.I.M.E. Trans. (1955), Vol. 203, pp. 965-967.
40. Wager, L. R., and W. A. Deer, Medd. om Gnon. (1939), No. 4, 352 pp.
41. Osborne, E. F., Am. Jour. Sci. (1959), Vol. 257, pp. 609-647.
42. Boyd, J. F., and England, Carnegie Inst. Washington Year Book
(1959-1960), pp. 47-52.
43. Slawson, C. B. and A. B. Peck, Am. Mineral. (1936), Vol. 21,
pp. 523-528.
44. Winchell, A. N. and H. Winchell, Elements of Optical Mineralogy,
Part II, Fourth Ed. (1952), p. 281.
45. Hess, H. H., Am. Mineral. (1949), Vol. 34, pp. 621-666.
46. Haughton, S. and F. Partridge, Trans. Geol. Soc. S. Africa (1938),
Vol. 41, pp. 205-210.
47. Carmichael, I. S. E., Jour. Petrology (1960), Vol. 1, pp. 309-336.
48. Berwerth, F., Sitzber. Math.-Natur. Kl. Akad. Wissen. Wien (1903),
Vol. 112, pp. 739-776.
49. Tsuboi, S., Mineralog. Mag. (1923), Vol. XX, pp. 108-122.
50. Smith, J. R., Am. Mineral. (1958), Vol. 43, pp. 1179-1194.
51. Smith, J. R., and H. S. Yoder, Jr., Am. Mineral. (1956), Vol. 41,
pp. 632-647.
52. Schairer, J. F., J. R. Smith, and F. Chayes, Carnegie Inst.
Washington Year Book (1955-1956), pp. 195-197.
53. Lovering, J. F., in Researches in Meteorites, (Edited by
C. B. Moore), pp. 179-198.
54. Fuchs, L., Paper presented at Annual Meeting of American Geophysical
Union, Washington, D. C., April, 1962.

55. Muan, A., and E. F. Osborne, *Am. Ceram. Soc. Jour.* (1956),
Vol. 39, pp. 121-140.
56. Urey, H. C., in Physics and Chemistry of the Earth, (Edited by
L. Ahrens, F. Press, K. Rankama and S. K. Runcom) (1957),
Vol. II, pp. 60-68.
57. Urey, H. C., in Space Science, (Edited by D. P. LeGalley) (1963),
pp. 123-168.
58. Mason, Brian, Personal communication, 1963.
59. Wager, L. R. and R. L. Mitchell, *Geochim. et Cosmochim. Acta* (1951),
Vol. 1, pp. 129-207.
60. Bate, G. L., H. A. Potratz, and J. R. Huizenga, *Geochim. et
Cosmochim. Acta* (1960), Vol. 18, pp. 101-107.
61. Schmitt, R. A., R. H. Smith, J. E. Lasch, D. A. Olehy, K. I. Perry
and A. W. Mosen, Annual Report, General Atomic (1962).
62. Patterson, C. C., *Geochim. et Cosmochim. Acta* (1955), Vol. 7,
pp. 151-153.
63. Reed, G. W., K. Kigoshi and A. Turkevich, *Geochim. et Cosmochim.
Acta* (1960), Vol. 20, pp. 122-140.
64. Hamaguchi, H., G. W. Reed and A. Turkevich, *Geochim. et Cosmochim.
Acta* (1957), Vol. 12, pp. 337-347.
65. Reynolds, J. H. and J. I. Lipson, *Geochim. et Cosmochim. Acta* (1957),
Vol. 12, pp. 330-336.
66. Eberhardt, P. and D. C. Hess, *Astrophys. Jour.* (1960), Vol. 131,
p. 38ff.
67. Anders, E., The Solar System, Chapter 11, Vol. 4, in Press (1963).
68. Stauffer, H., *Jour. Geophys. Res.*, (1962), Vol. 67, pp. 2023-2028.

69. Gast, P. W., *Geochim. et Cosmochim. Acta* (1962), Vol. 26, pp. 927-944.
70. Öpik, E. J., *Proc. Roy Irish Acad.* (1951), Vol. 54, p. 165
71. Urey, H. C., *Jour. Geophys. Res.* (1959), Vol. 64, pp. 1721-1737.
72. Shima, M., *Jour. Geophys. Res.* (1962), Vol. 67, pp. 4521-4523.
73. Brown, H., and I. Goddard, *Preprint*(1963).
74. Millard, H. T., Jr., and H. Brown, *Preprint*(1963)
75. Bjork, R. L., *Jour. Geophys. Res.* (1961), Vol. 66, pp. 3379-3387.
76. Fredriksson, K., P. S. DeCarli and A. Aaramae, *Space Science III(COSPAR)* (1962).
77. zur Strassen, H., *Zeit. anorg. Chemie* (1930), Vol. 191
78. Wänke, H., and H. König, *Zeit. Naturforsch.* (1959), Vol. 14a p. 860
79. Vinogradov, A. P., I. K. Zadorozhnii, and K. G. Knorre, *Meteoritika* (1960), Vol. 18, p. 92.
80. Gerling, E. K , and K. G. Rik, *Dokl. Akad. Nauk. U.S.S.R.* (1955), Vol 101, p. 433.
81. Gault, D. E., E. M. Shoemaker, and Henry J. Moore, *Transactions of the American Geophysical Union*(1962), Vol. 43, p. 405.

APPENDIX

PLATE 1

(a) Nuevo Laredo

Exterior, showing dull black fusion crust and glossy black rills.

(b) Nuevo Laredo

Exterior, showing the fragmental nature of the meteorite.

The dark gray lithic fragments have fine-grained textures and vary from 1mm to 5 cm in diameter. The larger fragments, such as the one near the upper edge, have some angular corners, but the fragments tend to be rounded and subspherical. The light gray matrix consists of a mixture of lithic and crystal fragments, some of which are sub-microscopic.

PLATE 2

(a) Nuevo Laredo (NL-1a) Plane light (20x)

Photomicrograph, showing texture of groundmass and lithic fragments. The boundaries are not well marked, in general, due to the very fine-grained textures of the fragments and groundmass. Arrows indicate lithic fragments.

(b) Nuevo Laredo (NL-1a) Plane light (120x)

Photomicrograph showing a contact between a lithic fragment and the matrix. An apparently gradational contact may result from overlapping of the matrix onto a subspherical lithic fragment. Note that some of the matrix material is very fine-grained and nearly opaque. The lithic fragment consists of colorless plagioclase plates and interstitial dark clinopyroxene.

PLATE 3

(a) Nuevo Laredo (NL-2b) Plane light (120x)

Photomicrograph, showing the zone of surficial fusion. The outer portion is isotropic brown glass filled with spherical cavities. The interior of the fused zone consists of colorless glass in which some plagioclase laths persist. This portion grades into normal crystalline material, but a slightly darkened portion indicated by the arrows may mark the limits of the fusion effects.

(b) Nuevo Laredo

Resistant fragments. The dark fragments are at the lower size limit for lithic or crystal fragments. They are dense (opaque) and commonly show smooth surfaces over hemispherical segments. The lighter fragments are composed of fragmental matrix material that is apparently more indurated than most of the matrix material.

PLATE 4

(a) Nuevo Laredo (NL-1) Crossed nicols (6x)

Photomicrograph showing distribution of black "glass" fragments in a vein-like feature. Note that the distribution is not continuous and may represent a post-accumulation redistribution of a single original fragment of "glass". The arrow points to the location of two phenocrysts (See Plate 4b).

(b) Nuevo Laredo (NL-1) Plane light (80x)

Photomicrograph, showing euhedral pigeonite phenocryst in the "glass".

PLATE 5

(a) Nuevo Laredo (NL GM 4) Plane light (80x)

Photomicrograph showing a fine-grained intergranular texture. Plagioclase(colorless), clinopyroxene(dark), cristobalite(c). The cristobalite is interpreted as a product of direct crystallization from the magma.

(b) Nuevo Laredo (NL GM 4) Plane light (80x)

Photomicrograph showing a medium-grained sub-ophitic texture with plagioclase(colorless), clinopyroxene(dark) and some interstitial opaque minerals. The plagioclase contains abundant bleb inclusions.

PLATE 6

(a) Nuevo Laredo (NL G-3) Plane light (80x)

Photomicrograph, showing inclusions in a plagioclase plate.

Both oriented, elongated inclusions and strings of bleb inclusions are present. The plagioclase (colorless) and clinopyroxene (dark) are intergrown in a sub-ophitic texture.

(b) Nuevo Laredo (NL GM 4) Plane light (80x)

Photomicrograph, showing a concentration of troilite and ilmenite in interstices with plagioclase (i) that is more sodic than that of the laths. Quartz may also occur in these interstitial areas, but it is not obvious here.

(c) Nuevo Laredo (NL-2) Reflected light (120x)

Photomicrograph, showing inclusions in a clinopyroxene grain

(p). The oriented rodlike inclusions (trending toward upper left) are parallel to (100). These, and the bleb inclusions, may be ilmenite. The (001) planes are marked by a material of higher reflectivity which gives the grain a lamellar appearance. The scattered grains of high reflectivity are troilite.

PLATE 7

(a) Nuevo Laredo (NL GM 4) Plane light (80x)

Photomicrograph, showing an inclusion-filled corroded pyroxene grain which occurs with quartz (Q) in the interstices of a lithic fragment. The appearance of the pyroxene can be contrasted to that shown in Plates 5a and 5b.

(b) Nuevo Laredo (NL-2) Crossed nicols (120x)

Photomicrograph, showing a recrystallization texture. Orthopyroxene (H), an unidentified material with low birefringence (M) and black opaque metallic iron occur in this fragment. Some of the areas of higher birefringence may be clinopyroxene. This is interpreted as a post-magmatic recrystallization texture, but the timing of recrystallization with respect to breccia accumulation has not been determined.

PLATE 8

(a) Sioux County

Exterior, showing a variety of lithic fragments set in a fine-grained fragmental matrix. Many of the lithic fragments have medium-grained gabbroic textures. The fragment marked with the arrow was separated for chemical and mineralogical analysis.

(b) Sioux County

Exterior, showing the coarsest-grained lithic fragment observed in the meteorite. The largest pyroxene (**hypersthene, dark**) grain may be greater than 1 cm across, which would make this the coarsest texture that has been observed in a basaltic achondrite.

PLATE 9

(a) Sioux County (SC-3) Crossed nicols (6x)

Photomicrograph, showing a medium-grained lithic fragment in finer-grained matrix. Plagioclase (p) is tabular, rather than lath-like as in Nuevo Laredo, and shows strong undulatory extinction and deformation of twin planes. Clinopyroxene (n) shows evidence of internal disruption and fracturing. The boundary marked by the arrow is shown in greater detail in Plate 10.

(b) Sioux County (SC-2) Crossed nicols (20x)

Photomicrograph, showing the irregular inversion of a twinned pigeonite grain. The overlying gives the details of the intergrowth relations.

PLATE 10

(a) Sioux County (SC-3) Plane light (50x)

Photomicrograph, showing the details of the boundary between a lithic fragment and the matrix. Much of the matrix is coarser than the Nuevo Laredo matrix, but there is some material that is submicroscopic. The colorless areas at the right are holes in the slide.

(b) Sioux County (SC-3) Crossed nicols (50x)

Photomicrograph showing the same field as Plate 10a with crossed nicols. The boundary between the lithic fragment and the matrix is more pronounced, as is the fragmental nature of the matrix. There is a faint lination in the matrix that is sub-parallel to the fragment boundary (marked with the arrow). This feature was not discussed in the text, but there are several similar vague features in the meteorite that suggest that some post-accumulation movement has occurred.

PLATE 11

(a) Sioux County (SC-2) plane light (80x)

Photomicrograph, showing corrosion of interstitial clinopyroxene. The large clinopyroxene grain (A) is structurally continuous into the areas marked (a). The interstitial material includes plagioclase, quartz (q), troilite and ilmenite.

(b) Sioux County (SC-2) Plane light (80x)

Photomicrograph, showing the recrystallization of dark clinopyroxene (X) to lighter clinopyroxene (Y). The colorless grains are plagioclase.

PLATE 12

(a) Sioux County (SC-1) Plane light (50x)

Photomicrograph, showing a reaction relation with clinopyroxene (brown) being replaced by orthopyroxene (colorless) and troilite (black). The troilite forms a discontinuous rim around the orthopyroxene.

(b) Sioux County (SC-1) Reflected light (50x)

Photomicrograph of the area shown in Plate 12c. The bright grains are metallic iron.

(c) Sioux County (SC-1) Plane light (50x)

Photomicrograph, showing the association of metallic iron with colorless orthopyroxene (O). The intergrowth occurs in a fragment that is entirely surrounded by matrix. It is not possible to fix the period of metal crystallization with respect to the time of breccia accumulation.

PLATE 13

(a) Sioux County (SC-2) Crossed nicols (80x)

Photomicrograph, showing a strongly deformed plagioclase grain.

(b) Sioux County (SC-2) Plane light (20x)

Photomicrograph of an area that is interpreted as recrystallized matrix. The colorless plagioclase grains have fragmental shapes, but show little undulatory extinction in contrast to other plagioclase fragments in the meteorite. There are a number of distinct boundaries (see overlay) which seem to be interrelated but do not fix a unique boundary to the area. At the location marked with an arrow there is an apparent boundary across which some pyroxene grains appear to be continuous. At the upper right, the boundary with more normal groundmass material is gradational.

PLATE 14

(a) Sioux County (SC-2) Plane light (50x)

Photomicrograph, showing the boundary between a crystal fragment and finer-grained fragmental matrix. The colorless plagioclase gives the impression that it is a continuous mesh. Boundaries between adjacent plagioclase grains are indistinct.

(b) Sioux County (SC-2) Crossed nicols (50x)

Photomicrograph, showing the same area as Plate 14a under crossed nicols. The fragmental nature of the matrix is pronounced and much of the interstitial dark material appears to be nearly isotropic. Most plagioclase fragments show strong undulatory extinction. The apparent continuity of plagioclase shown in plane light may indicate that this portion of the matrix has been slightly sintered, but it is not highly recrystallized.

PLATE 15

(a) Juvinas (scale in centimeters)

Exterior, showing black lithic fragments in fine-grained matrix.

(b) Juvinas (Juv-1) Crossed nicols (20x)

Photomicrograph, showing sub-ophitic texture in a lithic fragment. The pigeonite is tinted on (100). Dark striations parallel to (001) and conspicuous partings parallel to (110) are present. At the left, the brown pigeonite has been bleached and recrystallized. The recrystallized pyroxene has lower birefringence.

PLATE 16

(a) Juvinas (Juv-3) Plane light (6x)

Photomicrograph, showing a lithic fragment with ophitic texture. The dark pyroxene includes unoriented stubby colorless plagioclase laths. Note the "dusty" interiors and clear rims of the plagioclase grains.

PLATE 17

(a) Juvinas (Juv-1) Crossed nicols (20x)

Photomicrograph, showing a lithic fragment with sub-ophitic texture. Some of the clinopyroxene has been recrystallized to a finer-grained aggregate. Some of the cleavage traces of the unaltered grain can be followed into the recrystallized areas. Plagioclase is apparently unaffected by the pyroxene recrystallization.

(b) Juvinas (Juv-1) Plane light (80x)

Photomicrograph, showing recrystallized pigeonite. The original brown pigeonite has been replaced by a fine-grained aggregate of colorless pyroxene, primarily pigeonite, in a similar fashion to the texture shown in Plate 17a. The recrystallized portion has a higher abundance of opaque inclusions. Some original cleavage traces can be seen in the recrystallized portion.

PLATE 18

(a) Juvinas (Juv-1) Crossed nicols (120x)

Photomicrograph, showing recrystallized pigeonite. Note the clear rims of the twinned plagioclase grain, which do not appear to be related to the areas of recrystallized pyroxene.

(b) Juvinas (Juv-1) Crossed nicols (80x)

Photomicrograph showing a recrystallized pigeonite grain. Original (001) traces (direction of arrow) are marked by rows of minute inclusions. The grain has been recrystallized to a number of domains of different crystallographic orientation without redistributing the opaque inclusions marking original crystallographic directions.

PLATE 19

(a) Juvinas (Juv-2) Plane light (50x)

Photomicrograph showing the distribution of opaque minerals in the interstices of a sub-ophitic area. Most of the very fine-grained opaque material in the corroded pyroxene(dark) is troilite.

(b) Juvinas (Juv-2) Reflected light (50x)

Photomicrograph, showing the same area as Plate 19a. Metallic iron (m), and ilmenite (i) are the prominent opaque minerals.

PLATE 20

(a) Juvinas (Juv-1) Plane light (80x)

Photomicrograph, showing the concentration of troilite along fractures in pigeonite. Areas adjacent to the fractures have been bleached.

PLATE 21

(a) Stannern (scale in centimeters)

Exterior, showing a lithic fragment composed of plagioclase and pyroxene laths. The boundaries between lithic fragments and the matrix are very indistinct.

(b) Stannern (scale in centimeters)

Exterior, showing dark gray lithic fragments and light gray fine-grained matrix. The black vein is a conspicuous textural feature. The nature of the ovoidal structure near the top of the specimen is uncertain.

PLATE 22

(a) Stannern (St-3) Plane light (120x)

Photomicrograph, showing a portion of the fusion crust. The three regions present in the Nuevo Laredo fusion crust(Plate 3a) are present here, but not as well developed. Plagioclase laths tend to extend through the glass zone to the outer boundary. Cavities are not as abundant as they are in the fusion crust of Nuevo Laredo and the zone of darkening is not pronounced.

(b) Stannern (St-2) Crossed nicols (50x)

Photomicrograph, showing a twinned clinopyroxene grain that has inverted to hypersthene. The light lamellae(nearly vertical in lower part of twin) probably are exsolution lamellae from the original pigeonite.

PLATE 23

(a) Stannern (St-2) Plane light (50x)

Photomicrograph, showing subophitic texture. Quartz grains (q) are surrounded by opaque minerals, probably troilite, and are interpreted as due to direct crystallization from the magma. The clinopyroxene is dark, the plagioclase is colorless or gray, depending on the abundance of inclusions.

(b) Stannern (St-2) Plane light (50x)

Photomicrograph, showing the reaction of pigeonite to form troilite and quartz. See overly for details of the mineralogy. The crosshatched area indicates the original extent of the corroded pyroxene grain as determined from small areas in structural continuity with the unaltered portions. Contrast this textural occurrence of quartz with that shown in Plate 23a.

PLATE 24

(a) Stannern (BM-46790) Crossed nicols (50x)

Photomicrograph, showing a radiating aggregate of plagioclase laths with interstitial pyroxene.

(b) Stannern (BM-46790) Plane light (20x)

Photomicrograph, showing an intergranular texture with plagioclase laths and interstitial clinopyroxenes. The thin black veins are post-accumulation features. Note the offset of the lithic fragment along the black veins.

(c) Stannern (BM 46790) Plane light (6x)

Photomicrograph, showing a radiating texture consisting of plagioclase laths(colorless) and clinopyroxene(dark).

PLATE 25

(a) Stannern (St-2) Crossed nicols (80x)

Photomicrograph, showing a lithic fragment with sub-ophitic texture. Note the distorted twin planes in plagioclase grain (A) and the undulatory extinction in plagioclase grains (B) and (C).

(b) Stannern (St-1) Plane light (50x)

Photomicrograph, showing a vein of brown amorphous material. Note the fractures (see arrows) perpendicular to the vein walls at irregular intervals.

PLATE 26

(a) Stannern (St-1) Crossed nicols (20x)

Photomicrograph, showing a set of dark veins which are concentrated near the boundary of a lithic fragment (towards top) and finer-grained matrix (towards bottom). There are at least two sets of veins, but there is no obvious offset at their intersections. The veins are essentially isotropic in most portions.

(b) Stannern (St-1) Plane light (20x)

Photomicrograph, showing a brown amorphous vein (1-1') and a troilite vein (2-2'). It is difficult to determine whether there has been displacement along the veins. There does not appear to have been any displacement in the region just above 1' and 2'.

PLATE 27

(a) Pasamonte (scale in centimeters)

Exterior, showing fine- to medium-grained lithic fragments consisting of black pigeonite, brown iron-rich pigeonite and ferroaugite and white plagioclase.

(b) Pasamonte

Exterior, showing the fusion crust. Note the very fine light polygonal fractures in the crust.

PLATE 28

(a) Pasamonte (Pas-1) Crossed nicols (50x)

Photomicrograph, showing sheaf-like aggregates of clinopyroxene.

Dark areas are amorphous or opaque.

(b) Pasamonte (Pas-1) Plane light (20x)

Photomicrograph, showing a fragment with ophitic texture imbedded in fine-grained matrix with smaller lithic and crystal fragments. The interstices contain darker pyroxenes and troilite. The pyroxenes of Pasamonte are less filled with inclusions than most of the pyroxenes of the iron-rich basaltic achondrites.

PLATE 29

(a) Pasamonte (Pas-1) Plane light (20x)

Photomicrograph, showing a fine-grained lithic fragment with intergranular texture in a matrix of fine-grained lithic and crystal fragments. Note that many of the pyroxene crystal fragments show variable color due to compositional zoning.

(b) Pasamonte (Pas-1) Plane light (20x)

Photomicrograph, showing compositional zoning of pigeonite. Cores (c) are colorless and have compositions close to Fe/Fe Mg 0.5; rims are brown and have Fe/Fe Mg 0.7. Brown, inclusion-filled ferroaugite occurs in the rims and interstices. Tridymite (t) occurs in the interstices.

PLATE 30

(a) Bholghati (BM 1915,140) Crossed nicols (20x)

Photomicrograph, showing a medium-grained lithic fragment and fine-grained matrix, which is dark and amorphous except for the crystal fragments. The crystal fragments have strong undulatory extinction.

(b) Moore County

Exterior, Note irregular distribution of plagioclase (light) and pyroxene (dark) which gives small areas that are pyroxenitic and others that are anorthositic. Two dark veins are present at the left.

PLATE 31

(a) Moore County (MC-1) Crossed nicols (6x)

Photomicrograph, showing medium-grained gabbroic texture. Area at lower left represents an original pigeonite grain which has gone through a set of exsolution and inversion processes. The original pigeonite exsolved augite (A) in broad lamellae. The remaining pigeonite (X) then partially inverted to hypersthene (W). Within the hypersthene, thin lamellae parallel to (100) are present, which represent exsolution of augitic pyroxene after inversion to hypersthene.

(b) Moore County (MC-1) Partially crossed nicols (50x)

Photomicrograph, showing tabular pyroxene and plagioclase grains in gabbroic texture. The opaque grains tend to be concentrated along fractures and grain boundaries. The pyroxene grain marked (d) is a distinct grain of ferroaugite.

PLATE 32

(a) Serra de Mage (SdM-1) Crossed nicols (6x)

Photomicrograph, showing medium to coarse-grained gabbroic texture and strong concentration of plagioclase. A central zone trending towards the upper left consists almost in its entirety of plagioclase, making it an anorthosite. The pyroxene grains show complicated inversion and exsolution features (see Plate 34a).

(b) Serra de Mage (SdM-1) Crossed nicols (50x)

Photomicrograph, showing small areas in which quartz(?) and troilite are concentrated at the boundary between two pyroxene grains (L).

PLATE 33

(a) Serra de Mage (SdM-1) Plane light (50x)

Photomicrograph showing fusion crust developed on pyroxene grain.

(b) Serra de Mage (SdM-1) Plane light (50x)

Photomicrograph showing fusion crust developed on plagioclase grain.

PLATE 34

(a) Serra de Mage (SdM-1) Crossed nicols (20x)

Photomicrograph showing exsolution lamellae in an orthopyroxene grain(at extinction). Broader lamellae are parallel to the (001) direction of the original pigeonite. Narrower lamellae(nearly vertical in the picture) are parallel to the (100) direction in the hypersthene and have formed by exsolution after the original pigeonite inverted to hypersthene.

(b) Serra de Mage (SdM-1) Plane light (20x)

Photomicrograph showing the distribution of opaque minerals. Metallic iron and troilite occur as grains up to 0.5mm diameter. The metallic iron of Serra de Mage probably has crystallized directly from the magma rather than as a reaction product after the magmatic episode. Plagioclase in this picture is colorless and pyroxene is gray.

(c) Serra de Mage (SdM-1) Reflected light (20x)

Photomicrograph showing the same area as in Plate 34b. Metallic iron(m) and troilite(s) are concentrated at plagioclase-pyroxene grain boundaries.

PLATE 35

(a) Shergotty

Exterior. Note strong preferred orientation of colorless maskelynite laths.

(b) Shergotty (Sh-1) Plane light (6x)

Photomicrograph. Note color variation within brown clinopyroxene that suggests that the iron content increases towards the rims of some grains. Many maskelynite (colorless) laths have good feldspar forms.

PLATE 36

(a) Shergotty (Sh-1) Plane light (20x)

Photomicrograph, showing the relations between maskelynite (m), clinopyroxene (dark gray), whitlockite (w), amorphous brown material (b) and magnetite (black). Maskelynite has few fractures or cleavage traces.

(b) Shergotty (Sh-1) Crossed nicols (20x)

Photomicrograph, showing the same area as Plate 36a. The maskelynite is amorphous and the pyroxene shows irregular extinction.

PLATE 37

(a) Shergotty (USNM-321) Crossed nicols (50x)

Photomicrograph showing zonal relation of augite (A) and pigeonite (P) in a twinned clinopyroxene grain.

PLATE 38

(a) Petersburg

Exterior, showing the variety of lithic fragments. Note the conspicuous rims of metallic iron around some fragments. The arrow points to the metal rim shown in Plate 38b.

(b) Petersburg

Exterior, showing the metallic iron rim at higher magnification. The interior consists of a polygranular aggregate of plagioclase and orthopyroxene. Only a portion of the rim (R) is highly reflecting, due to terrestrial oxidation and poor polishing. At the right is a fine-grained lithic fragment.

PLATE 39

(a) Petersburg (Pet-1) Plane light (6x)

Photomicrograph showing a portion in which most fragments have textures resembling the sub-ophitic textures in Stannern or Juvinas.

(b) Petersburg (BM32053) Plane light (6x)

Photomicrograph showing a portion in which fragments with recrystallization textures and coarse orthopyroxene crystal fragments are abundant. A few lithic fragments have been outlined, as the boundaries with the matrix are not always clear.

PLATE 40

(a) Petersburg (BM 32053) Plane light (20x)

Photomicrograph, showing recrystallized lithic fragments referred to as granoblastic. Colorless plagioclase and gray pigeonite have irregular, but more or less equigranular, intergrowth relationships.

(b) Petersburg (BM32052) Plane light (6x)

Photomicrograph showing a recrystallized fragment. In a few areas, the plagioclase grain shape is suggestive of lathlike form, but the texture for the most part approaches the granoblastic textures shown in Plate 40a.

PLATE 41

(a) Petersburg (BM32053) Plane light (50x)

Photomicrograph, showing granoblastic texture. Note the subparallel set of fractures, primarily in the colorless plagioclase.

(b) Petersburg (BM 32053) Plane light (50x)

Photomicrograph showing the fracture pattern in a granoblastic portion of the fragment shown at the bottom of Plate 39b.

Although the pattern is most conspicuous in the plagioclase, it seems to be continuous through most of the pyroxene grains.

PLATE 42

(a) Petersburg (BM 32053) Plane light (50x)

Photomicrograph showing a sub-ophitic portion of the fragment at the bottom center of Plate 39b. The fractures tend to be perpendicular to the edges of the plagioclase laths. The pyroxene is granular, but the external boundaries of the granular aggregate may reflect the original shape of the pyroxene grains.

(b) Petersburg (BM 32053) Crossed nicols (50x)

Photomicrograph of the area shown in Plate 42a, with crossed nicols. Plagioclase has feathery extinction pattern of very fine-grained crystallites. The pyroxene has irregular interference patterns. The recrystallization of the plagioclase is interpreted as a shock metamorphic transformation.

PLATE 43

(a) Petersburg (BM 32053) Plane light (20x)

Photomicrograph, showing a fragment which consists of a very fine-grained nearly opaque matrix that surrounds a few small plagioclase grains.

(b) Petersburg (BM 32053) Crossed nicols (20x)

Photomicrograph, showing a medium-grained lithic fragment that consists primarily of equant pigeonite grains. The pigeonite shows lamellae that probably represent exsolution features. This fragment may represent a crystal accumulation texture.

PLATE 44

(a) Petersburg (Pet-1) Crossed nicols (20x)

Photomicrograph, showing a strongly strained orthopyroxene grain. Cleavage traces are distorted and the grain has strongly undulatory extinction. The light-colored rodlike areas within the extinguished portion of the grain may be clinopyroxene exsolved during an episode of non-hydrostatic deformation.

(b) Petersburg (BM 32053) Plane light (20x)

Photomicrograph, showing a deformed orthopyroxene fragment. Note the fractures (marked by arrows) at about 45° to the (100) cleavage.

PLATE 45

(a) Petersburg (Pet-1) Plane light (20x)

Photomicrograph, showing a metallic iron rim around fragmental material. The rims are easily separable from the surrounding groundmass, but not from the included silicates.

Only orthopyroxenes are found within the metal rims. The meteorite contains abundant un-rimmed orthopyroxene and clinopyroxene. It seems probable that the metal is genetically related to the silicates that the rims enclose.

PLATE 46

(a) Bialystok (Bial-1) Plane light (20x)

Photomicrograph, showing a lithic fragment that has subophitic texture set in a fragmental matrix. The plagioclase (white or gray) laths in the lithic fragment have somewhat irregular boundaries against the pyroxenes (dark gray) which suggests that the fragment has undergone some recrystallization.

(b) Bialystok (Bial-1) Plane light (20x)

Photomicrograph, showing a granoblastic lithic fragment. Some of the boundaries merge with the matrix, which suggests that post-accumulation recrystallization has occurred.

PLATE 47

(a) Bialystok (Bial-1) Plane light (20x)

Photomicrograph, showing a portion where dense opaque material encloses pyroxene and plagioclase fragments. This may be an oxidized remnant of a metallic rim around silicate fragments as is found in Petersburg. At the lower edge of the area there is a zone (z), bounded by a fracture, which has elongated crystal fragments sub-parallel to the fracture. This feature may be indicative of post-accumulation movement in the breccia. A fine-grained area that includes an angular plagioclase fragment (k) resembles the Petersburg fragment shown in Plate 43a.

(b) Bialystok (Bial-1) Plane light (20x)

Photomicrograph, showing lithic and crystal fragments. A conspicuous fragment consists of black opaque unidentified material intergrown with plagioclase.

PLATE 48

(a) Pavlovka (scale is in 1/5 inch)

Exterior, showing fragments of a variety of colors ranging from gray or yellow to black, set in a light gray fine-grained fragmental matrix.

(b) Pavlovka (BM 55255) Plane light (20x)

Photomicrograph, showing lithic and crystal fragments. The right side of the picture shows a lithic fragment which has a texture that resembles the fragmental texture shown by Sioux County (Plate 14 a, b) and is interpreted as a fragment of re-crystallized matrix.

PLATE 49

(a) Pavlovka (BM 55255) Plane light (6x)

Photomicrograph, showing a variety of fragment types. Note that the pyroxene crystal fragments(P) vary from colorless to dark brown(dark gray in picture) depending on their iron content. The dark fragment in the center consists of clinopyroxene grains and an unidentified black opaque matrix. At the right is an area of dense, nearly isotropic material that apparently grades into fine-grained matrix material.

(b) Pavlovka (BM 55255) Plane light (20x)

Photomicrograph, showing the recrystallization of an orthopyroxene grain. The recrystallized portions tend to be concentrated in a pattern that makes angles of about 45° with the (210) cleavage. The fracture pattern shown by the orthopyroxene fragment in Plate 44b may be a related feature. The recrystallization of a coarse crystal into a finer-grained aggregate without strong mechanical deformation of the grain is possibly a result of shock metamorphism.

PLATE 50

(a) Tatouhine(Tat-1) Crossed nicols (6x)

Photomicrograph, showing the recrystallization of orthopyroxene along two sets of fractures. The lighter portions consist of hypersthene and some clinohypersthene in different optical orientations from the host hypersthene grain which is at extinction. The original hypersthene grains were as much as 3 cm in length.

PLATE 51

(a) Yurtuk

Exterior, showing a variety of lithic and crystal fragments. The yellow pyroxenes are the more magnesian, the dark brown pyroxenes are the more iron-rich. The fragmental groundmass has a more brown than gray color due to the abundance of more magnesian crystal fragments. A black vein, probably similar to the veins in Stannem, is present.

(b) Pavlovka (55255 BM) Plane light (20x)

Photomicrograph showing crystal fragments surrounded by dense very fine-grained matrix. Note the color variation of the pyroxenes(p) as a function of iron content. The plagioclase and pyroxene fragments are of similar sizes, but rarely are the crystal fragments larger than 1mm. Plagioclase(Pl); Pyroxene (p).

PLATE 52

(a) Binda (scale in inches)

Exterior, showing a coarse-grained lithic fragment at the far right hand side of the picture and dense gray areas in the central portions. The color of the dark minerals seems to be uniform over the surface, which agrees with the optical studies that suggest the meteorite is a monomict breccia.

PLATE 53

(a) Binda (Bin-1) Plane light (6x)

Photomicrograph, showing the distribution of lithic and crystal fragments. The lithic fragment at the bottom left has a very strongly sheared plagioclase-pyroxene contact. The dark, nearly amorphous material in some areas appears to be fragmental, but in other areas apparently invades crystalline material (see arrows). In general, the finer the grain size, the darker the groundmass.

(b) Binda (Bin-1) Crossed nicols (6x)

Photomicrograph, showing the same area as Plate 53a under crossed nicols. Most of the crystal fragments have undulatory extinction. The dense black material is not truly isotropic. The gradational character of some of the black material is shown by comparison of the portions on Plates 53a and 53b marked with X. In crossed nicols, it appears that this region is finely granulated and seems to grade into the densest black portions shown in plane light. This suggests that the black material is extremely finely granulated material.

PLATE 54

(a) Binda (Bin-1) Crossed nicols (20x)

Photomicrograph, showing the sheared zone between the plagioclase and pyroxene grain shown at the lower left of Plate 53. The plagioclase is strongly strained and a mortar texture has developed along the sheared zone.

(b) Binda (Bin-1) Crossed nicols (6x)

Photomicrograph, showing deformed orthopyroxene. In some places, exsolution lamellae parallel (100) in the orthopyroxene have been contorted by later fracturing. Very fine-grained almost isotropic areas seem to grade into the more normal fragmental matrix.

PLATE 55

(a) Kapoeta (UCLJ-1) Plane light (50x)

Photomicrograph, showing lithic and crystal fragments. At the center is a fragment that consists of a plagioclase lath surrounded by brown pigeonite at the top and colorless pyroxene at the bottom. At the top, some colorless pyroxene surrounding the pigeonite may be due to recrystallization of the pigeonite. This lithic fragment is comparable to some fragments in iron-rich basaltic achondrites such as Nuevo Laredo and Stannern. At the left is a large hypersthene crystal fragment that represents a portion of a much more magnesian system than that represented by the lithic fragment.

(b) Kapoeta (UCLJ -1) Plane light (20x)

Photomicrograph. The lithic fragment at the top is similar to the Petersburg fragment shown in Plate 40b. Note the color variation of pyroxenes (p) due to variation of the iron content.

PLATE 56

(a) Kapoeta (UCLJ-1) Plane light (50x)

Photomicrograph, showing a fragment with a texture that resembles the Pavlovka and Sioux County textures which have been interpreted as recrystallized matrix. Angular plagioclase grains are set in a fine-grained matrix consisting of plagioclase and pyroxene.

(b) Kapoeta (UCLJ-1) Plane light 50x)

Photomicrograph, showing a fragment that consists of a few angular grains of pyroxene and plagioclase enclosed by a very fine-grained matrix. This may be similar to the texture shown by the fragment in Plate 43a.

PLATE 57

(a) Kapoeta (UCLJ-d) Plane light (20x)

Photomicrograph, showing a portion of the "light-dark" structure. The darker portions are located in strongly fractured areas. The original material was a coarse monomineralic aggregate of orthopyroxene, perhaps similar to the lithic fragment shown in Plate 43b(Petersburg).

(b) Kapoeta (UCLJ-d) Reflected light (20x)

Photomicrograph, showing the same area in reflected light. A conspicuous subparallel fracture pattern is present. The darker portions tend to occur where the fracture pattern is most pronounced.

PLATE 58

(a) Kapoeta (UCLJ-d) Plane light (20x)

Photomicrograph showing a "dark" portion of the meteorite. The nearly opaque groundmass contains high contents of "primordial" rare gases.

(b) Kapoeta (UCLJ-d) Reflected light (20x)

Photomicrograph, showing the same area as Plate 58a in reflected light. The fracture pattern is less pronounced in this portion. Note that some areas that stand out as fragments in reflected light are dark in transmitted light. This suggests that the transformation has occurred in place after the accumulation of the breccia.

PLATE 59

(a) Estherville (Est-1) Plane light (6x)

Photomicrograph The large clast at the left is olivine(O). Details of the reaction rim are shown in Plate 59a. Plagioclase grains (p) are irregular and appear to be fragmental. Some variation of color in the pyroxene grains(dark) can be seen. The recrystallization has produced some features that are similar to the texture described in Plate 13b(Sioux County). Plagioclase seems to extend apophyses into its surroundings and is generally lacking in undulatory extinction.

(b) Estherville (Est-1) Crossed nicols (20x)

Photomicrograph, showing details of the olivine nodule. The interior is marked by zones of recrystallization to finer-grained olivine, which tend to have higher concentrations of opaque minerals. A bordering reaction rim(arrow) has opaque grains(probably metallic iron) on the inside and orthopyroxene on the outside. The meteorite contains abundant tridymite.

PLATE 60

(a) Estherville (Est-1) Crossed nicols (20x)

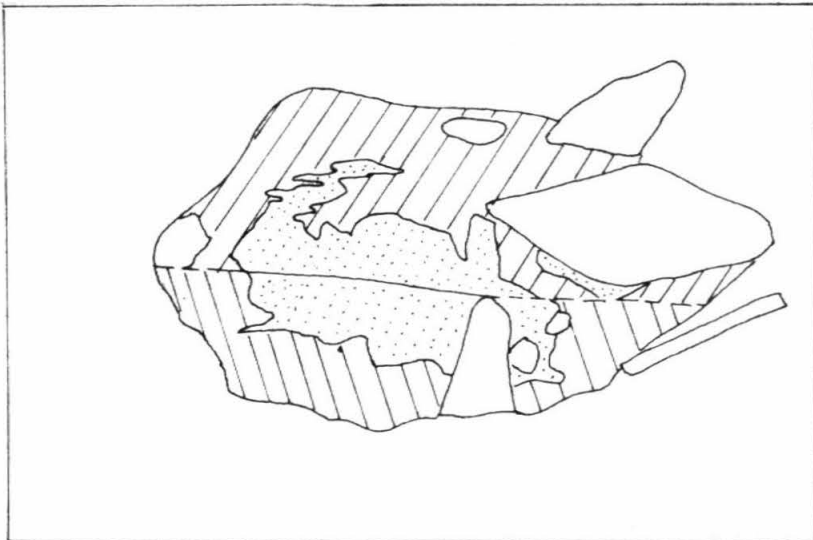
Photomicrograph, showing reaction(?) rim around an orthopyroxene grain and the distribution of metallic iron. The central orthopyroxene grain (P) has a zone that contains abundant bleb inclusions, possibly of clinopyroxene. There is an inclusion-free zone to the outside of the inclusion-filled zone (arrow). The metallic iron does not form a continuous network in this texture. Note the plagioclase penetration twin at the bottom center.

(b) Brent Crater impact breccia. Crossed nicols (20x)

Photomicrograph, showing the distribution of lithic and crystal fragments. There is a great range of fragment sizes. Most crystal fragments show strong undulatory extinction. The mineralogy consists of plagioclase, potassium feldspar and quartz.

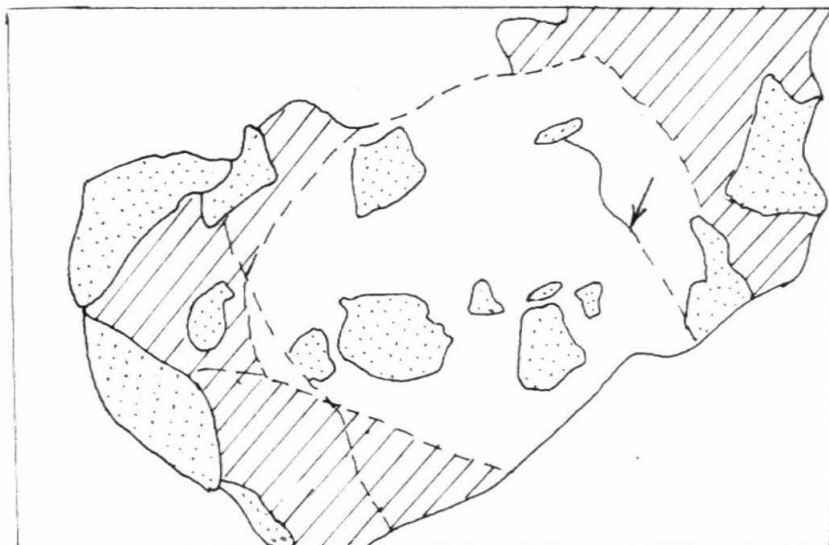
Overlay for Plate 9b

Stippled, hypersthene: crosshatched, pigeonite,
plain. plagioclase.

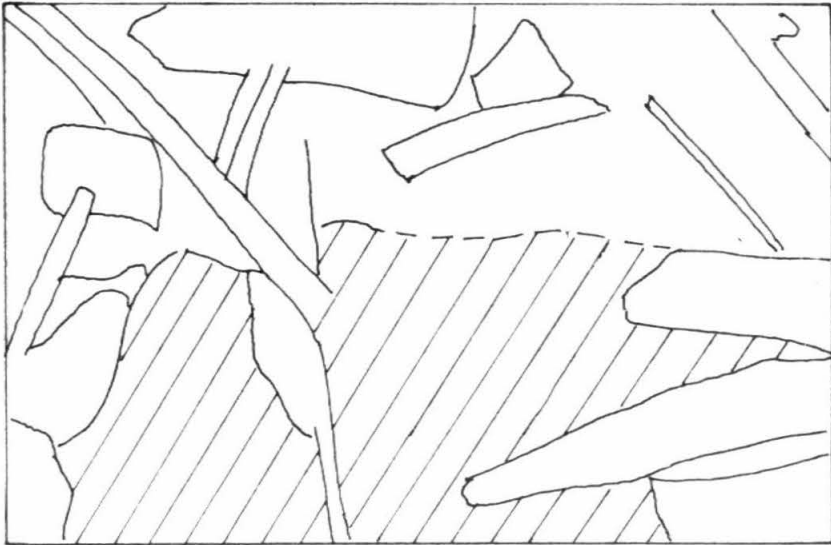


Overlay for Plate 13b

Stippled, plagioclase; Plain, fine-grained mass of pyroxene and plagioclase.



Overlay for plate 23b



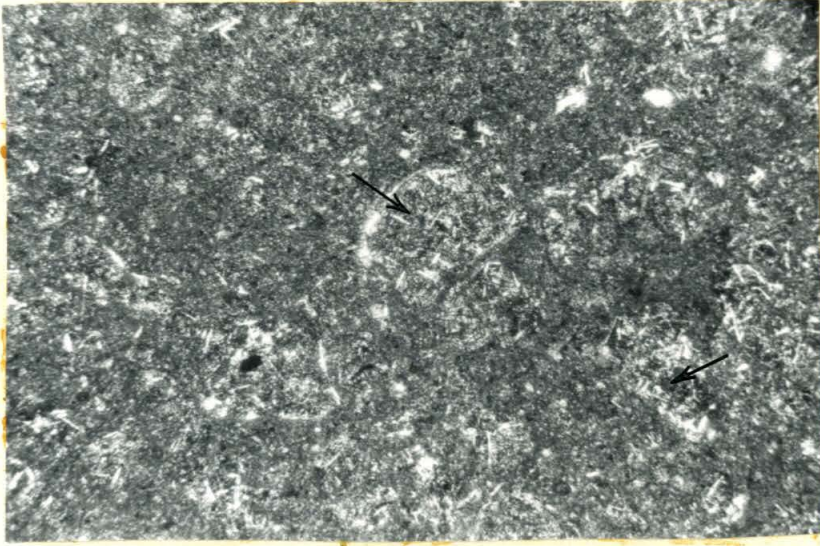
-303-



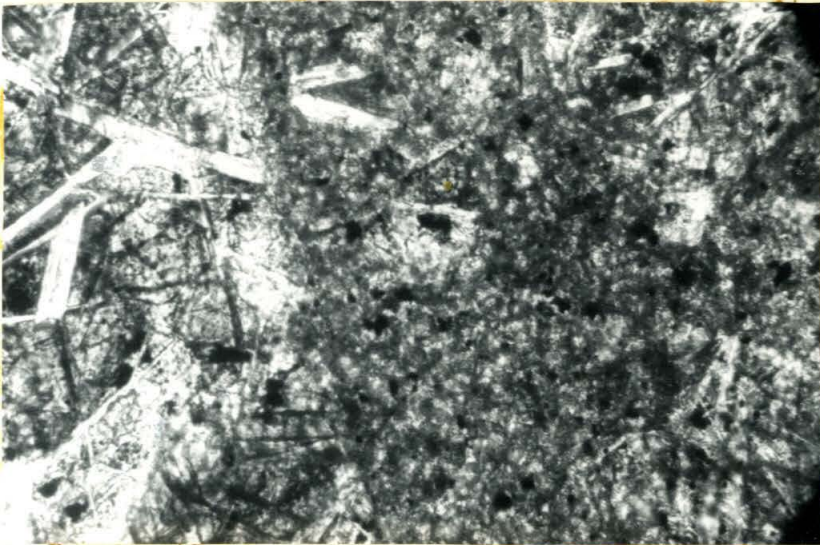
(a)



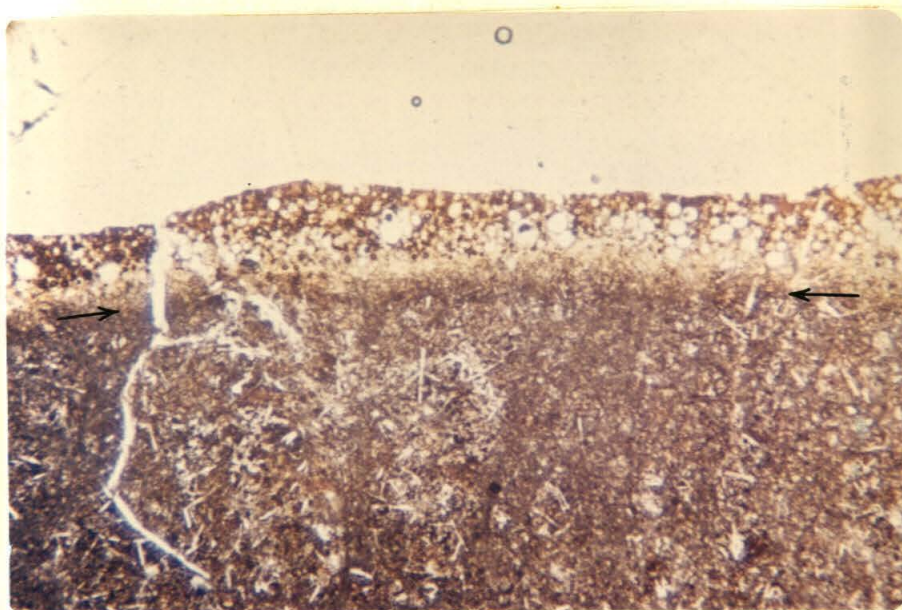
(b)



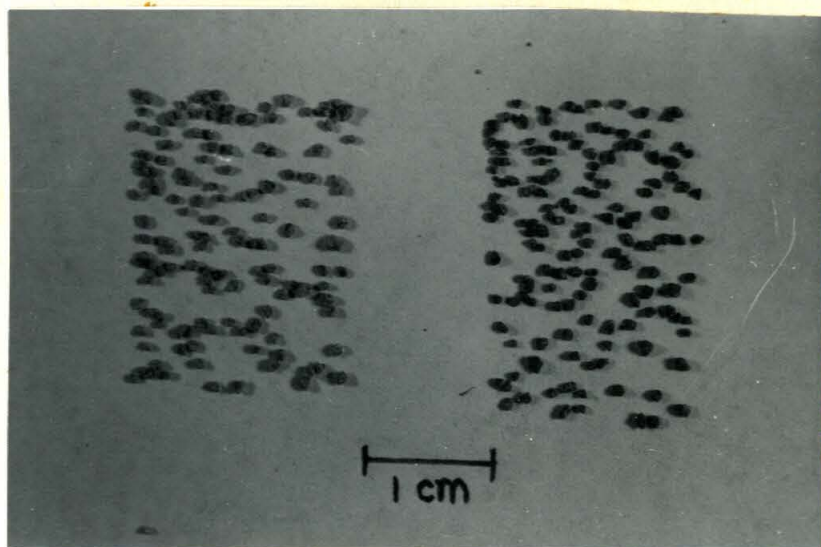
(a)



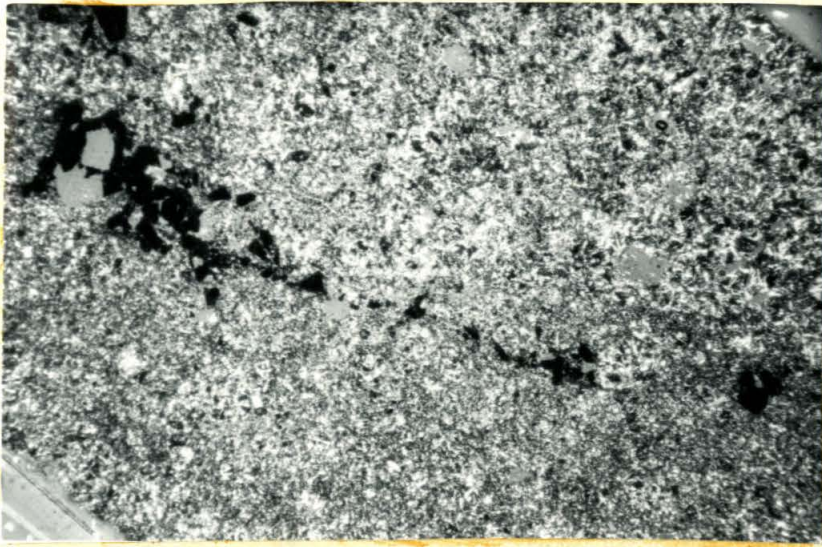
(b)



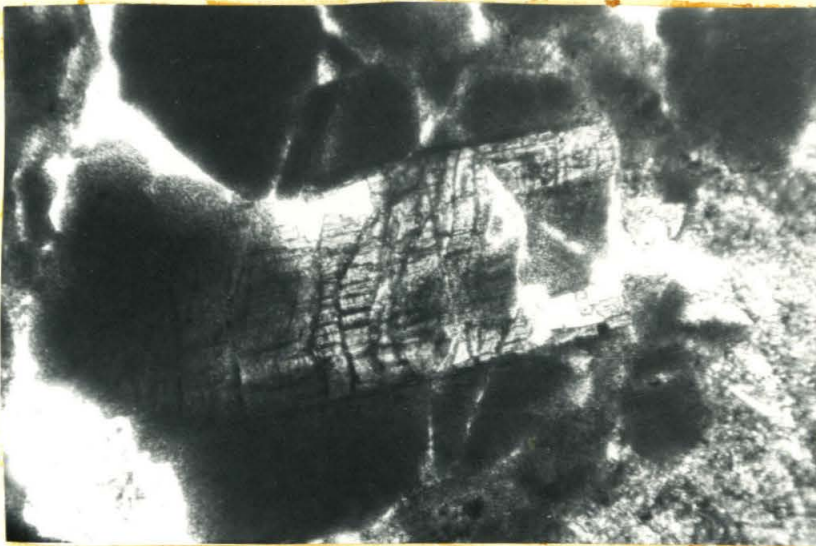
(a)



(b)



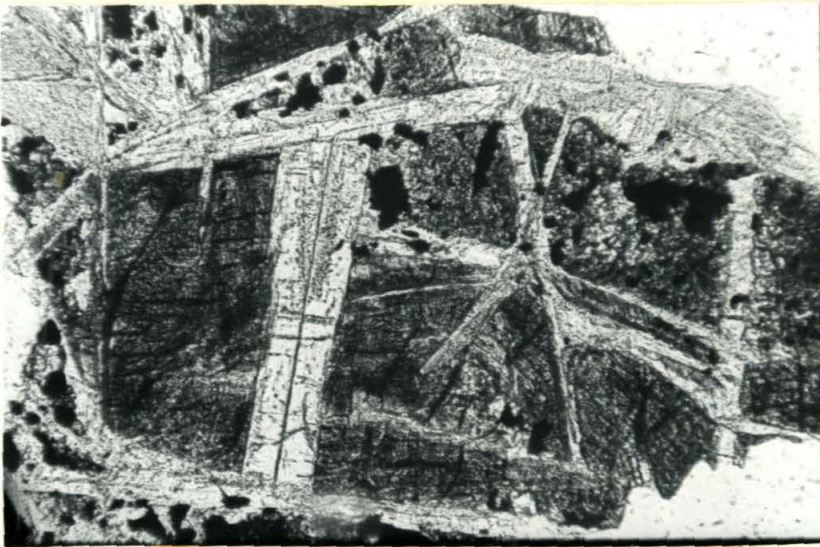
(a)



(b)



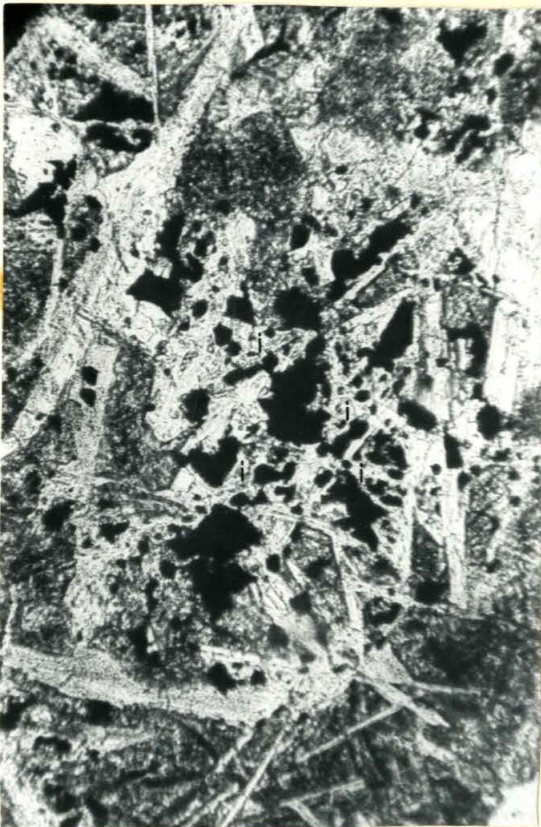
(a)



(b)



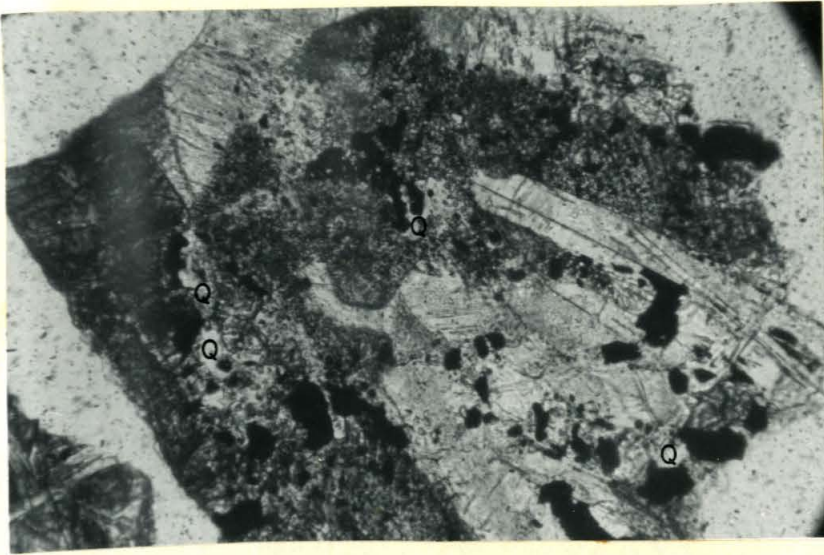
(a)



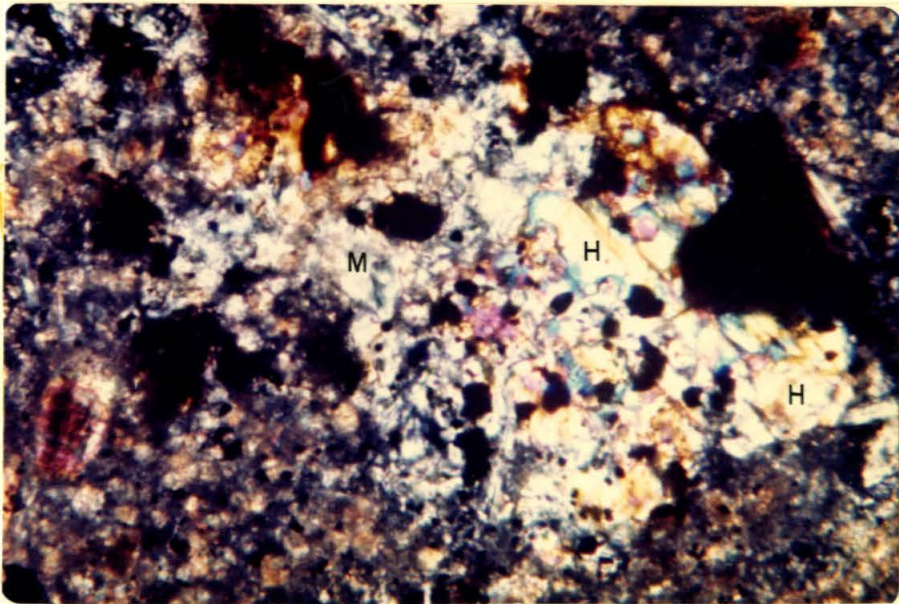
(b)



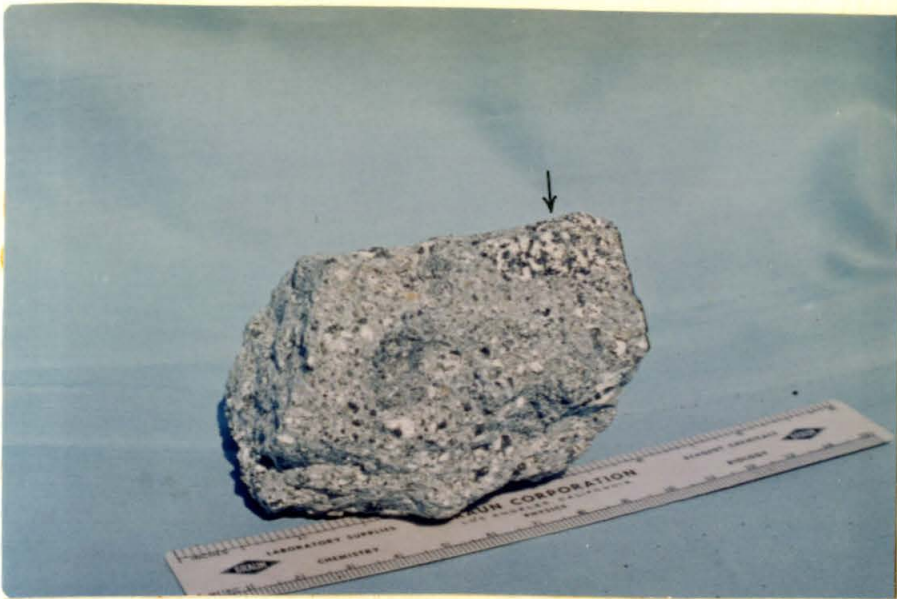
(c)



(a)



(b)



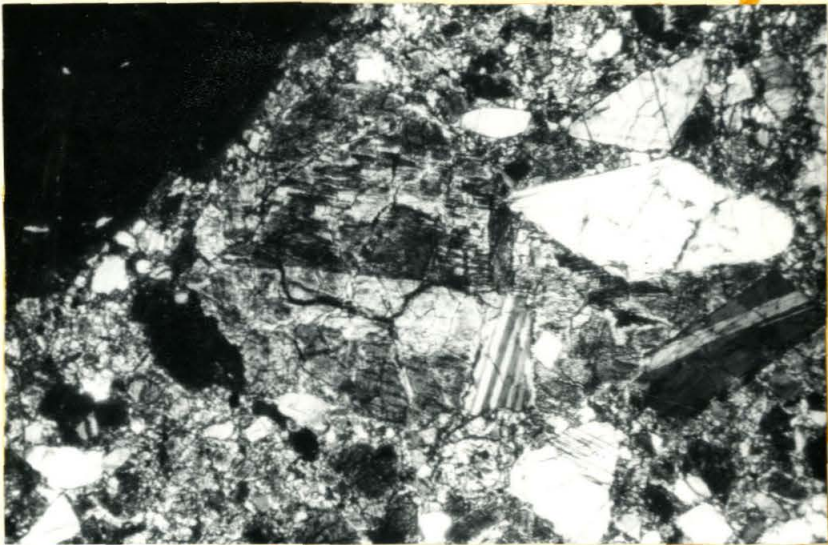
(a)



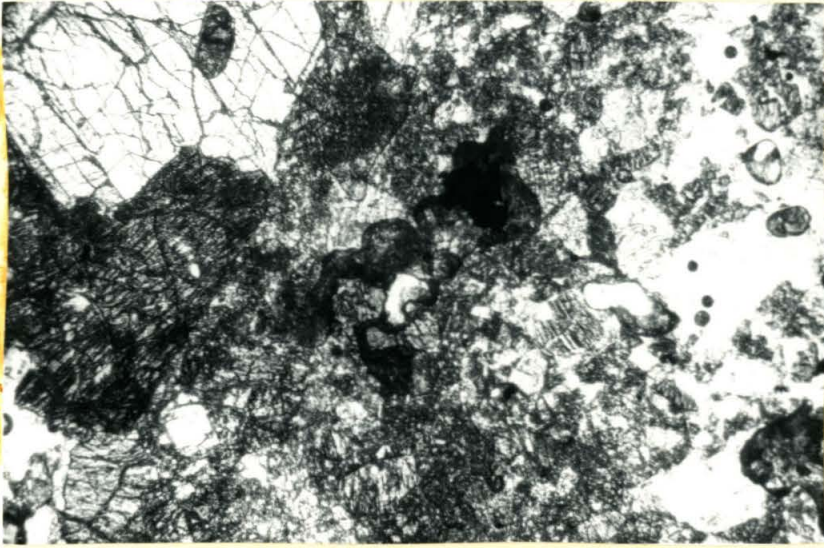
(b)



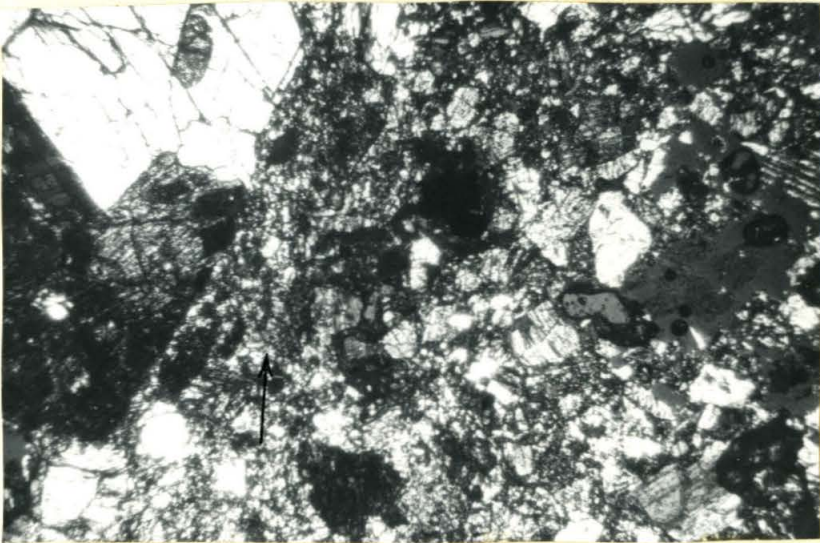
(a)



(b)



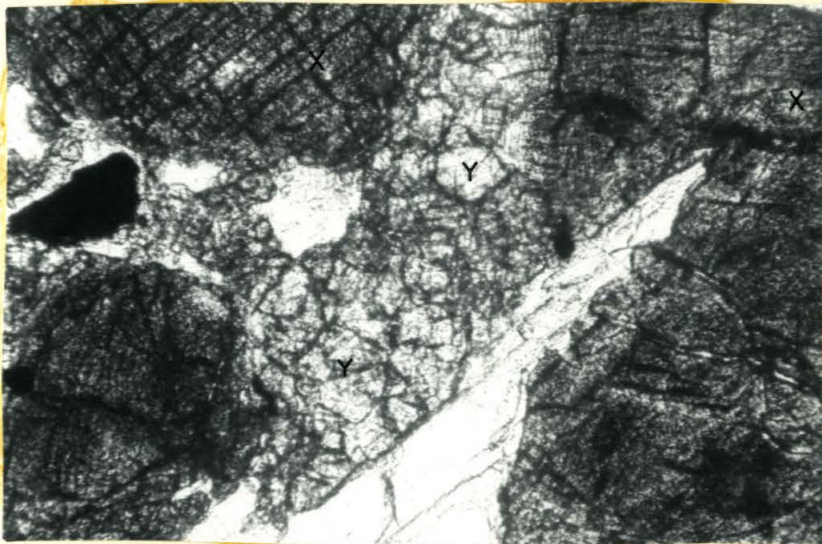
(a)



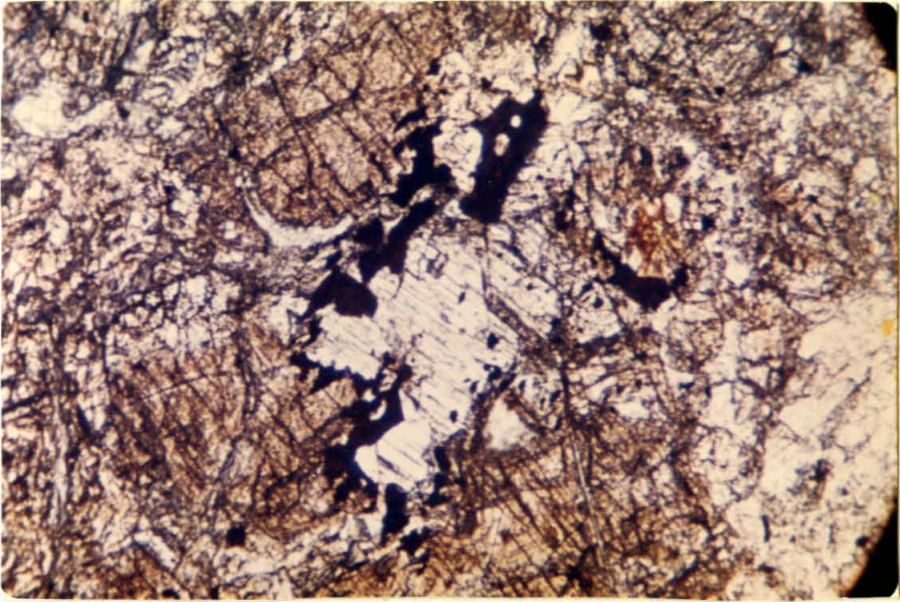
,(b)



(a)



(b)



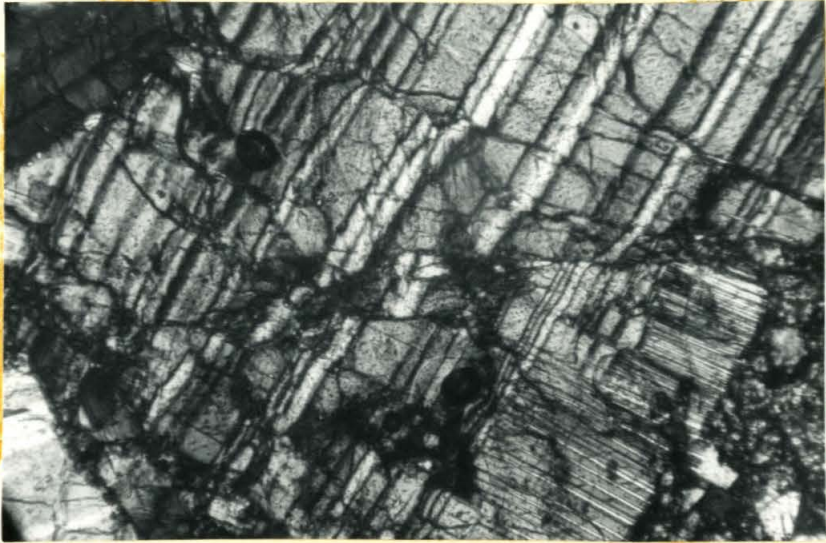
(a)



(b)



(c)



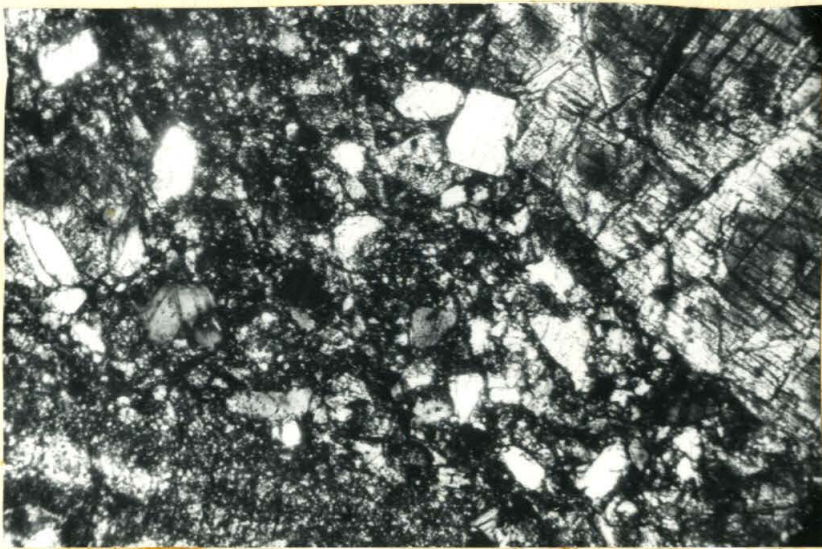
(a)



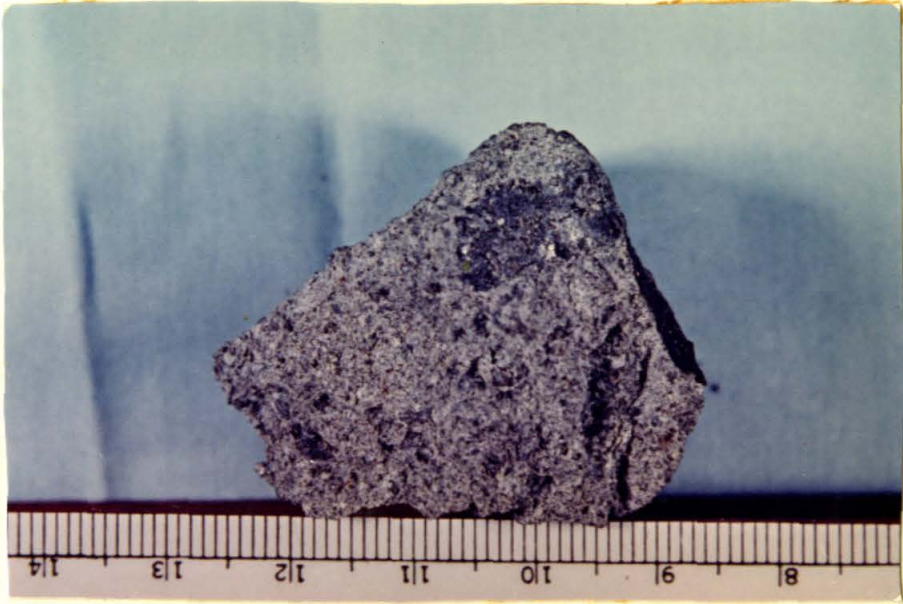
(b)



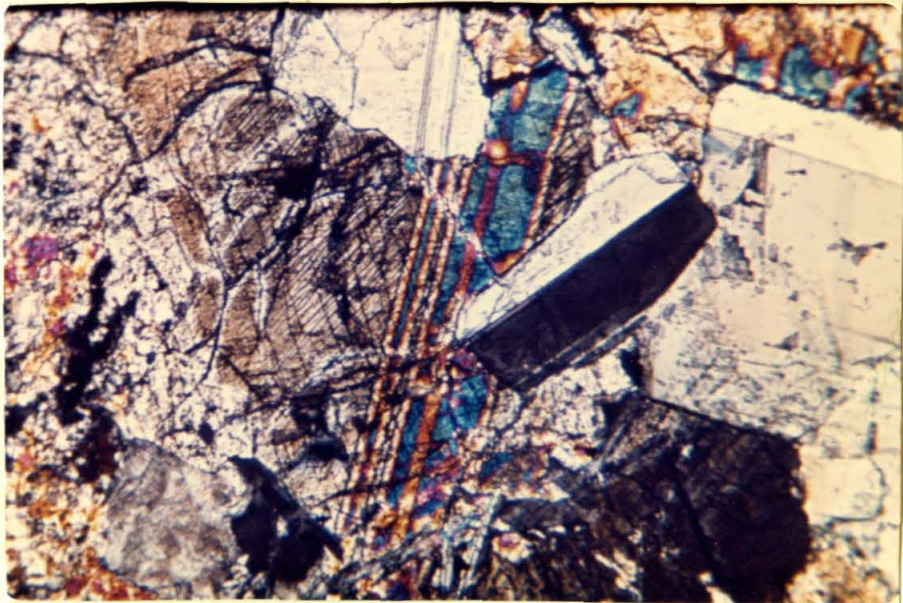
(a)



(b)



(a)

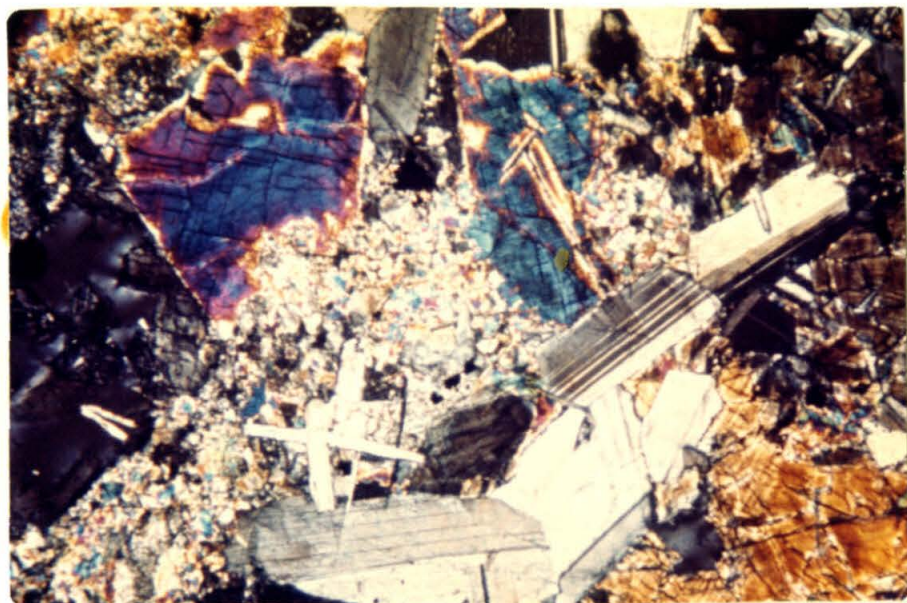


(b)

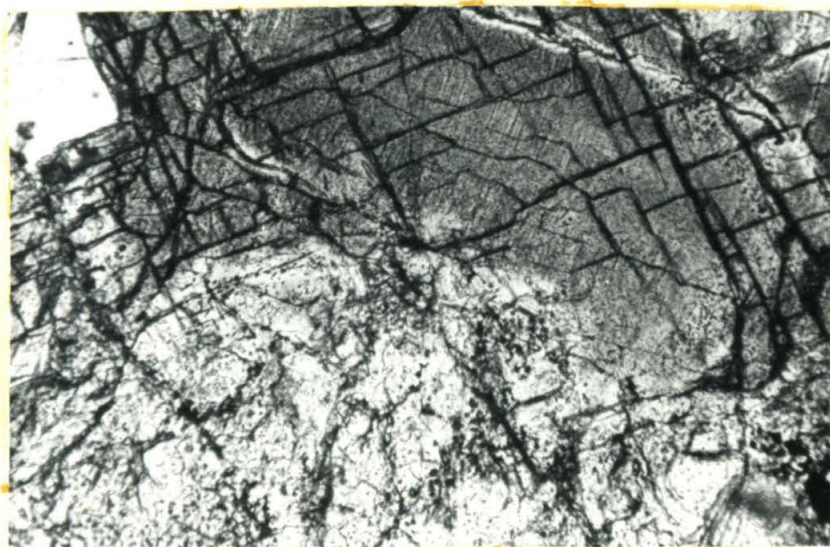


(a)

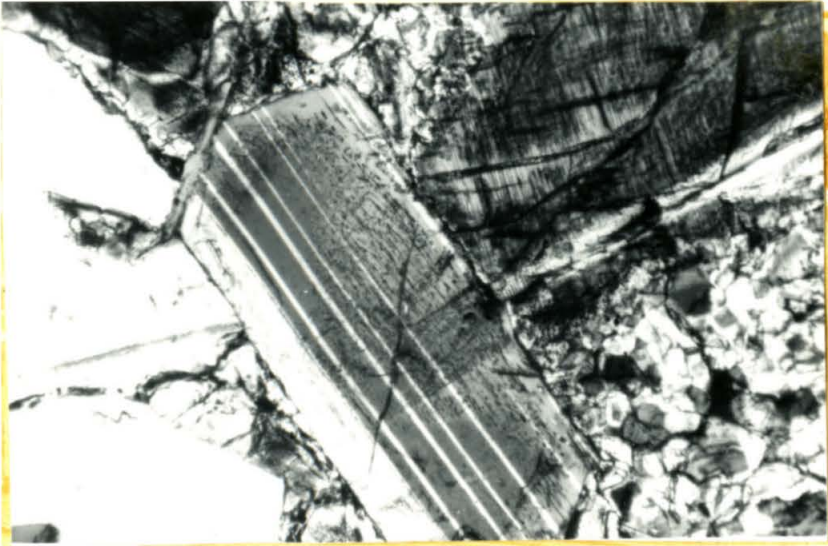
PLATE 16



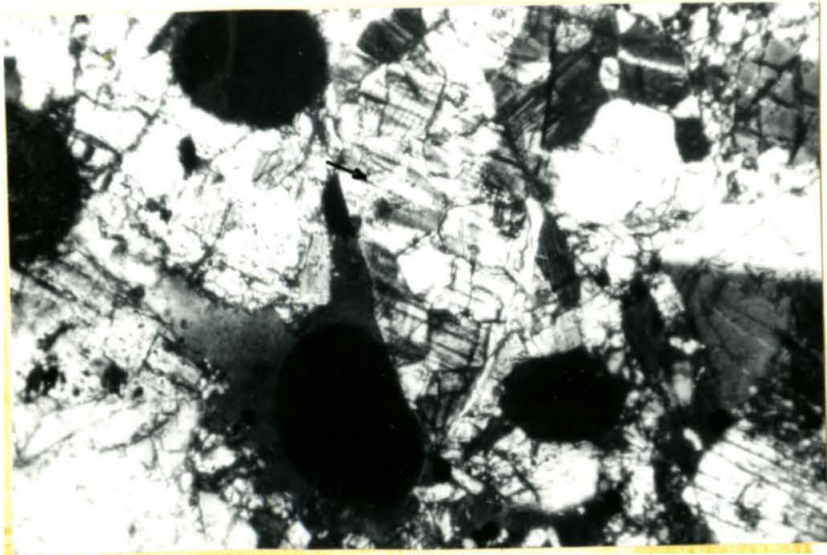
(a)



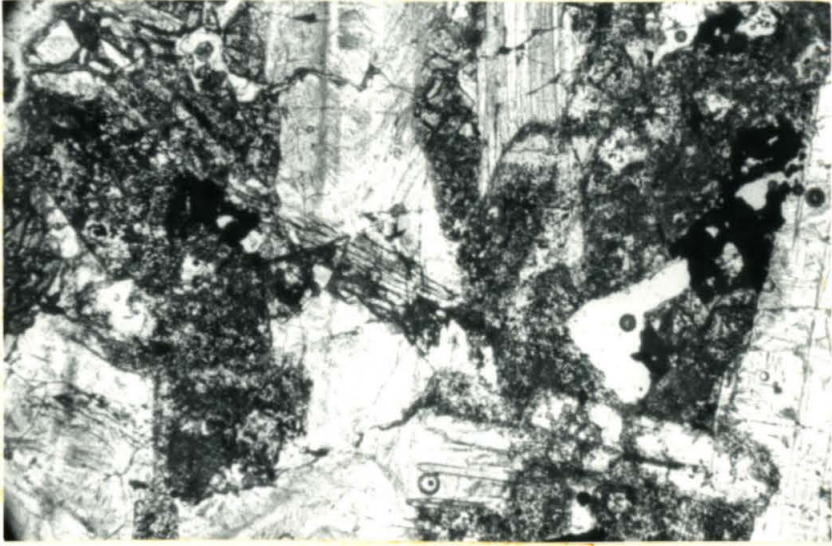
(b)



(a)



(b)



(a)



(b)

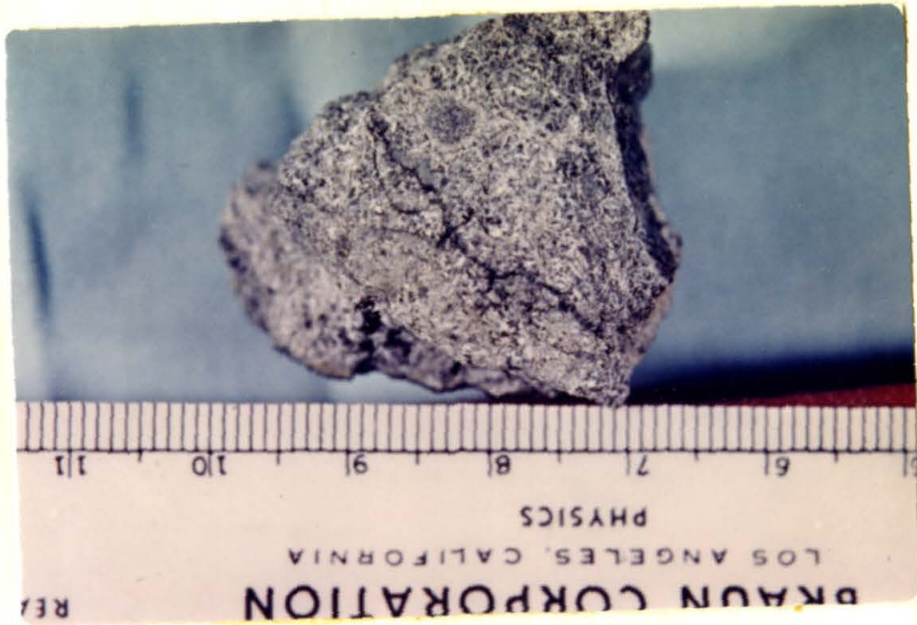


(a)

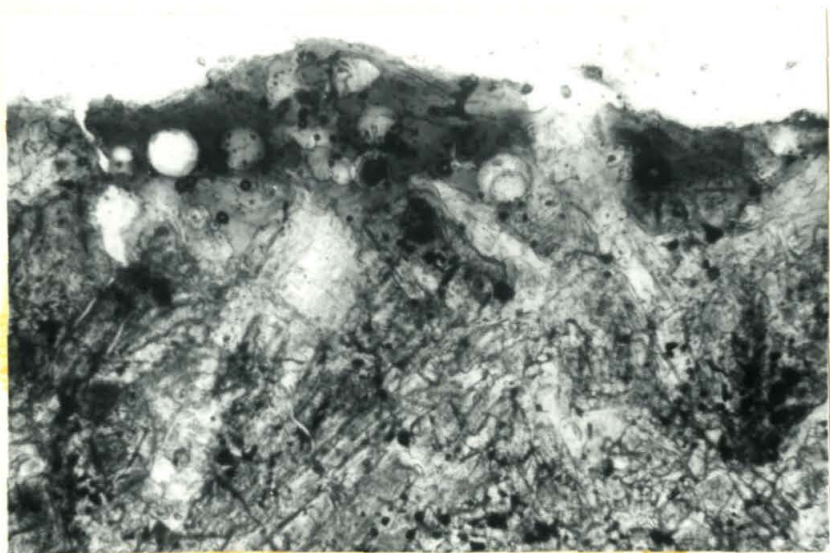
PLATE 20



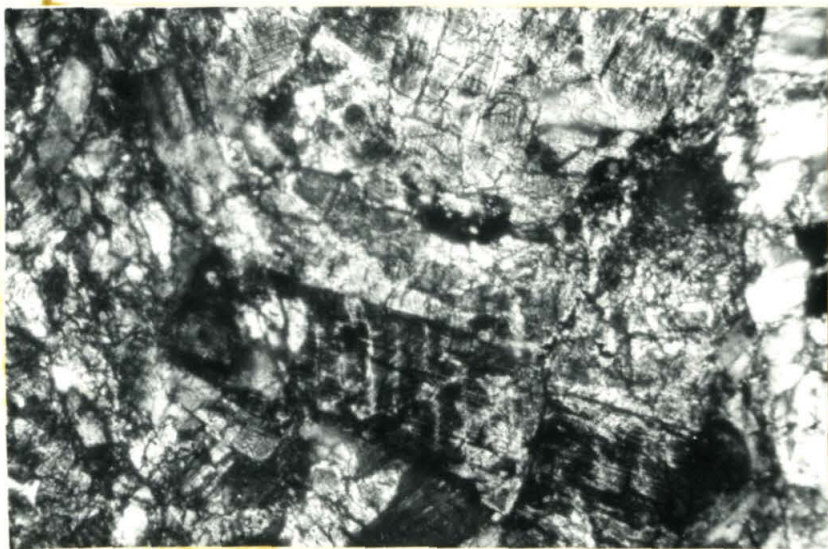
(a)



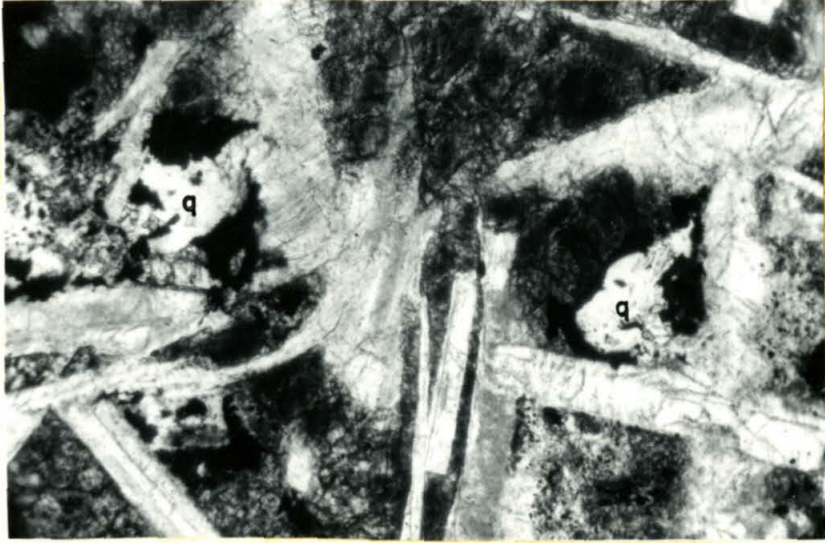
(b)



(a)



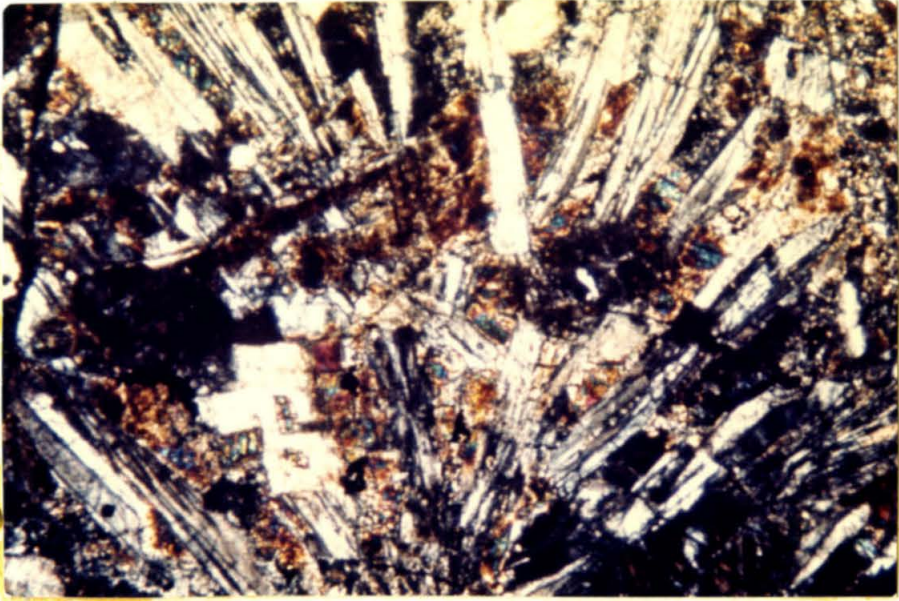
(b)



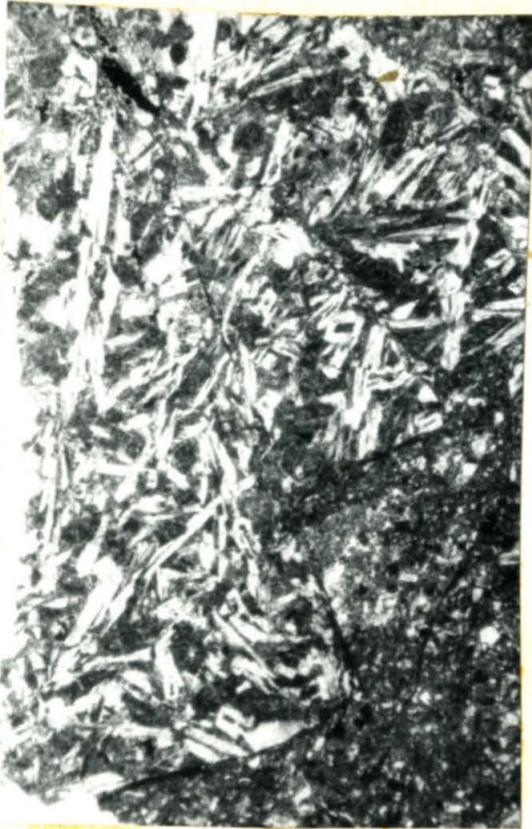
(a)



(b)



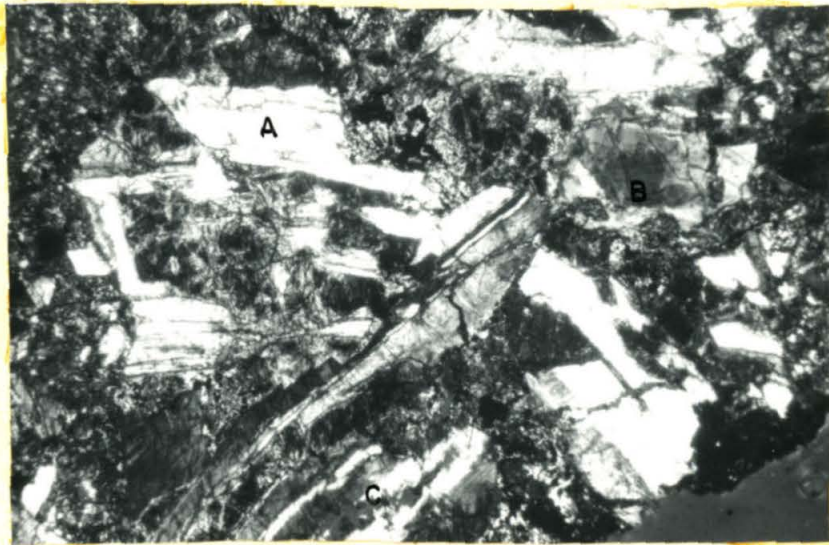
(a)



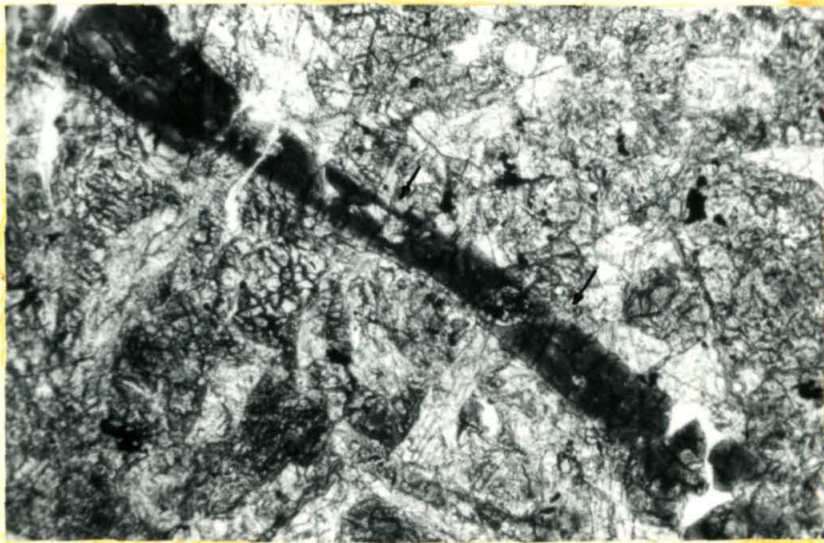
(b)



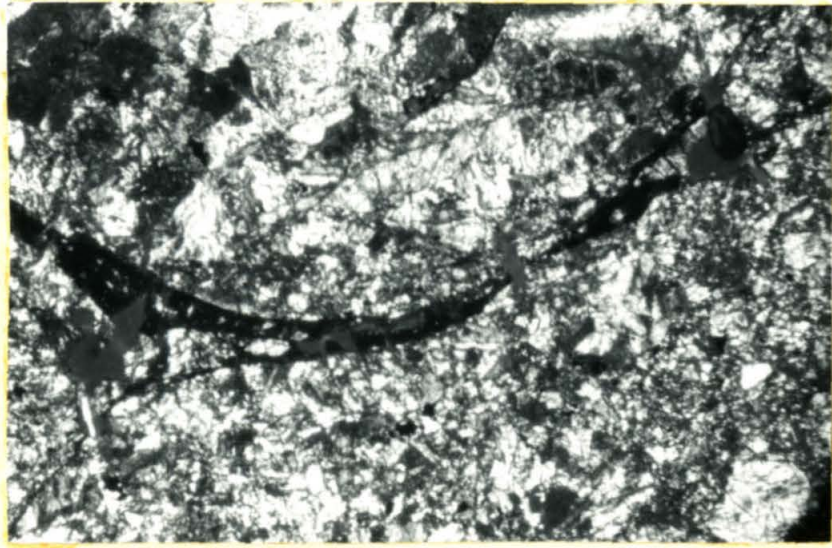
(c)



(a)



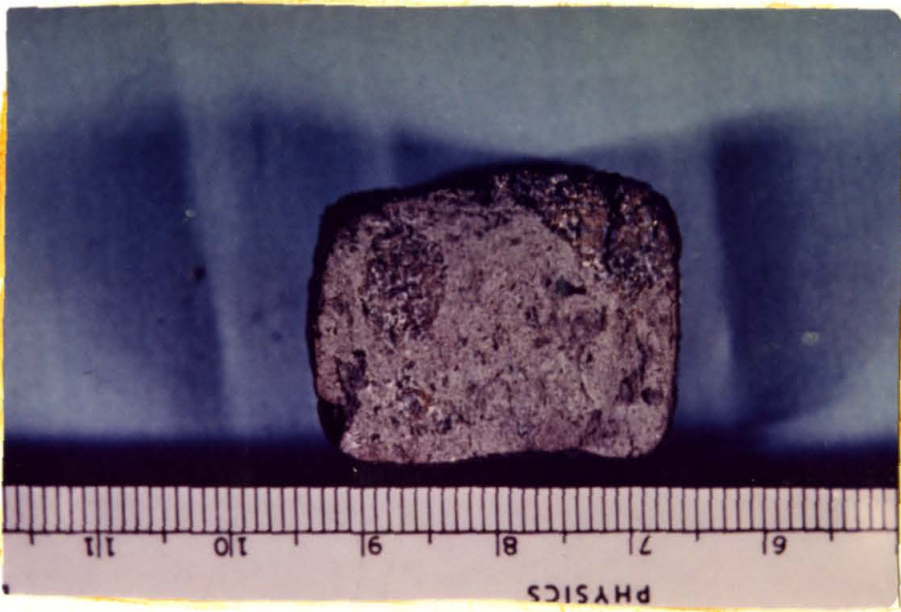
(b)



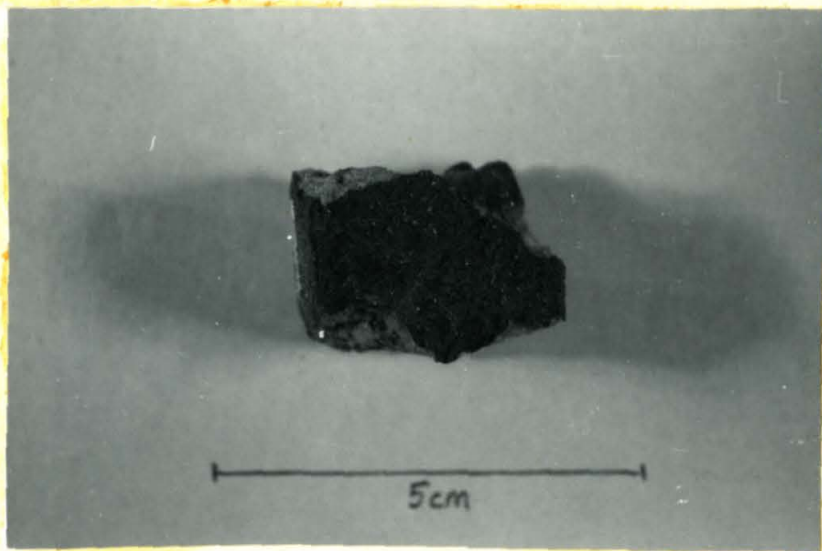
(a)



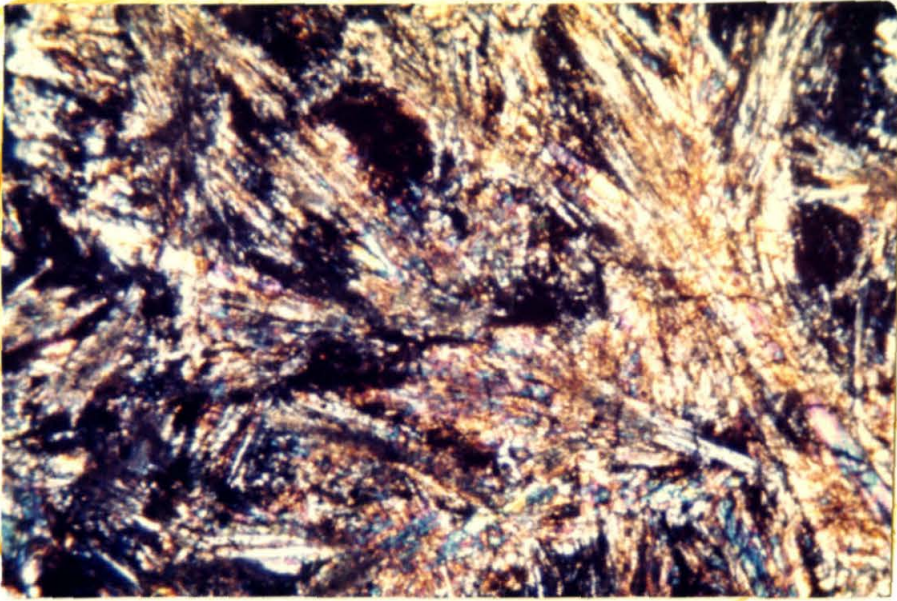
(b)



(a)



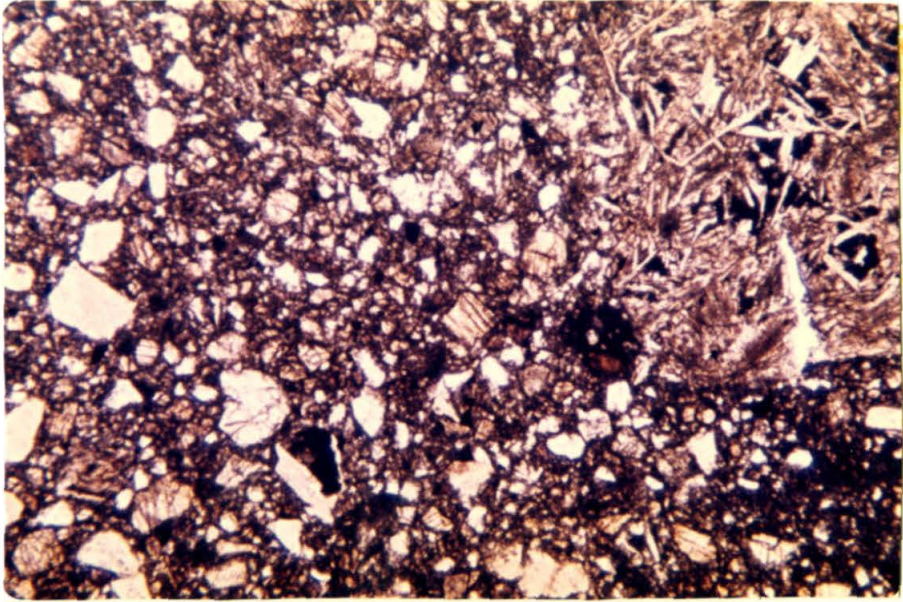
(b)



(a)



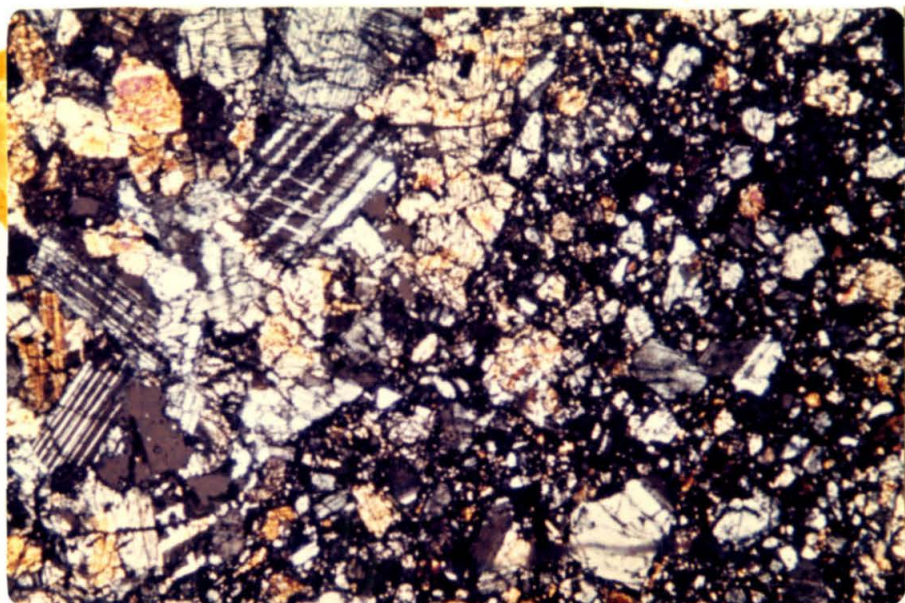
(b)



(a)



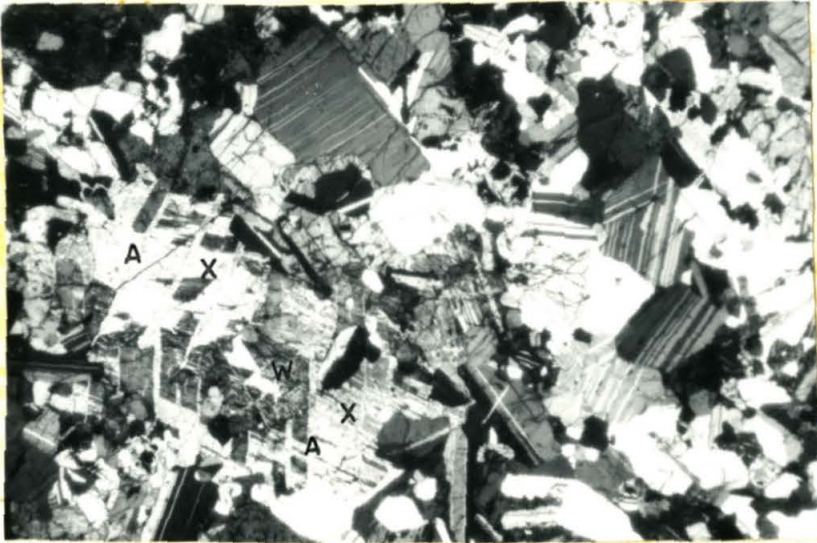
(b)



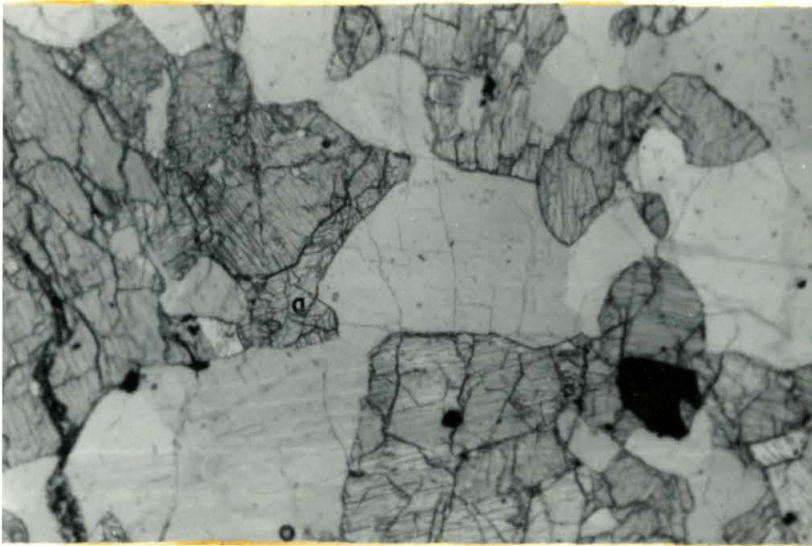
(a)



(b)



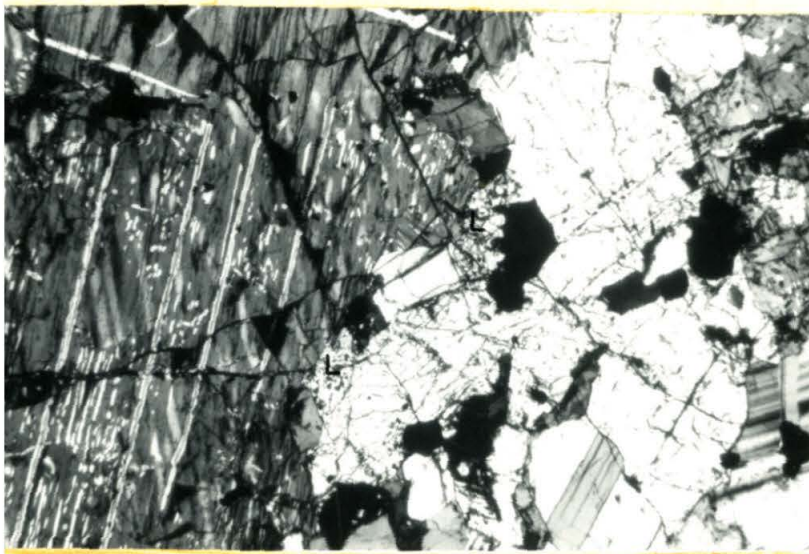
(a)



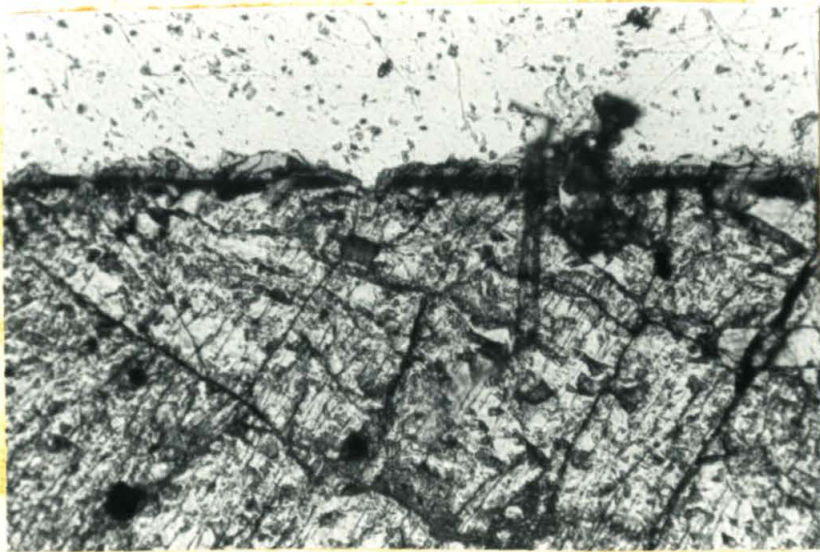
(b)



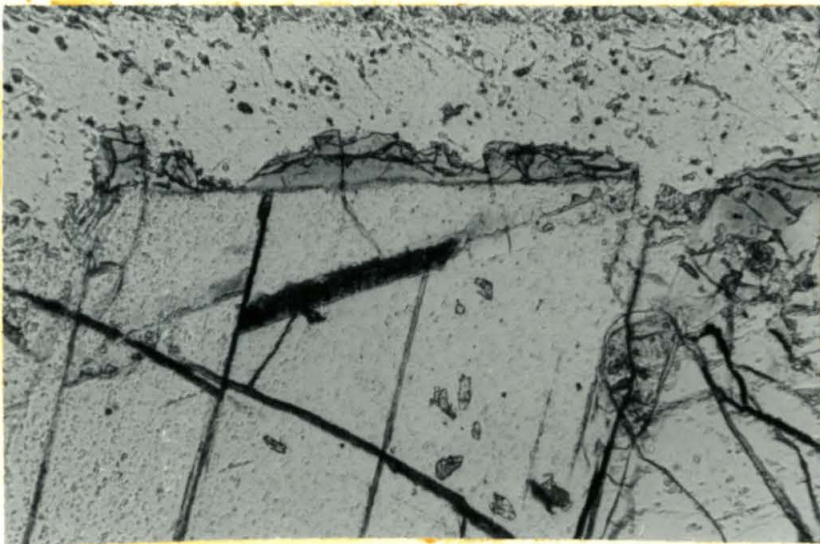
(a)



(b)



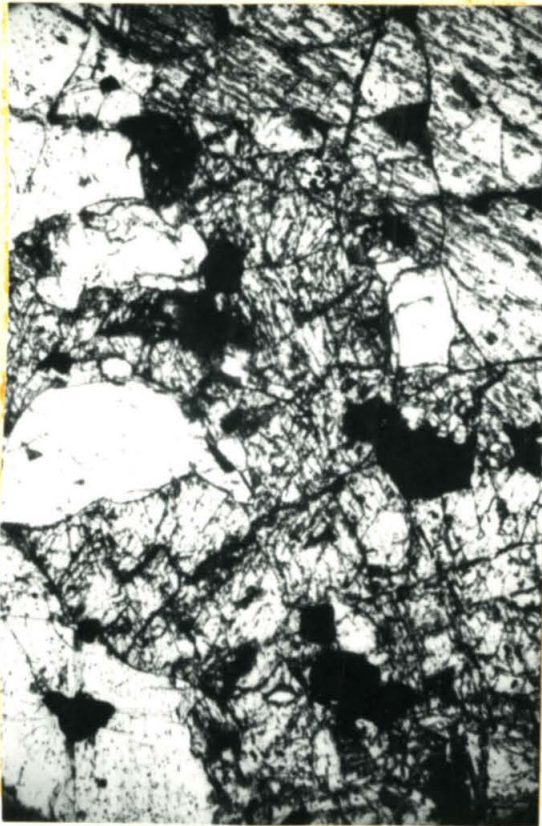
(a)



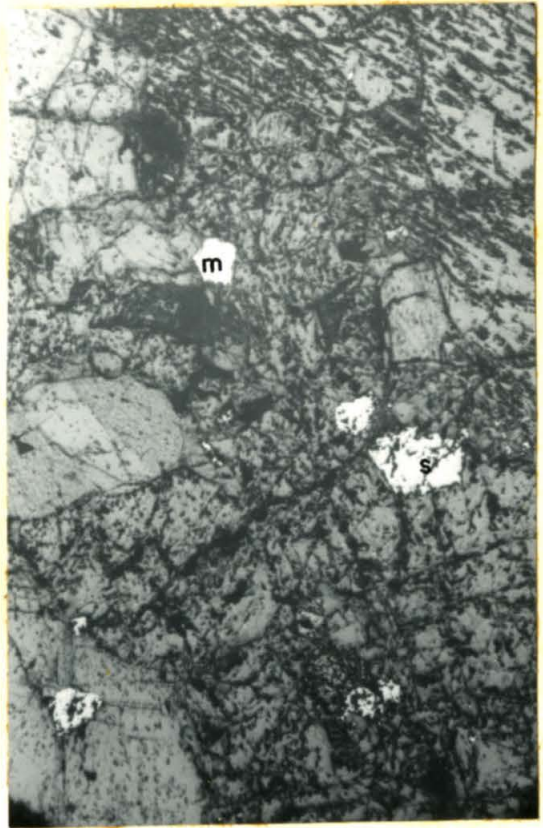
(b)



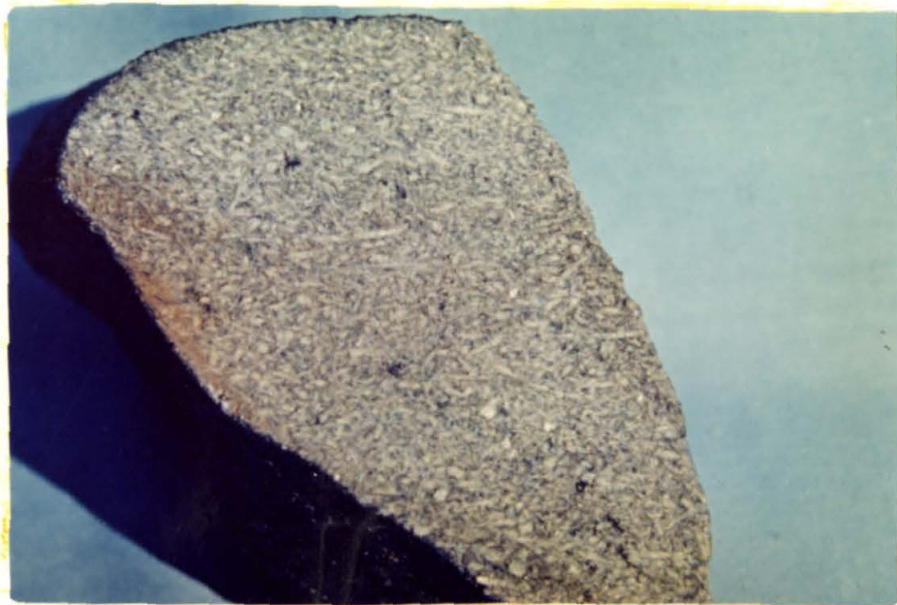
(a)



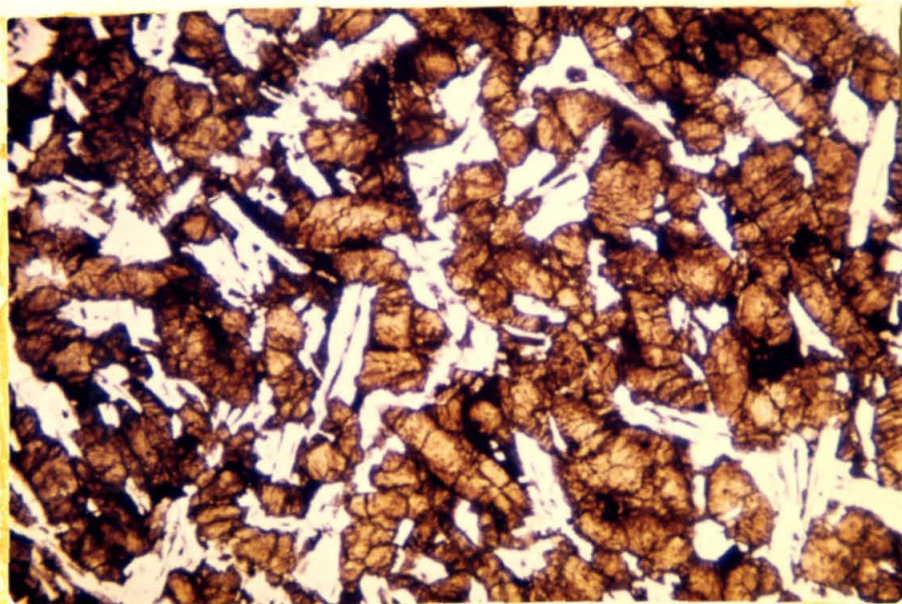
(b)



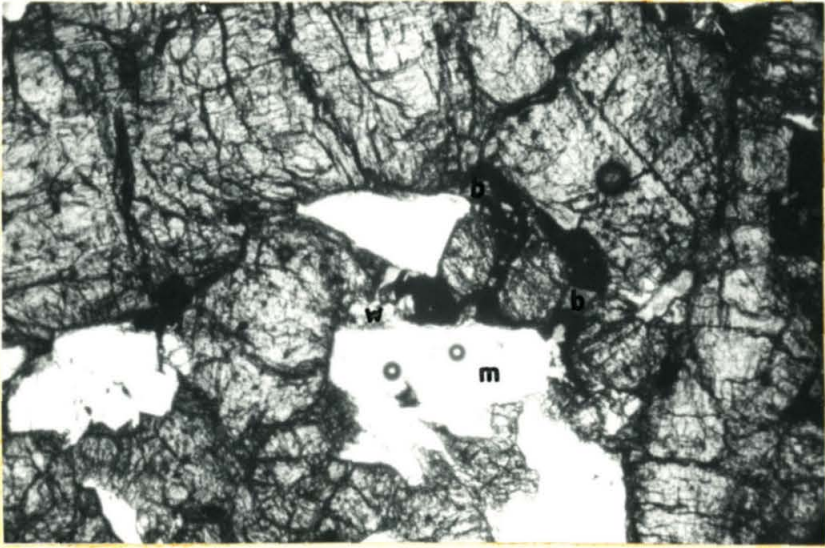
(c)



(a)



(b)



(a)

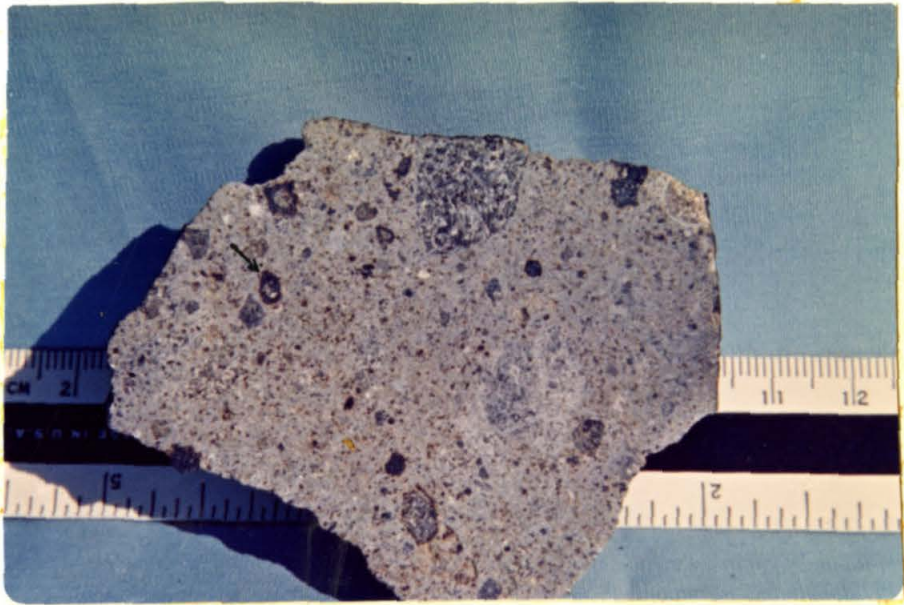


(b)



(a)

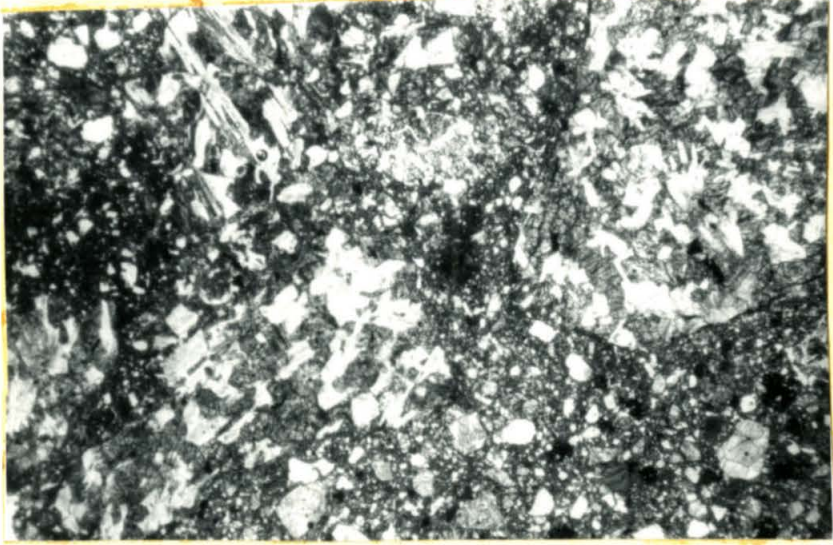
PLATE 37



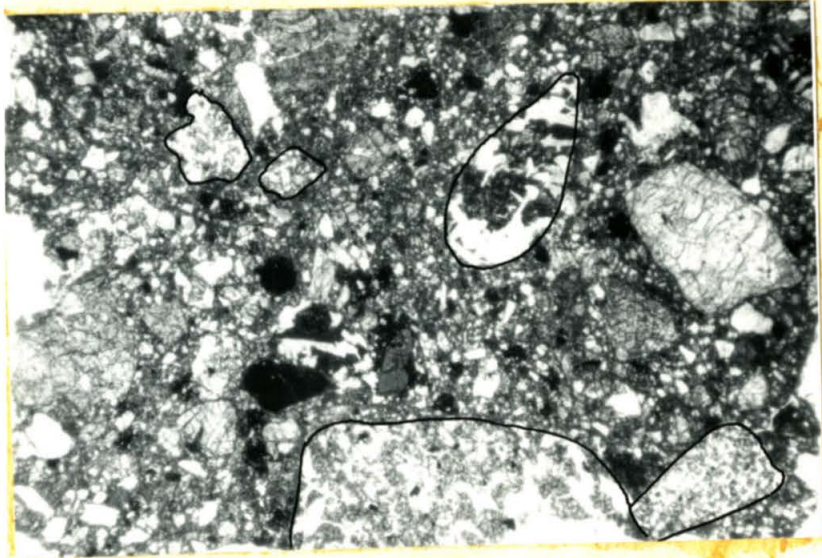
(a)



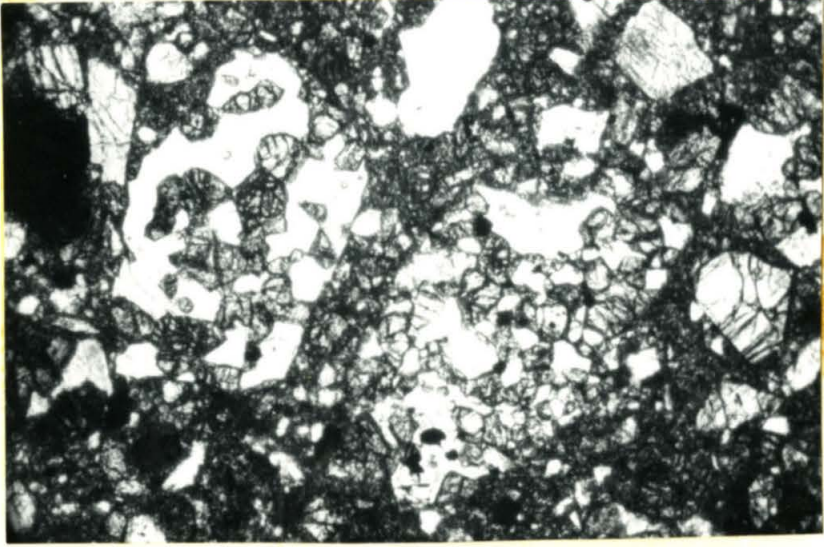
(b)



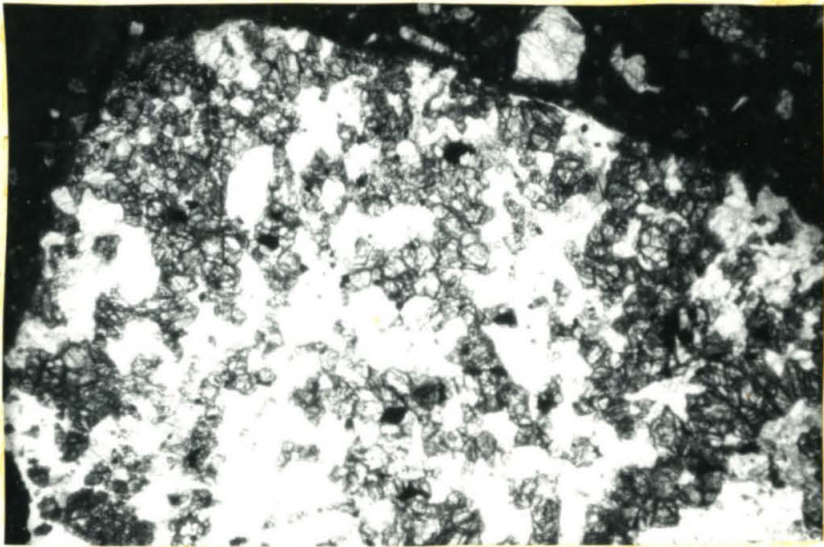
(a)



(b)



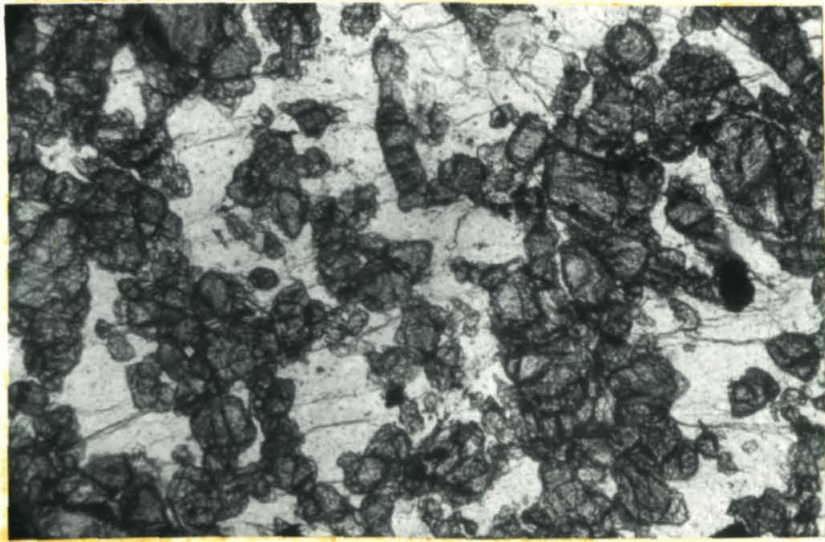
(a)



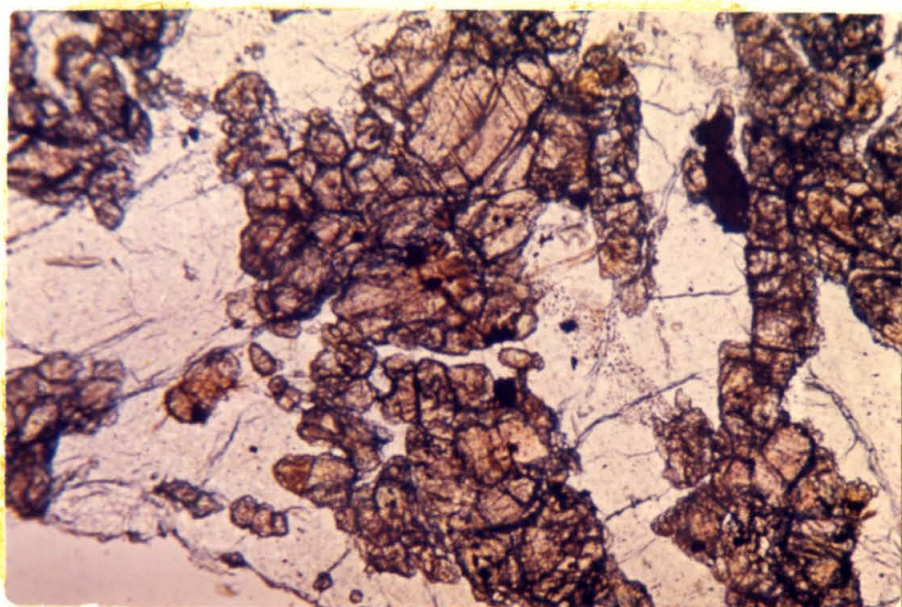
(b)



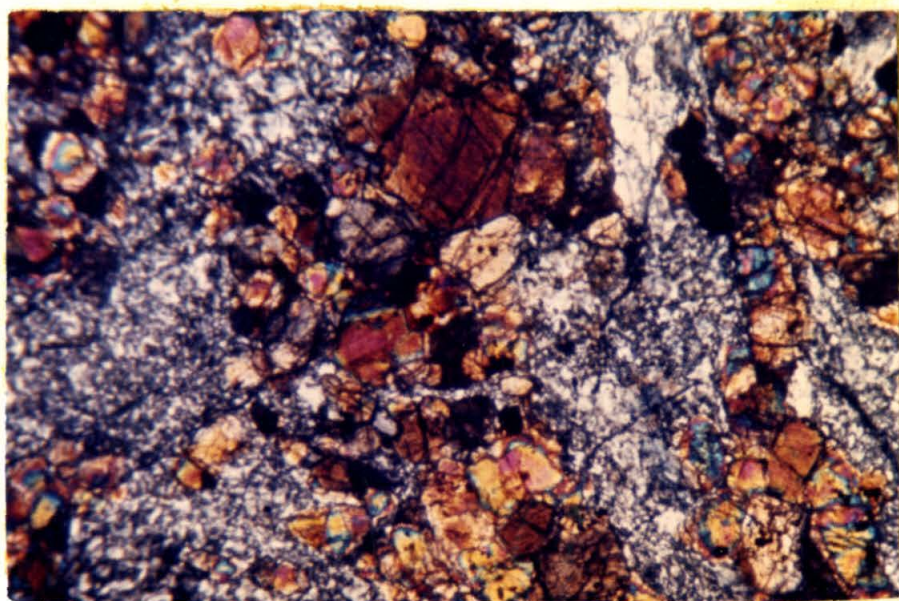
(a)



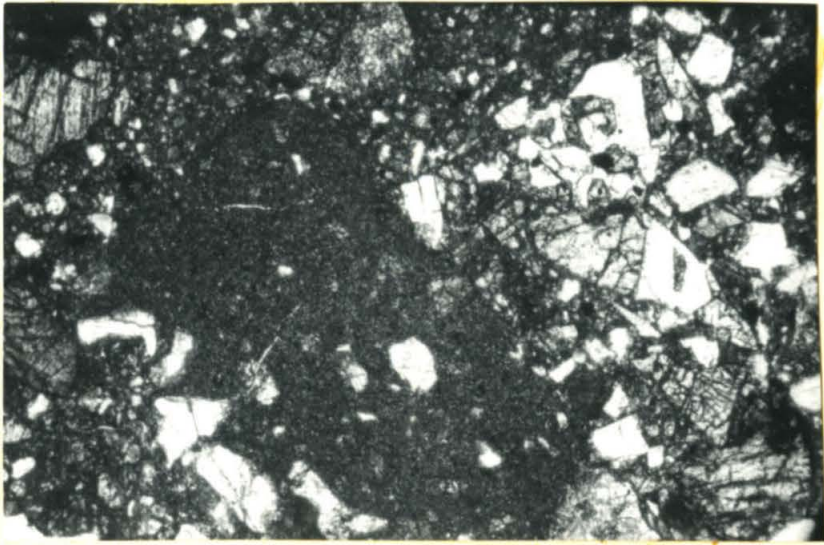
(b)



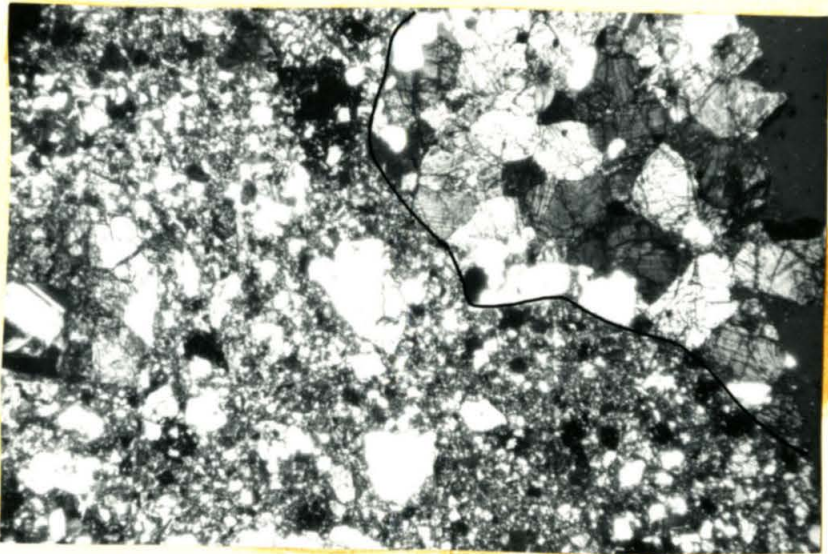
(a)



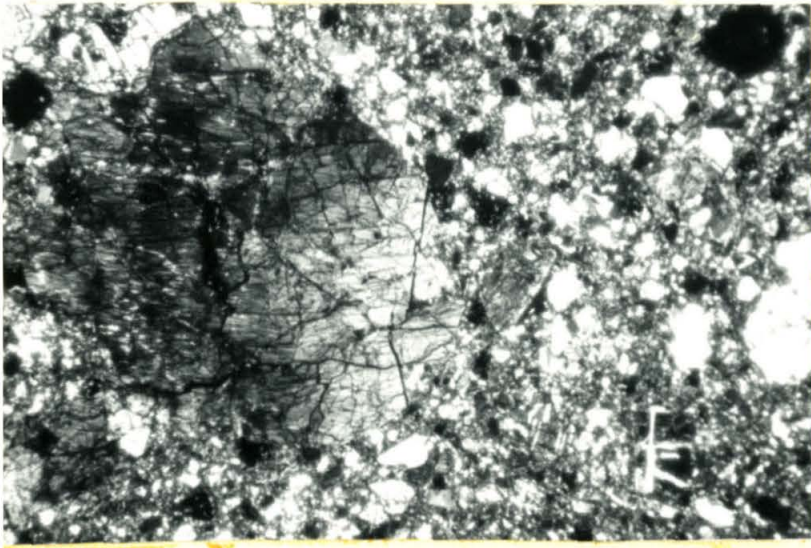
(b)



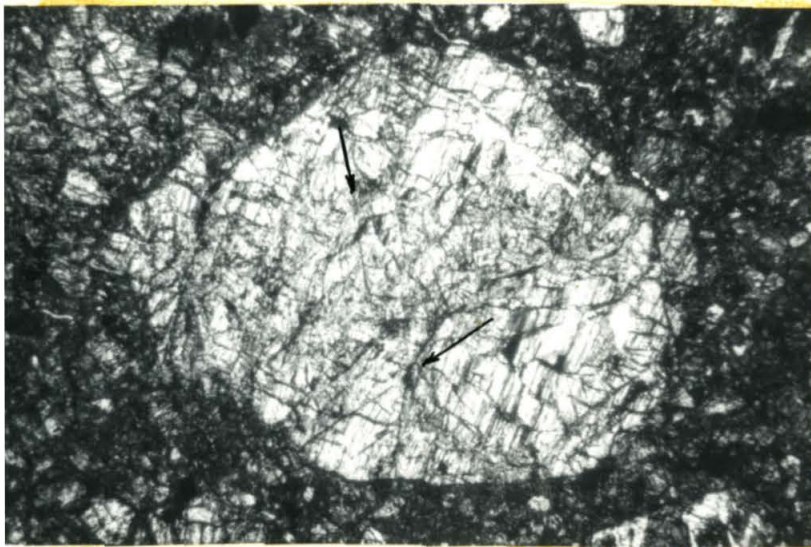
(a)



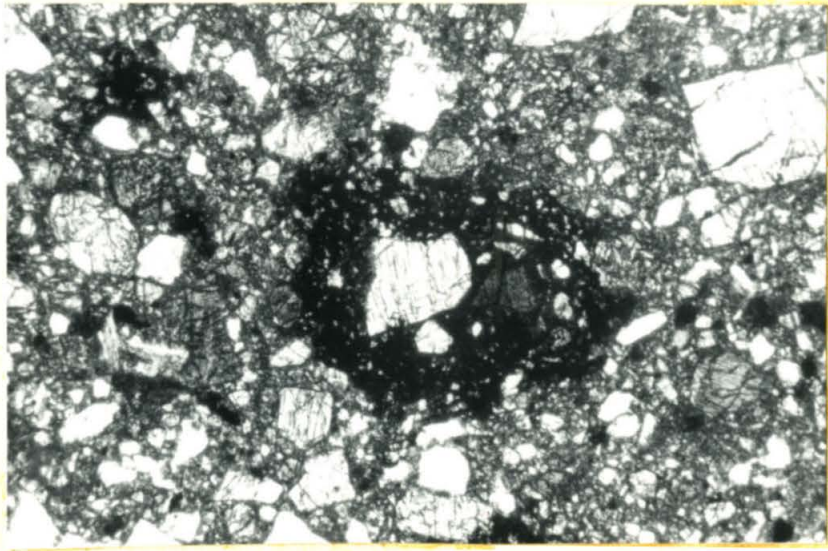
(b)



(a)

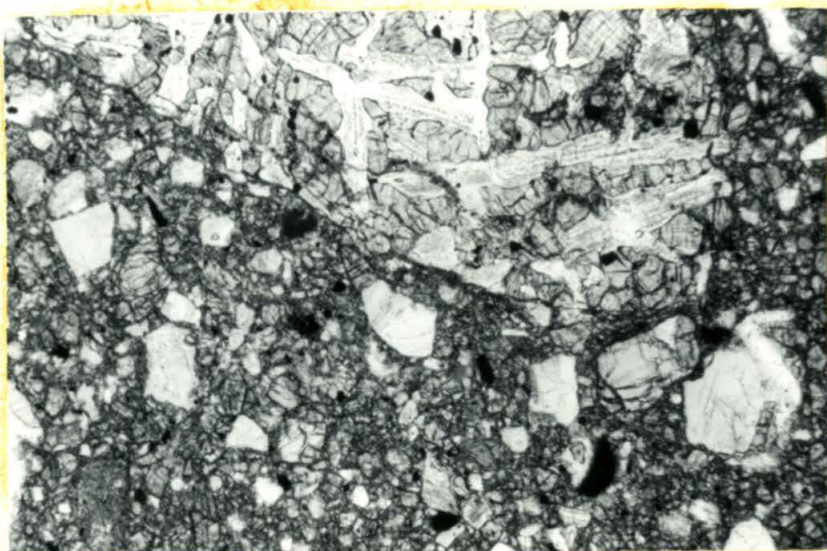


(b)

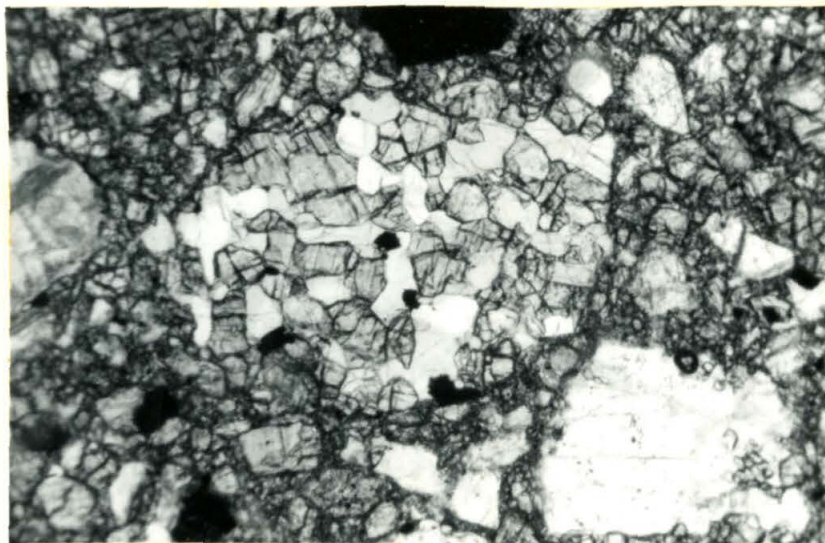


(a)

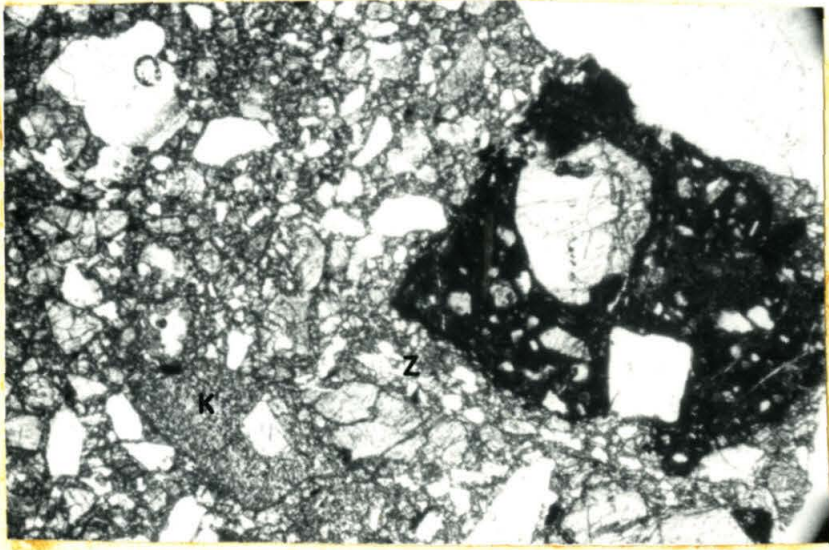
PLATE 45



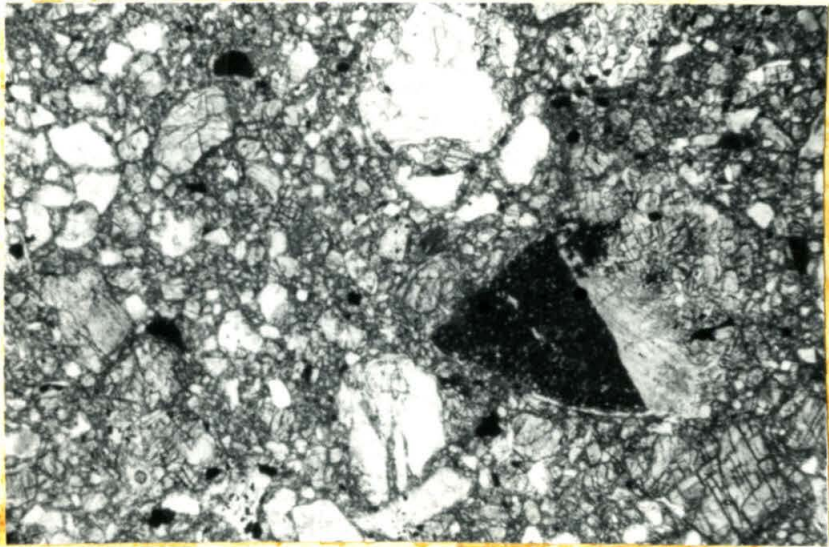
(a)



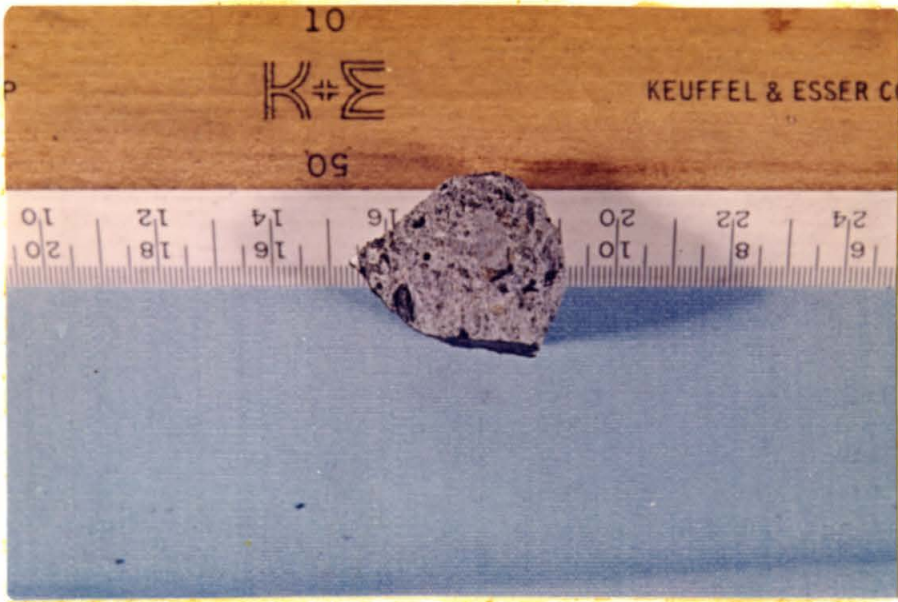
(b)



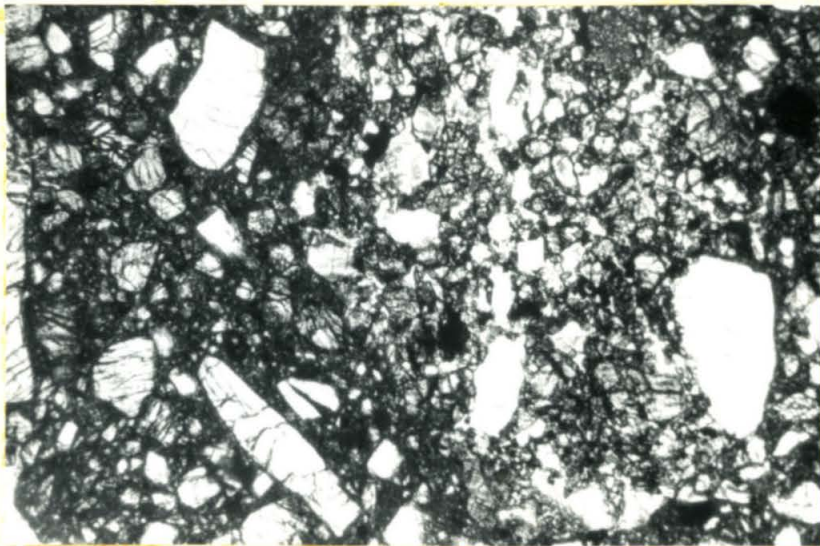
(a)



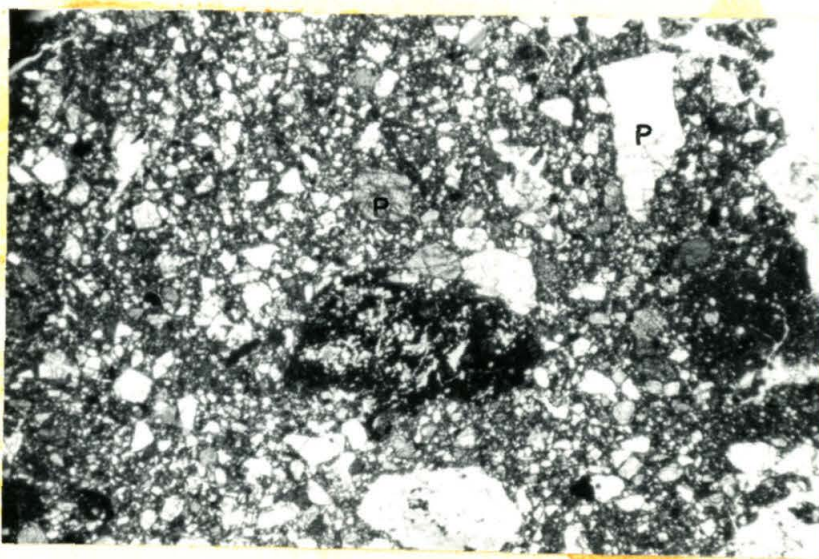
(b)



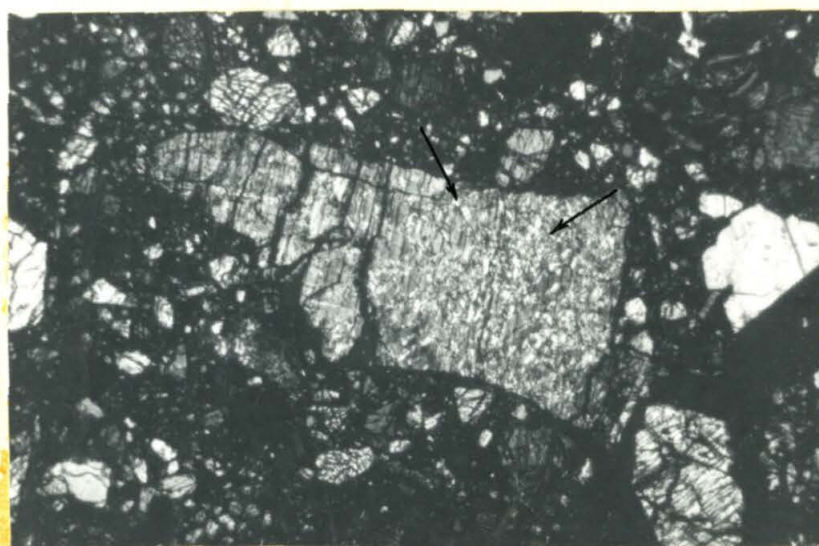
(a)



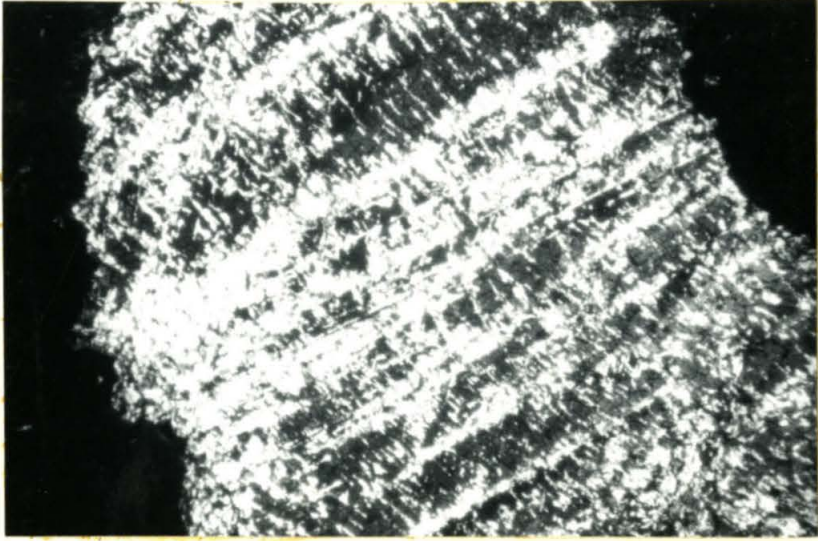
(b)



(a)



(b)

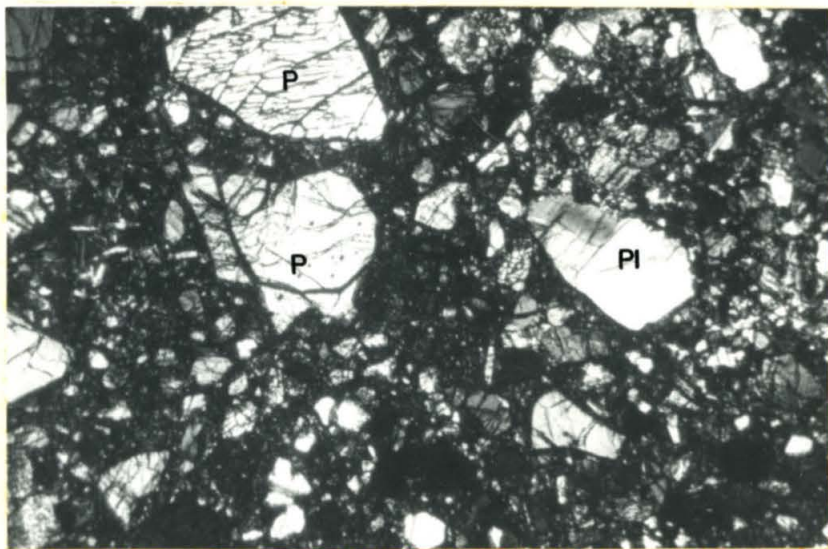


(a)

PLATE 50



(a)

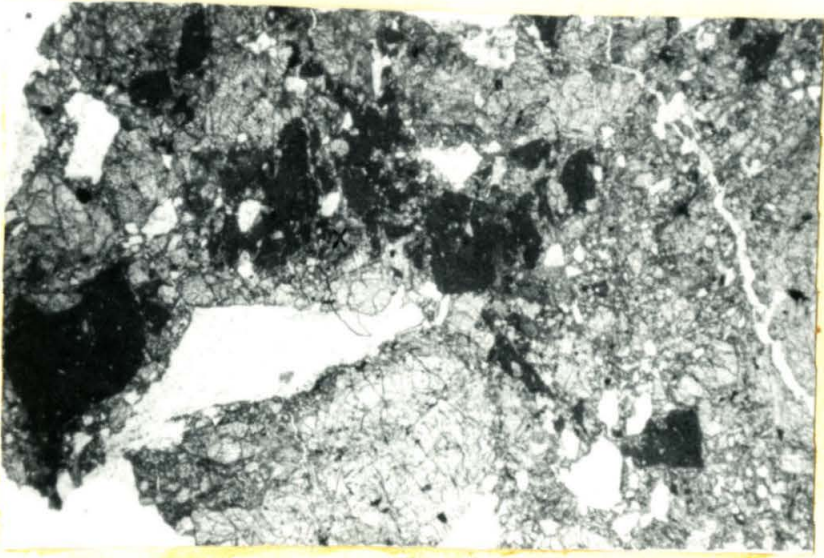


(b)

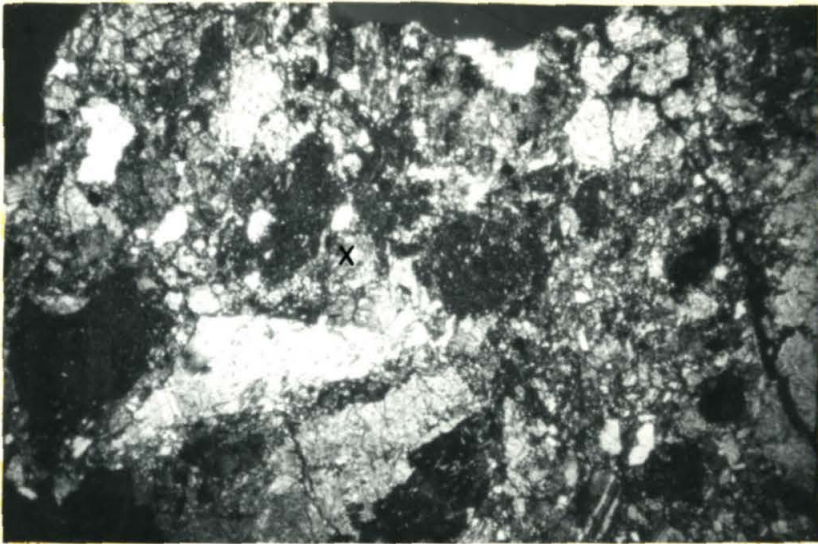


(a)

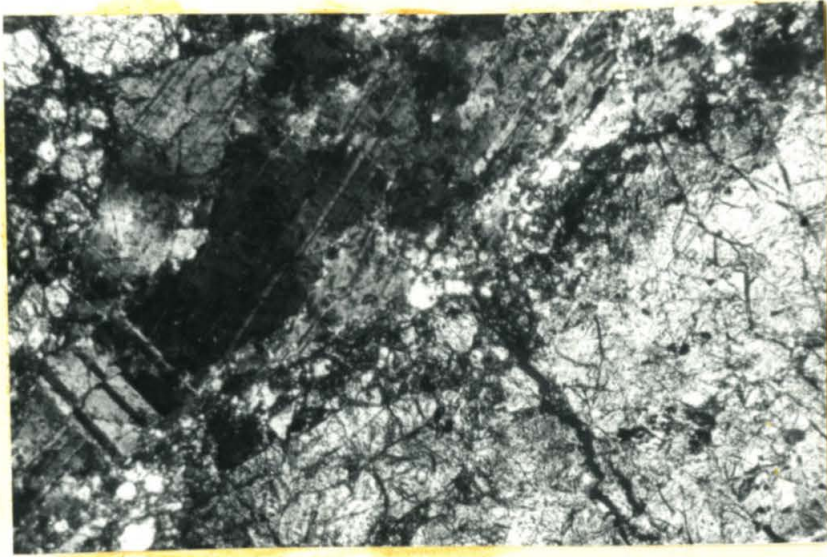
PLATE 52



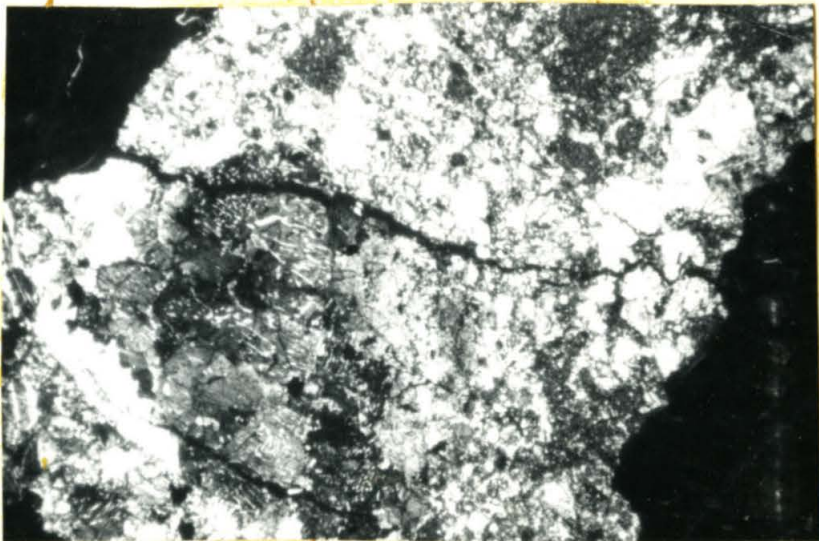
(a)



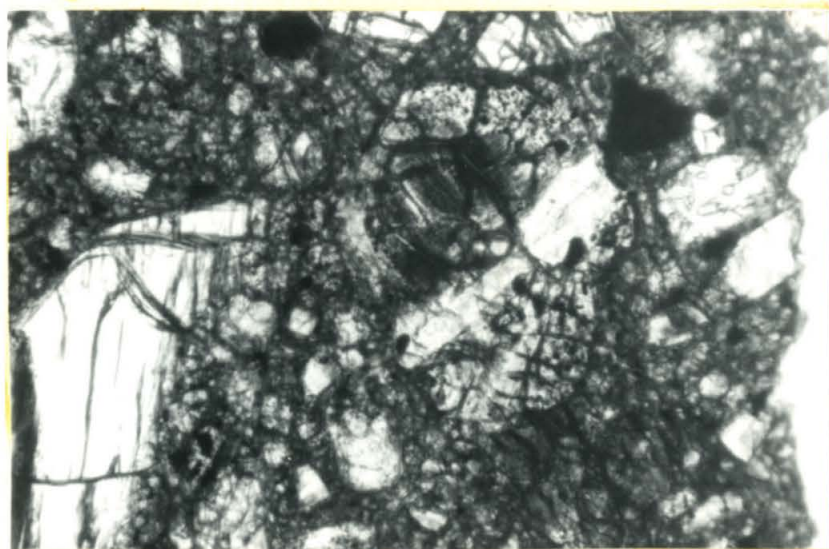
(b)



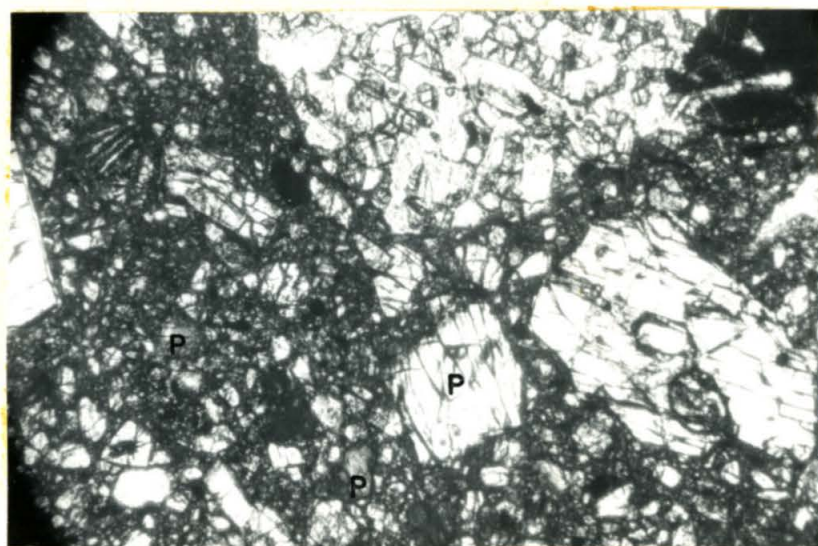
(a)



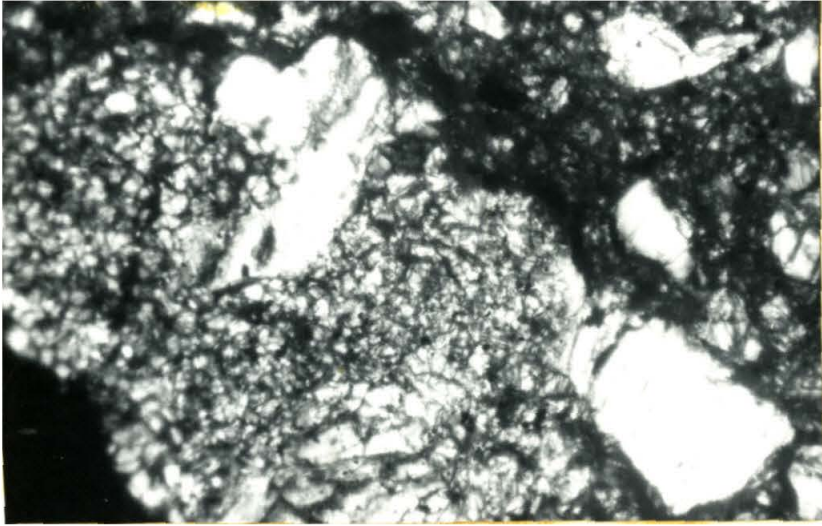
(b)



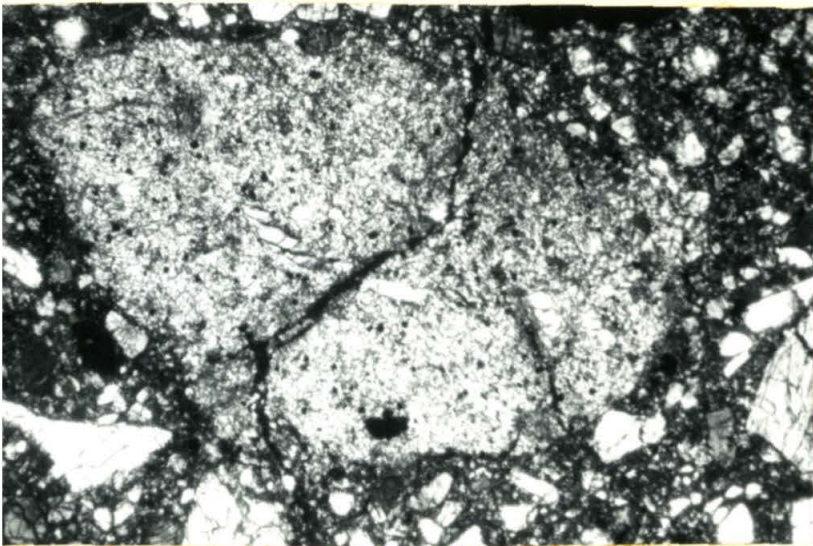
(a)



(b)



(a)



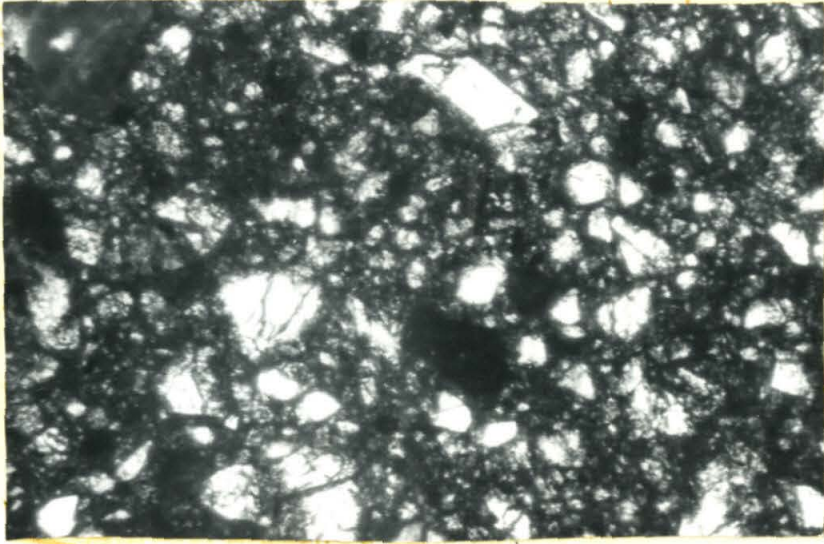
(b)



(a)



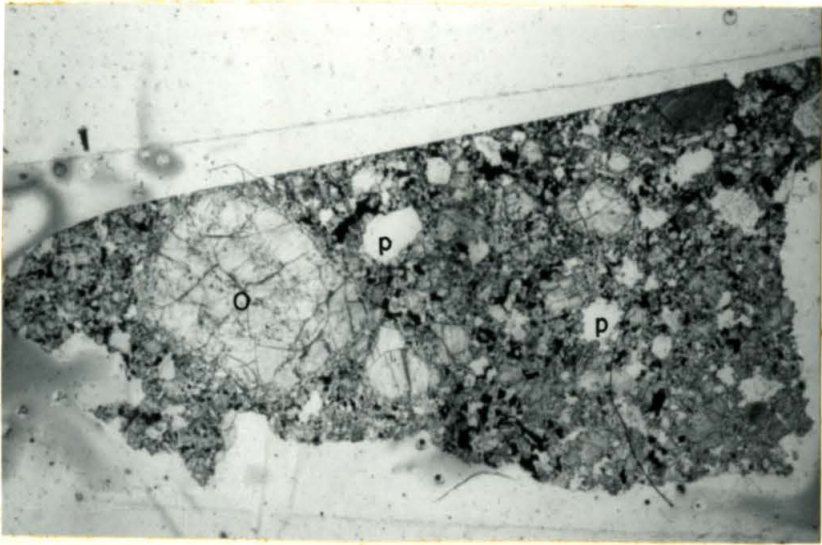
(b)



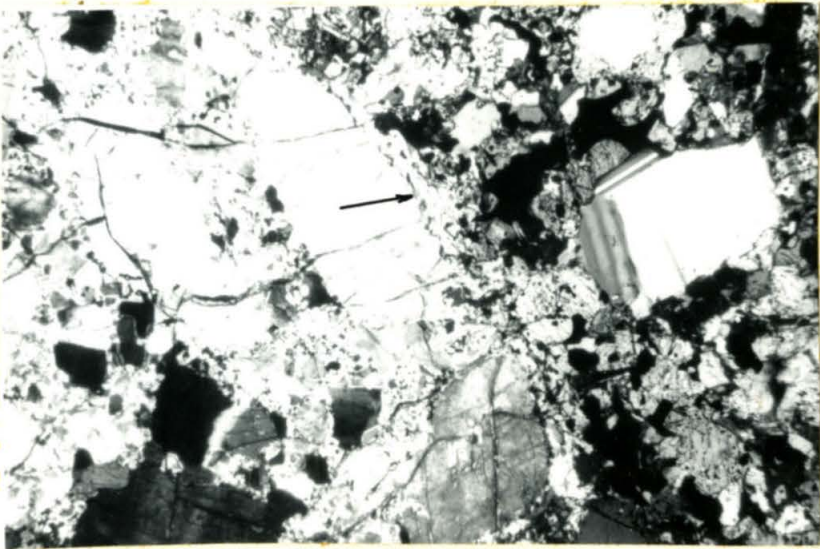
(a)



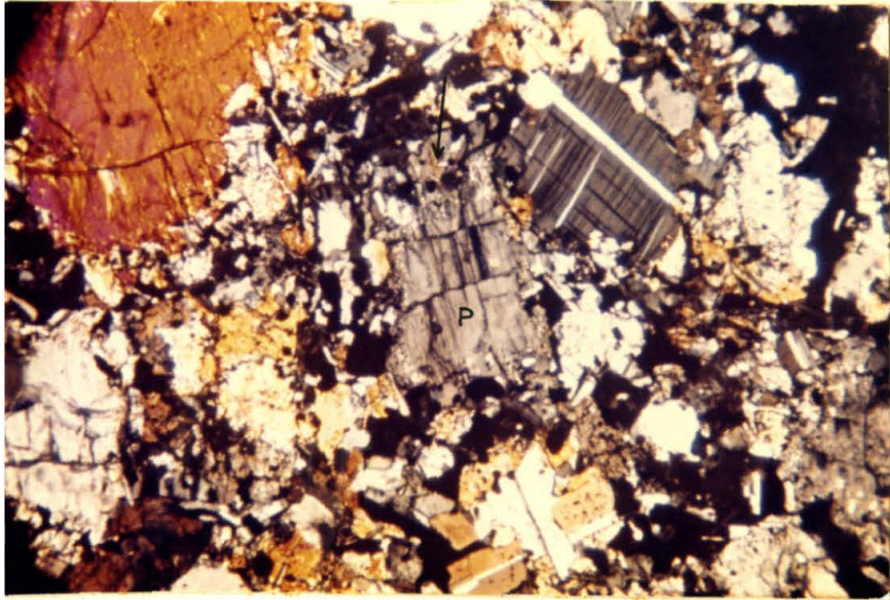
(b)



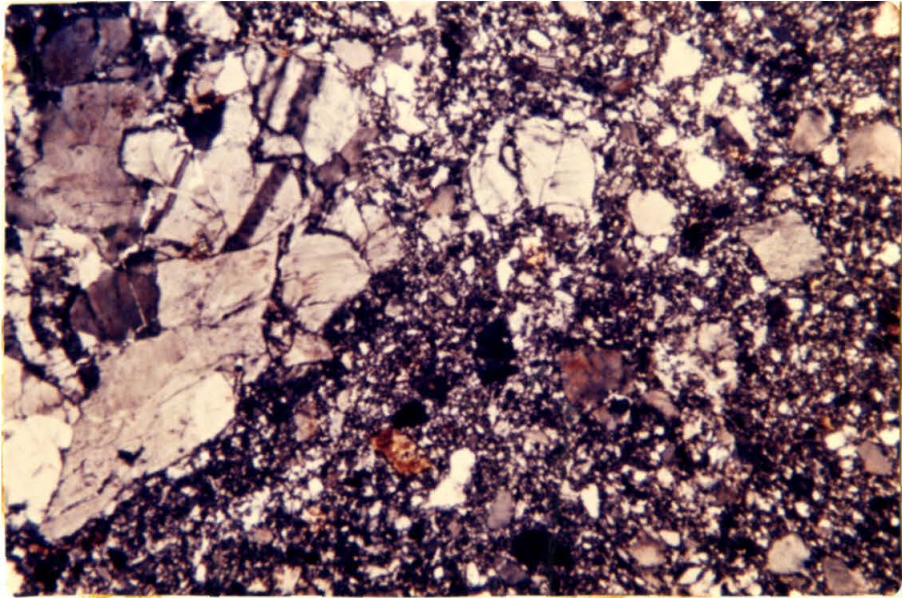
(a)



(b)



(a)



(b)